UNIVERSIDADE FEDERAL DE GOÍAS

INSTITUTO DE CIÊNCIAS BIOLÓGICAS

PROGRAMA DE PÓS-GRADUAÇÃO EM GENÉTICA E BIOLOGIA MOLECULAR

FABIANA RIBEIRO DA MATA

METABOLISMO DO ACETATO ENTRE MEMBROS DO GÊNERO *Paracoccidioides* spp.

TESE DE DOUTORADO

GOIÂNIA

2017

sistema de bibliotecas ufg

PRPG
PRÓ-REITORIA DE PÓS-GRADUAÇÃO

UFG

TERMO DE CIÊNCIA E DE AUTORIZAÇÃO PARA DISPONIBILIZAR VERSÕES ELETRÔNICAS DE TESES E DISSERTAÇÕES NA BIBLIOTECA DIGITAL DA UFG

Na qualidade de titular dos direitos de autor, autorizo a Universidade Federal de Goiás (UFG) a disponibilizar, gratuitamente, por meio da Biblioteca Digital de Teses e Dissertações (BDTD/UFG), regulamentada pela Resolução CEPEC nº 832/2007, sem ressarcimento dos direitos autorais, de acordo com a Lei nº 9610/98, o documento conforme permissões assinaladas abaixo, para fins de leitura, impressão e/ou *download*, a título de divulgação da produção científica brasileira, a partir desta data.

1. Identificação do material bibliográfico: **[ ] Dissertação** **[x] Tese**

2. Identificação da Tese ou Dissertação:

Nome completo do autor: Fabiana Ribeiro da Mata

Título do trabalho: **Metabolismo do acetato entre membros do gênero Paracoccidioides spp.**

3. Informações de acesso ao documento:

Concorda com a liberação total do documento [x] SIM [ ] NÃO[1]

Havendo concordância com a disponibilização eletrônica, torna-se imprescindível o envio do(s) arquivo(s) em formato digital PDF da tese ou dissertação.

Fabiana Ribeiro da Mata
Assinatura do(a) autor(a)[2]

Ciente e de acordo:

Assinatura do(a) orientador(a)[2]

Data: 21 / 09 / 2017

[1]Neste caso o documento será embargado por até um ano a partir da data de defesa. A extensão deste prazo suscita justificativa junto à coordenação do curso. Os dados do documento não serão disponibilizados durante o período de embargo.

Casos de embargo:
- Solicitação de registro de patente
- Submissão de artigo em revista científica
- Publicação como capítulo de livro
- Publicação da dissertação/tese em livro

[2]A assinatura deve ser escaneada.

Versão atualizada em maio de 2017.

UNIVERSIDADE FEDERAL DE GOÍAS

INSTITUTO DE CIÊNCIAS BIOLÓGICAS

PROGRAMA DE PÓS-GRADUAÇÃO EM GENÉTICA E BIOLOGIA MOLECULAR

METABOLISMO DE ACETATO ENTRE MEMBROS DO GÊNERO *Paracoccidioides* spp.

Tese apresentada ao Programa de Pós-Graduação em Genética e Biologia Molecular da Universidade Federal de Goiás, como requisito para a obtenção do **título de Doutor em Genética e Biologia Molecular.**

Candidata: Fabiana Ribeiro da Mata

Orientadora: Profa. Dra. Célia Maria de Almeida Soares

GOIÂNIA

2017

Ficha de identificação da obra elaborada pelo autor, através do
Programa de Geração Automática do Sistema de Bibliotecas da UFG.

Ribeiro da Mata, Fabiana
METABOLISMO DO ACETATO ENTRE MEMBROS DO GÊNERO Paracoccidioides spp. [manuscrito] / Fabiana Ribeiro da Mata. - 2017.
xxi, 200 f.: il.

Orientador: Profa. Dra. Célia Maria de Almeida Soares.
Tese (Doutorado) - Universidade Federal de Goiás, Instituto de Ciências Biológicas (ICB), Programa de Pós-Graduação em Genética e Biologia Molecular, Goiânia, 2017.
Bibliografia.
Inclui abreviaturas, gráfico, tabelas, lista de figuras, lista de tabelas.

1. Paracoccidioides spp.. 2. Proteômica. 3. Fonte de dois carbonos. 4. Acetato de sódio. 5. Metabolismo. I. de Almeida Soares, Célia Maria, orient. II. Título.

CDU 577.2

SERVIÇO PÚBLICO FEDERAL
UNIVERSIDADE FEDERAL DE GOIÁS
INSTITUTO DE CIÊNCIAS BIOLÓGICAS
PROGRAMA DE PÓS-GRADUAÇÃO EM GENÉTICA E BIOLOGIA MOLECULAR

ATA DA SESSÃO PÚBLICA DE DEFESA DE TESE DE Nº 003

Aos treze dias do mês de abril do ano de dois mil e dezessete, às 14 horas, no Anfiteatro do ICB II/UFG, reuniram-se os componentes da banca examinadora: **Profa. Dra. Célia Maria de Almeida Soares; Prof. Dr. Alexandre Melo Bailão; Prof.Dr. Cirano José Ulhoa; Prof. Dr. Wesley de Almeida Brito e Prof. Dr. Carlos André Ornelas Ricart** para, em sessão pública presidida pela primeira examinador citada, procederem à avaliação da defesa de tese intitulada: **"METABOLISMO DO ACETATO ENTRE MEMBROS DO GÊNERO** *Paracoccidioides* **spp"**, em nível de doutorado, área de concentração em **Genética e Biologia Molecular**, de autoria de **Fabiana Ribeiro da Mata**, discente do Programa de Pós-Graduação em Genética e Biologia Molecular da Universidade Federal de Goiás. A sessão foi aberta pela presidente, que fez a apresentação formal dos membros da banca. A palavra, a seguir, foi concedida à autora da tese que, em cerca de 50 minutos, procedeu à apresentação de seu trabalho. Terminada a apresentação, cada membro da banca arguiu a examinada, tendo-se adotado o sistema de diálogo sequencial. Terminada a fase de arguição, procedeu-se à avaliação da tese. Tendo-se em vista o que consta na Resolução nº 1294 de 06 de Junho de 2014 do Conselho de Ensino, Pesquisa, Extensão e Cultura (CEPEC), que regulamenta o Programa de Pós-Graduação em Genética e Biologia Molecular, a tese foi APROVADA, considerando-se integralmente cumprido este requisito para fins de obtenção do título de Doutor (a) em Genética e Biologia Molecular pela Universidade Federal de Goiás. A conclusão do curso dar-se-á quando da entrega da versão definitiva da tese na secretaria do programa, com as devidas correções sugeridas pela banca examinadora, no prazo de trinta dias a contar da data da defesa. Cumpridas as formalidades de pauta, às 18 horas e 00 minutos, encerrou-se a sessão de defesa

SERVIÇO PÚBLICO FEDERAL
UNIVERSIDADE FEDERAL DE GOIÁS
INSTITUTO DE CIÊNCIAS BIOLÓGICAS
PROGRAMA DE PÓS-GRADUAÇÃO EM GENÉTICA E BIOLOGIA MOLECULAR

e, para constar, eu, Gleizilene Braz Pereira dos Santos, Assistente em Administração da Universidade Federal de Goiás, lavrei a presente ata que, após lida e aprovada, será assinada pelos membros da banca examinadora em três vias de igual teor.

Profa. Dra. Célia Maria de Almeida Soares
Presidente da Banca
ICB/UFG

Prof. Dr. Alexandre Melo Bailão
ICB/UFG

Prof.Dr. Cirano José Ulhoa
ICB/UFG

Prof. Dr. Wesley de Almeida Brito
UEG/GO.

Prof. Dr. Carlos André Ornelas Ricart.
UNB/DF

BANCA EXAMINADORA

TITULARES:

Profa. Dra. Célia Maria de Almeida Soares

Instituto de Ciências Biológicas. Universidade Federal de Goiás. UFG.

Prof. Dr. Carlos André Ornelas Ricart
Instituto de Ciências Biológicas. Universidade de Brasília. UnB.

Prof. Dr. Cirano José Ulhoa
Instituto de Ciências Biológicas. Universidade Federal de Goiás. UFG.

Prof. Dr. Alexandre Melo Bailão
Instituto de Ciências Biológicas. Universidade Federal de Goiás. UFG.

Prof. Dr. Wesley de Almeida Brito
Universidade Estadual de Goiás. UEG

SUPLENTES:

Profa. Dra. Juliana Alves Parente Rocha
Instituto de Ciências Biológicas. Universidade Federal de Goiás. UFG.

Profa. Dra. Ângela Adamski da Silva Reis
Instituto de Ciências Biológicas. Universidade Federal de Goiás. UFG.

“..Seja forte e corajoso! Não fique desanimado nem tenha medo por que eu o Senhor seu Deus estarei com você em qualquer lugar para onde você for! ”

Josué 1:9

À Deus criador de tudo, meu Senhor e Pai ...

Aos meus filhos Isabela e Christian Filho amores da minha vida que alegram meu coração todos os dias....

Dedico este trabalho também .....

...À minha família benção de Deus na minha vida meu porto seguro

.... Aos meus filhos Isabela e Christian amores da minha vida! Sempre me auxiliando e apoiando dia após dia. Mesmo na ausência durante o trabalho compreenderam ajudaram e torceram por mim. Amo muito vocês.

....À minha mãe pelo amor e dedicação em todos os momentos principalmente nas horas difíceis.

.... Ao meu pai pelo incentivo, amor e cuidado em toda minha vida.

.... Aos meus irmãos Márcia, Viviane, Sara e Fernando. Sempre ao meu lado diariamente apoiando, torcendo, chorando e sorrindo juntos. Admiro e amo vocês.

.... Aos meus cunhados Albert, Fábio, Carlos, Fábio Júnior e Josymarry pelo apoio. carinho e incentivo sempre.

As minhas cunhadas Cleusa, Nara Cristina e Marcia Christianne irmãs do coração sempre incentivando e torcendo por mim.

Aos meus sogros Elpídio e Fátima (*in memoriam*) pelo amor, carinho e apoio sempre. Aprendi muito com vocês ao longo desses anos de convivência. Amo muito vocês!

As minhas amigas Ariane e Celiny pela compreensão, carinho, amor e apoio nos momentos mais difíceis. Agradeço a Deus por colocá-las no meu caminho. Amo vocês.

Ao meu tio João pelo amor e carinho em todos os momentos. Pelos ensinamentos e apoio em todos os momentos

Aos meus Apóstolos Liberato e Elizângela instrumentos de Deus na minha vida principalmente nas horas mais sofridas trazendo Palavras de força e amor do Senhor.

AGRADECIMENTOS

À Deus criador de tudo e de todos o início e o fim. Tudo foi feito por Ele. Para Ele e por meio Dele. Deus de graça e amor. Obrigada Senhor por me amar e me escolher primeiro. Tu me levas a lugares onde jamais podia imaginar e me sustentas. Fortalece e protege em todos os momentos durante a caminhada. Estas sempre comigo minha rocha inabalável e por isso tenho a certeza que tudo correrá bem. A Ti Senhor toda honra. Toda glória. Todo louvor e todo domínio. Amem!!!

À Profª. Dra. Célia Maria de Almeida Soares pela orientação e ensinamentos durante a execução deste trabalho. Um exemplo de dedicação e competência na pesquisa científica não medindo esforços para a produção de trabalhos com excelência. Admiro sua dedicação e trabalho árduo na produção do conhecimento. Minha gratidão!

Aos professores do LBM Clayton Luiz Borges, Juliana Alves Parente Rocha e Alexandre Bailão pelo apoio e auxilio diário. Principalmente a Prof.ª Maristela Pereira pelas contribuições importantes na execução deste trabalho.

Aos colegas e professores do Departamento de Morfologia Ana Cristina. Augusto, Paulo César, João, Karina e Edson pelo apoio principalmente no período inicial onde conciliava aulas e disciplinas do doutorado. Obrigada pelas aulas que muitos permutaram comigo para em horários de experimento e disciplinas

A Lilian e a Laurine pela amizade e parceria neste estudo principalmente nos dois últimos meses de trabalho intenso. Admiro a dedicação e a responsabilidade de vocês como pesquisadoras principalmente como pessoa. Obrigada pela convivência alegre e agradável. Pela força e incentivo nos momentos difíceis. Pela amizade e companhia. E também pelas contribuições inestimáveis neste estudo.

A Vanessa e a Marta pela amizade e apoio em todos os momentos onde por vezes choramos. Mas também sorrimos juntas. Muito obrigada!

A Juliana DeCurcio, Lucas Nojosa, Marielle e Luciana Casalleti, pelo apoio e auxílio no início do doutorado.

Ao Luis Paulo e Leandro pela amizade, disposição e auxilio nas análises.

A todos os alunos do LBM: Carlos, Patrícia, Aparecido, André, Igor, Lanna, Danielle, Laura, Santiago, Davi, André, Andreia, Alex, Rosi, Lívia, Kassyo, Kleber, Amanda, Mariana Pedrosa e Mariana Tomazett pela amizade, convivência diária e contribuição direta ou indiretamente neste estudo.

A todos que de alguma maneira contribuíram para a realização deste trabalho.....

Muito obrigada a todos!

Deus abençoe!

SUMARIO

LISTA DE FIGURAS

Capítulo 1

Capítulo 2

of the biological triplicates of independent experiments. Student's *t*-test was used. * significantly different from the glucose condition, at a *p*-value of ≤0.05.

Figure 4: Comparison of protein profiles related to the cell wall metabolism in *P. lutzii* **and isolates of** *P. brasiliensis* Dataset comparisons were carried out, as cited in Figure 2, legend. **A**- Representative diagram of the cell wall metabolism pathways depicting down regulated (green) and up regulated (red) in the isolates, as cited above. **B**- Changes in expression levels upon yeast cells incubated with acetate in *Pb*01, *Pb*03, *Pb*339, and *Pb*EPM83, are represented in a heat map format. Black means that no significant difference was observed.

Figure 5: Comparison of protein profiles related to TCA and glyoxylate cycle in *P. lutzii* **and isolates of** *P. brasiliensis*. Dataset comparisons were carried out, as cited in Figure 2, legend. **A**- Representative diagram of the TCA and glyoxylate cycle depicting down regulated (green) and up regulated (red) in the isolates. B- Changes in expression levels upon yeast cells incubated with acetate in *Pb*01, *Pb*03, *Pb*339, and *Pb*EPM83 are represented in a heat map format. Black means that no significant difference was observed.

Figure 6: Comparison of protein profiles related to β-oxidation and methylcitrate cycle in *P. lutzii* **and isolates of** *P. brasiliensis*. Dataset comparisons were carried out as cited in Figure 2, legend. A-Representative diagram of the β-oxidation and methylcitrate cycle pathways depicting down regulated (green) and up regulated (red) in the isolates B- Changes in expression levels in yeast cells incubated with acetate in *Pb*01, *Pb*03, *Pb*339, and *Pb*EPM83 are represented in a heat map format. Black means that no significant difference was observed.

Figure 7: Comparison of protein profiles related to amino acids catabolism in *P. lutzii* **and isolates of** *P. brasiliensis*. Dataset comparisons were carried out as cited in Figure 2, legend. **A**- Changes in expression levels in yeast cells incubated with acetate in *Pb*01, *Pb*03, *Pb*339, and *Pb*EPM83 are represented in a heat map format. **B**- Representative diagram of the amino acid catabolism pathways depicting down regulated (green) and up regulated (red) in the isolates, as cited above. Black means that no significant difference was observed.

Figure 8: Comparison of protein profiles related to detoxification mechanisms against oxidative stress in the *P. lutzii* **and isolates of** *P. brasiliensis*. Dataset comparisons were carried out with as cited in Figure 2, legend. **A**- Changes in expression levels upon yeast cells incubated with acetate in Pb01, *Pb*03, *Pb*339, and *Pb*EPM83 are represented in a heat map format. **B**- Representative diagram of the detoxification mechanisms against oxidative stress pathways depicting down regulated (green) and up regulated (red) in the isolates as cited above. Black means that no significant difference was observed. *Glutathione (GSH*); Glutathione reductase (GR); Glutathione disulfide (GSSG).

Figure 9: Overview of the metabolic features of members of the *Paracoccidioides* genus, in sodium acetate as carbon source. The metabolic pathways were identified by the analysis of the up regulated proteins in *P. lutzii* (*Pb*01) and *P. brasiliensis Pb*03, *Pb*339, and *Pb*EPM83. The main metabolic pathways were represented: gluconeogenesis, fermentation, cycles of the tricarboxylic acid (TCA), glyoxalate (GC) and methylcitrate (MCC), respiratory chain, β- oxidation, amino acid degradation, detoxification / response to stress and cell wall components.

Supplemental Figure 1. Growth of *P. lutzii* (*Pb*01) and *P. brasiliensis* isolates *Pb*03, *Pb*339, and *Pb*EPM83 in glucose and sodium acetate as carbon sources. A total of $1x10^6$ cells/50 mL were incubated in MMcM medium with glucose (100 mM) or sodium acetate (100 mM) for 96 hours. Cells were collected at time intervals, killed by heat, lyophilized and the dry weight was determined. Data were expressed as mean and standard deviation of the triplicates of independent experiments. The data were analyzed by two-way ANOVA and Tukey's multiple comparisons test. Letters indicate significant differences at time points, in each condition.

Supplemental Figure 2. Functional classification of proteins regulated in yeasts of *P.lutzii* and *P. brasiliensis* grown in 100mM sodium acetate as carbon source for 48 hours and obtained by NanoUPLC-MS^E analysis. **(A)** Biological processes of induced proteins. **(B)** Biological processes of repressed proteins. The biological processes of the differentially expressed proteins in the isolates were obtained using the Pedant in MIPS for *P. lutzii* (http://pedant.helmholtzmuenchen.de/pedant3htmlview/pedant3view?Method=analysis&Db=p3_r48325_Par_lutzi), *Pb*03 (http://pedant.helmholtzmuenchen.de/pedant3htmlview/pedant3view?Method=analysis&Db=p3_p27779_Par_brasi_Pb03). and *Pb339*. *Pb*EPM83 (http://pedant.helmholtzmuenchen.de/pedant3htmlview/pedant3view?Method=analysis&Db=p3_p28733_Par_brasi_Pb18), Uniprot (http://www.uniprot.org/) and KEGG: Kyoto Encyclopedia of Genes and Genomes (www.genome.jp/kegg/).

Supplemental Figure 3. Evaluation of β-1,3 glucan quantities in the cell wall of *P. brasiliensis* isolate *Pb*03. (A) Aniline blue was used to evaluate, by fluorescence microscopy, the presence of β-1,3 glucan in the cell wall of *Pb*03, after growth in MMcM medium with sodium acetate or glucose for 48 h (increase of 40 times). **(B)** Fluorescence intensity graph. The values of fluorescence intensity (in pixels) and the standard error of each analysis were used to plot the graph. Data are expressed as mean ± standard error (represented using error bars), (*) represents $p \leq 0.05$.

Supplemental Figure 4: Comparison of protein profiles related to electron transport and membrane-associated energy conservation in *P. lutzii* and isolates of *P. brasiliensis*. Data of expression set comparisons were carried out with The MultiExperiment Viewer software V.4.8 (www.tm4.org/mev/) was used to group and compare data of expression and ANOVA test, applying a cut off at 1.5-fold expression changes. **A**- Changes in expression levels upon yeast cells incubated with acetate in

*Pb*01, *Pb*03, *Pb*339 and *Pb*EPM83 in presence of sodium acetate 100 mM are represented in a heat map format. Mean values of experimental triplicates are shown for down regulation (green) and up regulation (red). **B**- Representative diagram of the electron transport and membrane-associated energy conservation in pathways depicting down regulated (green) and up regulated (red) in the isolates. Black means that no significant difference was observed.

Supplemental Figure 5: Schematic representation of the degradation of the amino acids methionine, threonine, glycine, serine, alanine and aspartate in *P. lutzii* (*Pb*01) **and** *P. brasiliensis Pb*03, *Pb*339 and *Pb*EPM83 **in presence of sodium acetate 100 mM**. Proteins up regulated and down regulated in each isolate were depicted by colors red and green, respectively.

Supplemental Figure 6: Schematic representation of the degradation of the amino acids tryptophan, phenylalanine and tyrosine in *P. lutzii* (*Pb*01) **and** *P. brasiliensis Pb03, Pb339,* **and** *Pb*EPM83 **in presence of sodium acetate 100 mM.** Proteins up regulated and down regulated in each isolate were depicted by colors red and green, respectively.

Supplemental Figure 7: Schematic representation of the degradation of the amino acids arginine, glutamate and proline in *P. lutzii* (*Pb*01) **and** *P. brasiliensis Pb*03, *Pb*339, **and** *Pb*EPM83 **in presence of sodium acetate 100 mM**. Proteins up regulated and down regulated in each isolate were depicted by colors red and green, respectively.

Supplemental Figure 8: Schematic representation of the degradation of the amino acids valine, leucine and isoleucine in *P. lutzii* (*Pb*01) **and** *P. brasiliensis Pb*03, *Pb*339, and *Pb*EPM83 **in presence of sodium acetate 100 mM.** Proteins up regulated and down regulated in each isolate were depicted by colors red and green, respectively.

Supplemental Figure 9: Survival of *Paracoccidioides* **isolates to macrophages during infection.** *Paracoccidioides* yeast cells of the four isolates (*Pb*01, *Pb*03, *Pb*339 and *Pb*EPM83) were previously grown in BHI medium liquid ssupplemented with 4% of glucose up to 48 h and then were incubated with macrophages at a 1:5 macrophages: yeast ratio, for 24 hours. The number of viable cells was determined by quantifying the number of colony forming units/mL (CFUs/mL) during infection from culture supernatant (non-internalized cells removed by aspiration prior to macrophages lysis) and after internalization. Data were expressed as mean ± standard error (represented using error bars) of the biological triplicates of independent experiments, using analysis of variance (ANOVA). There was no significant difference between the four isolates evaluated, for *p*-value of ≤0.05.

LISTA DE TABELAS

Supplementary Table 1. Total proteins identified in *P. lutzii* and *P. brasiliensis* grown in the presence of 100mM sodium acetate for 48 hours obtained by **N**anoUPLC-MS$^{E.}$ analysis.

Supplemental Table 2. Identified proteins after growth in 48 hours in sodium acetate as carbon source in *Paracoccidioides brasiliensis* isolate *Pb*339.

Supplemental Table 3. Identified proteins after growth in 48 hours in sodium acetate as carbon source in *Paracoccidioides brasiliensis* isolate *Pb*03.

Supplemental Table 4. Identified proteins after growth in 48 hours in sodium acetate as carbon source in *Paracoccidioides brasiliensis* isolate *Pb*EPM83.

Supplemental Table 5. Identified proteins after growth in 48 hours in sodium acetate as carbon source in *Paracoccidioides lutzii* (*Pb01*).

Supplemental Table 6. Functional categorization of proteins up-regulated 48 hours after growth in sodium acetate as carbon source in *Paracoccidioides lutzii* (*Pb01*).

Supplemental Table 7. Functional categorization of proteins down-regulated 48 hours after growth in sodium acetate as carbon source in *Paracoccidioides lutzii* (*Pb 01*).

Supplemental Table 8. Functional categorization of proteins up-regulated 48 hours after growth in sodium acetate as carbon source in *Paracoccidioides brasiliensis Pb*03.

Supplemental Table 9. Functional categorization of proteins down-regulated 48 hours after growth in sodium acetate as carbon source in *Paracoccidioides brasiliensis Pb*03.

Supplemental Table 10. Functional categorization of proteins up-regulated 48 hours after growth in sodium acetate as carbon source in *Paracoccidioides brasiliensis Pb*339 .

Supplemental Table 11. Functional categorization of proteins down-regulated 48 hours after growth in sodium acetate as carbon source in Paracoccidioides brasiliensis *Pb*339.

Supplemental Table 12. Functional categorization of proteins up-regulated 48 hours after growth in sodium acetate as carbon source in *Paracoccidioides brasiliensis Pb*EPM83 .

Supplemental Table 13. Functional categorization of proteins down-regulated 48 hours after growth in sodium acetate as carbon source in *Paracoccidioides brasiliensis Pb*EPM83.

LISTA DE ABREVIATURAS

DNA	Ácido desoxirribonucleico
RNA	Ácido ribonucleico
TFA	Ácido trifluoroacético
ATP	Adenosina trifosfato
ANOVA	Análise de variância
BCC	Biogêneses de componentes celulares *(Biogêneses of cellular componentes)*
MIPS	Centro de informação de sequências proteicas de Munique
CCDP	Ciclo celular e processamento do DNA (*Cell cycle and DNA processing*
TCA	Ciclo do ácido tricarboxílico
GC	Ciclo do glioxalato
MCC	Ciclo do metilcitrato
CoA	Coenzima A
CC/STM	Comunicação cellular/ mecanismos de transdução de sinal *(Cellular communication/signal transduction mechanism)*
Nano UPLC-MS^E	Cromatografia líquida de ultra performance acoplada à espectrometria de massas com aquisição independente de dados
D	*Desenvolvimento (Development)*
DTT	Ditiotreitol
cDNA	DNA complementar
CF	Endereçamento celular *(Cell fate)*
PF	Endereçamento proteico (*Protein fate*)
E	Energia *(Energy)*
ITS	Espaçador interno transcrito (*Internally transcribed spacer*)
S1	Espécie filogenética 1
PS2	Espécie filogenética 2
PS3	Espécie filogenética 3
ROS	Espécies reativas de oxigênio
MS	Espectometria de massas
g	Força centrífuga
PHB	Fosforilase B de coelho
P	Fosfato *(Phosphate)*
FBP1	Frutose-1.6 bifosfatase
GSSG	Glutationa dissulfite *(Glutathione disulfide)*
GR	Glutationa redutase *(Glutathione reductase)*
H	Hipotética (*Hypothetical*)
IWE	Interação com o ambiente *(Interaction with the environment)*
Fe^{+3}	Íon ferro oxidado
Fe^{+2}	Íon ferro reduzido
ICL	Isocitrato liase
*Pb*01	Isolado 01 de *Paracoccidioides lutzii*
*Pb*03	Isolado 03 de *Paracoccidioides brasiliensis*
*Pb*339	Isolado 339 de *Paracoccidioides brasiliensis*
*Pb*EPM83	Isolado EPM83 de *Paracoccidioides brasiliensis*
Log 2	Logaritmo na base 2
MLS	Malato sintase
MMcM	Meio mínimo Mc Veigh Morton
CCM	Metabolismo de compostos de carbono e carboidratos *(C-compound and carbohydrate metabolism*
M	Metabolismo (*Metabolism*)
ACM	Metabolismo de aminoácido *(Amino acid metabolismo)*

LFAIM	Metabolismo de lipidios, ácidos graxos e isoprenóide *(Lipid. fatty acid and isoprenoid metabolism)*
MIM	Metabolismo de mediadores intercelulares *(Metabolism of intercelular mediators)*
NNNM	Metabolismo de nitrogênio, enxofre e selênio *(Nitrogen. súlfur and selenium metabolism)*
MVCPG	Metabolismo de vitaminas, cofatores e grupos prostéticos *(Metabolism of vitamins. cofactors and prosthetic groups)*
PM	Metabolismo do fosfato *(Phosphate metabolismo)*
SM	Metabolismo secundário *(Secondary metabolismo)*
µg	Micrograma
µL	Microlitro
µM	Micromolar
mg	Miligrama
mL	Mililitro
NCBI	National Center for Biotechnology Information
NADP	Nicotinamida adenina dinucleotideo fosfato oxidado
NADPH	Nicotinamida adenina dinucleotideo fosfato reduzido
NAD	Nicotinamida adenina dinucleótido
PCM	Paracoccidioidomicose
pH	Potencial hidrogeniônico
PBFCR	Proteína com função de ligação ou requer cofactor *(Protein with binding function or cofactor requeriment)*
HSP	Proteína de choque térmico (*Heat shock protein*)
PCR	Reação em cadeia da polimerase
RT-PCR	Reação em cadeia da polimerase precedida por transcrição reversa
GCPSR	Reconhecimento de espécies filogenéticas por concordância genealógica
RMPF	Regulação do metabolism e função proteica *(Regulation of metabolismo and protein function)*
CRDV	Resgate cellular, defesa e virulência *(Cell rescue. defense and virulence)*
rpm	Rotações por minuto
PS	Síntese proteica (*Protein synthesis*)
PBS	Tampão Salina Fosfato
CTD	Tipo e diferenciação celular *(Cell type differentiation)*
T	Transcrição (*Transcription)*
CTTFTR	Transporte cellular, facilitado e rotas de transporte *(Cellular transport. transport facilities and transport routes)*

RESUMO

Membros do gênero Paracoccidioides são patógenos conhecidos de seres humanos que podem ser isolados de diferentes locais de infecção. Para investigar as taxas de expressão das proteínas expressas por diferentes isolados, do gênero Paracoccidioides, incluindo um isolado de P. lutzii (Pb01) e três isolados de P. brasiliensis (Pb03, Pb339 e PbEPM83) usando acetato de sódio, como fonte de carbono, As quantidades de proteínas foram determinadas usando o uso de LC-MSE independente de etiquetas e de dados. A análise estatística proporcionou a comparação de perfis de proteínas nos isolados. Um total de 1160, 1211, 1280 e 1462 proteínas foram identificadas de forma reprodutiva, e relativamente quantificadas em isolados de P. lutzii e P. brasiliensis Pb03, Pb339 e PbEPM83, respectivamente. Nomeadamente, um total de 526, 435, 744 e 747 proteínas foram diferencialmente expressas entre P. lutzii e os isolados de P. brasiliensis Pb03, Pb339 e PbEPM83, respectivamente, com uma mudança de dobra igual ou superior a 1,5. A análise revelou a reorganização do metabolismo através da indução de proteínas relacionadas à gliconeogênese, resposta ao estresse e degradação de aminoácidos nos quatro isolados avaliados. As diferenças entre os isolados foram observadas como segue: maiores aumentos nos níveis de expressão de proteínas pertencentes ao ciclo do glioxalato, TCA e cadeia respiratória, produção de etanol e β-oxidação foram observadas nos isoladosn*Pb*EPM83 e *Pb*01; As proteínas do ciclo da e do ciclo do metilcitrato apresentaram induzidas no *Pb*339. Os perfis proteômicos indicam que os quatro isolados reorganizam o metabolismo para o uso do acetato como fonte de carbono.

Palavras-chave: *Paracoccidioides* spp .; proteômica; fonte de dois carbonos; acetato de sódio; metabolismo.

ABSTRACT

Members of the genus *Paracoccidioides* are known pathogens of humans that can be isolated from different infection sites. To investigate the expression rates of proteins expressed by different isolates, of the genus *Paracoccidioides*, including one isolate of *P. lutzii* (*Pb*01), and three isolates of *P. brasiliensis* (*Pb*03, *Pb*339 and *Pb*EPM83) using sodium acetate, as carbon source, proteins quantities were determined using label-free and data independent LC-MS^E. Statistical analysis provided the comparison of proteins profiles in the isolates. A total of 1160, 1211, 1280 and 1462 proteins were reproducibly identified, and relatively quantified in *P. lutzii* e *P. brasiliensis* isolates *Pb*03, *Pb*339 e *Pb*EPM83, respectively. Notably, a total of 526, 435, 744 and 747 proteins were differentially expressed among *P. lutzii* and the *P. brasiliensis* isolates *Pb*03, *Pb*339 and *Pb*EPM*83*, respectively with a fold change equal or higher than 1.5. The analysis revealed the reorganization of metabolism through the induction of proteins related to gluconeogenesis, stress response and amino acid degradation in the four isolates evaluated. The differences between the isolates were observed as follows: greater increases in the expression levels of proteins belonging to the cycle of glyoxalate, TCA and respiratory chain, ethanol production and β-oxidation were observed in the isolatesPPEPM83 and Pb01; Cyclic and cyclocyclic proteins of the methylcitrate were induced in Pb339. Proteomic profiles indicate that the four isolates reorganize the metabolism for the use of acetate as a carbon source.

Key words: *Paracoccidioides* spp.; proteomic; two-carbon source, sodium acetate, metabolism.

Capítulo 1

Introdução

1. INTRODUCÃO

1.1. Aspectos morfológicos de *Paracoccidioides* spp.

Paracoccidioides spp. é o agente etiológico da Paracoccidioidomicose (PCM), micose sistêmica localizada geograficamente na América do Sul e Central (RESTREPO & TOBÓN. 2005) tendo infectado cerca de 10 milhões de pessoas, com o maior número de relatos de casos no Brasil (BRUMMER *et al*., 1993; PRADO *et al*., 2009).

Paracoccidioides spp. é um fungo associado a infecções sistêmicas em humanos e outros mamíferos e classificado como termodimórfico, sendo capaz de alternar entre duas formas morfológicas conforme condições ambientais específicas. O estímulo principal para o seu dimorfismo é a temperatura assim quando cultivado a 22-25°C o fungo apresenta-se na forma filamentosa, com aspecto algodonoso e microscopicamente observa-se a formação de hifas septadas, multinucleadas com finos filamentos e clamidósporos intercalares e terminais (BRUMMER *et al*., 1993; SAN-BLAS, 1993). Na temperatura 36-37°C *in vitro* ou no hospedeiro vertebrado os filamentos se diferenciam em leveduras, forma patogênica, assemelham-se a "roda de leme" célula mãe cercada perifericamente por células filhas com ou vários brotamentos e/ou brotamento único, sendo ambas as formas multinucleadas (McEWEN *et al*., 1987; QUEIROZ-TELLES 1994). Análises do transcriptoma demonstrou reprogramação genética durante a mudança dimórfica (FELIPE *et al*., 2003; GOLDMAN *et al*., 2003; BASTOS *et al*., 2007). A capacidade de o fungo transitar da forma de micélio para levedura é fundamental para o estabelecimento da infecção sendo não virulentos os isolados incapazes de se diferenciar (DEMORAES BORBA & SCHAFFER. 2002; ROONEY & KLEIN. 2002). Desta forma, o dimorfismo térmico é uma característica importante para a virulência e patogenicidade de *Paracoccidioides* spp. (SAN-BLAS *et al*., 2002); contudo, as bases celulares e moleculares envolvidas na transição morfológica deste patógeno humano ainda não foram completamente elucidadas (RESTREPO-MORENO *et al*., 2003). A temperatura parece ser o principal fator para a diferenciação dimórfica em leveduras; contudo há relatos também da influência do hormônio feminino 17-β-estradiol (NEMECEK *et al*., 2006; RAPPLEYE & GOLDMAN 2006; SAN-BLAS *et al*., 2002) e de resposta imunológica diferencial entre os gêneros (PINZAN *et al.,* 2010). Estudos verificaram a inibição da transição micélio para levedura de modo dose-dependente *in*

vitro (RESTREPO, 1985) e *in vivo* (SANO et al., 1999) pelo hormônio feminino 17-β-estradiol. Isto ocorre devido à interação do hormônio com a proteína fúngica denominada EBP (*Estradiol Binding Protein* ou *E2-Binding Protein*) atrasando e bloqueando a transição da fase infectiva para a patogênica (SHANKAR *et al.*, 2011). Além disso, o tipo de resposta imunológica em cada gênero sexual também pode estar relacionado à progressão da doença, como observado no desenvolvimento da doença em camundongos machos e fêmeas infectados com *Paracoccidioides spp*., sendo que as fêmeas se mostraram mais resistentes à infecção pelo fungo. Este fato foi atribuído em parte, aos hormônios sexuais, modulando a resposta imune, via estimulação da paracoccina, uma lectina presente na superfície do fungo que se liga à laminina da superfície dos macrófagos. Esta ligação induz a produção de altos níveis de TNF-α (fator de necrose tumoral alfa) e óxido nítrico pelos macrófagos, os quais estão envolvidos na atividade fungicida destas células (PINZAN *et al*., 2010).

O hábitat do fungo tem sido alvo de muitos estudos, sendo o mesmo encontrado no solo como saprófita, utilizando de matéria orgânica em decomposição como fonte de nutrientes e energia (SILVA-VERGARA *et al.*, 1998; TERÇAROLI *et al*., 2007; THEODORO *et al*., 2005). O fungo tem sido encontrado em associação a animais de sangue quente, tendo sido isolado de tatus de regiões endêmicas (*Dasypus novemcinctus* - Brasil e *Cabassous centralis* - Colômbia) sendo esses animais considerados reservatórios naturais (BAGAGLI *et al*., 2003; 1998; CORREDOR *et al*., 1999). O contato desses animais com o solo, vivendo em túneis e cavando tocas poderia contribuir para disseminação dos esporos fúngicos (BOCCA et al., 2013). O fungo também tem sido isolado de outros animais como cães (FARIAS *et al*., 2011; ONO *et al*., 2001), preguiças de dois dedos (TREJO-CHAVEZ *et al*., 2011), morcegos e pinguins (GEZUELE *et al*., 1989).

A reprodução de isolados de *Paracoccidioides* spp. ocorre através de múltiplos brotamentos de células leveduriformes ou na fase micélio pela produção de conídios, esporos assexuais importantes na disseminação do fungo na natureza (TERÇARIOLI *et al*., 2007; SAN-BLAS *et al.,* 2002). Há também relatos de características sexuais e estruturas de acasalamento como recombinação presente no lócus MAT (*Mating type)* com expressão de genes relacionados ao sexo e formação de ascocarpo; contudo ainda não foi observado o estágio teleomórfico (LI *et al*., 2010; TEIXEIRA *et al*., 2013).

1.2. Classificação Taxonômica

A Paracoccidioidomicose (PCM) foi descrita pela primeira vez por Adolfo Lutz em 1908, que em seus pacientes em São Paulo observou características microscópicas que diferenciava este fungo de outros espécimes causadores de coccidioidomicose, como ausência de esférulas com esporos (LUTZ, 1908). O pesquisador observou também a natureza dimórfica do fungo e descreveu a doença como uma "nova enfermidade pseudococcídica" sul americana. O fungo foi identificado como *Zymonema brasiliensis* por Splendore (1912) estudando a morfologia em novos casos de pacientes em São Paulo. Em 1930, Almeida, após comparação morfológica com *Coccidioides immitis* e características distintas, propôs o nome *Paracoccidioides brasilensis* sendo considerado como fungo anamórfico devido ao desconhecimento da fase teleomórfica (DEL NEGRO *et al*., 1992).

Comparações filogenéticas de fungos dimórficos baseadas na subunidade ribossomal 28S classificaram *Paracoccidioides* spp. como sendo pertencentes ao filo Ascomycota, ordem Onygenales, família Onygenaceae, juntamente com outros fungos como, *Blastomyces dermatitidis* e *Histoplasma capsulatum, Emmonsia parva, Emmonsia crescens e Lacazia loboi*. Estes organismos se desenvolveram em associação com hospedeiros vertebrados apresentando uma fase saprobiótica no solo e/ou fezes e outra parasitária nos tecidos do hospedeiro (BAGAGLI *et al*., 2008).

Desde sua descoberta até o ano de 2006 *P. brasiliensis* era considerado como uma única espécie, como o agente etiológico da PCM. No entanto, estudos baseados em dados de polimorfismo genético baseados na análise de oito regiões de cinco genes nucleares em 65 isolados de *P. brasiliensis* propuseram a existência de três diferentes clados para *P. brasiliensis*: S1 grupo parafilético com 38 isolados, PS2 grupo monofilético com seis isolados e PS3 grupo monofilético com 21 isolados (MATUTE *et al.*, 2006; CARRERO *et al*., 2008). Análises da região 18S do DNA ribossomal, apontam como tempo de divergência entre PS2 e PS3 cerca de 8,04 - 8,37 milhões de anos sugerindo que a especiação de PS3 restrito a Colômbia poderia ser atribuído a dispersão ou qualquer evento que levou ao isolamento genético de PS3 a partir de S1 (especiação alopátrica); já o evento que gerou especiação em PS2 ainda é pouco conhecido (MATUTE *et al*., 2007).

Carrero e colaboradores (2008) analisaram as relações filogenéticas de 21 isolados pertencentes às espécies filogenéticas S1 e PS3 por meio da comparação de sequências

de regiões codantes, não codantes e ITS (sequência espaçadora interna) e observaram que um dos isolados, o *Pb*01, se diferenciava claramente dos demais e poderia ser uma nova espécie do gênero *Paracoccidioides*. Embora os resultados sugerissem a possibilidade de uma nova espécie filogenética, havia a necessidade de identificação da existência de mais isolados agrupados com *Pb*01. Alguns estudos com isolados de *P. brasiliensis* apontavam nesta direção revelando características como variabilidade genética (SOARES *et al*., 1995; MONTOYA *et al*., 1997, 1999; CANO *et al*., 1998; MOLINARI-MADLUM *et al.,* 1999; NIÑO-VEGA *et al*., 2000; HAHN *et al*., 2002, 2003; HEBELER-BARBOSA *et al*., 2003), possível correlação entre genótipo e isolamento geográfico (NIÑO-VEGA *et al*., 2000), virulência (MOLINARI-MADLUM *et al*., 1999) e resistência a drogas (HAHN *et al*., 2003).

Assim, Teixeira e colaboradores (2009) empregando o método de GCPSR (*genealogic concordance method of phylogenetic species recognition)* identificaram um clado de 17 isolados genotipicamente semelhantes, incluindo o *Pb*01, e distintos das outras três espécies filogenéticas S1, PS2 e PS3. Posteriormente, agruparam os 17 isolados em um grupo chamado "*Pb01*" e propuseram uma nova espécie chamada *P. lutzii*. Estudos com 63 isolados do gênero *Paracoccidioides* pertencentes às espécies S1, PS2, PS3 e *P. lutzii*, empregando a técnica de SNPs (*single nucleotide polymorphism*), revelaram uma distribuição geográfica restrita a Colômbia dos isolados pertencentes à espécie PS3, *P. lutzii* nas regiões centrais do Brasil, especificamente nos estados de Mato Grosso e Goiás, e no Equador, PS2 no Brasil e na Venezuela, enquanto que os isolados pertencentes à espécie S1 apresentaram distribuição pelo Brasil, Argentina, Paraguai, Peru e Venezuela (THEODORO *et al.*, 2012) (Figura 1).

De acordo com inferências biogeográficas, a radiação de *Paracoccidioides* iniciou-se na região noroeste da América do Sul, cerca de 11-32 milhões de anos atrás. Eventos vicariantes seriam responsáveis pela divergência de S1/S2 e *P. lutzii* e uma dispersão recente originou PS3, geograficamente restrita a Colômbia (THEODORO *et al*., 2012). Contudo, a história evolucionária de *Paracoccidioides* spp. é bastante complexa devido a fatores como constante migração de hospedeiros humanos, período de latência longo da PCM, falta de informações sobre a história clínica de pacientes e dificuldade de localização exata do fungo devido à dificuldade de isolamento do fungo no solo (MATUTE *et al*., 2006).

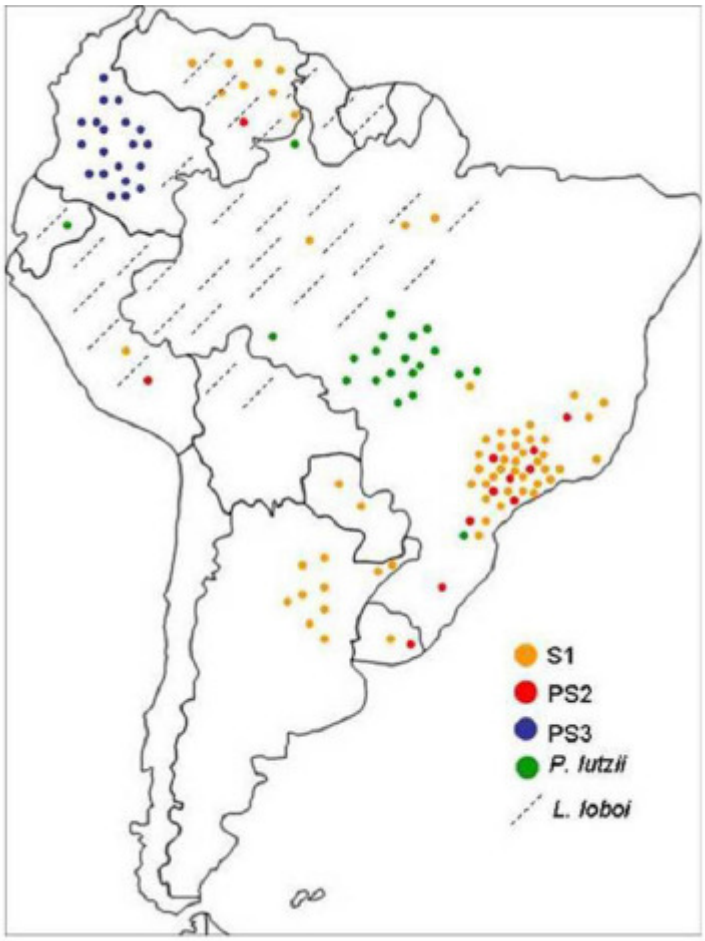

Figura 1- Distribuição geográfica do gênero *Paracoccidioides*. Distribuição geográfica das espécies filogenéticas de *P. brasiliensis* (S1, PS2, PS3) e *P. lutzii*. O fungo patogênico *Lacazia loboi* também pertencente à família Ajellomycetaceae considerada espécie irmã de *Paracoccidioides* spp. Fonte: THEODORO *et al*., 2012.

Análises baseadas em sequências parciais do gene Gp 43 (glicoproteína de 43 kDa) revelaram mais um grupo filogenético, o PS4, no qual parece ser uma população monofilética de isolados clínicos recuperados da Venezuela (BOCCA *et al.*, 2013; SALGADO-SALAZAR *et al*., 2010).

A organização genômica também tem sido investigada em espécies do gênero *Paracoccidiodes.* Os genomas estruturais dos isolados *Pb*01 *(P. lutzii/'Pb01'*), *Pb*18 *(P. brasiliensis*/S1) e *Pb*03 (*P. brasiliensis*/PS2) foram depositados no *Broad Institute* (http://www.broadinstitute.org/annotation/genome/paracoccidioides_brasiliensis/MultiHome.html). Análises comparativas entre *Pb*01 demonstraram divergência genética entre *Pb*18/*Pb*03 sendo o genoma de *Pb*01 composto de 32,94 Mb, com um total de 9,132 genes, apresentando maior genoma tanto em número de bases, quanto em quantidade de genes comparado aos outros dois isolados *Pb*03 e *Pb*18 analisados, os quais apresentaram

genomas do tamanho de 29,06 e 29,95 Mb e número de genes de 7,875 e 8,741 respectivamente. Estes dados corroboraram para melhor compreensão das diferenças entre os isolados e importantes na caracterização de regiões promotoras contribuindo para caracterização da biologia de *Paracoccidioides* (DESJARDINS *et al*., 2011).

A visão atual na literatura quanto ao gênero *Paracoccidioides* é a de que este é composto pelas espécies *P. brasiliensis* (por sua vez composta pelas espécies filogenéticas S1a, S1b, PS2, PS3 e PS4) e *P. lutzii*, conforme estudos subsequentes realizados que agregaram novas informações importantes quanto à filogenia em *Paracoccidioides* spp., além disso, ambas as espécies são capazes de causar PCM (TEIXEIRA *et al*., 2014; MUÑOZ *et al*., 2016).

1.3. Paracoccidioidomicose PCM

Paracoccidioidomicose (PCM) é uma micose sistêmica granulomatosa causada por fungos do gênero *Paracoccidioides.* Os portadores dessa doença são infectados através das vias respiratórias pela inalação de propágulos de micélio e conídios (BAGAGLI *et al*., 2006). Ao atingir o hospedeiro, o fungo pode ser eliminado ou se disseminar através das vias hematogênica e/ou linfática (SAN-BLAS, 1993; VALERA *et al*., 2008). A PCM pode variar de pouco sintomática até severa e potencialmente disseminada e fatal com período de latência desconhecido (Bocca *et al*., 2013). No Colóquio Internacional da PCM realizado em 1986 em Medellín, Colômbia a PCM foi classificada de acordo segundo os aspectos clínicos e a história da doença em duas formas: aguda/subaguda (tipo juvenil) após a infecção primária sendo moderada ou severa; forma crônica (tipo adulto) após longo período de latência com lesões multifocais ou unifocal e sequelas (FRANCO *et al*., 1987). A primeira, (forma aguda) é a mais severa da doença e acomete crianças e jovens, representando 3-5% dos casos. Seu quadro clínico caracteriza-se por um rápido desenvolvimento e pelo acometimento de órgãos como: fígado, baço, gânglios linfáticos e medula óssea. Já a segunda, conhecida por fase adulta, é a forma mais branda da doença tendo uma representação de 95% dos casos entre homens com mais de 40 anos (FRANCO, 1987). Ao contrário da forma aguda, a forma crônica apresenta um quadro clínico com desenvolvimento lento e evidente comprometimento pulmonar (BRUMMER *et al*., 1993). O progresso da patologia e a diversidade das formas clínicas dependem dos fatores imunológicos do

hospedeiro (FRANCO, 1987) e dos diferentes níveis de virulência dos isolados do fungo (SAN-BLAS & NIÑO-VEGA, 2001; PANUNTO-CASTELO *et al*., 2003).

A PCM é considerada uma enfermidade de alta prevalência e morbidade que acomete parcelas da população com menor capacidade de acesso a serviços de saúde, em áreas limitadas a somente alguns países da América Latina. No Brasil, a PCM representa 51,2% das causas de morte entre as micoses sistêmicas, seguida por criptococose, candidose e histoplasmose. Com relação à idade e sexo, 53,4% dos pacientes portadores da PCM possuem 30-59 anos e 87,9% são do sexo masculino (PRADO *et al.*, 2009). Essas diferenças podem estar relacionadas a capacidade dos estrógenos inibirem a transformação de micélio ou conídio para levedura ou a maior exposição de homens do que mulheres ao solo em áreas rurais (SHANKAR *et al*., 2011).

Cerca de 80% dos casos de PCM relatados ocorreram no Brasil, e o restante na Venezuela, Colômbia e Argentina. No Brasil, existe uma grande área endêmica que compreende as regiões sudeste (Estados de São Paulo, Rio de Janeiro, Espírito Santo e Minas Gerais), Centro-Oeste (principalmente os Estados de Goiás e Mato Grosso do Sul), e Sul (do Paraná ao norte do Rio Grande do Sul) (MARTINEZ, 2015). Uma segunda área endêmica no Brasil está localizada ao longo da fronteira da Amazônia, incluindo os estados do Pará, Maranhão e Tocantins (DE MATOS *et al*., 2012). Uma terceira área, tornou-se relevante no início do século XXI incluindo a região amazônica ocidental e o estado de Rondônia (VIEIRA *et al*., 2014). Casos autócnes, foram relatados casos nos Estados Unidos, Europa e Ásia (BUITRAGO *et al*., 2011). No Brasil, a PCM é responsável por 200 mortes ao ano e dessa forma, o país é considerado o maior centro endêmico da doença, De acordo com estudo realizado por Araújo e colaboradores (2009), a PCM é responsável por aproximadamente metade dos casos de óbito por micoses sistêmicas no Brasil, sendo que, as maiores taxas de mortalidade foram registradas nos estados de São Paulo e Paraná.

As atividades ou profissões relacionadas à manipulação do solo como atividades agrícolas, jardinagem, preparo do solo, atividades agropecuárias, entre outras, constituem o grande fator de risco para a infecção. Assim a doença é endêmica nas populações rurais afetando principalmente trabalhadores da agricultura, que realizam manipulação do solo, gerando aerossóis contendo esporos do fungo que podem ser inalados (FRANCO *et al*., 2000). Verificam-se focos emergentes em regiões periurbanas (BLOTTA *et al*., 1999) com movimentos migratórios (RESTREPO 1985; McEWEN *et al*., 1995). Nas áreas

endêmicas a incidência varia de 1 a 4 novos casos por 100,000 habitantes (MARTINEZ, 2015; SHIKANAI-YASUDA *et al*., 2006), sendo que em Rondônia essa incidência foi de 9,4 casos por 100,000 habitantes, por ser uma área com grande impacto sócio-ambiental, devido à expansão das fronteiras agrícolas (VIEIRA *et al*., 2014).

Aproximadamente 15,000 casos de PCM foram relatados na América Latina, entre 1930 e 2012 esse número reflete parcialmete a prevalência da doença (MARTINEZ, 2015). Por não ser uma doença de notificação compulsória, o impacto da PCM nas áreas endêmicas é de difícil quantificação e, talvez por isso, possua baixa visibilidade como um problema de saúde pública, o que enquadra a PCM na lista de doenças negligenciadas. Porém, apenas o Hospital Universitário da Faculdade de Medicina de Ribeirão Preto recebe, aproximadamente, 40 novos casos da doença por ano (MARTINEZ, 2010). Estima-se que sejam 3,360 novos casos por ano em todo o Brasil (MARTINEZ, 2010) e que a taxa de mortalidade seja de 5 a 27% dentro da população infectada (BROWN *et al*., 2012).

O diagnóstico pode ser realizado através da identificação do patógeno em microscopia direta de material como granulomas, drenagem de nódulos linfáticos, exsudato e expectoração (TALHARI *et al*., 2008). Os testes sorológicos revelam a existência do microrganismo antes mesmo dos exames de cultura e histopatológico e são de amplo uso na confirmação da doença (BLOTTA *et al*., 1999).

O tratamento da PCM é realizado com a quimioterapia antifúngica contudo, não há garantia de eliminação completa do fungo e a duração pode variar de 2 a 6 meses conforme a severidade da doença, incluindo sulfonamidas, anfotericina B em casos graves, e derivados azólicos, como itraconazol, cetoconazol e fluconazol (TRAVASSOS & TABORDA, 2012). Conforme as diretrizes brasileiras, itraconazol oral é a droga de escolha para tratamento da PCM (SHIKANAI-YASUDA 2005; SHIKANAI-YASUDA *et al*., 2006; TRAVASSOS & TABORDA, 2011).

1.4 . Ciclo do glioxalato

A glicose ocupa uma posição central no metabolismo de plantas, animais e microrganismos. Além de ser um bom combustível é também um precursor versátil, capaz de suprir intermediários metabólicos em reações biossintéticas (LENINGHER *et al*., 2011). A glicose é a fonte preferencial de carbono para muitos organismos e metabolicamente é oxidada a piruvato, através da glicólise, fornecendo energia na forma de ATP e intermediários para outras vias metabólicas. Ao ser oxidada pela via das pentoses fosfato produz ribose-5-fosfato e NADPH para processos biossintéticos redutores, conforme as necessidades do organismo. A descarboxilação oxidativa do piruvato pelo complexo da enzima piruvato desidrogenase converte o piruvato produzido pela glicólise em acetil CoA, principal combustível para o ciclo do ácido tricarboxílico (TCA) e também precursor para a síntese de ácidos graxos (HARVEY & FERRIER, 2012). Assim o TCA tem um papel importante não somente para oxidação completa da glicose a gás carbônico e água com produção de energia, mas atua também como reservatório de precursores metabólicos para síntese de aminoácidos, ácidos graxos e açúcares, cujas enzimas são reguladas de acordo com a necessidade da célula (HAMEL & APPANNA, 2001).

O ciclo de glioxalato (GG) é uma via anaplerótica de carbono que faz um desvio nos passos de descarboxilação do ciclo de ácido tricarboxílico (TCA), para produzir malato e succinato, utilizando acetil-CoA em condições em que a produção de piruvato a partir da glicólise é reduzida (LORENZ & FINK, 2002, FLECK *et al*., 2011). Desta forma, microrganismos e plantas têm o ciclo do glioxalato como uma via metabólica que possibilita a síntese de carboidratos a partir de fontes de carbono não fermentáveis como acetato, etanol e ácidos graxos (KORNBERG, 1966).

A capacidade de oxidar compostos de dois carbonos (C2) com produção de energia e compostos precursores de materiais celulares foi verificada em plantas e vários microrganismos e invertebrados. Estudos realizados Kornberg & Krebs (1957) a partir de bactérias capazes de utilizar acetato como fonte única de carbono e a germinação de sementes com a conversão de ácidos graxos em carboidratos, identificaram duas enzimas exclusivas do CG a isocitrato liase (ICL) e a malato sintase (MLS) que possibilitam a síntese anaplerótica do succinato a partir de acetil CoA. Através do compartilhamento de algumas reações com o TCA, o CG contorna duas etapas que impedem a síntese de

compostos de quatro carbonos (C4) como a reação de descarboxilação do isocitrato pela isocitrato desidrogenase (IDH) no TCA, e produção de succinato a partir de acetil CoA com a anaplerose do oxalacetato, que de acordo com as necessidades metabólicas da célula pode ser direcionado para a gliconeogênese para geração de energia ou como precursores estruturais (KORNBERG & KREBS, 1957). Assim através do CG, plantas, microrganismos como *Escherichia coli* e leveduras são capazes de utilizar outras fontes de carbono não preferenciais como acetato e ácidos graxos, para produzir energia e/ou síntese de componentes estruturais. As enzimas chaves deste ciclo são a isocitrato liase (ICL) que cliva isocitrato com 6 carbonos em glioxalato com 2 carbonos e succinato 4 carbonos, enquanto a malato sintase (MLS) condensa glioxalato com uma molécula de acetil CoA produzindo malato (LORENZ & FINK, 2002; FLECK *et al*., 2011), Figura 2. O ciclo do glioxalato ocorre nos glioxissomos e no compartimento citosólico em eucariotos e procariotos respectivamente (TRELEASE *et al*., 1974). A ICL e as demais enzimas do ciclo do glioxalato são induzidas em condições como baixos níveis de glicose e baixa tensão de oxigênio (FERNANDEZ *et al*.,1993; WAYNE & LIN, 1982), fontes de carbono como acetato e etanol e altas temperaturas (BOWYER et al., 1994).

Assim o ciclo do glioxalato possibilita a síntese de compostos de quatro carbonos a partir de compostos de dois carbonos como acetato, etanol (KORNBERG, 1966), sendo uma via alternativa ao TCA possibilitando a oxidação de acetato e a síntese de ácidos dicarboxílicos como succinato, malato e oxaloacetato (PLAVELL &WOOWARD, 1970). Em plantas durante a germinação de sementes ricas em lipídios o CG possibilita a conversão de acetil-CoA, produzido pela β- oxidação de ácidos graxos, em oxaloacetato, e subsequentemente em açúcar (SMITH, 2000).

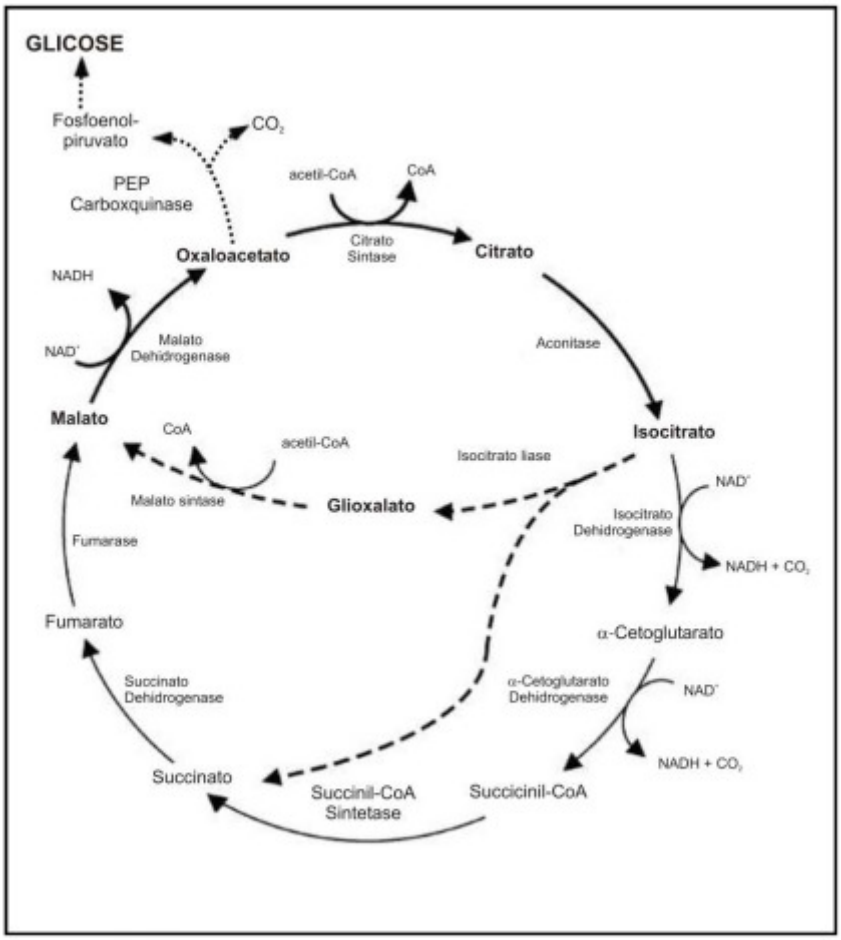

Figura 2. Esquema representativo do ciclo do ácido cítrico e glioxalato e gliconeogênese. São evidenciados os passos enzimáticos do TCA (linhas finas) comuns para todos os organismos, e o CG (linhas tracejadas) presente em microrganismos e plantas. Reações comuns entre os dois ciclos (linhas grossas) e a reação inicial da gliconeogênese (linhas sombreadas). Fonte: LORENZ & FINK, 2002.

A MLS é a enzima que catalisa a condensação da acetil-CoA e glioxalato com produção de malato, sendo uma reação altamente específica que requer Mg^{2+} como cofator (DIXON *et al*., 1960). A enzima também participa na degradação de purinas convertendo o glioxalato produzido a partir de ácido úrico, alantoína e ácido alantoico em malato (HARTIG *et al*., 1992). MLS localiza-se no citosol em leveduras com crescimento em etanol e nos peroxissomos, quando em crescimento com ácido oleico (KUNZE *et al*., 2002). A enzima apresenta-se em duas isoformas ou famílias A (MSA) e G (MSG), classificadas com base nas sequências de aminoácidos. A MSA ocorre em bactérias como *E. coli* (KORNBERG, 1966) e fungos, como *S. cerevisiae* (LORENZ & FINK, 2001), possuindo massa molecular em torno de 65 kDa. A MSG ocorre somente em bactérias e apresenta massa molecular em torno de 80 kDa (NAKAZAWA *et al*., 2005).

Zambuzzi-Carvalho e colaboradores (2009) caracterizaram a sequência codificante para a malato sintase de *Paracoccidioides* (*Pb*MLS), constituída por 539 resíduos de aminoácidos, com massa molecular de 60 kDa, pI de 8,45, apresentando assinatura característica da família das MLSs, resíduos catalíticos essenciais para a atividade enzimática, localização peroxissomal/glioxissomal e motivos reguladores na região de promotora do gene que poderiam indicar sua regulação por fontes de carbono e nitrogênio. Em *Paracoccidioides*, *Pb*MLS está associada à parede celular, sendo capaz de se ligar a componentes da matriz extracelular, como fibronectina e colágeno tipo I e IV mediando à aderência e internalização de células cultivadas *in vitro*, o que sugere o seu papel potencial no estabelecimento da infecção (NETO *et al*., 2009).

A isocitrato liase é presente em bactérias, arqueobactérias, fungos, plantas (NAKAZAWA *et al*., 2005; WANG *et al*., 2003; EBEL *et al*., 2006; e também em animais invertebrados e vertebrados (VAN EYK *et al*., 1993). A enzima apresenta massa molecular de 47 kDa em bactérias e 60 e 64 kDa em eucariotos (NAKAZAWA *et al*., 2005). Tanto a isocitrato desidrogenase (IDH) quanto a isocitrato liase utilizam o mesmo substrato o isocitrato, porém as enzimas fazem parte do TCA e GC respectivamente. Assim em *E. coli* crescida em meio com acetato, observou-se a divisão do fluxo de carbono em ambos os ciclos através da regulação da IDH por fosforilação reversível, possibilitando a utilização do isocitrato em diferentes condições, como variações de fontes de carbono (COZZONE, 1998).

A ICL possui um papel importante para a sobrevivência de patógenos no interior de macrófagos como *Mycobacterium tuberculosis, Cândida albicans* e bactérias gram-positivas (LORENZ & FINK, 2001; McKINNEY *et al*., 2000). Sua importância na virulência foi observada também em fungos patogênicos de plantas como *Magnaporthe grisea* e *Leptosphaeria maculans* nos quais verificou-se a presença do glicerol formado a partir de triglicérides no processo infeccioso, sendo este utilizado para produção de energia dependente da atividade da ICL (WANG *et al*., 2003). A deleção da ICL levou a uma forte atenuação da virulência atribuída as baixas concentrações de fontes preferenciais de carbono, com predomínio de ácidos graxos no local da infecção (IDNURM & HOWLETT, 2002).

Em *Aspergilus fumigatus* a ICL foi observada durante o crescimento em fontes não preferenciais de carbono como acetato, em conídios e hifas, sugerindo a utilização de lipídios durante a germinação e após a fagocitose por macrófagos (EBEL *et al*., 2006). Quanto ao mecanismo regulatório da ICL, verificou-se em *E. coli* sua ativação após

fosforilação, enquanto a desfosforilação leva à inativação da enzima. Em *S. cerevisiae* na presença de glicose a ICL foi inativada por fosforilação (LOPEZ-BOADO *et al*.,1988).

Em fungos patogênicos de plantas e insetos como *M. grisea, Colletotrichum lagenarium, Metarhizium anisopliae* e *Beauveria bassiana* observou-se a expressão da ICL aumentada durante a infecção e penetração da cutícula do hospedeiro (WANG *et al*., 2003; ASAKURA *et al*., 2006; PADILLA-GUERRERO *et al*., 2011). Verificou-se também o atraso na formação do apressório, conidiogênese e penetração da cutícula resultando em desenvolvimento reduzido da doença em cepas mutantes para a ICL (IDNURM & HOWLETT, 2002; WANG *et al*., 2003).

Em *P. lutzii*, a ICL apresenta homologia com as sequencias de outros fungos e massa molecular de 60 kDa. A enzima é induzida por acetato de potássio, ácido glicólico, etanol e reprimida em glicose após 24 horas de crescimento. A presença de proteínas com diferentes valores de p*I*s nas análises de *Western blot* sugerem regulação pós-traducional em nível de fosforilação (CRUZ *et al*., 2011).

Microrganismos conseguem utilizar fontes de carbono como lipídios, ácidos graxos, acetato e ativar vias para metabolizar esses compostos e obter energia (LORENZ & FINK, 2002). Durante a infecção fúngica ocorre a fagocitose pelos macrófagos como mecanismo de defesa do hospedeiro na tentativa de eliminar o patógeno. No fagolissosomo então formado tem se um ambiente de privação de nutrientes, como a glicose desta forma, torna-se fundamental a necessidade de reorganização metabólica do patógeno para a utilização de fontes de carbono não preferenciais como acetato, etanol, lipídios entre outros (SELITRENNIKOFF & NAKATA, 2003). Assim, para a utilização destes compostos com dois carbonos é requerido o ciclo do glioxalato (CG) ausente em mamíferos (NAKATA & SELITRENNIKOFF, 2002).

Desta forma, a importância do CG em situações de privação de nutrientes tem sido observada em microrganismos como *S. cerevisiae*, sob fagocitose com a indução da enzima frutose-1,6-bifosfatase (FBP1), apontando o papel do GC para a produção de glicose no interior do macrófago, cujo ambiente é restrito em glicose (LORENZ & FINK 2001). Em *C. albicans* a fagocitose promoveu a indução de enzimas do ciclo do glioxalato, reforçando a importância da aquisição de fontes de carbono não preferenciais por essas células e a função do GC na síntese de glicose (LORENZ & FINK, 2001).

O CG possui um papel importante na gliconeogênese, pois possibilita a produção de oxaloacetato, o qual ao ser convertido em fosfoenolpiruvato pela enzima

fosfoenolpiruvato carboxicinase (PEP carboxicinase) é direcionado para a síntese de glicose (KORNBERG & MADSEN, 1957) onde as enzimas PEP carboxicinase e frutose-1,6-bifosfatase atuam como regulatórias na gliconeogênese. O GC também contribui para a sobrevivência do patógeno no interior do macrófago que se apresenta pobre em compostos carbônicos complexos e rico em ácidos graxos e seus produtos de degradação como acetil-CoA, consistindo em única via para síntese de glicose (COZZONE, 1998).

Estudos tem evidenciado o papel importante do ciclo do glioxalato na patogenicidade e virulência de patógenos humanos como *A. fumigatus* (OLIVAS *et al*., 2007), *C. albicans* (LORENZ &, FINK, 2001, 2002) e *M. tuberculosis* (McKINNEY *et al*.,2000; MUÑOZ-ELÍAS & McKINNEY, 2005). Em fungos patogênicos de plantas e insetos como o *M. grisea, C. lagenarium, Metarhizium ansiopliae* e *Beauveria bassiana* houve um aumento na expressão da ICL durante a infecção e a penetração da cutícula do hospedeiro (WANG *et al*., 2003; ASAKURA *et al*.,2006; PADILLA-GUERRERO *et al*., 2011). Em *P. lutzii* também houve regulação positiva dos transcritos da *icl* (FELIPE *et al*., 2005) e *mls* (NUNES *et al*., 2005) em células leveduriformes durante a transição de micélio para levedura (BASTOS *et al*., 2007) e no processo infeccioso (COSTA *et al*., 2007). Desta forma, o ciclo do glioxalato constitui uma via metabólica importante na assimilação de fontes de carbono não preferenciais como observado em *C. albicans, Aspergillus* spp. e *M. tuberculosis* (LORENZ & FINK, 2002; DUNN *et al*., 2009; FLECK *et al*., 2011) e também na patogenicidade de fungos (PRICE *et al*., 2011; VYLKOVA *et al*., 2011).

Desta forma, o GC é uma via metabólica que desempenha um importante papel na relação patógeno-hospedeiro, permitindo a síntese de glicose a partir de fontes não preferenciais de carbono e cujo conhecimento contribuirá também no desenvolvimento de inibidores das enzimas ICL e MLS ausentes em mamíferos (DUNN *et al*., 2009).

1.5. Assimilação de fontes não preferenciais de carbono

Os seres vivos bem como os microrganismos estão sujeitos a inúmeras variações em seu ambiente como tensão de oxigênio, temperatura, pH, disponibilidade de nutrientes entre outros. Assim, para sobreviver e crescer os microrganismos desenvolveram mecanismos de resposta adaptativa coordenada e circuitos de regulação para ajustar sua fisiologia e manter a homeostase (GERSTMEIR *et al*., 2003). Desta forma são favorecidos aqueles que conseguem se adaptar as mudanças ocorridas no ambiente, reorganizando seu metabolismo para a utilização de diversas fontes de carbono.

Na relação patógeno-hospedeiro, ambos utilizam mecanismos complexos na busca de estratégias onde o hospedeiro tenta eliminar o patógeno através de mecanismos de defesa e o patógeno tenta evadir para sobreviver e crescer. Em infecções sistêmicas o patógeno alcança os mais diversos tecidos e órgãos como fígado com reserva de glicogênio e a corrente sanguínea rica em grandes quantidades de nutrientes como glicose, proteínas, aminoácidos e vitaminas (FLECK *et al*., 2011). Assim, o sucesso na infecção requer do patógeno uma adaptação rápida às diferentes condições microambientais (BROCK, 2009) para garantir sua nutrição (ASKEW, 2009) utilizando os nutrientes disponíveis nos tecidos do hospedeiro. Bactérias e fungos apresentam mecanismos de invasão celular considerados de importância fundamental para o início da infecção (FILLER & SHEPPARD, 2006).

A concentração de glicose na corrente sanguínea varia de 4,5 a 5 mM (EGI *et al.*, 2008). Contudo, outras fontes não preferenciais como lipídios, proteínas, acetato entre outros, podem estar presentes no local da infecção e serem utilizados pelos patógenos (BROCK, 2009). A maioria dos microrganismos possui a capacidade de remodelar o metabolismo conforme a disponibilidade de nutrientes utilizando uma variedade de compostos como fontes de carbono, nitrogênio, fósforo e enxofre (LORENZ, 2013). Fontes alternativas ou não preferenciais de carbono como etanol, aminoácidos, ácidos graxos, acetato, as quais podem ser metabolizadas em microrganismos principalmente por três vias: ciclo do glioxalato, gliconeogênese e beta oxidação, vias que são importantes para produção de energia, reposição anaplerótica dos intermediários do TCA e produção de glicose como observado em *C. albicans* (LORENZ *et al*., 2004) (Figura 3).

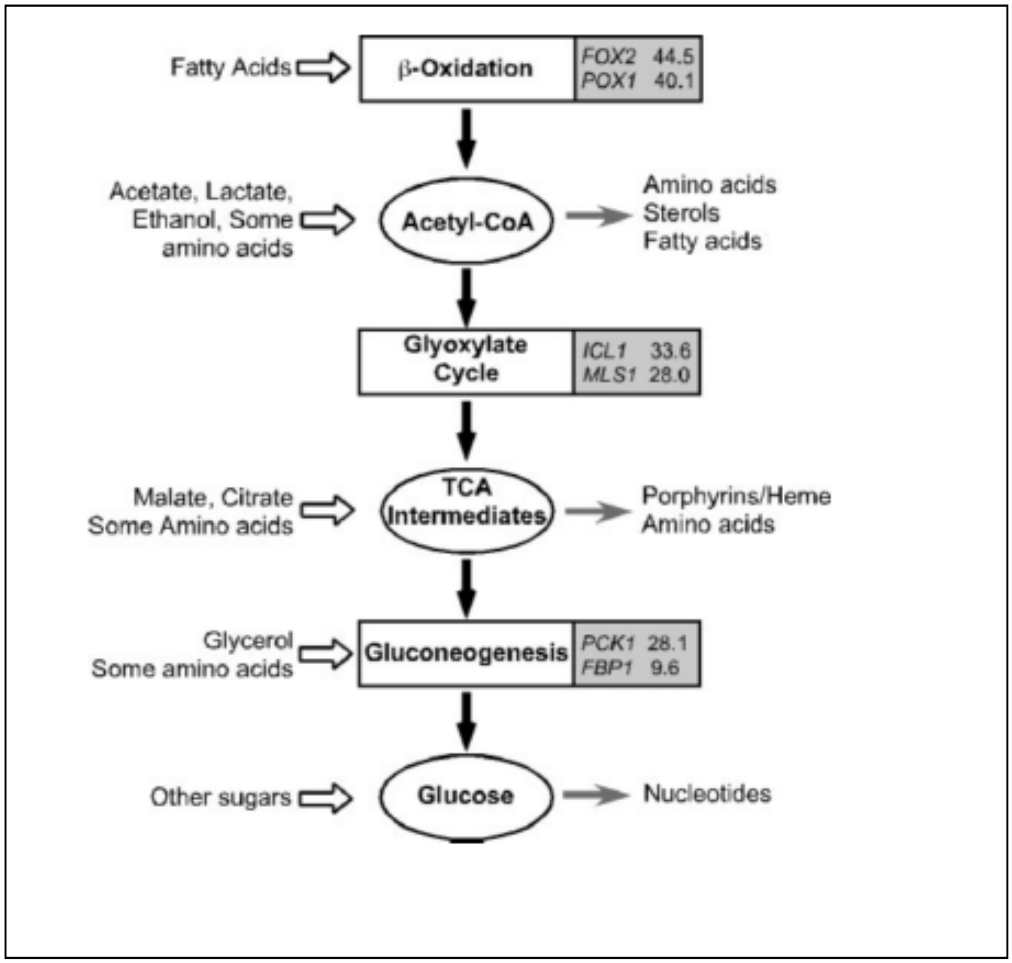

Figura 3. Metabolismo central na ausência de glicose em microrganismos. As vias bioquímicas são mostradas nos retângulos com a indução de genes importantes após fagocitose. Em oval estão representados os intermediários críticos. Entrada de substâncias está à esquerda (setas abertas) e os produtos do catabolismo indicados à direita (setas cinzas). Fonte: LORENZ *et al*., 2004.

O acetato é uma importante fonte de acetil-CoA e uma molécula central no metabolismo de substratos de carbono. É utilizado em procariotos, eucariotos (YAMASHITA *et al*., 2002) podendo ser encontrado no solo (CONRAD & KLOSE, 1999). Para entrar no metabolismo central deve ser primeiramente ativado a acetil-CoA, um metabólito intermediário chave utilizado em vias anabólicas e catabólicas, conforme as necessidades do organismo. Acetil-CoA também pode ser produzida a partir da oxidação de ácidos graxos, glicose e aminoácidos (SHIMAZU *et al*., 2010). Procariotos, ao utilizarem o etanol como fonte de energia promovem a sua conversão em acetato e a seguir, a ativação em acetil-CoA (CHAKIR *et al*., 1993) enquanto alguns microrganismos utilizam acetato diretamente como fonte de carbono (KORNBERG, 1966). Microrganismos em condições onde há uma redução na produção do piruvato pela glicólise utilizam o acetato através do ciclo do glioxalato, com a produção de malato e

succinato (LORENZ & FINK. 2002; DUNN *et al*., 2009; FLECK *et al*., 2011). Protozoários como a *Entamoeba histolitica* e bactérias, em condições de privação de glicose utilizaram fontes alternativas de carbono onde acetil-CoA é convertido em acetaldeído e reduzido a etanol na via piruvato-etanol (TOVY*et al*., 2011).

O acetato desempenha também um papel central na manutenção da homeostase energética em eucariotos superiores como mamíferos (SHIMAZU *et al*., 2010), como ilustrado na Figura 4. A interconversão de acetil-CoA em acetato é catalisada por duas classes de enzimas acetil-CoA hidrolases que catalisam a hidrólise de acetil-CoA gerando acetato, enquanto acetil-CoA sintetases (ACS em bactérias e leveduras e AceCS em mamíferos) sintetizam acetil-CoA a partir do acetato, ATP e CoA (STARAI & ESCALANTE-SEMERENA, 2004) essas enzimas são conservadas de bactérias a humanos (WOLFE, 2005).

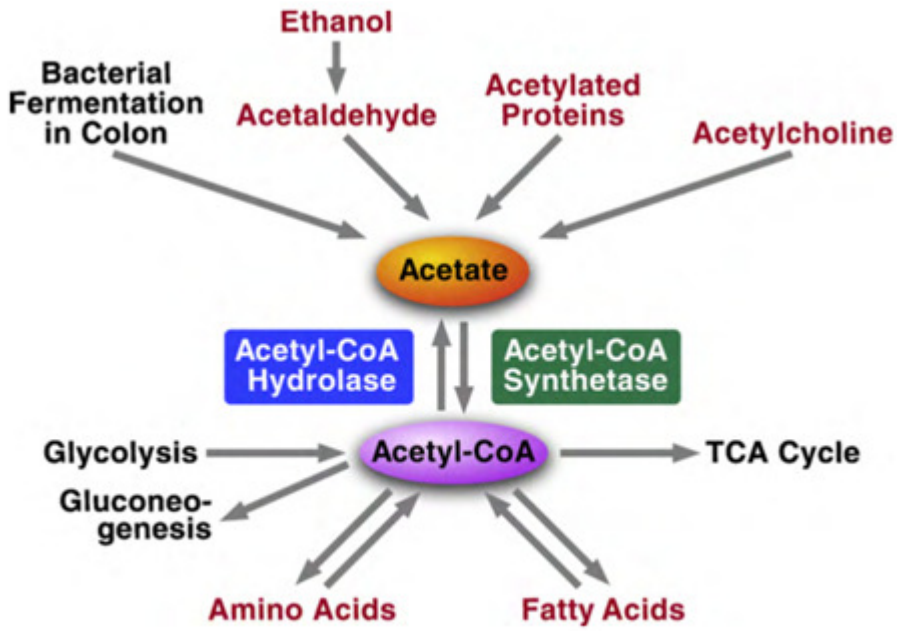

Figura 4. Regulação do metabolismo do acetato em tecidos de mamíferos. A interconversão em acetil-CoA é regulada pela atividade de competição da acetil-Coa hidrolase e acetil-CoA sintase. As múltiplas origens do acetato e acetil-CoA dentro do organismo mamífero são mostradas. Fonte: SHIMAZU *et al*., 2010.

Em *Salmomella entérica* a atividade da ACS é regulada pós- traducionalmente, pela acetilação no resíduo de lisina-509 inativando-a e a desacetilação pela CobB um

ortólogo bacteriano das desacetilases Sir2 em levedura e das sirtuínas em mamíferos (STARAI et al., 2002; STARAI & ESCALANTE-SEMERENA, 2004) ativando-a, possibilitando o crescimento em acetato e propionato (STARAI *et al*., 2002, 2003). Em eucariotos há duas isoformas da ACS localizadas no citosol e mitocôndria, controlando a ativação do acetato a acetil-CoA para ser utilizado em processos anabólicos como biossíntese de ácidos graxos e geração de energia no TCA, respectivamente (KISPAL *et al*., 1991; WOODNUTT & PARKER, 1986; DE VIRGILIO *et al*., 1992; VAN DEN BERG & STEENSMA, 1995; IKEDA *et al*., 2001; LOIKKANEN *et al*., 2002; YAMASHITA *et al*., 2002). Em *S. cereviseae* as duas isoformas estão presentes, sendo importantes na regulação metabólica; ACS1 mitocondrial necessária para o crescimento em condições de gliconeogênese enquanto a ACS2 citosólica promove o crescimento anaeróbio em glicose (KLEIN & JAHNKE, 1979; VAN DEN BERG & STEENSMA, 1995). Isolados duplos mutantes ACS1/ACS2 de *S. cerevisiae* apresentaram não viáveis, sugerindo que outras fontes de acetil-CoA (piruvato) não compensam a falta de ACS (DE VIRGILIO *et al*., 1992; VAN DEN BERG & STEENSMA, 1995).

Durante o brotamento, S. *cerevisae* e outros microrganismos utilizam glicose como fonte de carbono, através da via glicolítica, entretanto fontes alternativas de carbono como sacarose, maltose, galactose, etanol, glicerol, acetato, lactato são assimiladas em ambientes com privação de carbono, para geração de energia e biomassa celular, demonstrando a necessidade de regulação metabólica para assimilação de carbono (TURCOTTE *et al*., 2010). A mudança de uma fonte de carbono para outra é designada de crescimento diauxico onde há a exaustão da fonte preferencial, redução no crescimento e readaptação metabólica, que ocorre, por exemplo, na mudança do metabolismo fermentativo para não fermentativo em leveduras com consequente regulação de genes relacionados a vias metabólicas como metabolismo do carbono, síntese proteica e estocagem de carboidratos (DE RISI *et al*., 1997).

Desta forma, *S. cerevisiae* utiliza glicerol como fonte de carbono e para a osmoregulação (HOHMANN, 2002) sendo a conversão em glicerol-3-fosfato e diidroxiacetona fosfato direcionada à glicólise ou gliconeogênese (TURCOTTE *et al*., 2010). Nas células *Saccharomyces cerevisiae* o lactato é assimilado através da permease JEN 1 (CASAL *et al*., 2008) cuja expressão é induzida em lactato e reprimida em glicose (LODI & FERRERO, 1999). Enzimas da gliconeogênese como frutose-1,6-bifosfatase (FBP1), malato desidrogenase (MLD1) e fosfoenolpiruvato carboxicinase (PCK1) são degradadas em cepas de *Saccharomyces cerevisiae* oriundas do Euroscarf (European

Saccharomyces cerevisiae Archive for Functional Analysis) na presença de glicose (HUNG *et al*., 2004; SANTT *et al*., 2008), e a ativação de PCK1 pelo complexo NuA4 acetiltransferase é essencial para o crescimento de leveduras em fonte de carbono não fermentáveis (LIN *et al*., 2009). Na presença de ácido oleico como fonte de carbono ocorre a regulação positiva de genes codificantes de enzimas para β-oxidação e proteínas envolvidas no aumento dos peroxissomos em *Saccharomyces cerevisiae (*HILTUNEN *et al*., 2003; GURVITZ & ROTTENSTEINER, 2006a).

A capacidade de utilizar fontes alternativas de carbono possibilita a muitos patógenos superar a restrição de nutrientes que pode ser encontrada no hospedeiro durante a infecção. Portanto, a capacidade de adaptação metabólica e ao estresse em vários ambientes no hospedeiro tem um papel importante na virulência em fungos (BARELLE *et al*., 2006; FLECK *et al*., 2011; FRADIN *et al*., 2005). Os pulmões consistem em um nicho para o patógeno com limitação de nutrientes, pois não há contato direto com nutrientes ingeridos da dieta (TRAVIS *et al*., 1999) e microrganismos inalados são rapidamente fagocitados por macrófagos, neutrófilos e células dendriticas (IBRAHIM-GRANET *et al*., 2010). *C. albicans* pode encontrar no hospedeiro ambiente pobre em carbono durante o crescimento e a capacidade de utilizar múltiplas fontes de carbono não fermentáveis pode determinar a virulência (RAMÍREZ & LORENZ, 2007).

Atenuação da virulência foi observada em *C. albicans* na ausência de enzimas chaves para assimilação de carbono como ICL e frutose 1,6- bifosfatase (FBP1) do ciclo do glioxalato e gliconeogênese respectivamente (BARELLE *et al*., 2006; RAMÍREZ & LORENZ, 2007). O metabolismo do carbono foi avaliado em cepas mutantes de *C. albicans* para os genes FBP1 (fructose-1,6-bisphosphatase). FOX2 (β-oxidation multifunctional protein) e ICL1 (isocitrate lyase) pra gliconeogênese, oxidação de ácidos graxos e ciclo do glioxalato respectivamente, nas fontes de carbono glicose. glicerol, etanol, acetato e ácido cítrico, onde os mutantes para FOX2 não conseguiram crescer na presença de ácidos graxos etanol e ácido cítrico e mutantes para ICL tiveram maior comprometimento na utilização de carbono (LORENZ, 2013). *M. tuberculosis* ativa vias metabólicas para assimilação de carbono dentro de macrófagos e mutações nessas vias atenuam a virulência (HÖNER ZU *et al*., 1999; McKINNEY *et al*., 2000; MUÑOZ-ELÍAS & McKINNEY, 2005).

Condições de privação de nutrientes são observadas em macrófagos com redução de glicose e aminoácidos (BARELLE *et al*., 2006; LORENZ *et al*., 2004) e utilização de fontes de carbono disponíveis no interior destas células foram observados em *C. albicans*

e *C. neoformans* (LORENZ *et al*., 2004; COONEY & KLEIN, 2008; FAN *et al*., 2005). Macrófagos e neutrófilos fagocitam patógenos com formação de um ambiente hostil no fagolissosomo com pH ácido, limitação de nutrientes e estresse oxidativo (FERNÁNDEZ-ARENAS *et al*., 2007; FROHNER *et al*., 2009). Em *C. albicans* observou-se que para sobreviver e propagar o patógeno necessita de estratégias para sobreviver e escapar do fagócito como elongação rápida da hifa criando uma força mecânica para romper a membrana celular e escapar, invadir e crescer em outros tecidos (LORENZ *et al*., 2004). Contudo, crescimento e elongação de hifas consome energia, portanto sem nutrição o estabelecimento da infecção será prejudicada (FLECK *et al*., 2011).

A complexidade das interações que ocorrem em *C. albicans* e fagócitos foi confirmada através do estudo do perfil de expressão gênica com a regulação diferencial de mais de 500 genes durante a fagocitose por macrófagos e neutrófilos (FRADIN *et al*., 2005; LORENZ *et al*., 2004; RUBIN-BEJERANO *et al*., 2003). Verificou-se regulação metabólica em *C. albicans* fagocitadas por macrófagos, semelhantes ao ambiente com privação de nutrientes com inibição da glicólise e ativação de vias que permitem a assimilação de fontes alternativas de carbono como ciclo do glioxalato, gliconeogênese e beta oxidação (PRIGNEAU *et al*., 2003). A regulação destas vias possibilita ao patógeno a conversão de lipídios a acetato e glicose para seu crescimento e sobrevivência (LORENZ *et al*., 2004). Também genes para o ciclo do glioxalato apresentaram-se induzidos em *C. albicans* e *S. cerevisae* fagocitados por macrófagos (LORENZ & FINK, 2001).

Em micoses sistêmicas como na PCM, para o estabelecimento e a progressão da doença em hospedeiros susceptíveis, torna-se importante a sobrevivência do patógeno no interior dos macrófagos, possibilitando a latência do fungo e/ou disseminação para outros tecidos (FELDMESSER *et al*., 2000; FRANCO, 1987). Assim os macrófagos constituem um mecanismo de defesa importante na infecção por *P. brasiliensis* (BRUMMER *et al*., 1988a; 1988b).Tavares e colaboradores (2007) observaram após a fagocitose de *P. brasiliensis* em macrófagos murinos durante 6h, a repressão do transcrito da fosfofrutoquinase-1 indicando a repressão da via glicolítica e aumento de transcritos relacionados ao estresse oxidativo, síntese de metionina e da parede celular. Desta forma a capacidade de metabolizar fontes alternativas de carbono em ambientes com limitação nutricional no hospedeiro tem um papel importante na sobrevivência e virulência de

Paracoccidioides spp. (DERENGOWSKI *et al*., 2008; TAVARES *et al*., 2007), *C. albicans* e *C. neoformans* (LORENZ *et al*., 2004; FAN *et al*., 2005).

Em leveduras de *P. brasiliensis* recuperadas do fígado de camundongos infectados foi observado a utilização de múltiplas fontes de carbono durante a infecção e o aumento na expressão de genes codificantes para enzimas, reguladores e transportadores de carboidratos, lipídios e produção de etanol (COSTA *et al*., 2007). Em leveduras de *P. lutzzi,* em fontes de carbono não preferenciais como acetato, etanol e ácido glicólico, verificou-se a produção de malato pelo ciclo do glioxalato e a regulação da PbMLS a nível transcricional (ZAMBUZZI-CARVALHO *et al*., 2009).

Edwards e colaboradores (2013), utilizando dois isolados de *Histoplasma* pertencentes a diferentes espécies filogenéticas verificaram que ambos dependem de diferentes mecanismos para sobreviver no hospedeiro como a evasão do fagócito ou mecanismos de defesa aumentados como elevação nos níveis de transcritos de genes de defesa ao estresse oxidativo. Em *Paracoccidioides* spp. isolados de espécies filogenéticas de *P. lutzii* e *P. brasiliensis* após infectar humanos podem variar a virulência e induzir diferentes respostas imune no hospedeiro (SCORZONI *et al.,* 2015).

Análise metabólica comparativa do proteoma de membros das quatro linhagens filogenéticas do gênero *Paracoccidioides*, na presença de glicose mostrou diferenças bioquímicas e aspectos metabólicos diferenciais entre as linhagens (PIGOSSO *et al.*, 2013). Assim as vias metabólicas preferenciais entre os isolados foram assim caracterizadas: *Pb*339 (S1) utilizou preferencialmente a via de oxidação de ácidos graxos importante para fornecer acetil-CoA para o metabolismo central de carbono deste grupo filogenético; em *Pb*02 (PS2) predominou a via das pentoses-fosfato e a degradação de aminoácidos; *Pb*Epm83 (PS3), utilizou preferencialmente carboidratos em rotas aeróbicas de produção de energia; *P. lutzii* utilizou a glicólise e fermentação alcoólica para produção de energia e resposta ao estresse oxidativo. A melhor resposta a espécies reativas de oxigênio foi observada em *Pb*02 e *Pb*339, enquanto proteínas antigênicas de 27 kDa e gp43 foram menos abundantes em *Pb*02 e *P. lutzii*, indicando diferenças metabólicas entre os membros analisados. Portanto avaliar as diferenças metabólicas, em acetato de sódio como fonte de carbono, entre as espécies filogenéticas de membros do gênero *Paracoccidioides* pode contribuir no conhecimento da biologia do patógeno, bem como, essas adaptações podem contribuir para o entendimento da sobrevivência ao ambiente hostil encontrado no hospedeiro.

2 Justificativa

2. JUSTIFICATIVA

A assimilação de diferentes fontes de carbono pelos microrganismos é fundamental para sua sobrevivência, replicação e persistência, tanto no meio ambiente quanto no hospedeiro. Patógenos enfrentam mudanças drásticas no hospedeiro como diferenças de temperatura, pH, tensão de oxigênio, privação de nutrientes, espécies reativas de oxigênio, nitrogênio e cloro para impedir o seu crescimento. Assim, o sucesso na infecção requer uma adaptação rápida para garantir nutrientes e consequentemente a sobrevivência nos tecidos do hospedeiro.

A utilização de fontes alternativas de carbono possibilita a muitos patógenos superar a restrição de nutrientes que pode ser encontrada no hospedeiro durante a infecção. Macrófagos e neutrófilos fagocitam patógenos com formação de um ambiente hostil no fagolissosomo com pH ácido, limitação de nutrientes e estresse oxidativo assim para sobrevivência e propagação do patógeno torna-se importante a reorganização metabólica. O acetato é uma fonte de dois carbonos utilizado em procariotos, eucariotos e importante fonte de acetil-CoA uma molécula central no metabolismo de substratos de carbono. Em condições de privação de glicose microrganismos podem utilizar o acetato através do ciclo do glioxalato para produção de energia e precursores biossintéticos. Desta forma, o ciclo do glioxalato possui um papel importante na patogenicidade e virulência de fungos patógenos humanos.

A adaptação metabólica e ao estresse em vários ambientes do hospedeiro tem um papel importante na virulência em fungos. Estudos sugerem variações na virulência e indução de diferentes respostas imune em isolados membros de espécies filogenéticas de *P. lutzii* e *P. brasiliensis* após infecção em humanos. Análise metabólica comparativa do proteoma de membros das quatro linhagens filogenéticas do gênero *Paracoccidioides*, na presença de glicose mostrou diferenças bioquímicas e aspectos metabólicos diferenciais entre as linhagens. Portanto compreender o papel das vias metabólicas utilizadas por isolados de diferentes espécies filogenéticas de *P. brasiliensis* e *P. lutzii* em fontes não preferenciais de carbono como o acetato de sódio torna-se importante visto que a assimilação de carbono tem um papel importante no estabelecimento da infecção e contribui para avaliar possíveis diferenças metabólicas entre membros de espécies filogenéticas do gênero *Paracoccidioides.*

3 Objetivos

3. OBJETIVOS

3.1. OBJETIVO GERAL

Analisar o proteoma de membros do gênero *Paracoccidioides* isolados *Pb*339, *Pb*03, *Pb*EPM83 e *P. lutzii* em fase leveduriforme na presença de acetato de sódio comparativamente com a glicose como fontes de carbono para verificar possíveis alterações no perfil metabólico.

3.2.OBJETIVOS ESPECIFICOS

- Comparar o crescimento dos isolados de *P. brasiliensis* e *P. lutzii* na presença de diferentes fontes de carbono como glicose e acetato de sódio, utilizando o peso seco celular.
- Proceder a análise proteômica comparativa dos diferentes isolados de *Paracoccidioides* spp. cultivados na presença de glicose e acetato de sódio;
- Comparar e interpretar aspectos metabólicos diferenciais entre as linhagens de *P. brasilensis* e *P. lutzii* na presença de acetato como fonte de carbono.

Capítulo 2

Manuscrito

Frontiers: Manuscript Submitted

Frontiers Microbiology Editorial Office <microbiology.editorial.office@frontiersin.org>
Para
frbdamata@yahoo.com.br
Ago 9 em 7:39 PM

Dear Dr da Mata,

We are pleased to inform you that we have received the manuscript below, which will be considered for publication in Frontiers in Microbiology, section Fungi and Their Interactions.

Title: "TWO-CARBON METABOLISM ACROSS MEMBERS OF THE Paracoccidioides GENUS"
Article type: Original Research
Submitted By: Célia Maria de Almeida Soares
Submitted On: 09 Aug 2017

You can access the review forum and track the progress of your manuscript by registering a Frontiers account following this link:
http://www.frontiersin.org/Registration/Register.aspx?invitationnumber=319c3b98-8cb5-4c4e-9126-ace0cde0d1a0

If you have already created a Frontiers account using a different email address, please add this one as a secondary email to your Frontiers profile following this link:

http://loop.frontiersin.org/settings/email

You can contact support@frontiersin.org for any questions on the above.

Best regards,

Your Frontiers in Microbiology team

Frontiers | Editorial Office - Collaborative Peer Review Team
www.frontiersin.org
EPFL Innovation Square, Building I, Lausanne, Switzerland
Office T 41 21 510 17 25

For technical issues, please contact our IT Helpdesk (support@frontiersin.org) or visit our Frontiers Help Center (zendesk.frontiersin.org/hc/en-us)

TWO-CARBON METABOLISM ACROSS MEMBERS OF THE *Paracoccidioides* GENUS

Fabiana Ribeiro da Mata[a#],Lilian Cristiane Baeza[a#], Laurine Lacerda Pigosso[a#], Maristela Pereira[a], Gustavo Henrique Martins Ferreira de Souza[b], Alexandre Siqueira Guedes Coelho[c], Célia Maria de Almeida Soares[a*]

[#]Equal contributors

[a]Laboratório de Biologia Molecular, Instituto de Ciências Biológicas, Universidade Federal de Goiás, Goiânia, GO, Brazil

[b]Mass Spectrometry Applications Research & Development Laboratory, Waters Corporation, São Paulo, SP, Brazil

[c]Laboratório de Genética e Genômica de Plantas, Escola de Agronomia, Universidade Federal de Goiás, Goiânia, GO, Brazil.

*Corresponding author

Celia Maria de Almeida Soares

Laboratório de Biologia Molecular

Instituto de Ciências Biológicas

Universidade Federal de Goiás

70690-900-Goiânia-Goiás-Brazil

e-mail: cmasoares@gmail.com

ABSTRACT

Members of the genus *Paracoccidioides* are known pathogens of humans that can be isolated from different infection sites. To investigate the expression rates of proteins expressed by different isolates, of the genus *Paracoccidioides*, including one isolate of *P. lutzii* (*Pb*01), and three isolates of *P. brasiliensis* (*Pb*03, *Pb*339 and *Pb*EPM83) using sodium acetate, as carbon source, proteins quantities were determined using label-free and data independent LC-MS^E. Statistical analysis provided the comparison of proteins profiles in the isolates. A total of 1160, 1211, 1280 and 1462 proteins were reproducibly identified, and relatively quantified in *P. lutzii* e *P. brasiliensis* isolates *Pb*03, *Pb*339 e *Pb*EPM83, respectively. Notably, a total of 526, 435, 744 and 747 proteins were differentially expressed among *P. lutzii* and the *P. brasiliensis* isolates *Pb*03, *Pb*339 and *Pb*EPM*83*, respectively with a fold change equal or higher than 1.5. The analysis revealed the reorganization of metabolism through the induction of proteins related to gluconeogenesis, stress response and amino acid degradation in the four isolates evaluated. The differences between the isolates were observed as follows: greater increases in the expression levels of proteins belonging to the cycle of glyoxalate, TCA and respiratory chain, ethanol production and β-oxidation were observed in the isolatesPPEPM83 and Pb01; Cyclic and cyclocyclic proteins of the methylcitrate were induced in Pb339. Proteomic profiles indicate that the four isolates reorganize the metabolism for the use of acetate as a carbon source.

Key words: *Paracoccidioides* spp.; proteomic; two-carbon source, sodium acetate, metabolism.

1. INTRODUCTION

The *Paracoccidioides* genus includes fungal pathogens causing paracoccidioidomycosis, a disease geographically restricted to subtropical areas of Latin America (San-Blas et al., 2002). About 80% of the cases reported of paracoccidioidomycosis occurred in Brazil, followed by Colombia, Venezuela and Argentina (Martinez, 2015). Members of this genus are thermally dimorphic fungi that grow in a hyphal form in the environment, but exist as budding yeast in mammalian hosts. The infection is initiated by inhalation of fungal propagules, which after reaching the alveolar epithelium differentiate into the yeast form (Restrepo et al., 2001).

Multilocus sequencing typing (MLST) allowed, at first, the proposal of four cryptic studies in the genus *Paracoccidioides*, as following: S1, PS2 and PS3 in the *P. brasiliensis* complex and *P. lutzii*, the last a single monophyletic population (Matute et al., 2006a; Teixeira et al., 2009). Additionally, a new lineage PS4 was proposed, belonging to a region of Venezuela (Teixeira et al., 2014). Recently, the S1 group was divided into lineages S1a and S1b. Analysis of the dating time of the separation of the lineages above, indicated that S1b was the earliest diverging lineage of *P. brasiliensis* (Munõz et al., 2016).

There is a plenty of information on genomes in the genus *Paracoccidioides*. Analysis demonstrated a reduced number of genes involved in the metabolism of carbohydrates and proteins, as well as in the synthesis of secondary metabolites (Desjardins et al., 2011; Munõz et al., 2014). Additionally, genomes of 31 isolates representing the lineages S1, PS2, PS3 and PS4 were sequenced and provided new reference genomes for two lineages from PS3 and PS4 (Munõz et al., 2016). In this way, further functional analysis can provide more data at the fungus biology.

To grow, a pathogen has to assimilate carbon and must have a metabolic flexibility in order to assimilate available nutrients in different niches of the host. Data from transcriptional and proteomic profiles are consistent with this assumption. In this way, it has been shown that *Candida albicans* demands isocitrate lyase (ICL), a key enzyme of the glyoxylate cycle for virulence (Lorenz and Fink, 2001). Due to the fact that ICL is repressed by glucose, its expression in the host is restricted to the nutrient-limited environment of the phagosome of immune cells (Barelle et al., 2006). Members of the *Paracoccidioides* genus regulate genes upon different carbon sources. Upon carbon starvation, *P. lutzii* yeast cells shift the metabolism to gluconeogenesis and ethanol production, supported by the degradation of amino acids and fatty acids and by the modulation of glyoxylate and tricarboxylic cycles (Lima et al., 2014). During macrophage infection, *P. brasiliensis* regulates positively proteins involved in alternative carbon metabolism, such as those related to gluconeogenesis, beta oxidation and amino acids catabolism (Parente-Rocha et al., 2015). At the initial stages of lung infection, *P. brasiliensis* alters the expression of genes related to several functional categories including energy metabolism and cell wall metabolism. *P. brasiliensis* remodels cellular lipid metabolism to catabolize its own lipid stores via beta oxidation, glyoxylate cycle, which were strongly induced during the first 6 hours of lung infection (Pigosso et al., 2017).

Proteomic characterization of members in the *Paracoccidioides* genus was performed using 2D electrophoresis and mass spectrometry. Comparing the protein expression profiles from yeast cells growing in glucose as carbon source, depicted different metabolic aspects among members of four phylogenetic species (Pigosso et al., 2013). In this way, it was proposed that *P. lutzii* used more preferentially anaerobic pathways for energy production; *P. lutzii* and *P. brasiliensis* (*Pb*2 and *Pb*339) presented

100 a better response to ROS compared to *Pb*EPM83 and *Pb*2 presented a higher abundance
101 of enzymes from the pentose phosphate pathway compared to the others. Also, antigenic
102 proteins were differentially accumulated (Pigosso et al., 2013). Comparative proteomic
103 analyses were confirmed by biochemical assays (Pigosso et al., 2013). Additionally, the
104 hierarchical clustering of proteins reflects the phylogenetic relationships among the
105 studied *Paracoccidioides* species, where S1 is an independent species (*Pb*339), PS3
106 (*Pb*EPM83) is phylogenetically closer to S1 than PS2 (*Pb*2), and *P. lutzii* (*Pb*01) is highly
107 divergent from the other phylogenetic species (Matute et al., 2006a; Matute et al., 2006b;
108 Teixeira et al., 2009).

109 Macrophages are an important part of the innate immune system and constitute,
110 with neutrophils the front-line phagocytes that act to eliminate pathogens. During the
111 infection by members of the *Paracoccidioides* genus, alveolar macrophages constitute
112 one of the primary defense mechanisms (Brummer et al., 1988). It is generally believed
113 that the phagosome is a nutrient-poor environment (Haas, 2007), whose carbon sources
114 could be derived from the breakdown of fatty acids via Beta-oxidation, rendering acetyl-
115 CoA (Lorenz and Fink, 2002).

116 Metabolic peculiarities in members of the *Paracoccidioides* genus, as cited above,
117 led us to investigate their metabolism in the presence of acetate, a two-carbon component.
118 Acetate utilization requires the tricarboxilic acid (TCA) shunting through the glyoxylate
119 cycle, which allows the utilization of two-carbon sources. In this work, we used the
120 isolates *Pb*339 (ATCC 200273), *Pb*03, *Pb*EPM83 and *P. lutzii* (ATCC-MYA-826)
121 (Carrero et al., 2008; Teixeira et al., 2009) to investigate the metabolic aspects of the
122 utilization of two-carbon sources by those organisms.

123

124

2. MATERIAL AND METHODS

2.1. Strains and growth conditions

*Paracoccidioides brasiliensis Pb*339 (ATCC 200273), *Pb*03, *Pb*EPM83 (Matute *et al*., 2006a) and *P. lutzii* (ATCC-MYA-826) (Carrero et al., 2008; Teixeira et al., 2009) were used in this study. The fungus was maintained in brain heart infusion (BHI) medium, which was supplemented with 4% (w/v) glucose at 36ºC, to cultivate the yeast form. After three days in BHI liquid medium, at 36ºC with agitation at 150 rpm, yeast cells were washed twice with phosphate buffered saline solution 1X (1X PBS; 1.4 mM KH_2PO_4, 8 mM Na_2HPO_4, 140 mM NaCl, 2.7 mM KCl; pH 7.2) and inoculated in chemically defined McVeigh/Morton (MMcM) medium (Restrepo & Jiménez, 1980). The defined medium was added of glucose (100 mM) (control) or sodium acetate (100 mM) (test), as carbon sources and cells were grown for 48 h at 36ºC, with agitation at 150 rpm.

2.2. Isocitrate lyase activity

Following *Paracoccidioides Pb*01, *Pb*03, *Pb*339 and *Pb*EPM83 growth under the conditions of acetate and glucose (both 100 mM), the cells were centrifuged at 1,500 x g, resuspended in a solution containing 20 mM Tris-HCl, pH 8.8, 2 mM $CaCl_2$ (Fonseca et al., 2001) and disrupted using glass beads and bead beater apparatus (BioSpec, Oklahoma, USA) in 5 cycles of 30 sec, while on ice. The cell lysate was centrifuged at 10,000 x g for 15 min at 4°C and the supernatant was quantified using the Bradford reagent (Sigma-Aldrich) (Bradford, 1976). The amount of protein 50 µg was used to perform the dosage (Lima et al., 2014).

Isocitrate lyase activity was determined by measuring the formation of glyoxylate as its phenylhydrazone derivative (Ebel et al., 2006). Glyoxylate-phenylhydrazone formation

150 was determined by measuring the absorbance at 324 nm, using an extinction coeficient
151 of 16.8 mM^{-1} cm^{-1}, in a reaction mixture containing 2 mM threo-D,L-isocitrate (Sigma
152 Aldrich, Co.), 2 mM $MgCl_2$, 10mM phenylhydrazine HCl (Sigma Aldrich, Co.), 2 mM
153 dithiothreitol and 50 mM potassium phosphate at pH 7.0. Specific activity was
154 determined as the amount of enzyme required to form 1 µmol of glyoxylate-
155 phenylhydrazone per min per mg of total protein. Statistical comparisons were performed
156 using the Student's *t test* and *p*-values ≤ 0.05 were considered statistically significant.
157
158 **2.3.** *Paracoccidioides* spp. **cell dry weight assay**
159 *Paracoccidioides* spp. yeast cells were grown as described in the previous item. The
160 amount of 10^6 cells/50 mL was inoculated in the chemically defined MMcM medium
161 (Restrepo & Jiménez, 1980), containing the carbon sources, glucose or sodium acetate
162 and were incubated at 36ºC. In each time-point, aliquots of 10 ml of culture were
163 centrifuged at 1,500 x g and the supernatants were carefully removed. The cells were
164 ressuspended in 1X PBS up to 500 µL and subjected to the temperature of 95ºC, heating
165 for 1 h. The cells were centrifuged, frozen in liquid nitrogen and lyophilized for 24 h
166 (Lima et al., 2014). Data are expressed as the mean ± standard deviation of the triplicates
167 of independent experiments. Statistical comparisons were performed using Student's *t*
168 *test*, and *p* value ≤ 0.05 were considered significant.
169
170 **2.4. Obtaining protein extracts**
171 To obtain cytoplasmic protein extract, the cells were centrifuged at 10,000 x g for 5 min,
172 followed by washing in 1X PBS twice, and by the addition of Tris-Ca buffer (20 mM
173 Tris–HCl pH 8.8; 2 mM $CaCl_2$). This suspension was distributed in tubes containing glass
174 beads (425-600 µm) in equal volume of the cell pellet. The cells were disrupted by

vigorous mixing in bead beater apparatus (BioSpec, Oklahoma, USA) during 5 cycles of 30 sec, while on ice. The cell lysate was submitted to cycles of centrifugation at 10,000 x g for 15 min at 4°C, until no pellet formations was observed. The supernatant was quantified for protein concentration, using the Bradford reagent (Sigma-Aldrich, Co.) (Bradford, 1976), whit bovine serum albumin (BSA) as standard.

2.5. Protein digestion for nanoUPLC-MS^E analysis

Enzymatic digestion proteins was processed according to the (Murad et al., 2011) with some modifications. Briefly, approximately 150 µg of protein (previous item) was added to 10 µl of 50 mM ammonium bicarbonate pH 8.5, in a microcentrifuge tube. Then 75 µl of RapiGEST^{TM} SF Surfactante (0.2% v/v) (Waters Corporation) was added, and the sample was vortexed and incubated in a dry bath at 80ºC for 15 min. Following we performed the reduction of disulfide bonds with 2.5 µl of 100 mM dithiothreitol (DTT) (GE Healthcare) at 60 ºC for 30 min, and alkylation of cysteine with 2.5 µl of 300 mM iodocetamide (GE Healthcare) for 30 minutes at room temperature, in the dark. The proteins were subsequently digested with 30 µl of trypsin 0.05 µg/µl (Promega) at 37ºC in dry bath for 16 h. Trypsin digestion was stopped. To precipitate the RapiGEST, samples were acidified whit 30 µl of a 5% (v/v) trifluoracetic acid solution (Sigma-Aldrich, Co.) and the mixture was incubated for 90 min at 37ºC in a dry bath, followed by centrifugation at 18,000 x *g*, 4ºC for 30 min. The supernatants were dried in speed vaccum (Eppendorf). All obtained peptides were suspended in 80 µl of solution containing 20 mM of ammonium formiate and 80 fmol/µl of PHB (Rabbit Phosphorylase B) (Waters Corporation) (MassPREP^{TM} protein) as internal standard. Samples were transferred to a Waters Total Recovery vial (Waters Corporation). The samples were then placed in the auto-sampler and kept at 4 °C for the nanoUPLC-MS^E analysis.

2.6. Mass spectrometry

The mass spectrometric experiments were performed on a Synapt G2-Si HDMS (High Definition Mass Spectrometry) (Waters, Corporation) equipped with mass analyzers type a hybrid quadrupole/ion mobility mass spectrometry/orthogonal acceleration time-of-flight (Q-IMMS-*o*αTOF) MS geometry, and coupled to nanoAcquity^{TM} UPLC (Ultra Performance Liquid Chromatography) system (Waters, Corporation). The peptide mixture was loaded online for 5 min at a flow rate of 8 µl/min of phase A (0.1% formic acid) using a Symmetry C18 trapping column (5 µm particles, 180 µm × 20 mm length; Waters, Corporation). The mixture of trapped peptides was subsequently separated by elution with a gradient of 7–35% of phase B (0.1% formic acid in acetonitrile) through a BEH 130 C18 column (1.7 µm particles, 75 × 150 mm; Waters, Corporation) in 93 min, at 275 nl/min. Data were acquired in the in data-independent mode (UDMS^{E}) (Distler et al., 2014) in the m/z range of 50–1600 in resolution mode. Collision energies were alternated between 4 eV and a ramp of 17–60 eV for precursor ion and fragment ions, respectively, using scan times of 1.25 s. The nano electrospray ionization in the positive mode (nanoESI+) source was operated with a capillary voltage of 3.0 kV, block temperature of 70°C, and cone voltage of 50 V. For lock mass correction, [Glu1]-Fibrinopeptide B solution (500 fmol/mL in 50% acetonitrile, 0.1 formic acid; Waters, Corporation) was infused through the reference sprayer at 500 nl/min and sampled every 60 s (Abreu et al., 2017; Garrido et al., 2016). The peptides fractions were analyzed in triplicate.

223 **2.7. Data processing and protein identification**

224 Mass spectrometry raw data of peptide fractions were loaded in Progenesis QI for
225 Proteomics (Nonlinear Dynamics). A reference run for the triplicates was automatically
226 selected. Precursor ion retention times were processed for alignment, peak picking and
227 normalized to a reference run with default parameters. The MS data were processed by
228 the Apex3D module using low energy threshold of 150 counts, elevated energy threshold
229 of 30 counts and intensity threshold of 750 counts. The MS/MS spectra were exported as
230 a *.pkl file through ProteinLynx Global Server version 3.0.2 (PLGS) (Waters
231 Corporation) and processed spectra were search against the *Paracoccidioides* database
232 (http://www.broadinstitute.org/annotation/genome/paracoccidioides_brasiliensis/Multio
233 me.html) according to the isolate, together with reverse sequences: (i) *Pb*339 and
234 *Pb*EPM83 with *P. brasiliensis Pb*18 protein sequences; (ii) *Pb*03 with *P. brasiliensis*
235 (strain *Pb*03) protein sequences; (iii) *P. lutzii* (*Pb*01) protein sequences.

236 The mass error tolerance for peptide identification was under 10 ppm. Protein
237 identification criteria included: (i) the detection of at least 2 fragment ions per peptide,
238 (ii) 5 fragments per protein, (iii) the determination of at least 1 peptide per protein, (iv)
239 carbamidomethylation of cysteine as a fixed modification, (v) phosphorylation of serine,
240 threonine and tyrosine, and oxidation of methionine were considered as variable
241 modifications, (vi) maximum protein mass (600 kDa), (vii) one missed cleavage site was
242 allowed for trypsin, (viii) maximum false positive ratio (FDR) of 4% was allowed.
243 Peptide ion data were exported from Progenesis QI as *.csv files and edited in Excel
244 (Microsoft®). Only features detected above the intensity threshold of 150 and in at least
245 2 out of 3 replicates were considered for further analysis. For analysis comparing the
246 ratios between samples and control (glucose) and test (sodium acetate), were accounted
247 proteins that presented, at least. 50% differences in expression values compared to the

control were considered to be regulated. The Uniprot (http://www.uniprot.org) and Pedant on MIPS (http://mips.helmholtz muenchen.de/funcatDB/) database were used for functional classification. NCBI database was employed for annotation of uncharacterized proteins (https://www.ncbi.nlm.nih.gov/).

2.8. Data treatment

Quantitative data on the expression of each of the proteins were converted to logarithmic scale (base 2) for analysis purposes. For each protein, the significance of the effects associated with isolates, carbon sources and interaction between these two factors was evaluated using the variance analysis procedure (ANOVA) using the factorial model, followed by the *Tukey* test. All comparisons were performed using the critical significance level of 0.05. All analyzes were performed in R (R Core Team, 2017) software.

TheMultiExperiment Viewer software V.4.8 (www.tm4.org/mev/) was used to group the comparative proteomic data. To analyze the isolates, the up- and down-regulated proteins were combined and the expression levels that were estimated for each protein were used to build a heat map. In this way, the differences in the proteomic profiles were examined by hierarchical clustering using the Pearson correlation as a measure of similarity.

2.9. Ethanol quantification assay

The quantification of concentration of ethanol was performed by enzymatic detection kit according to the manufacturer's instruction (UV-test for ethanol, RBiopharm, Darmstadt, Germany). Briefly, ethanol is oxidized to acetaldehyde by the enzyme alcohol dehydrogenase, in the presence of nicotinamide-adenine dinucleotide (NAD). Acetaldehyde is quantitatively oxidized to acetic acid in the presence of aldehyde

dehydrogenase, releasing NADH, which is determined by means of its absorbance at 340 nm. *Paracoccidioides Pb*01, *Pb*03, *Pb*339 and *Pb*EPM83 yeast cells were cultivated in minimal media with acetate (100 mM) and glucose (100 mM), and 10^6 cells were used to assay. Briefly, cells were centrifuged, and lysed using glass beads and bead beater apparatus (BioSpec, Oklahoma, USA) in 5 cycles of 30 sec, keeping the samples on ice. The cell lysate was centrifuged at 10,000 x g for15 min at 4°C and the supernatant was used for enzymatic assay according to the manufacturer's instructions. The concentrations of ethanol were obtained in triplicate. Statistical differences was performed using Student's *t test*, and p value ≤ 0.05 were considered significant.

2.10. Analysis of glucans by fluorescence microscopy

To evaluate the glucan content of the cell wall, staining was performed with aniline blue solution 100% (v/v) (Sigma, catalog n.B8563). The yeast cells of different isolates cultured in the presence of acetate or glucose were incubated with aniline blue for 5 min under stirring and subsequently washed twice with PBS 1X (DeCurcio et al., 2017; Renshaw et al., 2016). Samples stained with aniline blue were visualized under a fluorescence microscope (Zeiss Axiocam MRc-Scope A1). The minimum of 100 cells for each microscope slides, in triplicates, were used to evaluate fluorescence intensity. The software provided the fluorescence intensity (in pixels) and the standard error of each analysis. Statistical comparisons were performed using the Student's t *test* and p-values ≤ 0.05 were considered statistically significant.

2.11. Macrophage infection assays

The survival of the *Paracoccidioides* isolates was determined by quantifying the number of colony-forming units (CFUs) recovered from macrophage infection. J774 1.6

298 macrophages (Rio de Janeiro Cell Bank – BCRJ/ UFRJ, accession number 0273),
299 maintained in RPMI medium (RPMI 1640, Vitrocell, Brazil), with 10% FBS (fetal bovine
300 serum, [v/v]) and MEM non-essential amino acid solution (Sigma Aldrich, Missouri,
301 USA) at 36 ºC and 5% CO_2 until completely confluent, were used in assays. The
302 phagocytosis assay was performed in 12-well polypropylene plates (Greinner Bio-One,
303 USA). A total of 10^6 J774 macrophages were plated per well, in RPMI medium containing
304 IFN-γ (1U/mL) (Sigma Aldrich) and incubated for 24 h at 36 ºC and 5% CO_2 for
305 adherence and activation. Prior to co-cultivation, *Paracoccidioides* yeast cells were
306 grown in BHI liquid medium (4% [w/v] glucose, 3.7% [w/v] brain heart infusion, pH 7.2)
307 for 48 h. Then, $5x10^6$ yeast cells per well were added to the macrophages, resulting in a
308 yeast macrophage cell ratio of 5:1. The cells were incubated for 24 h at 36 ºC and 5%
309 CO_2 in RPMI medium containing IFN-γ (1U per mL). Non-phagocytized/non-adhered
310 yeast were washed off 3 times with PBS (Parente-Rocha et al., 2015). Then, macrophages
311 were lysed with water and fungal cells recovered. The number of viable cells was
312 determined based on the number of CFUs. The lysates were plated in BHI medium
313 supplemented with 5% FBS (fetal bovine serum, [v/v]). CFUs were determined after
314 growth at 36ºC, in 5% CO2, for 10 days. Data were expressed as the mean value deviation
315 from triplicates and the statistical analyses were performed using ANOVA.
316
317 **3. RESULTS AND DISCUSSION**
318
319 **3.1. ICL activity**
320 In order to determine the adequate time of exposure of the isolates to sodium acetate for
321 the proteomic assays, the enzymatic activity of ICL was performed in the four isolates at
322 different time intervals (6 h, 18 h, 24 h, and 48 h). An increase in ICL activity was

observed in all the four isolates at 48 hours, indicating activation of the glyoxalate cycle; so this time was used for proteomic analysis (Figure 1). As known, isocitrate lyase is an exclusive enzyme of the glyoxalate cycle, an anaplerotic carbon pathway that deviates in the decarboxylation steps of the TCA cycle, to produce malate and succinate, using acetyl-CoA under conditions in which the production of pyruvate from glycolysis is reduced (Lorenz and Fink, 2002; Fleck et al., 2011). In this way, the ICL activity can be taken as an indicator of the glyoxylate cycle functioning.

3.2. Growth of *P. lutzii* and isolates of *P. brasiliensis* in the presence of glucose and sodium acetate as carbon sources.

Yeast cells of *P. lutzii* (*Pb*01) and of *P. brasiliensis*: *Pb*03, *Pb*339 and *Pb*EPM83 were grown in glucose and sodium acetate. The growth was evaluated by dry weight analysis at several time intervals. For all the isolates, the growth was significantly reduced in the presence of sodium acetate, compared to glucose, as depicted in Supplemental Figure 1. Probably, the lower growth in acetate reflect the lower content of proteins extracted in this condition, as following: *Pb*01 glucose (14.6 µg/µl), *Pb*01 acetate (10.76 µg/µl); *Pb*03 glucose (10.22 µg/µl), *Pb*03 acetate (8.82 µg/µl); *Pb*339 glucose (8.6 µg/µl), *Pb*339 acetate (7.04 µg/µl); *Pb*EPM83 glucose (11,14 µg/µl), *Pb*EPM83 acetate (10.78 µg/µl). Similar results were described in *Escherichia coli* grown on acetate or glucose (Treitz et al., 2016).

3.3. The proteome of *P. lutzii* and of *P. brasiliensis* isolates in the presence of sodium acetate

We identified proteins differentially expressed among *P. lutzii* (*Pb*01) and three members of the species *P. brasiliensis*, as following: *Pb*03, *Pb*339 and *Pb*EPM83. The proteins

identified in the four analyzed groups of the genus *Paracoccidioides* are depicted in Supplementary Table 1. A total of 1,160, 1,211, 1,280 and 1,462 proteins were identified in *P. lutzii* (*Pb*01), *Pb*03, *Pb*339 and *Pb*EPM83 respectively, after filtering, using the criterion of minimum repeat rate of 2, totalizing 5,112 proteins (Supplemental Table 1). The proteins in each isolate, growing in the presence of acetate, were compared to the counter parts in yeast cells growing in the presence of glucose. From the total of proteins, the statistical analysis allowed the identification of those differentially expressed comparing all the analyzed fungi isolates. Upon considering a fold change of at least 1.5 we obtained 526, 442, 744 and 569 differentially expressed proteins, respectively for *P. lutzii* (*Pb*01) and *Pb*03, *Pb*339 and *Pb*EPM83, as depicted in Supplementary Table 1. The number of differentially expressed proteins comparing the four isolates to each other corresponds to 45.3%, 36.5%, 58.1% and 38.9%, respectively of the total of proteins identified in each isolate, what means *P. lutzii* (*Pb*01) and *Pb*03, *Pb*339 and *Pb*EPM83. This data indicate a highly metabolic flexibility in members of the *Paracoccidioides* genus. Similar results were observed by Pigosso and colleagues, which demonstrated significant differences in the protein expression profiles among the representatives of different phylogenetic clades of the genus *Paracoccidioides Pb*01, *Pb*02, *Pb*339 and *Pb*EPM83 (Pigosso et al., 2013).

3.4. The differentially regulated proteins in the analyzed *Paracoccidioides* isolates

By using statistical analysis, we have been able of classifying the differentially expressed proteins. Tables supplemental 2 to 9, present the proteins of the analyzed isolates, which were significantly up or down-regulated, upon growth in the two-carbon source, acetate. Those proteins were classified according to the functional categories present in FunCat2. The functional categories for up and down-regulated proteins were similar, comparing

the four analyzed isolates, as depicted in Supplemental Figure 2, panels A and B, respectively. Some proteins were assigned as unclassified, what means unknown function, comprising 20-30% of the analyzed proteins in the isolates (data not shown).

3.5. Comparative analysis of metabolic processes among *P. lutzii* and phylogenetic groups of *P. brasiliensis* upon acetate as the carbon source

We selected the metabolic pathways, glycolysis/gluconeogenesis and ethanol production, cell wall metabolism, glyoxylate shunt and the TCA cycle, beta-oxidation and the methylcitrate cycle, electron transport chain and oxidative phosphorylation, amino acids degradation and response to oxidative stress in order to be analyzed among isolates, as depicted in Supplemental Table 10.

3.5.1. Regulation of Glycolysis / Gluconeogenesis and alcoholic or ethanol production

To assess changes in protein expression in the isolates, related to glycolysis/gluconeogenesis we compared the levels of concerned enzymes, listed in Supplemental Tables 2 to 9. As depicted in Figure 2, panels A and B, fructose 1,6-biphosphatase (PAAG_02682; PADG_01706) was significantly induced in *Pb*01, *Pb*339 and *Pb*EPM83, suggesting increased gluconeogenesis. Regulatory enzymes of glycolysis, phosphofructokinase-I (PAAG_01583; PABG_03640; PADG_00192) and hexokinase (PADG_03813) were repressed in *Pb*01, *Pb*03, *Pb*339 and *Pb*EPM83, respectively. The reciprocal regulation of phosphofructokinase-I and fructose 1,6-biphosphatase clearly indicate increased gluconeogenesis and decrease in glycolysis, in the isolates of *P. lutzii* and *P. brasiliensis*, as depicted in Figure 2, panels A and B. A shift to gluconeogenesis has been described as a metabolic hallmark of fungal cells exposed to two-carbon sources.

Studies of response of *C. albicans* upon internalization by macrophages, reveals a reprogramming of transcription, including gluconeogenic growth (Lorenz et al., 2004).

Three enzymes involved in ethanol production were differentially expressed in the presence of acetate. Pyruvate decarboxylase (PAAG_02050; PADG_00714) and aldehyde dehydrogenase (PAAG_03910) were induced in *Pb*01 and *Pb*EPM83 and alcohol dehydrogenase (PAAG_00403; PABG_04316; PADG_11405) was induced in all studied isolates. Acetate could provide ethanol due to the increase of aldehyde dehydrogenase and alcohol dehydrogenase. The high level of enzymes involved in ethanol production was observed, principally for *Pb*01 and *Pb*EPM83, that presumably produce ethanol from pyruvate, acetate and acetaldehyde, as depicted in Figure 2, panels A and B. Ethanol measurement was performed, and the results showed that up to 48 h in presence of sodium acetate, a significantly higher level of ethanol was produced compared to cells cultured in glucose, in all isolates, confirming the data of proteomic analysis (Figure 3). In *P. lutzii* during carbon starvation there was induction of enzymes related to the production of ethanol such as alcohol dehydrogenase and pyruvate decarboxylase, as well as increase in ethanol production, in relation to cells cultured in glucose (Lima et al., 2014). Comparative proteomic studies among isolates *Pb*01, *Pb*2 *Pb*339 and *Pb*EPM83 in nutrient-rich media, demonstrated high level of ethanol production in *Pb*01 compared to the other isolates suggesting as here, differential production of ethanol among isolates (Pigosso et al., 2013). Ethanol production has been related to fungi virulence. The influence of alcohol dehydrogenase in fungal pathogenesis was observed in invasive pulmonary aspergillosis with increase in the inflammatory response in lung of mice infected with an alcohol dehydrogenase null mutant strain, and reduction in fungal burden (Grahl et al., 2011).

3.5.2. Regulation of the cell wall metabolism

Figure 4 depicts differences in the expression of cell wall metabolic enzymes in the presence of acetate in the analyzed isolates. *Pb*03 is the only one that up regulates the enzyme glucan 1,3-beta-glucosidase, which catalyzes successive hydrolysis of beta-D-glucose units from the non-reducing ends of (1-3)-beta-D-glucans, releasing beta glucose. Aniline blue which selectively stains 1,3-beta-D-glucan, was employed to estimate the amount of this polymer at the cell wall, as depicted in Supplemental Figure 3. As depicted in panel A, fluorescence was visible reduced in *Pb*03, when grown upon acetate as the carbon source. Quantitative analyzes of the fluorescence intensity (in pixels) in yeast cells of isolate *Pb*03 in the presence of sodium acetate, demonstrated a significant decrease of the fluorescence in cells ($p \leq 0.05$), panel B, strongly suggesting decrease in the glucan content, as indicated by proteomic analysis. Glucosamine-fructose-6-phosphate aminotransferase (PAAG_00850; PADG_03984) is down regulated in *Pb*EPM83, *Pb*01 and *Pb*339. It catalyzes the formation of glucosamine 6-phosphate and is the first and rate-limiting enzyme of the hexosamine biosynthetic pathway controlling the flux of glucose into the hexosamine pathway. The final product of the hexosamine pathway, UDP-N-acetyl-glucosamine, is an active precursor of numerous macromolecules containing amino sugars, including chitin in fungi and arthropods (Badet et al., 1987). In our analysis, *Pb*EPM83 is the only one that up regulate the enzymes glucosamine-6-phosphate-deaminase (PADG_00401), Phosphoacetylglucosamine mutase (PADG_00604) and UDP-N-acetylglucosamine pyrophosphorylase (PADG_04312). Those enzymes participate in amino sugars metabolism to cell wall biosynthesis. Phosphoacetylglucosamine mutase converts N-acetyl-alpha-D-glucosamine-1-phosphate to N-acetyl-D-glucosamine-6-phosphate, which is a reversible step. The products from this reaction are substrates to the enzymes glucosamine-6-phosphate-

deaminase and UDP-N-acetylglucosamine pyrophosphorylase, respectively. The first one convert glucosamine-6-phosphate and H_2O to NH_3 and fructose-6-phosphate, which is used to glycolysis and gluconeogenesis; the second one convert N-acetyl-alpha-D-glucosamine-1-phosphate to UDP-N-acetyl-D-glucosamine, which is used to produce chitin to the cell wall. The down regulation of glucosamine: fructose-6-phosphate-aminotransferase (PADG_03984) and up regulation of glucosamine-6-phosphate-deaminase (PADG_03984) suggests that *Pb*EPM83 uses glucosamine-6-phosphate mainly to glucose production. Those results suggest that *Pb*EPM83 is the isolate that more efficiently respond to the presence of acetate as the carbon source, using polymeric carbohydrates precursors to obtain glucose by gluconeogenesis, and at the same time it synthesizes the chitin polymer into the cell wall.

3.5.3. Regulation of the glyoxylate shunt and the TCA cycle

Acetyl-CoA synthase (PADG_01677) and pyruvate dehydrogenase (PAAG_11035; PABG_03494; PADG_07213) can promote the synthesis of acetyl-CoA from acetate and pyruvate, respectively, as depicted in Figure 5, panels A and B. The major fate of acetyl-CoA is the TCA cycle, in which most of enzymes are induced in the analyzed isolates, mainly in *Pb*01 and *Pb*EPM83 (Figure 5 A and B). The glyoxylate shunt which is a shortcut of the decarboxylation steps of the TCA cycle, can allow the use of acetyl-CoA for synthesis of cellular components (Chung et al., 1988). Isocitrate lyase (PAAG_06951; PADG_01483) malate synthase (PAAG_04542; PADG_04702) were increased in isolates *Pb*01 and *Pb*EPM83. This aspect is of relevance, since isocitrate lyase and malate synthase allows the use of two carbon compounds, from the glyoxalate cycle. Induction of transcripts encoding isocitrate lyase and malate synthase was observed in phagocytized *C. albicans* upon macrophage infection, enhancing the importance of acquiring non-

preferential carbon sources and the glyoxylate cycle function in glucose synthesis (Lorenz and Fink, 2001). Thus, the activation of this metabolic pathway enables the pathogen to survive and persist in the host, in tissues where there is a limitation of nutrients such as inside the macrophages. As already noted, there is an induction of the glyoxalate cycle in fungi and bacteria during phagocytosis as a response to the environment of nutrient deprivation found in the phagolysosome (Brock, 2009). Genes encoding the enzymes of the glyoxylate cycle, isocitrate lyase and malate synthase, were induced in *C. albicans* upon phagocytosis by murine macrophages (Lorenz et al., 2004) and human neutrophils (Fradin et al., 2015). This metabolic pathway enables the fungus to utilize two-carbon molecules as a carbon source, and the induction of this pathway probably reflects the nutrient-deprived environment inside the phagocytes (Miramón et al., 2012). The role of the glyoxylate cycle for virulence has been described in organisms, such as *A. fumigatus* (Olivas et al., 2007), *C. albicans* (Lorenz and Fink 2001, 2002), *M. tuberculosis* (McKinney et al., 2000; Muñoz-Elías and McKinney, 2005).

Regarding to the genus *Paracoccidioides*, the induction of isocytrate lyase was observed in *Pb*01 during transition from mycelium to yeast cells (Bastos et al., 2007) and in yeast cells recovered from kidney of infected mice (Costa et al., 2007). The glyoxylate cycle was positively regulated in yeast cells of *P. lutzii* (Felipe et al., 2005) and the level of malate synthase transcript was higher in yeast cells in the presence of a two-carbon source in relation to glucose (Zambuzzi-Carvalho et al., 2009). An increase in expression of the isocytrate lyase was also observed in *Pb*01 from 6 to 12 hours under carbon starvation (Lima et al., 2014).

3.5.4. Regulation of the β-oxidation and the methylcitrate cycle

In general, the beta-oxidation of fatty acids is up regulated in all isolates, producing acetyl-CoA and propionyl-CoA. Acetyl-CoA can be consumed in the glyoxylate cycle, for biosynthetic purposes, or in the TCA cycle for generation of cellular energy as reduced cofactors. Of relevance, beta oxidation was induced in mitochondria, as well as in peroxisomes, as evidenced in Figure 6, depicting the up regulation of enzymes from both compartments. Carnitine O-acetyl transferase (PADG_07023), related to the entering of acyl fatty acid in the mitochondria and acyl-CoA dehydrogenase mitochondrial (PAAG_05454; PABG_01791; PADG_06805) which catalyzes the initial step in each cycle of fatty acid β-oxidation, were up regulated in *Pb*01, *Pb*03, *Pb*339 and *Pb*EPM83, suggesting higher fatty acid degradation in those isolates, when in the presence of acetate.

Regarding to the methylcitrate cycle, methylcitrate synthase was increased in *Pb*01, *Pb*339 and *Pb*EPM83 (PAAG_04550; PADG_04710), and methylisocitrate lyase was induced in the isolates (PABG_04323; PADG_0470), as depicted n Figure 6. The enzyme level was maintained in *Pb*03, as determined by proteomic analysis. Methylcitrate synthase is a key enzyme in the methylcitrate cycle, essential for the degradation of propionyl-CoA in fungi and some bacteria, avoiding accumulation of propionyl which is toxic (Ibrahim-Granet et al., 2008). The accumulation of propionyl in *Aspergillus nidulans* and *A. fumigatus* inhibits growth and secondary metabolism, and occurs when there are defects in the enzyme methylcitrate synthase (Brock and Buckel, 2004; Zhang et al., 2004; Maerker et al., 2005). In *A. fumigatus* methylcitrate synthase is essential for the manifestation of invasive aspergillosis, suggesting that amino acids serve as nutritional support for the growth and invasion of *A. fumigatus* (Ibrahim-Granet et al., 2007).

3.5.5. Electron transport chain and oxidative phosphorylation

Additionally, the electron transport chain and the ATP synthase complex were predominantly induced in *Pb*EPM83, without any class of repressed protein, as depicted in Supplementary Figure 4. Proteins of the different respiratory chain complexes were regulated differentially among isolates, Supplemental Figure 4. In synthesis, *Pb*EMP83 presented the highest number of induced respiratory chain proteins/enzymes, whereas in *Pb*01, most of the components of the electron transport system and membrane associated energy conservation were not induced, corroborating with the study of Pigosso and colleagues that demonstrated that *P. lutzii* (*Pb*01) is metabolically more anaerobic than *P. brasiliensis* (Pigosso et al., 2013).

3.5.6. Regulation of amino acids degradation

The degradation of amino acids providing precursors for the TCA, pyruvate or acetyl-CoA was induced in the analyzed isolates, as depicted in Figure 7. The degradation of methionine by cystathionine gamma-lyase (PADG_02456) was up regulated in *Pb*339, as shown in Figure 7, panels A and B. The higher production of succinyl-CoA seems to occur in *Pb*01 from the degradation of methionine and threonine, due to the induction of the adenosylhomocysteinase (PAAG_02859) and threonine dehydratase (PAAG_03168), depicted in Figure 7 and Supplemental Figure 5. The conversion of valine and isoleucine to succinyl-CoA could be more predominant in *Pb*EPM83, and *Pb*01 due to the up regulation of the enzymes acyl-CoA dehydrogenase (PAAG_05454; PADG_06805;), enoyl-CoA hydratase (PAAG_06309; PADG_01209;) in both (Figure 6, Supplemental Figure 8), as well as the up-regulation of 2-oxovalerate dehydrogenase (PAAG_01194) and methylmalonate-semialdehyde dehydrogenase (PAAG_07036) in *Pb*01 and 3-

hydroxyisobutyrate dehydrogenase (PADG_03466) and branched-chain amino acid aminotransferase (PADG_04570) in *Pb*EPM83 (Figure 7, Supplemental Figure 8).

The pyruvate production from the degradation of glycine was observed in *Pb*01, *Pb*03 and *Pb*EPM83 with the induction of the enzyme glycine dehydrogenase (PAAG_1568; PABG_04990) (Figure 7 and Supplemental Figure 5). The *Pb*01 also induced the alanine aminotransferase (PAAG_08207) alanine degradation enzyme. Of special note *Pb*03 seems to induce the interconversion of alanine and glyoxylate to pyruvate and glycine, due to the up regulation of alanine glyoxylate aminotransferase (PABG_00589) allowing pyruvate synthesis from the transamination of alanine and glyoxylate synthesized by the glyoxylate cycle (Figure 7 and Supplemental Figure 6). *Pb*03 seems to be the most efficient in the production of oxaloacetate from asparagine, up regulating the enzyme aspartate aminotransferase (PABG_02806), Figure 7 and Supplemental Figure 6.

The conversion of arginine and ornithine to alpha-ketoglutarate seems to predominate in *Pb*339, *Pb*03 and *Pb*EPM83, since the enzymes of this pathway, arginase (PADG_00637), ornithine aminotransferase (PABG_02827; PADG_01328) were up regulated in the three isolates, as depicted in Figure 7 and Supplemental Figure 7. The degradation of phenylalanine to acetoacetyl-CoA could be very similar in *Pb*01 and *Pb*03, due to the up regulation of the three enzymes of this pathway homogentisate-1,2-dioxygenase (PAAG_08164; PABG_07392), maleylacetoacetate isomerase (PAAG_08162; PABG_07390) and fumarylacetoacetase (PAAG_00869) (Figure 7; Supplemental Figure 6). The isolates *Pb*EPM83 and *Pb*339, also induced two enzymes of this pathway, respectively homogentisate 1,2-dioxygenase (PADG_08466) and fumarylacetoacetase (PADG_03964) Figure 7; Supplemental Figure 6. The degradation of tryptophan rendering acetyl-CoA could be higher in *Pb*EPM83, and *Pb*03 due to the up regulation of kyneurinase (PADG_00349; PABG_01965) and kynurenine-

572 oxoglutarate transaminase (PABG_03129) as depicted in Figure 7 and Supplemental
573 Figure 6.

574 The isolates *Pb*EPM83 and *Pb*339 are supposed to produce more efficiently acetyl-
575 CoA from leucine, due to the induction of the enzyme methylcrotonyl-CoA carboxylase
576 (PADG_07370) in both isolates, as depicted in Figure 7 and Supplemental Figure 8. Also,
577 related to this pathway, the enzymes isovaleryl-CoA dehydrogenase (PADG_07369) and
578 methylglutaconyl-CoA hydratase (PADG_00643), were induced in *Pb*339 and
579 *Pb*EPM83, respectively. However, *Pb*01, and *Pb*03 are supposed to be the less efficient
580 in producing acetoacetate from leucine, since the cited up regulated enzymes in this
581 pathway were not observed and the methylcrotonyl-CoA carboxylase (PAAG_04103)
582 was repressed, as depicted in Figure 7 and Supplemental Figure 8.

583 In synthesis, the catabolism of amino acids is highly induced in members of the
584 *Paracoccidioides* genus. In this way, in the presence of a non-preferential carbon source,
585 there was a metabolic shift to the catabolism of amino acids that can render the TCA
586 intermediates. Similar results were obtained in *E. coli*, which in acetate as the carbon
587 source activates the amino acids degradation (Treitz et al., 2016). *C. albicans* upon
588 nutrient deprivation utilizes amino acids as the main carbon source; the process leads to
589 ammonia excretion that promotes a rise in the environmental pH that contributes to
590 morphogenesis (Vylkova et al., 2011). *P. lutzii*, upon carbon deprivation, activates
591 degradation of aminoacids in order to provide precursors to gluconeogenesis (Lima et al.,
592 2014). Also, upon phagocytosis *P. brasiliensis* induces the enzymes glutamate
593 dehydrogenase, alanine glyoxylate aminotransferase and aspartate aminotransferase,
594 evidencing the importance of the catabolism of aminoacids for obtaining glucose
595 precursors and energy, in the phagolysosome harsh environment (Parente-Rocha et al.,
596 2015).

3.5.7. The regulation of the response to stress

Comparing the expression of heat shock proteins (HSPs) depicted in Figure 8, it is evident that *Pb*339 is more efficient in the production of those proteins, when compared to *Pb*03, *Pb*EPM83 and *Pb*01. We also observed the induction of several proteins and enzymes related to ROS (reactive oxygen species) detoxification in pathogenic microorganisms, in the different isolates of *P. brasiliensis* and *P. lutzii,* when yeast cells were cultured in the presence of sodium acetate. Detoxifying molecules are involved in the pathogenesis and virulence of pathogens in phagocytes (Enjalbert et al., 2007; Youseff et al., 2012). We detected the increase, in all analyzed isolates, of the superoxide dismutases (SODs), Cu/Zn-containing SOD1 (PAAG_04164; PABG_03954; PADG_07418), Fe/Mn-containing SOD2 (PAAG_02725; PABG_03204; PADG_01755) as well as peroxisomal catalase (PADG_00324; PAAG_01454; PABG_01943). Superoxide dismutase (SOD) is a primary antioxidant defense against ROS, it dismutases the superoxide radical ($O_2^{\cdot-}$) into molecular oxygen and H_2O_2 (Turrens, 2003). It has been previously suggested that one of the mechanisms used by *P. brasiliensis* to eliminate ROS is the expression of proteins from the antioxidant system, such as SOD enzymes, to neutralize superoxide and convert them into less harmful molecules such as hydrogen peroxide and oxygen molecules (Campos et al., 2005; Grossklaus et al., 2013). The *Paracoccidioides* genome database exhibit six SODs isoforms. The levels of gene expression between phylogenetic lineages of *Paracoccidioides*, depicted the induction of *SOD1* and *SOD3* during the transition from mycelium-to-yeast , exposure to oxidative agents and interaction with phagocytic cells (Tamayo et al., 2016). Amongst the enzymes capable of catabolizing hydrogen peroxide are catalase and peroxidases. *Paracoccidioides* isolates encode three catalases *PbCatA*, *PbCatP* and *PbCatB*, which catalyze the decomposition of hydrogen

622 peroxide (H_2O_2) into oxygen and water (Chagas et al., 2008; Tamayo et al., 2017). CATP
623 was up regulated in all isolates of *Paracoccidioides,* here analyzed (Figure 8).
624 Cytochrome C peroxidase (PABG_00720) and glutathione peroxidase (PABG_04219)
625 were increased only in *Pb*03, compared to the other isolates, upon incubation with acetate
626 as the only carbon source. It has been demonstrated by proteomic analysis, that during
627 the infection in macrophages, *P. brasiliensis* induced the expression of gamma glutamyl-
628 transpeptidase, cytochrome c peroxidase, Cu/Zn superoxide dismutase, and thioredoxins.
629 Cytochrome C peroxidase knockdown mutant strains have reduced survival upon
630 macrophage interaction and during infection in mouse (Parente-Rocha et al., 2015).
631 Although those considerations, all the isolates here analyzed, presented similar survival
632 rates upon macrophage phagocytosis (Supplemental Figure 9), suggesting that they could
633 have equivalent mechanisms to avoid oxidative stress caused by phagocytes.
634
635 **3.6. The most induced processes in *P. lutzii* and *P. brasiliensis* isolates /Concluding**
636 **Remarks**
637 By comparing the metabolic pathways that reflect carbon flux distribution it was possible
638 to propose preferential metabolic strategies in the analyzed isolates of the
639 *Paracoccidioides* genus, in the presence of acetate, as the only carbon source. Figure 9
640 depicts the variations of *in vivo* carbon flux distribution of enzymes involved in the central
641 metabolism. Gluconeogenesis is supposed to occur at similar rates comparing *P.*
642 *brasiliensis* and *P. lutzii* since similar induction of the enzymes of the pathway, as
643 depicted in Figure 2. *Pb*03 and *Pb*EPM83 are supposed to use intermediates of the cell
644 wall catabolism in order to produce glucose, as depicted in Figures 4 and 9. *Pb*01 and
645 *Pb*EPM83 are supposed to present a higher increase in the glyoxylate cycle and TCA,
646 when compared to *Pb*03 and *Pb*339, as depicted in Figures 5 and 8. β-oxidation

predominates in *Pb*339, *Pb*01 and *Pb*EPM83 , as depicted in Figures 6 and 9. The methylcitrate cycle predominates in *Pb*03 and *Pb*339 and *Pb*EPM83, as evidenced in Figures 6 and 9. Regarding to the oxidative phosphorylation and ATP synthesis, *Pb*EPM83 seems to have the most induced process, compared to the other isolate of the *Paracoccidioides* genus, here analyzed. The catabolism of aminoacids rendering intermediates to the TCA was prominent among the isolates. *Pb*03 is the most efficient obtaining precursors to TCA from aminoacids metabolism; it uses α-ketoglutarate, aspartate, oxaloacetate, acetoacetyl-CoA, glyoxylate and pyruvate. *Pb*339 could more efficiently produce α-ketoglutarate and acetyl-CoA; *Pb*EPM83 could more efficiently produce α-ketoglutarate, succinyl CoA and acetyl CoA; *Pb*01 could more efficiently produce succinyl CoA, acetoacetyl-CoA and pyruvate. Regarding to the detoxification process, all the analyzed isolates of the *Paracoccidioides* genus are supposed to be able to detoxify H_2O_2 through catalase P. *Pb*03 presents additionally the induction of glutathione peroxidase and cytochrome C peroxidase, that may account to higher potential to eliminate hydrogen peroxide (Figures 8 and 9). In synthesis, taken together we suggest that *Pb*EPM83 presents the more aerobic metabolism, through TCA and glyoxylate shunt, rendering ATP through the oxidative phosphorylation.

In synthesis, taken together we suggest that all isolates utilizes acetate as source for all pathways less to glycolysis since sugar is not present. In general, there are not a pathway preferential to each isolate obtaining energy and intermediars to componds necessary to survive. This is in accordance with the fact of all isolates had growth *in vitro* in the presence of acetate or *ex vivo* inside macrophage.

AUTHOR CONTRIBUTIONS

CMAS conceived and finalized the manuscript

LCB, FRM, and LLP performed the experiments

GHMFS carried out proteomic data

ASGC carried out statistical analyzes

LCB, FRM, LLP, MP, and CMAS designed the study, discussed, analyzed, interpreted the data and writing the manuscript

ACKNOWLEDGMENTS

This work at Universidade Federal de Goiás was supported by grants from Conselho Nacional de Desenvolvimento Científico e Tecnológico (CNPq), Fundação de Amparo à Pesquisa do Estado de Goiás (FAPEG) and Programa Nacional de Pós Doutorado - Coordenação de Aperfeiçoamento de Pessoal de Nível Superior (PNPD-CAPES). This work is part of the INCT program of Strategies of Host Pathogen Interaction (HPI).

REFERENCES

Abreu, T. F., Sumitomo, B. N., Nishiyama, M. Y. Jr., Oliveira, U. C., Souza, G. H., Kitano, E. S., et al. (2017). Peptidomics of *Acanthoscurria gomesiana* spider venom reveals new toxins with potential antimicrobial activity. *J. Proteomics*. 151, 232-242. doi: 10.1016/j.jprot.2016.07.012

Badet, B., Vermoote, P., Haumont, P. Y., Lederer, F., and Legoffic, F. (1987). Glucosamine synthetase from *Escherichia coli*: purification, properties, and glutamine-utilizing site location. *Biochem*. 26, 1940-1948.

698 Barelle, C.J., Priest, C.L., MacCallum, D. M., Gow, N. A., Odds, F. C., and Brown, A. J.
699 (2006). Niche-specific regulation of central metabolic pathways in a fungal pathogen.
700 *Cell Microbiol*. 8, 961-971. doi: 10.1111/j.1462-5822.2005.00676.x
701
702 Bastos, K. P., Bailão, A. M., Borges, C. L., Faria, F. P., Felipe, M. S., Silva, M. G., et al.
703 (2007). The transcriptome analysis of early morphogenesis in *Paracoccidioides*
704 *brasiliensis* mycelium reveals novel and induced genes potentially associated to the
705 dimorphic process. *BMC Microbiol*. 10, 7-29. doi: 10.1186/1471-2180-7-29
706
707 Bradford, M. M. (1976). A rapid and sensitive method for the quantitation of microgram
708 quantities of protein utilizing the principle of protein-dye binding. *Anal. Biochem.* 72,
709 248-254.
710
711 Brock, M. (2009). Fungal metabolism in host niches. *Curr. Opin. Microbiol.* 12, 371–
712 376. doi: 10.1016/j.mib.2009.05.004
713
714 Brock, M., and Buckel, W. (2004). On the mechanism of action of the antifungal agent
715 propionate. *Eur. J. Biochem*. 271, 3227-3241. doi: 10.1111/j.1432-1033.2004.04255.x
716
717 Brummer, E., Hanson, L. H., Restrepo, A., and Stevens, D. A. (1988). *In vivo* and *in vitro*
718 activation of pulmonary macrophages by IFN-gamma for enhanced killing of
719 *Paracoccidioides brasiliensis* or *Blastomyces dermatitidis*. *J. Immunol.* 140, 2786-2789.
720
721 Campos, E. G., Jesuíno, R. S., Dantas, A. S., Brígido, M. M., and Felipe, M. S. (2005).
722 Oxidative stress response in *Paracoccidioides brasiliensis*. *Genet. Mol. Res*. 4, 409-429.

723

724 Carrero, L. L., Niño-Vega, G., Teixeira, M. M., Carvalho, M. J., Soares, C. M., Pereira,
725 M., et al. (2008). New *Paracoccidioides brasiliensis* isolate reveals unexpected genomic
726 variability in this human pathogen. *Fungal Genet. Biol*. 45, 605-612. doi:
727 10.1016/j.fgb.2008.02.002

728

729 Chagas, R. F., Bailão, A. M., Pereira, M., Winters, M. S., Smullian, A. G., Deepe, G. S.
730 Jr., et al. (2008). The catalases of *Paracoccidioides brasiliensis* are differentially
731 regulated: protein activity and transcript analysis. *Fungal Genet. Biol*. 45, 1470-1478.
732 doi: 10.1016/j.fgb.2008.08.007

733

734 Chaves, G. M., Bates, S., MacCallum, D. M., and Odds, F. C. (2007). *Candida albicans*
735 GRX2, encoding a putative glutaredoxin, is required for virulence in a murine model.
736 *Genet. Mol. Res*. 6, 1051-1063.

737

738 Chung, T., Klumpp, D. J., and Laporte, D. C. (1988). Glyoxylate bypass operon of
739 *Escherichia coli*: cloning and determination of the functional map. *J. Bacteriol*. 170, 386-
740 392.

741

742 Costa, M., Borges, C. L., Bailão, A. M., Meirelles, G. V., Mendonça, Y. A., Dantas, S.
743 F., et al. (2007). Transcriptome profiling of *Paracoccidioides brasiliensis* yeast-phase
744 cells recovered from infected mice brings new insights into fungal response upon host
745 interaction. *Microbiol*. 153 (Pt 12), 4194–4207. doi: 10.1099/mic.0.2007/009332-0

746

De Curcio, J. S., Silva, M. G., Siva-Bailão, M. G., Báo, S. N., Casaletti, L., Bailão, A. M., et al. Identification of membrane proteome of *Paracoccidioides lutzii* and its regulation by zinc. (2017). *Future Sci.* doi.org/10.4155/fsoa-2017-0044

Desjardins, C. A., Champion, M. D., Holder, J. W., Muszewska, A., Goldberg, J., Bailão, A. M., et al. (2011). Comparative genomic analysis of human fungal pathogens causing paracoccidioidomycosis. *PLoS Genet*. 7,e1002345. doi: 10.1371/journal.pgen.1002345

Distler, U., Kuharev, J., Navarro, P., Levin, Y., Schild, H., and Tenzer, S. (2014). Drift time-specific collision energies enable deep-coverage data-independent acquisition proteomics. *Nat. Methods*. 11, 167-170. doi: 10.1038/nmeth.2767

Ebel, F., Schwienbacher, M., Beyer, J., Heesemann, J., Brakhage, A. A., and Brock, M. (2006). Analysis of the regulation. expression. and localization of the isocitrate lyase from *Aspergillus fumigatus*. a potential target for antifungal drug development. *Fungal Genet. Biol*. 43, 476-489. doi: 10.1016/j.fgb.2006.01.015

Enjalbert, B., MacCallum, D. M., Odds, F. C., and Brown, A. J. (2007). Niche-specific activation of the oxidative stress response by the pathogenic fungus *Candida albicans*. *Infect Immun*. 75, 2143-2151. doi: 10.1128/IAI.01680-06.

Felipe, M. S., Andrade, R. V., Arraes F. B., Nicola, A. M., Maranhão, A. Q., Torres, F. A., et al. (2005). Transcriptional profiles of the human pathogenic fungus *Paracoccidioides brasiliensis* in mycelium and yeast cells. *J. Biol. Chem.* 280, 24706–24714. doi: 10.1074/jbc.M500625200

772

773 Fleck, C. B., Schobel, F., and Brock, M. (2011). Nutrient acquisition by pathogenic fungi:
774 nutrient availability. pathway regulation. and differences in substrate utilization. *Int. J.*
775 *Med. Microbiol.* 301, 400–407. doi: 10.1016/j.ijmm.2011.04.007

776 Fonseca, C. A., Jesuíno, R. S., Felipe, M. S., Cunha, D. A., Brito, W. A., and Soares, C.
777 M. A. (2001). Two-dimensional electrophoresis and characterization of antigens from
778 *Paracoccidioides brasiliensis*. *Microbes Infect*. 3, 535-342. doi: 10.1016/S1286-
779 4579(01)01409-5

780

781 Fradin, C., Bernardes, E. S., Jouault, T. (2015). *Candida albicans* phospholipomannan: a
782 sweet spot for controlling host response/inflammation. *Semin Immunopathol*. 37, 123-
783 130. doi: 10.1007/s00281-014-0461-5

784

785 Garrido, B. C., Souza, G. H., Lourenço, D. C., and Fasciotti, M. (2016). Proteomics in
786 quality control: Whey protein-based supplements. *J. Proteomics*. 147, 48-55. doi:
787 10.1016/j.jprot.2016.03.044

788

789 Grahl, N., Puttikamonkul, S., Macdonald, J. M., Gamcsik, M. P., Ngo, L. Y., Hohl, T.
790 M., et al. (2011). *In vivo* hypoxia and a fungal alcohol dehydrogenase influence the
791 pathogenesis of invasive pulmonary aspergillosis. *PLoS Pathog*. 7, e1002145. doi:
792 10.1371/journal.ppat.1002145

793

794 Grossklaus, de A. D., Bailão, A. M., Vieira Rezende, T. C., Borges, C. L., Oliveira, M.
795 A. P., Parente, J. A., et al. (2013). Response to oxidative stress in *Paracoccidioides* yeast

cells as determined by proteomic analysis. *Microbes Infect.* 15, 347-364. doi: 10.1016/j.micinf.2012.12.002

Haas, A. The phagosome: compartment with a license to kill. (2007). *Traffic*. 8, 311-330. doi: 10.1111/j.1600-0854.2006.00531.x

Ibrahim-Granet, O., Dubourdeau, M., Latgé, J. P., Ave, P., Huerre, M., Brakhage, A. A., et al. (2008). Methylcitrate synthase from *Aspergillus fumigatus* is essential for manifestation of invasive aspergillosis. *Cell Microbiol.* 10, 134-148. doi: 10.1111/j.1462-5822.2007.1025.x

Lima, P. de S., Casaletti, L., Bailão, A. M., Vasconcelos, A. T., Fernandes, G. da R., and Soares, C. M. (2014). Transcriptional and proteomic responses to carbon starvation in *Paracoccidioides*. *PLoS Negl. Trop. Dis*. 8, e2855. doi: 10.1371/journal.pntd.0002855

Lorenz, M. C., and Fink, G. R. (2001). The glyoxylate cycle isrequired for fungal virulence. *Nature*. 412, 83-86. doi: 10.1038/35083594

Lorenz, M. C., and Fink, G. R. (2002). Life and death in a macrophage: role of the glyoxylate cycle in virulence. *Eukaryot. Cell*. 1, 657-662. doi: 10.1128/EC.1.5.657-662.2002

Lorenz, M. C., Bender, J. A., and Fink, G. R. (2004). Transcriptional response of *Candida albicans* upon internalization by macrophages. *Eukaryot Cell*. 3:1076–1087. doi: 10.1128/EC.3.5.1076-1087.2004

821

822 Maerker, C., Rohde, M., Brakhage, A. A., and Brock, M. (2005). Methylcitrate synthase
823 from *Aspergillus fumigatus*. Propionyl-CoA affects polyketide synthesis, growth and
824 morphology of conidia. *FEBS J.* 272, 3615-3630. doi: 10.1111/j.1742-
825 4658.2005.04784.x

826

827 Martinez, R. (2015). Epidemiology of Paracoccidioidomycoses. *Rev. Soc. Bras. Med.*
828 *Trop*. 57 (Suppl. 19), 11-20. doi: 10.1590/S0036-46652015000700004

829

830 Matute, D. R., McEwen, J. G., Puccia, R., Montes, B. A., San-Blas, G., Bagagli, E., et al.
831 (2006a). Cryptic speciation and recombination in the fungus *Paracoccidioides*
832 *brasiliensis* as revealed by gene genealogies. *Mol. Biol. Evol.* 23, 65–73. doi:
833 10.1093/molbev/msj008

834

835 Matute, D. R., Sepulveda, V. E., Quesada, L. M., Goldman, G. H., Taylor, J. W.,
836 Restrepo, A., et al. (2006b). Microsatellite analysis of three phylogenetic species of
837 *Paracoccidioides brasiliensis*. *J. Clin. Microbiol.* 44, 2153-2157. doi:
838 10.1128/JCM.02540-05

839

840 McKinney, J. D., Höner zu Bentrup, K., Muñoz-Elías, E. J., Miczak, A., Chen, B., Chan,
841 W. T., et al. (2000). Persistence of *Mycobacterium tuberculosis* in macrophages and mice
842 requires the glyoxylate shunt enzyme isocitrate lyase. *Nature*. 406, 735-738. doi:
843 10.1038/35021074

844

Miramón, P., Dunker, C., Windecker, H., Bohovych, I. M., Brown, A. J., Kurzai, O., et al. (2012). Cellular responses of *Candida albicans* to phagocytosis and the extracellular activities of neutrophils are critical to counteract carbohydrate starvation, oxidative and nitrosative stress. *PLoS One*. 7, e52850. doi: 10.1371/journal.pone.0052850

Muñoz, J. F., Farrer, R. A., Desjardins, C. A., Gallo, J. E., Sykes, S., Sakthikumar, S., et al. (2016). Genome diversity, recombination, and virulence across the major lineages of *Paracoccidioides*. *mSphere*. 1, pii: e00213-16. doi: 10.1128/mSphere.00213-16.

Muñoz, J. F., Gallo, J. E., Misas, E., Priest, M., Imamovic, A., Young, S., et al. (2014). Genome update of the dimorphic human pathogenic fungi causing paracoccidioidomycosis. *PLoS Negl. Trop. Dis.* 8, e3348. doi: 10.1371/journal.pntd.0003348

Munõz-Elias, E. J., and McKinney, J. D. (2005). *Mycobacterium tuberculosis* isocitrate lyases 1 and 2 are jointly required for *in vivo* growth and virulence. *Nat. Med.* 11, 638–644. doi: 10.1038/nm1252

Murad, A. M., Souza, G. H., Garcia, J. S., and Rech, E. L. (2011). Detection and expression analysis of recombinant proteins in plant-derived complex mixtures using nanoUPLC-MS$^{(E)}$. *J. Sep. Sci.* 34, 2618-2630. doi: 10.1002/jssc.201100238

Olivas, I., Royuela, M., Romero, B., Monteiro, M. C., Mínguez, J. M., Laborda, F., et al. (2007). Ability to grow on lipids accounts for the fully virulent phenotype in neutropenic

mice of *Aspergillus fumigatus* null mutants in the key glyoxylate cycle enzymes. *Fungal Genet. Biol.* 45, 45-60. doi: 10.1016/j.fgb.2007.05.002

Parente-Rocha, J. A., Parente, A. F., Baeza, L. C., Bonfim, S. M. R. C., Hernández, O., McEwen, J. G., et al. (2015). Macrophage interaction with *Paracoccidioides brasiliensis* yeast cells modulates fungal metabolism and generates a response to oxidative stress. *PLoS One*. 10, e0137619. doi: 10.1371/journal.pone.0137619

Pigosso, L. L., Baeza, L. C., Tomazett, M. V., Batista, M. R. F., Moura, V. M. B. D., Bailão, A. M., et al. (2017). *Paracoccidioides brasiliensis* presents metabolic reprogramming and secretes a serine proteinase during murine infection. *Virulence*. 13:0. doi: 10.1080/21505594.2017.1355660.

Pigosso, L. L., Parente, A. F. A., Coelho, A. S. G., Silva, L. P., Borges, C. L., Bailão, A. M., et al. (2013). Comparative proteomics in the genus *Paracoccidioides*. *Fungal Genet. Biol.* 60, 87-100. doi: 10.1016/j.fgb.2013.07.008

Renshaw, H., Vargas-Muñiz, J. M., Richards, A. D., Asfaw, Y. G., Juvvadi, P. R., and Steinbach, W. J. (2016). Distinct roles of myosins in *Aspergillus fumigatus* hyphal growth and pathogenesis. *Infect Immun*. 84, 1556-1564. doi: 10.1128/IAI.01190-15.

Restrepo, A., and Jiménez, B. E. (1980). Growth of *Paracoccidioides brasiliensis* yeast phase in a chemically defined culture medium. *J. Clin. Microbiol.* 12, 279-281.

893 Restrepo, A., McEwen, J. G., and Castañeda, E. (2001). The habitat of *Paracoccidioides*
894 *brasiliensis*: how far from solving the riddle? *Med. Mycol.* 39, 233-241.
895
896 San-Blas, G., Niño-Vega, G., and Iturriaga, T. (2002). *Paracoccidioides brasiliensis* and
897 paracoccidioidomycosis: molecular approaches to morphogenesis, diagnosis,
898 epidemiology, taxonomy and genetics. *Med. Mycol.* 40, 225-242.
899
900 Tamayo, D., Muñoz, J. F., Almeida, A. J., Puerta, J. D., Restrepo, A., Cuomo, C. A., et
901 al. (2017). *Paracoccidioides* spp. catalases and their role in antioxidant defense against
902 host defense responses. *Fungal Genet. Biol.* 100, 22-32. doi: 10.1016/j.fgb.2017.01.005
903
904 Tamayo, D., Muñoz, J. F., Lopez, A., Urán, M., Herrera, J., Borges, C. L., et al. (2016).
905 Identification and analysis of the role of superoxide dismutases isoforms in the
906 pathogenesis of *Paracoccidioides* spp. *PLoS Negl. Trop. Dis.* 10, e0004481. doi:
907 10.1371/journal.pntd.0004481
908
909 Teixeira, M. M., Theodoro, R. C., Carvalho, M. J., Fernandes, L., Paes, H. C., Hahn, R.
910 C., et al. (2009). Phylogenetic analysis reveals a high level of speciation in the
911 *Paracoccidioides* genus. *Mol. Phylogenet. Evol.* 52, 273–283. doi:
912 10.1016/j.ympev.2009.04.005
913
914 Teixeira, M. M., Theodoro, R. C., Niño-Vega, G., Bagagli, E., and Felipe, M. S. (2014).
915 *Paracoccidioides* species complex: ecology, phylogeny, sexual reproduction, and
916 virulence. *PLoS Pathog*. 10, e1004397. doi: 10.1371/journal.ppat.1004397
917

Treitz, C., Enjalbert, B., Portais, J. C., Letisse, F., and Tholey, A. (2016). Differential quantitative proteome analysis of *Escherichia coli* grown on acetate versus glucose. *Proteomics*. 16, 2742-2746. doi: 10.1002/pmic.201600303

Turrens, J. F. (2003). Mitochondrial formation of reactive oxygen species. *J. Physiol.* 552 (Pt 2), 335–344. doi: 10.1113/jphysiol.2003.049478

Vylkova, S., Carman, A. J., Danhof, H. A., Collette, J. R., Zhou, H., and Lorenz, M. C. (2011). The fungal pathogen *Candida albicans* autoinduces hyphal morphogenesis by raising extracellular pH. *MBio.* 2, e00055–e00011. doi: 10.1128/mBio.00055-11

Youseff, B. H., Holbrook, E. D., Smolnycki, K. A., and Rappleye, C. A. (2012). Extracellular superoxide dismutase protects *Histoplasma* yeast cells from host-derived oxidative stress. *PLoS Pathog.* 8, e1002713. doi: 10.1371/journal.ppat.1002713

Zambuzzi-Carvalho, P. F., Cruz, A. H. S., Santos-Silva, L, K., Goes, A. M., Soares, C. M. A., and Pereira, M. (2009). The malate synthase of *Paracoccidioides brasiliensis* Pb01 is required in the glyoxylate cycle and in the allantoin degradation pathway. Med Mycol. 47, 734-744. doi: 10.3109/13693780802609620

Zhang, Y. Q., Brock, M., and Keller, N. P. (2004). Connection of propionyl-CoA metabolism to polyketide biosynthesis in *Aspergillus nidulans*. *Genetics*. 168, 785-794. doi: 10.1534/genetics.104.027540

Conflict of Interest Statement: The authors declare that the research was conducted in the absence of any commercial or financial relationships that could be construed as a potential conflict of interest.

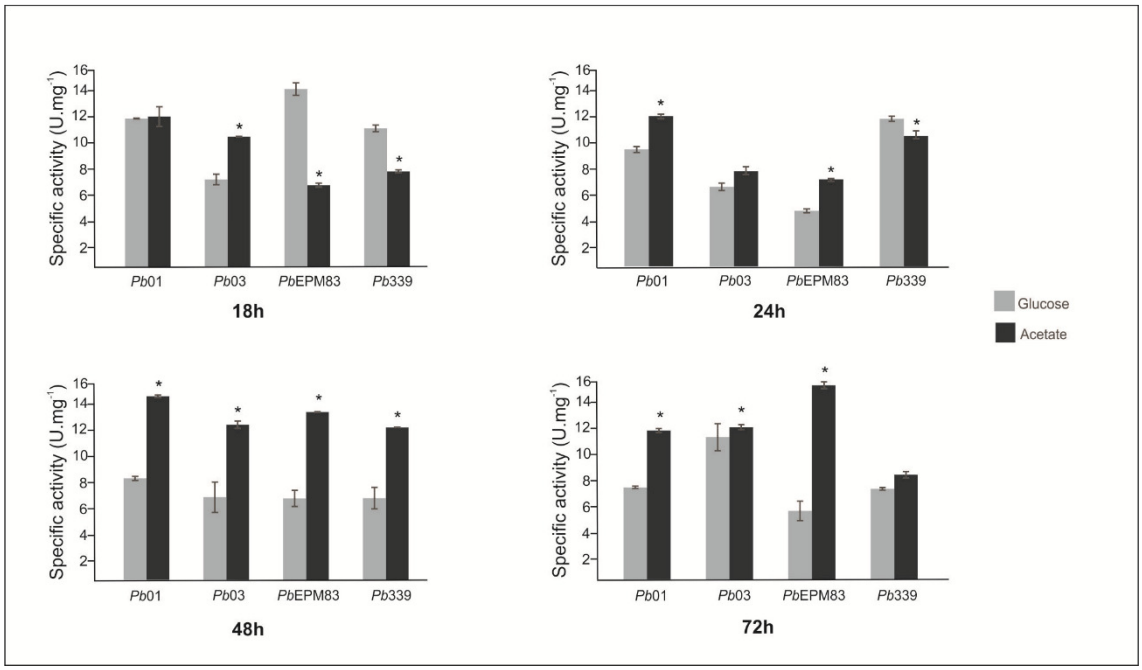

Figure 1: Isocitrate lyase (ICL) activity assay. The activity was determined by measuring the formation of glyoxylate as its phenylhydrazone derivative in each condition. A total of 50 mg of each total protein extract of *Paracoccidioides* isolates *Pb*01, *Pb*03, *Pb*339 and *Pb*EPM83 yeast cells, were cultivated in minimal media with sodium acetate (100 mM) and glucose (100 mM) at different time intervals (6 h, 18 h, 24 h, and 48 h). The specific activity of ICL was determined as the amount of enzyme required to form 1 μmol of glyoxylate-phenylhydrazone per minute, per mg of total protein, and represented as $U.mg^{-1}$. Errors bars represent standard deviation from three biological replicates while * represents $p \leq 0.05$.

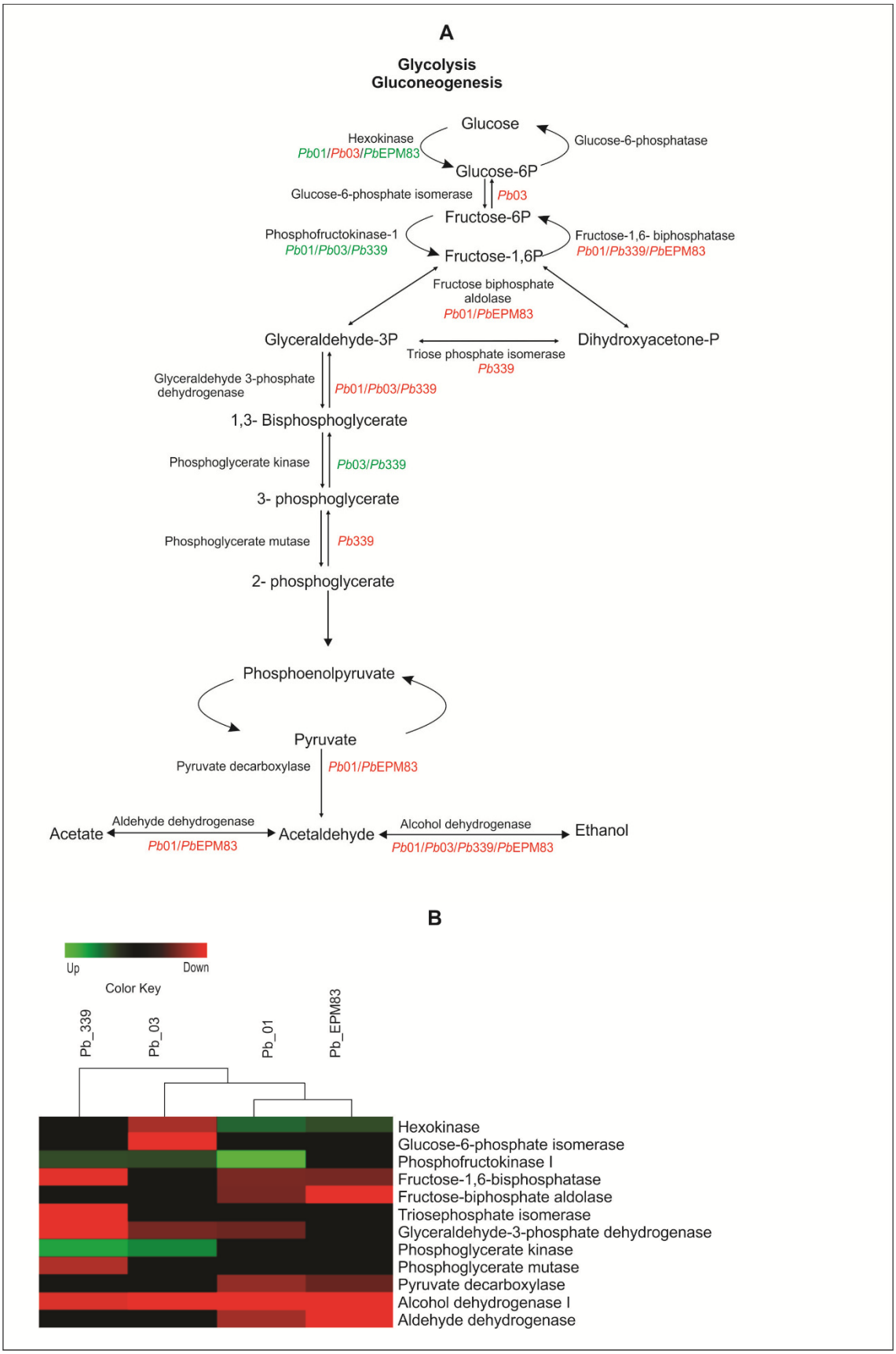
A
Glycolysis
Gluconeogenesis
Glucose
Hexokinase
Pb01/Pb03/PbEPM83
Glucose-6-phosphatase
Glucose-6P
Glucose-6-phosphate isomerase
Pb03
Fructose-6P
Phosphofructokinase-1
Pb01/Pb03/Pb339
Fructose-1,6- biphosphatase
Pb01/Pb339/PbEPM83
Fructose-1,6P
Fructose biphosphate aldolase
Pb01/PbEPM83
Glyceraldehyde-3P
Triose phosphate isomerase
Pb339
Dihydroxyacetone-P
Glyceraldehyde 3-phosphate dehydrogenase
Pb01/Pb03/Pb339
1,3- Bisphosphoglycerate
Phosphoglycerate kinase
Pb03/Pb339
3- phosphoglycerate
Phosphoglycerate mutase
Pb339
2- phosphoglycerate
Phosphoenolpyruvate
Pyruvate
Pyruvate decarboxylase
Pb01/PbEPM83
Acetate
Aldehyde dehydrogenase
Pb01/PbEPM83
Acetaldehyde
Alcohol dehydrogenase
Pb01/Pb03/Pb339/PbEPM83
Ethanol
B
Up
Down
Color Key
Pb_339
Pb_03
Pb_01
Pb_EPM83
Hexokinase
Glucose-6-phosphate isomerase
Phosphofructokinase I
Fructose-1,6-bisphosphatase
Fructose-biphosphate aldolase
Triosephosphate isomerase
Glyceraldehyde-3-phosphate dehydrogenase
Phosphoglycerate kinase
Phosphoglycerate mutase
Pyruvate decarboxylase
Alcohol dehydrogenase I
Aldehyde dehydrogenase

Figure 2: Comparison of protein profiles related to glycolysis and gluconeogenesis in *P. lutzii* and isolates of *P. brasiliensis*. ANOVA test was applied to compare expression values among isolates, applying a cut off of 1.5-fold. Data of expression were carried out with the MultiExperiment Viewer software V.4.8 (www.tm4.org/mev/), that was used to group and compare data of expression. **A**- Representative diagram of the glycolysis/gluconeogenesis and fermentation pathways depicting down regulated (green) and up regulated (red) in the isolates, as cited above. **B**- Changes in expression levels upon yeast cells incubated with acetate in the four analyzed isolates, are represented in a heat map format. Mean values of experimental triplicates are shown for down regulation (green) and up regulation (red) of genes of isolates, *Pb*01, *Pb*03, *Pb*339, and *Pb*EPM83 in presence of sodium acetate. Black means that no significant difference was observed.

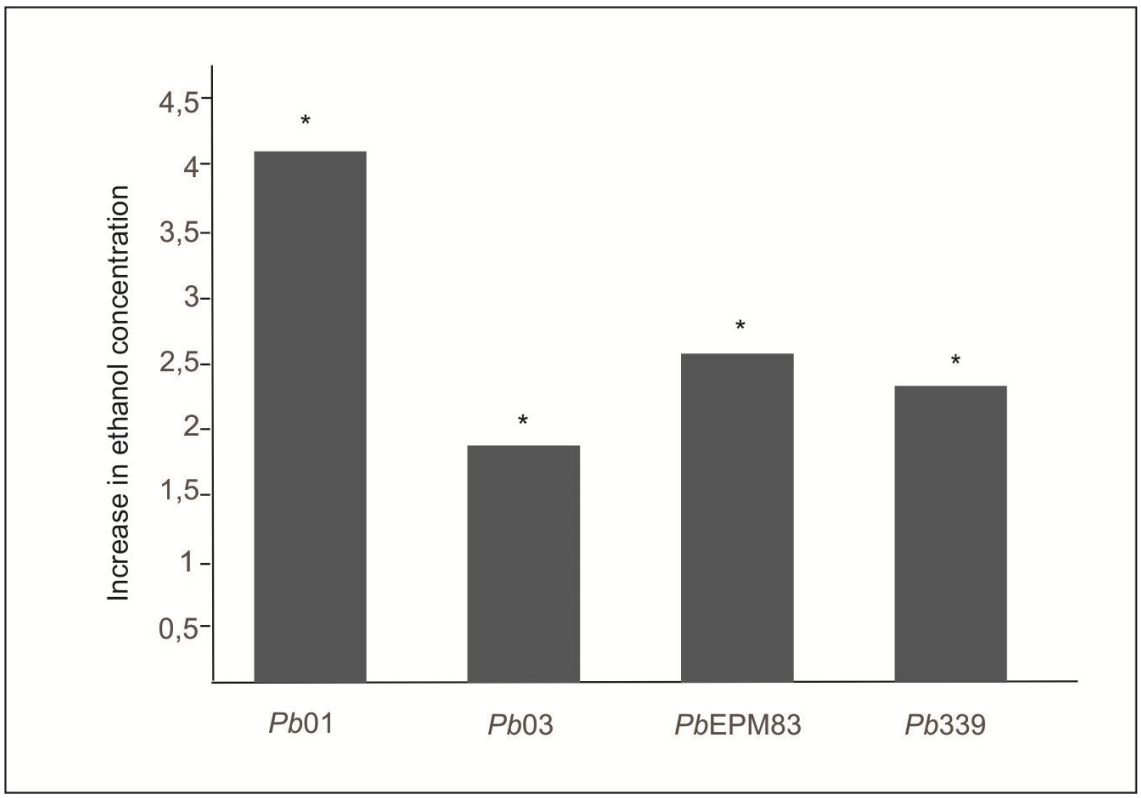

Figure 3: Ethanol measurement in *P. lutzii* and *P. brasiliensis*. The concentration of ethanol (g/L) was determined in yeast cells of the isolates *Pb*01, *Pb*03, *Pb*339 and *Pb*EPM83 upon growth in minimal media with sodium acetate (100 mM) and glucose (100 mM) for 48 h. A total of 10^6 cells were used for each sample, and the ethanol compound was quantified using the enzymatic detection kit (UV-test for ethanol, RBiopharm, Darmstadt, Germany). Data are expressed as the mean ± standard deviation of the biological triplicates of independent experiments. Student's *t*-test was used. * significantly different from the glucose condition, at a *p*-value of ≤0.05.

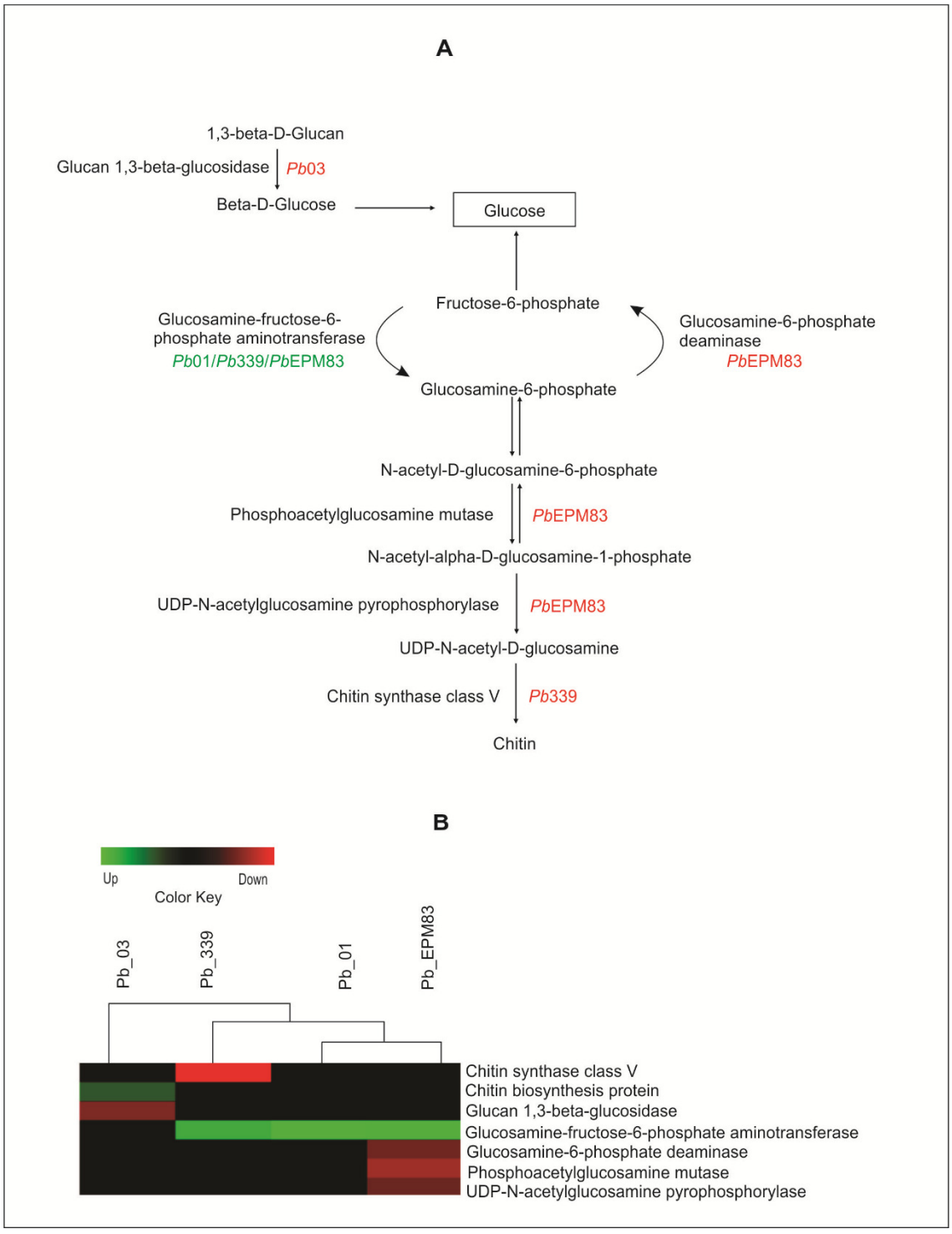

Figure 4: Comparison of protein profiles related to the cell wall metabolism in *P. lutzii* **and isolates of** *P. brasiliensis* Dataset comparisons were carried out, as cited in Figure 2, legend. **A**- Representative diagram of the cell wall metabolism pathways depicting down regulated (green) and up regulated (red) in the isolates, as cited above. **B**- Changes in expression levels upon yeast cells incubated with acetate in *Pb*01, *Pb*03, *Pb*339, and *Pb*EPM83, are represented in a heat map format. Black means that no significant difference was observed.

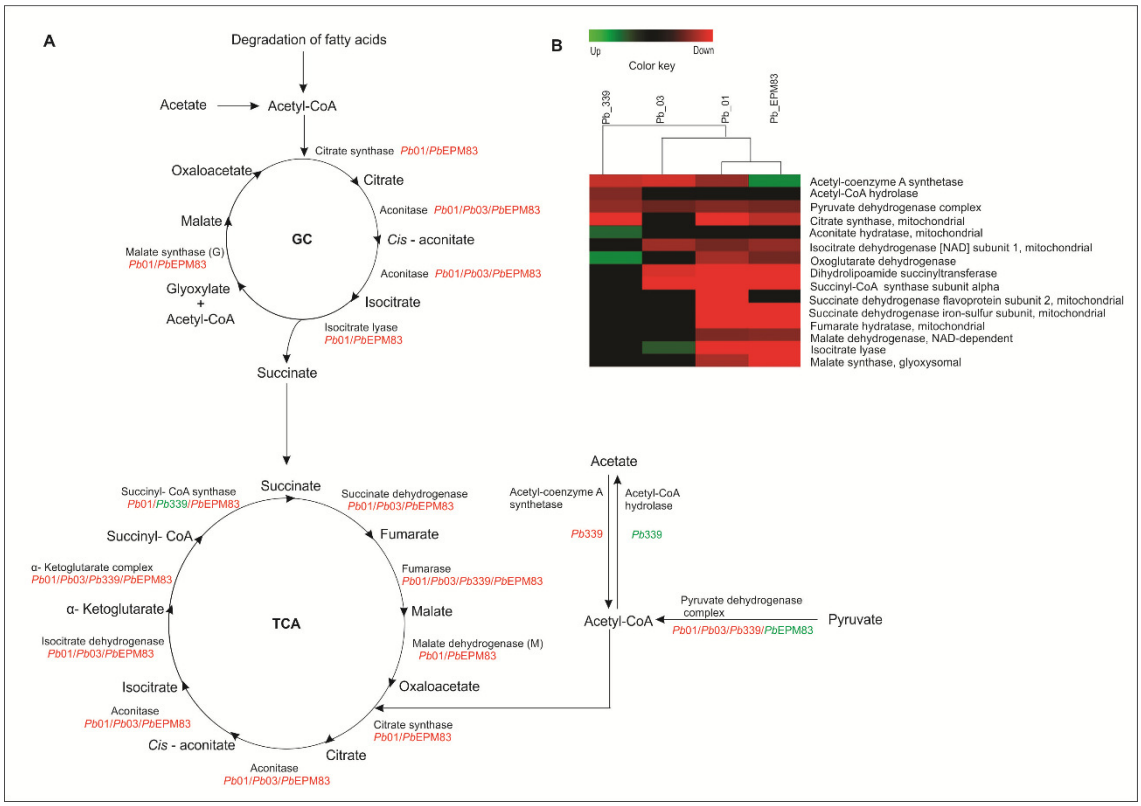

Figure 5: Comparison of protein profiles related to TCA and glyoxylate cycle in *P. lutzii* **and isolates of** *P. brasiliensis*. Dataset comparisons were carried out, as cited in Figure 2, legend. **A**- Representative diagram of the TCA and glyoxylate cycle depicting down regulated (green) and up regulated (red) in the isolates. B- Changes in expression levels upon yeast cells incubated with acetate in *Pb*01, *Pb*03, *Pb*339, and *Pb*EPM83 are represented in a heat map format. Black means that no significant difference was observed.

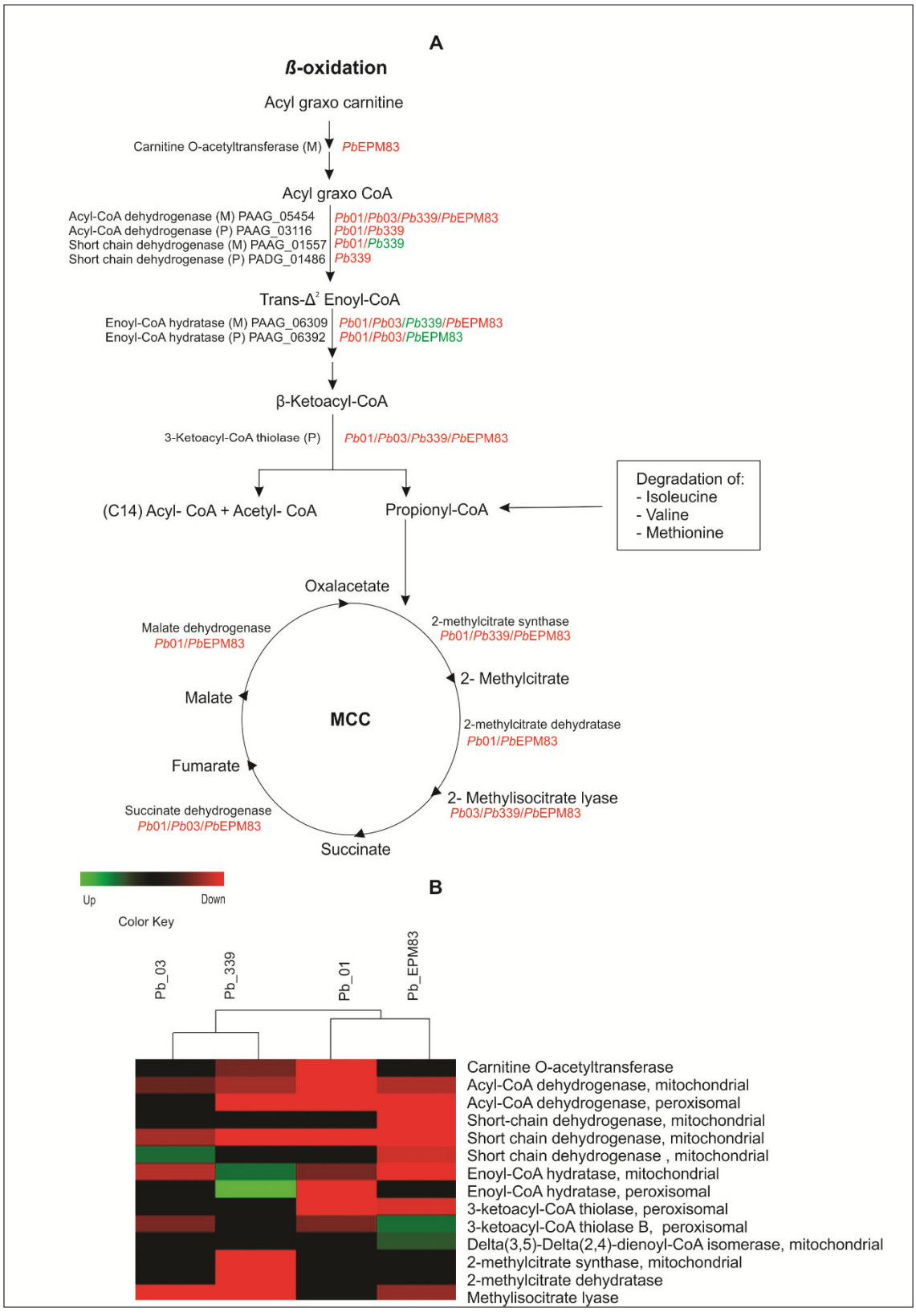

Figure 6: Comparison of protein profiles related to β-oxidation and methylcitrate cycle in *P. lutzii* **and isolates of** *P. brasiliensis*. Dataset comparisons were carried out as cited in Figure 2, legend. A-Representative diagram of the β-oxidation and methylcitrate cycle pathways depicting down regulated (green) and up regulated (red) in the isolates B-Changes in expression levels in yeast cells incubated with acetate in *Pb*01, *Pb*03, *Pb*339,

and *Pb*EPM83 are represented in a heat map format. Black means that no significant difference was observed.

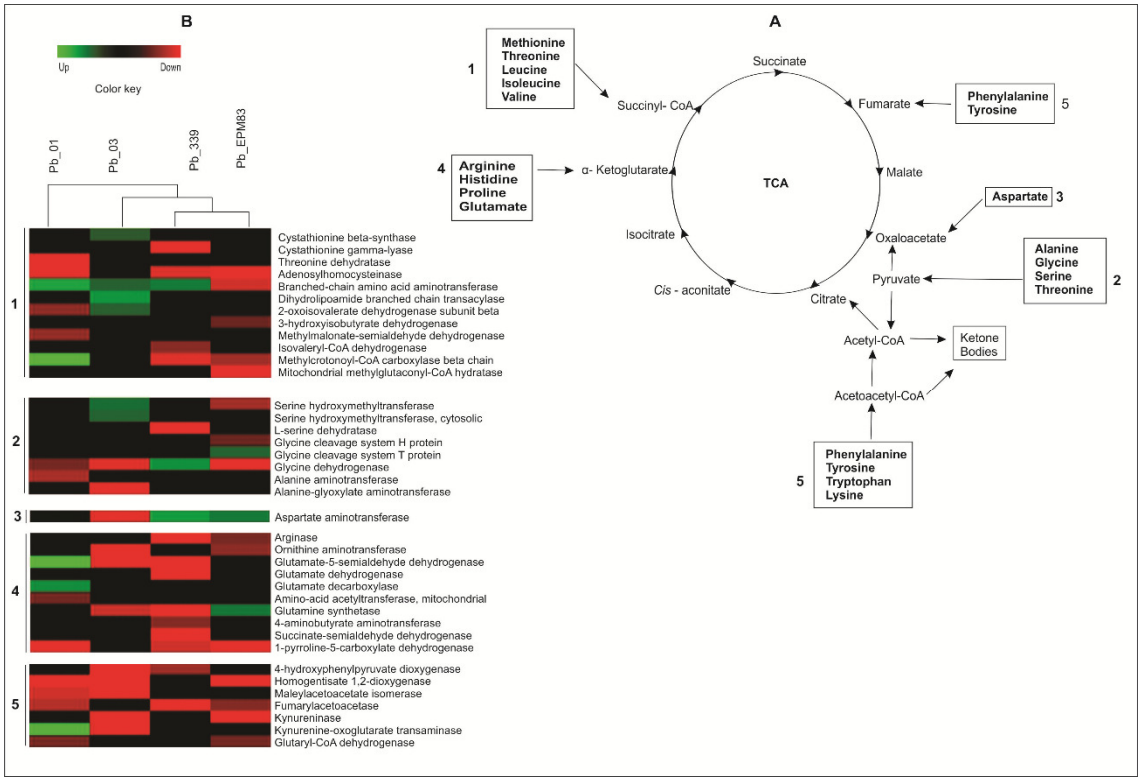

Figure 7: Comparison of protein profiles related to amino acids catabolism in *P. lutzii* **and isolates of** *P. brasiliensis*. Dataset comparisons were carried out as cited in Figure 2, legend. **A**- Changes in expression levels in yeast cells incubated with acetate in *Pb*01, *Pb*03, *Pb*339, and *Pb*EPM83 are represented in a heat map format. **B**- Representative diagram of the amino acid catabolism pathways depicting down regulated (green) and up regulated (red) in the isolates, as cited above. Black means that no significant difference was observed.

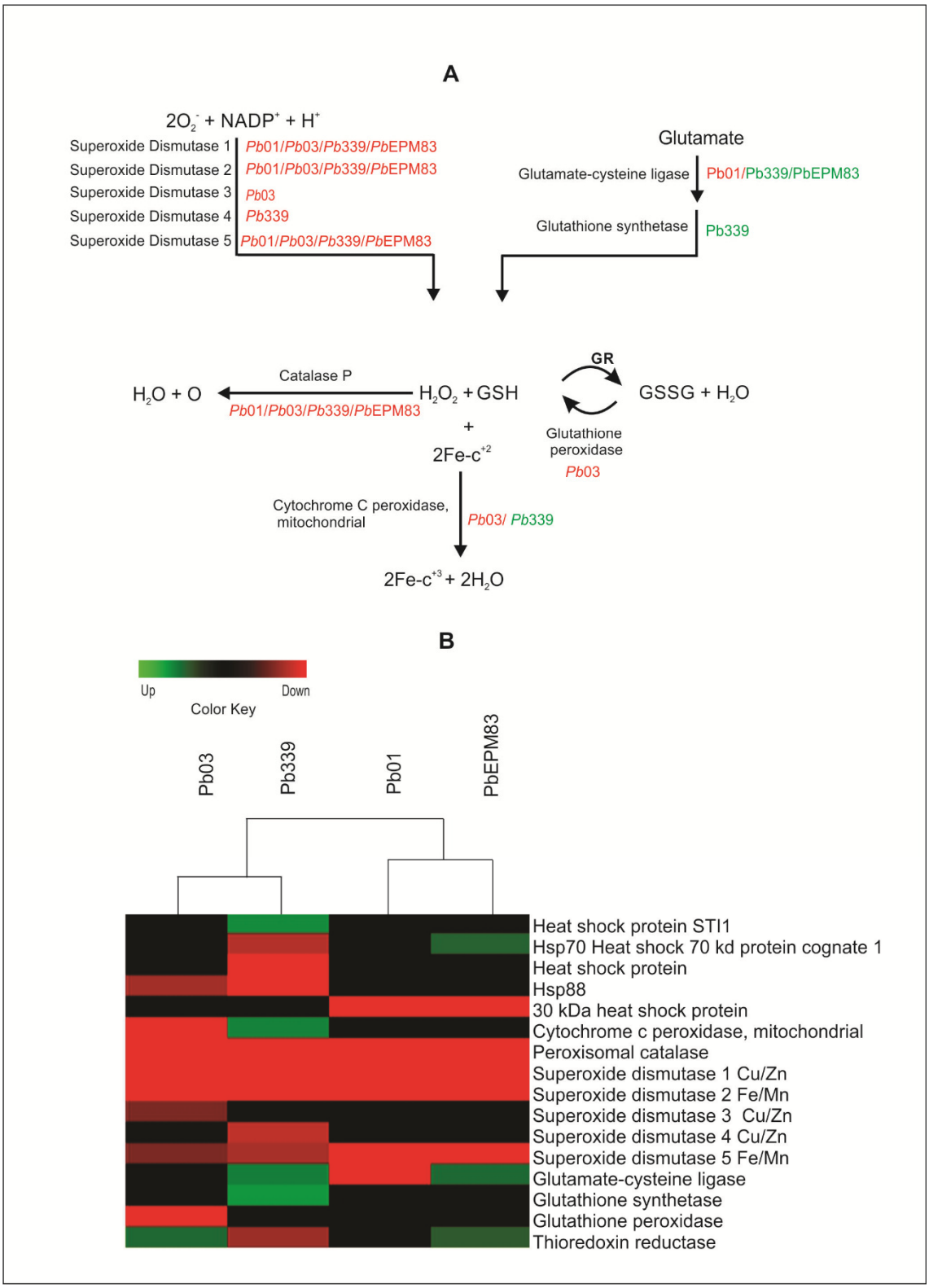

Figure 8: Comparison of protein profiles related to detoxification mechanisms against oxidative stress in the *P. lutzii* and isolates of *P. brasiliensis*. Dataset comparisons were carried out with as cited in Figure 2, legend. **A**- Changes in expression levels upon yeast cells incubated with acetate in Pb01, *Pb*03, *Pb*339, and *Pb*EPM83 are represented in a heat map format. **B**- Representative diagram of the detoxification mechanisms against oxidative stress pathways depicting down regulated (green) and up

regulated (red) in the isolates as cited above. Black means that no significant difference was observed. *Glutathione (GSH*); Glutathione reductase (GR); Glutathione disulfide (GSSG).

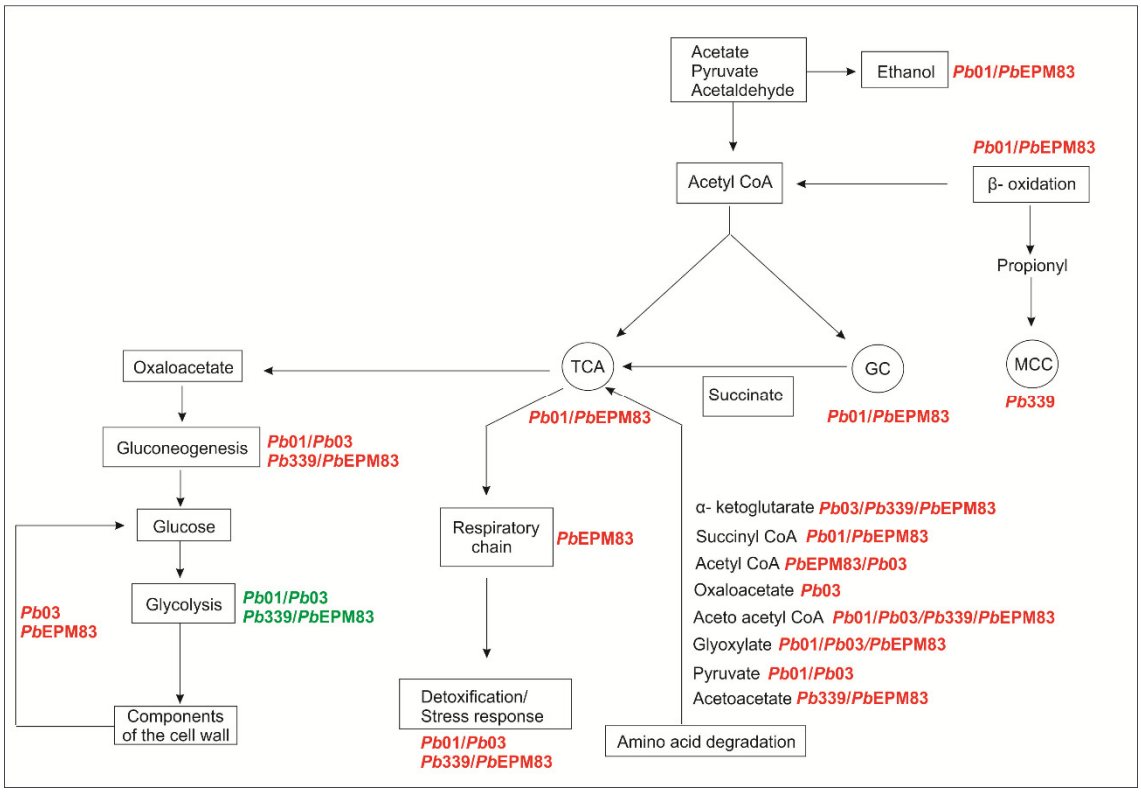

Figure 9: Overview of the metabolic features of members of the *Paracoccidioides* genus, in sodium acetate as carbon source. The metabolic pathways were identified by the analysis of the up regulated proteins in *P. lutzii* (*Pb*01) and *P. brasiliensis Pb*03, *Pb*339, and *Pb*EPM83. The main metabolic pathways were represented: gluconeogenesis, fermentation, cycles of the tricarboxylic acid (TCA), glyoxalate (GC) and methylcitrate (MCC), respiratory chain, β- oxidation, amino acid degradation, detoxification / response to stress and cell wall components.

SUPPORTING INFORMATION

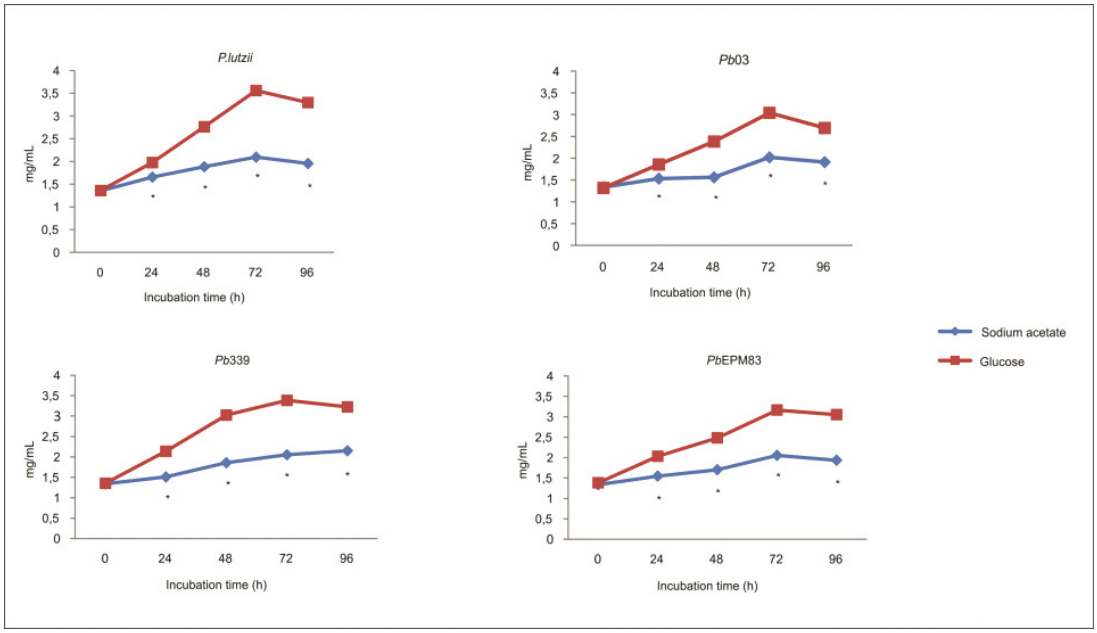

Supplemental Figure 1: Growth of *P. lutzii* (*Pb*01) **and** *P. brasiliensis* **isolates** *Pb*03, *Pb*339, **and** *Pb*EPM83 **in glucose and sodium acetate as carbon sources**. A total of $1x10^6$ cells/50 mL were incubated in MMcM medium with glucose (100 mM) or sodium acetate (100 mM) for 96 hours. Cells were collected at time intervals, killed by heat, lyophilized and the dry weight was determined. Data are expressed as the mean ± standard deviation of the triplicates of independent experiments. Student's *t-test* was used.*, significantly different from in glucose condition, at *p*-value of ≤ 0.05.

Supplemental Figure 2: Functional classification of proteins regulated in yeast cells of *P.lutzii* and *P. brasiliensis* grown in 100mM sodium acetate as carbon source for 48 hours and obtained by NanoUPLC-MS^{E} analysis. **(A)** Biological processes of induced proteins. **(B)** Biological processes of repressed proteins. The biological processes of the differentially expressed proteins in the isolates were obtained using the Pedant in MIPS for *P. lutzii* (http://pedant.helmholtzmuenchen.de/pedant3htmlview/pedant3view?Method=analysis&Db=p3_r48325_Par_lutzi), *Pb*03 (http://pedant.helmholtzmuenchen.de/pedant3htmlview/pedant3view?Method=analysis&Db=p3_p27779_Par_brasi_Pb03). and *Pb339*. *Pb*EPM83 (http://pedant.helmholtzmuenchen.de/pedant3htmlview/pedant3view?Method=analysis&Db=p3_p28733_Par_brasi_Pb18), Uniprot (http://www.uniprot.org/) and KEGG: Kyoto Encyclopedia of Genes and Genomes (www.genome.jp/kegg/).

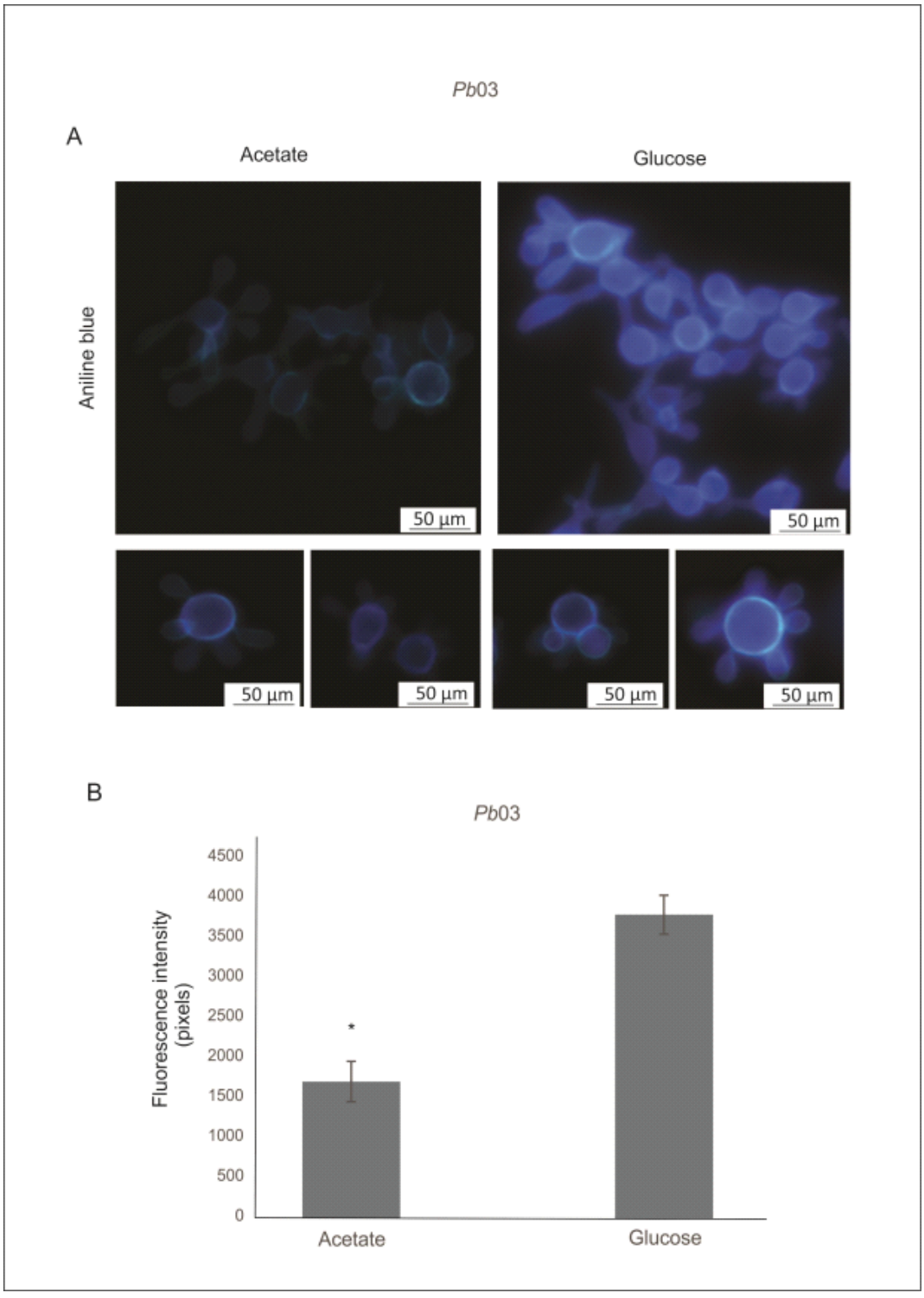

Supplemental Figure 3: Evaluation of β-1,3 glucan quantities in the cell wall of *P. brasiliensis* **isolate** *Pb*03**. (A)** Aniline blue was used to evaluate, by fluorescence microscopy, the presence of β-1,3 glucan in the cell wall of *Pb*03, after growth in MMcM medium with sodium acetate or glucose for 48 h. **(B)** Fluorescence intensity graph. The values of fluorescence intensity (in pixels) and the standard error of each analysis were used to plot the graph. Data are expressed as mean ± standard error (represented using error bars). (*) represents $p \leq 0.05$.

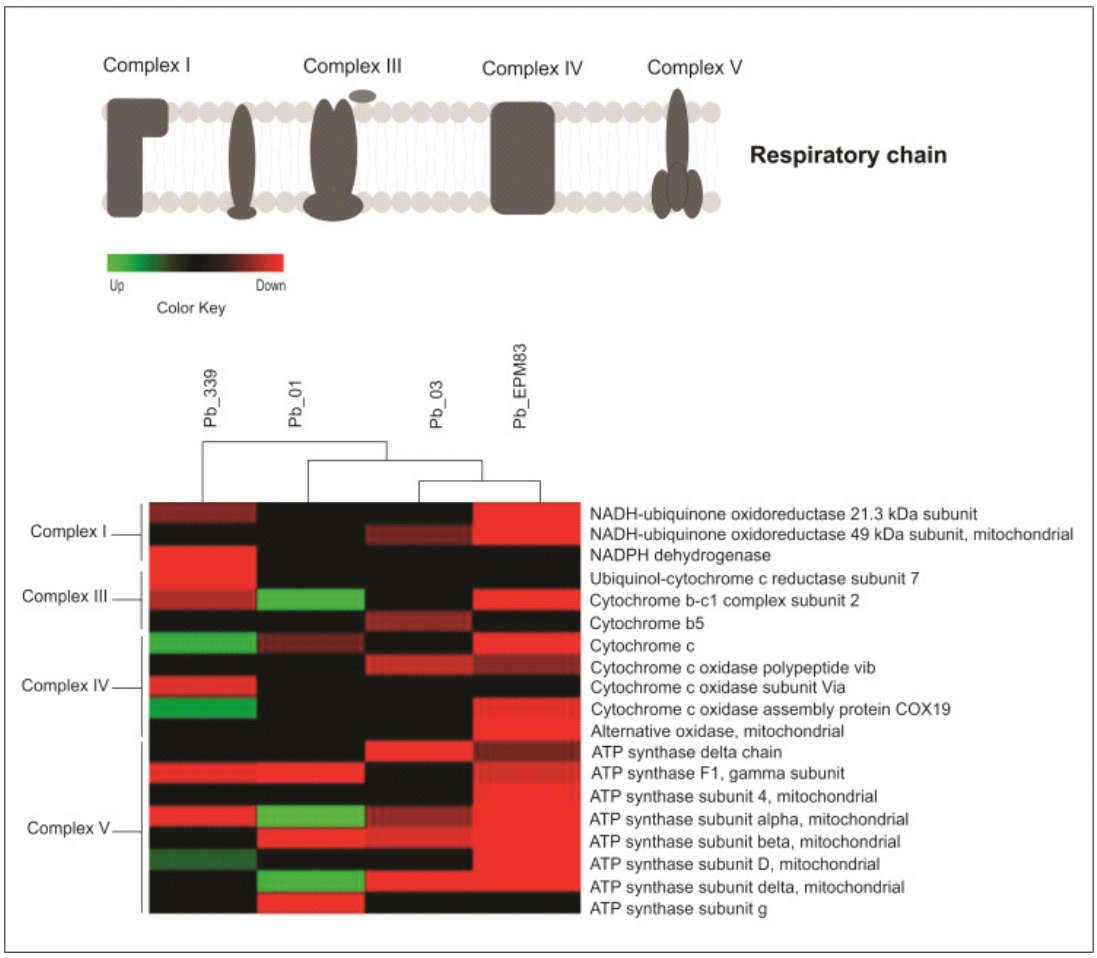

Supplemental Figure 4: Comparison of protein profiles related to electron transport and membrane-associated energy conservation in *P. lutzii* and isolates of *P. brasiliensis*. Data of expression set comparisons were carried out with the MultiExperiment Viewer software V.4.8 (www.tm4.org/mev/) that was used to group and compare data of expression and ANOVA test, applying a cut off at 1.5-fold expression changes. **A**- Changes in expression levels upon yeast cells incubated with acetate in *Pb*01, *Pb*03, *Pb*339 and *Pb*EPM83 in presence of sodium acetate 100 mM are represented in a heat map format. Mean values of experimental triplicates are shown for down regulation (green) and up regulation (red). **B**- Representative diagram of the electron transport and membrane-associated energy conservation in pathways depicting down regulated (green) and up regulated (red) in the isolates. Black means that no significant difference was observed.

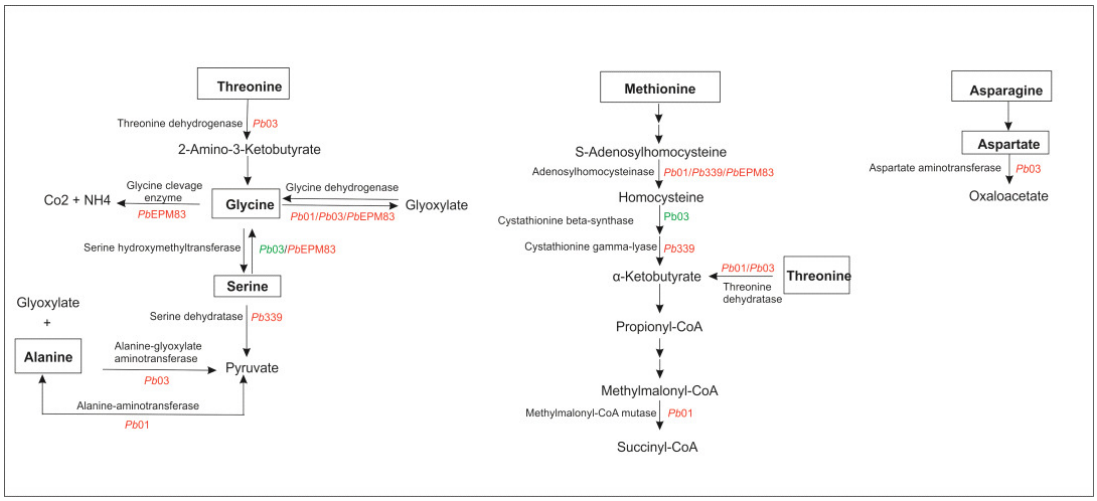

Supplemental Figure 5: Schematic representation of the degradation of the amino acids methionine, threonine, glycine, serine, alanine and aspartate in *P. lutzii* (*Pb*01) **and** *P. brasiliensis Pb*03, *Pb*339 and *Pb*EPM83 **in presence of sodium acetate 100 mM**. Proteins up regulated and down regulated in each isolate were depicted by colors red and green, respectively.

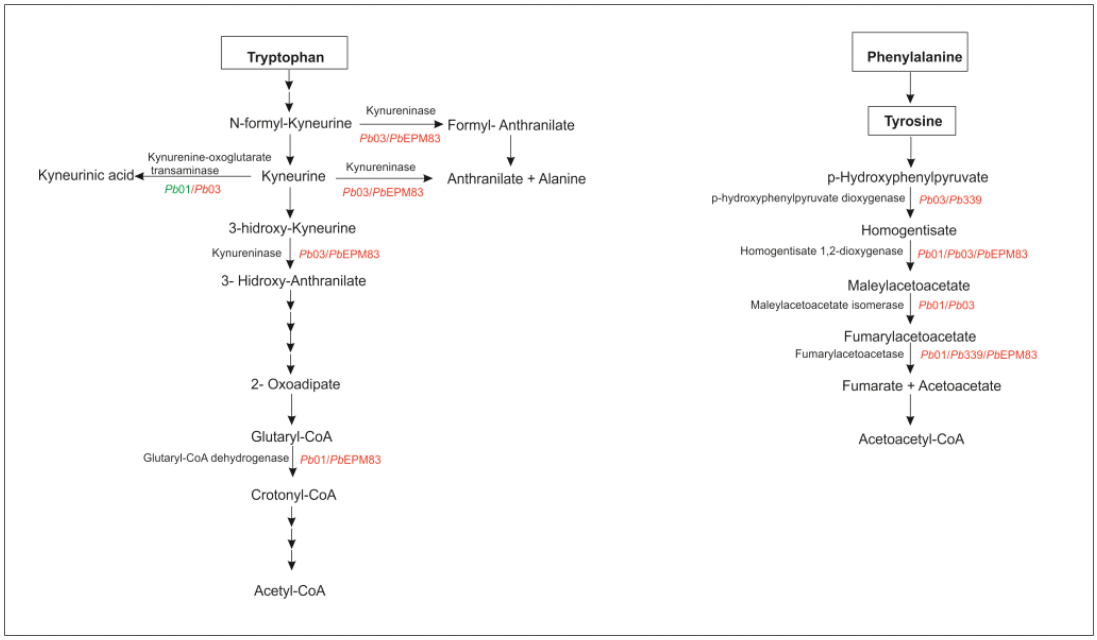

Supplemental Figure 6: Schematic representation of the degradation of the amino acids tryptophan, phenylalanine and tyrosine in *P. lutzii* (*Pb*01) **and** *P. brasiliensis Pb03, Pb339,* **and** *Pb*EPM83 **in presence of sodium acetate 100 mM.** Proteins up regulated and down regulated in each isolate were depicted by colors red and green, respectively.

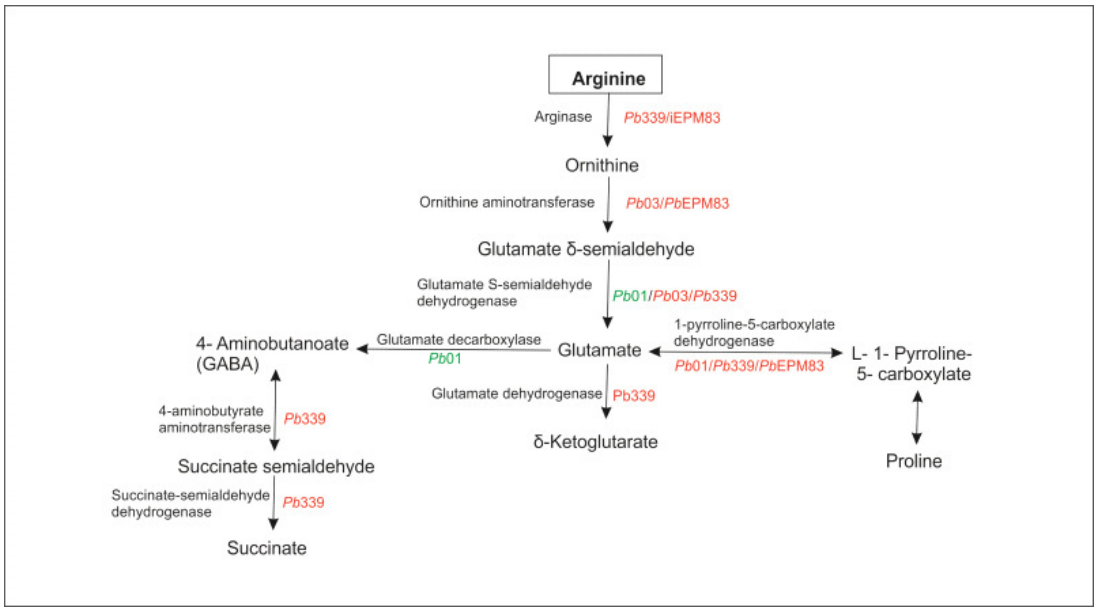

Supplemental Figure 7: Schematic representation of the degradation of the amino acids arginine, glutamate and proline in *P. lutzii* (*Pb*01) **and** *P. brasiliensis Pb*03, *Pb*339, **and** *Pb*EPM83 **in presence of sodium acetate 100 mM**. Proteins up regulated and down regulated in each isolate were depicted by colors red and green, respectively.

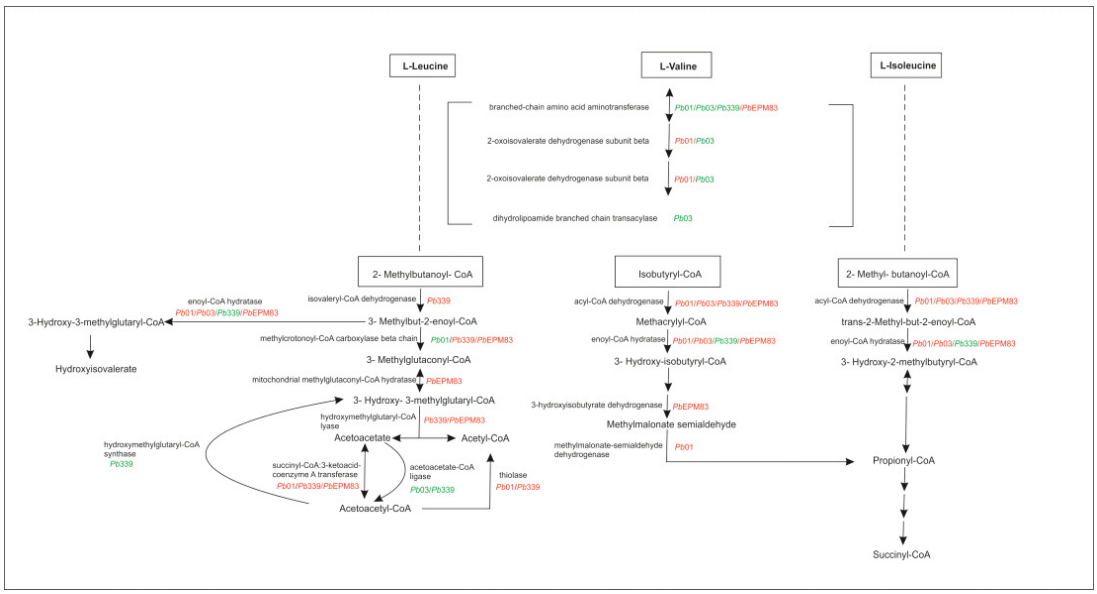

Supplemental Figure 8: Schematic representation of the degradation of the amino acids valine, leucine and isoleucine in *P. lutzii* (*Pb*01) **and** *P. brasiliensis Pb*03, *Pb*339, and *Pb*EPM83 **in presence of sodium acetate 100 mM.** Proteins up regulated and down regulated in each isolate were depicted by colors red and green, respectively.

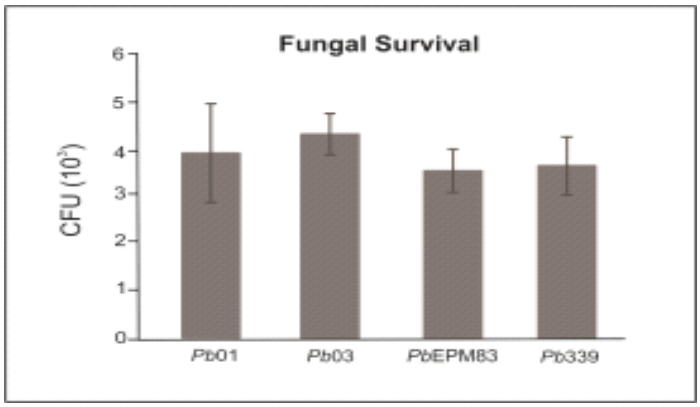

Supplemental Figure 9: Survival of *Paracoccidioides* isolates in macrophages during infection. *Paracoccidioides* yeast cells of the four isolates (*Pb*01, *Pb*03, *Pb*339 and *Pb*EPM83) were previously grown in BHI medium liquid ssupplemented with 4% (w/v) glucose up to 48 h and then were incubated with macrophages at a 1:5 macrophages: yeast cells ratio, for 24 h.The number of viable cells was determined by quantifying the number of colony forming units/mL (CFUs/mL) during infection from culture supernatant (non-internalized cells removed by aspiration prior to macrophages lysis) and after internalization. Data were expressed as mean ± standard error (represented using error bars) of the biological triplicates of independent experiments, using analysis of variance (ANOVA). There was no significant difference between the four isolates evaluated, for *p*-value of ≤0.05.

Supplemental Table 1: Proteins down-regulated in *Paracoccidioides lutzii* (Pb01) after growth for 48 hours in sodium acetate as carbon source.

Accession number[a]	Protein Description[b]	Acetate/Glucose Ratio[c]	Score
Functional categories[d]			
1. METABOLISM			
Amino acid metabolism			
PAAG_01383	3-deoxy-7-phosphoheptulonate synthase	0.35	80.55
PAAG_07605	Acetolactate synthase, small subunit	0.46	94.26
PAAG_04563	Amidophosphoribosyltransferase	0.38	68.93
PAAG_04401	Branched-chain amino acid aminotransferase	0.29	130.10
PAAG_03506	Glutamate decarboxylase	0.38	100.03
PAAG_00850	Glutamine-fructose-6-phosphate transaminase	0.10	350.67
PAAG_07089	Homocitrate synthase, mitochondrial	0.22	148.51
PAAG_01711	tRNA methyltransferase Trm5	0.51	107.16
PAAG_02603	Aspartate aminotransferase	0.45	164.90
PAAG_05743	Aromatic amino acid aminotransferase	0.55	10.86
PAAG_08900	2,2-dialkylglycine decarboxylase	0.37	48.37
PAAG_07566	Methionine aminopeptidase 2A	0.55	49.76

PAAG_04528	N-acetyl-gamma-glutamyl-phosphate reductase	0.39	155.54
PAAG_06289	Tryptophan synthase	0.26	92.44
PAAG_11922	3-hydroxyanthranilate 3,4-dioxygenase	0.43	18.54
Nitrogen, sulfur and selenium metabolism			
PAAG_06237	Urease accessory protein UreG	0.19	59.82
Nucleotide/nucleoside/nucleobase metabolism			
PAAG_06906	Adenine phosphoribosyltransferase	0.28	48.80
PAAG_08019	Adenylate kinase 1	0.66	65.27
PAAG_00316	Guanylate kinase	0.63	67.93
PAAG_06700	Uridylate kinase	0.33	77.05
PAAG_03466	5'-nucleotidase	0.45	32.68
PAAG_00886	Orotate phosphoribosyltransferase	0.41	10.58
PAAG_05613	Phosphoribosylglycinamide formyltransferase	0.34	17.28
PAAG_00211	Pyrimidine 5'-nucleotidase	0.23	15.96
PAAG_07682	Ribonucleoside-diphosphate reductase large chain	0.11	35.31
PAAG_08597	Thymidylate synthase	0.47	35.24
C-compound and carbohydrate metabolism			
PAAG_04888	4-coumarate-CoA ligase	0.30	69.57
PAAG_04602	Mannosyl-oligosaccharide glucosidase	0.34	37.84
PAAG_00889	Phosphomannomutase	0.61	169.26
PAAG_02382	Puinone oxidoreductase	0.27	178.56
PAAG_06817	UTP-glucose-1-phosphate uridylyltransferase	0.11	137.03
PAAG_04985	Magnesium-dependent phosphatase-1	0.30	18.42
PAAG_02767	Formamidopyrimidine-DNA glycosylase	0.56	6.55
Lipid, fatty acid and isoprenoid metabolism			
PAAG_01524	Fatty acid synthase subunit beta dehydratase	0.35	821.89
PAAG_03123	3-oxoacyl-(acyl-carrier-protein) reductase	0.20	10.60
PAAG_02007	Oxysterol binding protein	0.61	112.49
Metabolism of vitamins, cofactors, and prosthetic groups			
PAAG_00673	NUDIX domain-containing protein	0.63	17.04
PAAG_02418	Porphobilinogen deaminase	0.49	42.44
PAAG_05032	Uroporphyrinogen-III synthase	0.48	22.91
PAAG_06513	Biotin-protein ligase	0.63	49.10
PAAG_03464	Bleomycin hydrolase	0.19	90.89
2. ENERGY			
Glycolysis and gluconeogenesis			
PAAG_01583	6-phosphofructokinase subunit beta	0.59	220.05
PAAG_01015	Hexokinase	0.54	140.03

PAAG_02189	Aldolase	0.62	42.04
Pentose-phosphate pathway			
PAAG_01178	6-phosphogluconate dehydrogenase	0.62	316.09
PAAG_02633	Ribose-phosphate pyrophosphokinase 3	0.51	115.37
Tricarboxylic-acid pathway			
PAAG_07843	Aconitate hydratase	0.56	62.72
Electron transport and membrane-associated energy conservation			
PAAG_07586	Cytochrome b2	0.64	42.71
3. CELL CYCLE and DNA PROCESSING			
PAAG_02627	RuvB-like helicase 1	0.43	59.34
PAAG_09097	DNA mismatch repair protein Msh3	0.65	52.14
PAAG_02773	Ubiquitin-conjugating enzyme variant MMS2	0.44	45.34
PAAG_05197	Protein BCP1	0.18	41.13
PAAG_01325	Arf gtpase-activating protein	0.36	28.53
PAAG_03129	Dynein light chain	0.32	11.29
PAAG_04977	Ubiquitin-conjugating enzyme	0.66	34.66
PAAG_04846	COP9 signalosome complex subunit 4	0.55	17.31
PAAG_12506	Tubulin alpha-1 chain	0.17	94.72
PAAG_03031	Tubulin beta chain	0.43	73.92
PAAG_00317	Septin 4	0.45	83.35
4. TRANSCRIPTION			
PAAG_05734	DNA-directed RNA polymerases I and III	0.03	6.10
PAAG_02055	Histone chaperone asf1	0.52	41.84
PAAG_06917	KH domain RNA-binding protein	0.54	128.35
PAAG_06891	mRNA binding post-transcriptional regulator	0.40	73.27
PAAG_05121	Phosducin family protein	0.64	6.73
PAAG_08117	Transcriptional regulator	0.42	115.88
PAAG_04662	Cleavage and polyadenylation specificity factor subunit 5	0.61	134.41
PAAG_00723	Small nuclear ribonucleoprotein B and B'	0.66	66.05
PAAG_01062	Small nuclear ribonucleoprotein Sm D1	0.41	70.77
PAAG_08223	Small nuclear ribonucleoprotein Sm D3	0.65	23.75
PAAG_07775	Heat shock protein SSB1	0.61	336.29
PAAG_05711	Splicing factor U2AF 50 kDa subunit	0.47	44.94
PAAG_00847	Multifunctional methyltransferase subunit	0.46	11.71
PAAG_03941	G4 quadruplex nucleic acid binding protein	0.58	142.62
PAAG_05172	Zinc finger protein zpr1	0.48	76.86
PAAG_11028	DNA polymerase epsilon subunit C	0.50	12.00
5. PROTEIN SYNTHESIS			

PAAG_01097	Poly(rC)-binding protein	0.51	112.89
PAAG_00385	40S ribosomal protein S23	0.64	91.94
PAAG_09083	TCTP family protein	0.53	94.75
PAAG_00724	60S ribosomal protein L11	0.63	117.35
PAAG_00801	60S acidic ribosomal protein P0	0.45	53.61
PAAG_02578	Mitochondrial 54S ribosomal protein MRPL51	0.64	33.18
PAAG_05484	40S ribosomal protein S5	0.55	154.19
PAAG_09043	40S ribosomal protein S2	0.52	176.32
PAAG_08205	26S proteasome non-ATPase regulatory subunit 6	0.65	113.45
PAAG_05943	26S proteasome non-ATPase regulatory subunit 12	0.62	73.96
PAAG_00234	Translation initiation factor IF-2	0.50	41.56
PAAG_00689	ATP-dependent RNA helicase eIF4A	0.44	179.97
PAAG_01330	Eukaryotic translation initiation factor 3	0.28	29.64
PAAG_01425	Eukaryotic translation initiation factor 3	0.47	63.36
PAAG_01951	Eukaryotic translation initiation factor 3 subunit E	0.24	79.25
PAAG_06489	Eukaryotic translation initiation factor 3 subunit 8	0.48	139.32
PAAG_08817	Translation initiation factor 2 subunit beta	0.24	43.33
PAAG_09045	Eukaryotic translation initiation factor 4E-1	0.62	54.26
PAAG_00594	Elongation factor 2	0.57	857.93
PAAG_00376	Eukaryotic translation initiation factor 3 subunit F	0.35	60.89
PAAG_07283	ATP-dependent RNA helicase FAL1	0.39	117.76
PAAG_03652	Cap binding protein	0.28	41.56
PAAG_01698	Translation initiation factor eIF3	0.23	74.17
PAAG_04511	ATP-dependent RNA helicase SUB2	0.05	170.38
PAAG_07506	Nuclear cap-binding protein subunit 2	0.33	21.06
PAAG_02828	RNA binding domain-containing protein	0.62	30.26
PAAG_08680	RNA binding domain-containing protein	0.36	32.61
PAAG_11075	Eukaryotic translation initiation factor 5A	0.48	26.02
PAAG_11418	Elongation factor 1-alpha	0.40	464.33
PAAG_03556	Elongation factor 1 gamma domain-containing	0.60	359.69
PAAG_01292	Eukaryotic peptide chain release factor	0.39	89.84
PAAG_00338	Methionyl-tRNA synthetase	0.49	90.53
PAAG_02251	Asparaginyl-tRNA synthetase	0.60	120.98

6. PROTEIN FATE

PAAG_01727	T-complex protein 1 subunit delta	0.31	157.18
PAAG_05226	Hsp90 binding co-chaperone (Sba1)	0.65	60.15
PAAG_06068	T-complex protein 1 subunit beta	0.39	239.97
PAAG_07165	T-complex protein 1 subunit gamma	0.43	199.20
PAAG_00797	Chaperone DnaJ	0.30	113.76
PAAG_07039	Sorting nexin 3	0.54	29.09

PAAG_07286	Vacuolar protein sorting-associated protein	0.60	45.42
PAAG_05736	Ubiquitin mediated proteolysis	0.02	10.46
PAAG_04327	Ubiquitin carboxyl-terminal hydrolase	0.64	122.33
PAAG_01479	26S protease regulatory subunit 8	0.18	118.20
PAAG_01706	26S proteasome regulatory subunit RPN10	0.61	12.26
PAAG_02907	26S proteasome non-ATPase regulatory	0.49	87.45
PAAG_04899	26S protease regulatory subunit 4	0.43	40.52
PAAG_08020	26S proteasome regulatory subunit rpn-8	0.34	133.82
PAAG_00202	Ubiquitin carboxyl-terminal hydrolase	0.64	116.22
PAAG_00770	26S protease regulatory subunit	0.25	105.04
PAAG_11406	26S protease regulatory subunit 6B	0.64	118.98
PAAG_01926	26S proteasome regulatory subunit T5	0.22	91.50
PAAG_12272	26S proteasome regulatory subunit rpn11	0.67	29.64
PAAG_11969	Nuclear distribution protein PAC1	0.57	125.59
PAAG_02865	Translation initiation factor RLI1	0.58	136.92
PAAG_03018	26S proteasome complex ubiquitin receptor	0.24	62.92

7. PROTEIN WITH BINDING FUNCTION or COFACTOR REQUIREMENT

PAAG_05680	NTF2 and RRM domain-containing protein	0.33	22.76
PAAG_05087	RNA-binding domain-containing protein	0.37	152.85
PAAG_03970	Replication factor-A protein	0.37	16.42
PAAG_08356	AP-1 complex subunit beta-1	0.16	50.01
PAAG_00782	Small COPII coat GTPase sar1	0.52	91.82
PAAG_01452	ADP-ribosylation factor	0.65	6.56
PAAG_02820	GTP-dependent nucleic acid-binding protein engD	0.54	201.00
PAAG_08028	GTP-binding protein ypt1	0.47	97.85
PAAG_08703	Rheb small monomeric GTPase RhbA	0.63	5.75
PAAG_07444	Chaperone protein dnaK	0.53	60.16

8. CELLULAR TRANSPORT, TRANSPORT FACILITIES and TRANSPORT ROUTES

PAAG_04651	GTP-binding nuclear protein GSP1/Ran	0.58	239.90
PAAG_04904	ABC transporter ATP-binding protein ARB1	0.33	119.93
PAAG_04953	Reduced viability upon starvation protein	0.58	58.04
PAAG_12449	Importin beta-3 subunit	0.63	15.07
PAAG_06657	Importin subunit alpha-1	0.04	61.27

9. CELLULAR COMMUNICATION/SIGNAL TRANSDUCTION MECHANISM

PAAG_04197	Suppressor of G2 allele of SKP1	0.61	32.19
PAAG_03353	Signal recognition particle 14kD protein	0.35	24.53
PAAG_07634	Small GTPase RhoA	0.58	121.49
PAAG_02377	Rho GDP-dissociation inhibitor	0.62	173.86
PAAG_07900	Phosphatidylinositol-phosphatidylcholine transfer	0.67	117.81
PAAG_00783	Serine/threonine-protein phosphatase PP1	0.43	104.62
PAAG_05737	Calcium/calmodulin-dependent protein kinase	0.52	54.92

PAAG_04743	Casein kinase II subunit alpha	0.49	29.14
PAAG_07054	COP9 signalosome complex subunit 7a	0.34	17.97
PAAG_05449	RAC-alpha serine/threonine-protein kinase	0.33	19.03
PAAG_05129	Serine/threonine protein phosphatase 2A	0.55	34.11
PAAG_07339	S-phase kinase-associated protein 1A	0.52	97.30
PAAG_03659	Protein kinase gsk3	0.63	112.29
PAAG_03643	6-phosphofructo-2-kinase	0.66	72.71
10. CELL RESCUE, DEFENSE and VIRULENCE			
Stress response			
PAAG_05679	Heat shock protein	0.07	688.41
Detoxification			
PAAG_03290	Thioredoxin	0.41	49.66
PAAG_03216	Mitochondrial peroxiredoxin PRX1	0.33	165.36
PAAG_01849	Glutaredoxin	0.48	25.26
11. BIOGENESIS of CELLULAR COMPONENTS			
Cytoskeleton/structural proteins			
PAAG_03532	Actin	0.43	253.78
PAAG_00004	Actin binding protein	0.53	181.29
PAAG_05638	F-actin-capping protein subunit beta	0.26	57.91
PAAG_01272	F-actin-capping protein subunit alpha	0.27	72.11
PAAG_05414	Septum formation protein Maf	0.27	17.45
12. MISCELLANEOUS			
PAAG_08941	AmmeMemoRadiSam system protein B	0.65	36.22
PAAG_07829	Phosphatase family protein	0.20	37.39
PAAG_08992	Ttype 2A phosphatase activator tip41	0.46	45.23
PAAG_07874	Hepatocellular carcinoma down-regulated mitochondrial	0.21	43.57
13. UNCLASSIFIED			
PAAG_00059	Hypothetical protein	0.41	31.08
PAAG_00117	Hypothetical protein	0.53	24.78
PAAG_00220	Hypothetical protein	0.53	65.34
PAAG_00579	Hypothetical protein	0.48	126.90
PAAG_00828	Hypothetical protein	0.50	21.21
PAAG_01121	Hypothetical protein	0.01	9.88
PAAG_01695	Hypothetical protein	0.58	98.52
PAAG_01919	Hypothetical protein	0.62	20.42
PAAG_02072	Hypothetical protein	0.54	15.78
PAAG_02270	Hypothetical protein	0.23	16.00
PAAG_02353	Hypothetical protein	0.28	27.45
PAAG_02386	Hypothetical protein	0.65	10.25

PAAG_03179	Hypothetical protein	0.15	16.84
PAAG_03624	Hypothetical protein	0.55	109.99
PAAG_03636	Hypothetical protein	0.48	16.55
PAAG_04278	Hypothetical protein	0.27	10.74
PAAG_05315	Hypothetical protein	0.10	11.67
PAAG_06338	Hypothetical protein	0.57	4.54
PAAG_06679	Hypothetical protein	0.66	37.78
PAAG_06711	Hypothetical protein	0.06	5.21
PAAG_06837	Hypothetical protein	0.22	5.93
PAAG_07132	Hypothetical protein	0.49	26.37
PAAG_07521	Hypothetical protein	0.65	4.69
PAAG_07606	Hypothetical protein	0.63	45.73
PAAG_07633	Hypothetical protein	0.36	38.69
PAAG_07883	Hypothetical protein	0.17	38.79
PAAG_08058	Hypothetical protein	0.55	187.52
PAAG_08799	Hypothetical protein	0.02	10.44
PAAG_11167	Hypothetical protein	0.31	15.93
PAAG_11176	Hypothetical protein	0.48	10.65
PAAG_11364	Hypothetical protein	0.47	69.22
PAAG_11583	Hypothetical protein	0.34	16.82
PAAG_11610	Hypothetical protein	0.59	5.67
PAAG_11708	Hypothetical protein	0.49	31.87
PAAG_11835	Hypothetical protein	0.30	64.31
PAAG_12288	Hypothetical protein	0.40	319.63
PAAG_12503	Hypothetical protein	0.26	6.28
PAAG_12620	Hypothetical protein	0.59	140.68

[a] Identification of differentially regulated proteins from *Paracoccidioides* genome database (http://www.broadinstitute.org/annotation/genome/paracoccidioides_brasiliensis/MultiHome.html) using the ProteinLynx Global Server vs. 2.4 (PLGS) (Waters Corporation, Manchester, UK).

[b] Proteins annotation from *Paracoccidioides* genome database or by homology from NCBI database (http://www.ncbi.nlm.nih.gov/)

[c] Acetate/Glucose means: The level of expression in yeast cells derived from cultured in sodium acetate divided by the level in the control yeast cells cultured in glucose.

[d] Biological process of differentially expressed proteins from MIPS (http://mips.helmholtz-muenchen.de/funcatDB/) and Uniprot databases (http://www.uniprot.org/).

Supplemental Table 2: Proteins up-regulated in *Paracoccidioides lutzii* (Pb01) after growth for 48 hours in sodium acetate as carbon source.

Accession number[a]	Protein Description[b]	Acetate/Glucose Ratio[c]	Score
Functional categories[d]			
1. METABOLISM			
Amino acid metabolism			
PAAG_02975	2,4-dihydroxyhept-2-ene-1,7-dioic acid aldolase	2.32	60.36
PAAG_05481	2-isopropylmalate synthase	3.32	81.98
PAAG_01194	2-oxoisovalerate dehydrogenase subunit beta	1.64	81.87
PAAG_03978	3-hydroxyisobutyrate dehydrogenase	1.65	202.80
PAAG_05328	3-isopropylmalate dehydrogenase A	2.05	66.19
PAAG_02859	Adenosylhomocysteinase	1.99	337.84
PAAG_08207	Alanine aminotransferase	1.73	45.84
PAAG_08668	Anthranilate synthase component 2	1.93	260.85
PAAG_01969	Arginase	2.42	39.72
PAAG_01144	Aspartate aminotransferase	1.81	64.44
PAAG_08065	Aspartate-semialdehyde dehydrogenase	1.67	158.87
PAAG_09095	ATP phosphoribosyltransferase	5.32	40.67
PAAG_01365	Choline dehydrogenase	1.95	137.69
PAAG_05198	Chorismate mutase	4.96	96.77
PAAG_08405	Cystathionine beta-lyase	1.73	89.64
PAAG_05253	Delta-1-pyrroline-5-carboxylate dehydrogenase	3.71	283.08
PAAG_05776	Dihydroxy-acid dehydratase	1.61	145.93
PAAG_08163	Fumarylacetoacetase	1.85	177.34
PAAG_00869	Fumarylacetoacetate hydrolase domain-containing protein	1.77	73.60
PAAG_01649	Gamma-butyrobetaine dioxygenase	2.13	13.51
PAAG_07954	Gamma-glutamyl phosphate reductase	1.74	160.31
PAAG_08931	Glutamate carboxypeptidase	1.62	174.62
PAAG_01568	Glycine dehydrogenase	1.56	344.68
PAAG_05406	Histidine biosynthesis trifunctional protein	5.41	374.39
PAAG_08164	Homogentisate 1,2-dioxygenase	2.85	179.08
PAAG_01991	Homoserine dehydrogenase	1.55	98.08
PAAG_02644	Kynurenine-oxoglutarate transaminase	3.39	164.08
PAAG_02217	Isochorismatase domain-containing protein	3.32	124.54
PAAG_04083	Isochorismatase family hydrolase	2.96	13.75
PAAG_11161	L-serine dehydratase	1.76	18.19
PAAG_03092	TPA: putative Conserved lysine-rich protein	4.41	179.83
PAAG_08162	Maleylacetoacetate isomerase	1.86	69.23
PAAG_04103	Methylcrotonoyl-CoA carboxylase beta chain	1.55	206.48
PAAG_07036	Methylmalonate-semialdehyde dehydrogenase	1.66	206.70
PAAG_01302	S-methyl-5'-thioadenosine phosphorylase	2.09	120.37
PAAG_00047	Porphyrin and chlorophyll metabolism	2.00	62.76

PAAG_05847	Saccharopine dehydrogenase	2.10	11.58
PAAG_03168	Threonine dehydratase	2.35	88.86
PAAG_03537	Lysine decarboxylase-like protein	1.72	92.48
Nitrogen, sulfur and selenium metabolism			
PAAG_04233	2-nitropropane dioxygenase	1.82	59.48
PAAG_06606	Cyanate hydratase	1.87	56.15
PAAG_03333	Formamidase	2.03	202.65
PAAG_00954	Urease	1.57	273.15
Nucleotide/nucleoside/nucleobase metabolism			
PAAG_07312	CTP synthase	2.21	55.27
PAAG_02333	GMP synthase	1.62	51.87
PAAG_08438	Purine nucleoside phosphorylase	1.66	17.94
PAAG_01437	Uricase	2.76	89.60
PAAG_05242	Carbamoyl-phosphate synthase	1.76	176.96
PAAG_03904	DNA-directed RNA polymerase III subunit Rpc5	2.10	15.40
PAAG_04929	DNA-directed RNA polymerase III subunit RPC7	1.56	13.25
PAAG_04919	Nucleoside-diphosphate-sugar epimerase	2.00	41.97
Phosphate metabolism			
PAAG_00661	4-nitrophenylphosphatase	1.81	43.02
PAAG_08277	Nitroreductase family protein	2.03	130.99
C-compound and carbohydrate metabolism			
PAAG_03776	Inositol-3-phosphate synthase	2.16	83.51
PAAG_04181	Sorbitol utilization protein SOU2	1.61	78.13
PAAG_05416	NADP-dependent leukotriene B4	1.51	76.89
PAAG_03765	NADP-dependent glycerol dehydrogenase	1.80	49.12
PAAG_07276	Glycogen synthase	2.32	133.32
PAAG_03243	Aldose 1-epimerase family protein	1.65	147.72
PAAG_05287	Amidohydrolase	1.61	21.87
Lipid, fatty acid and isoprenoid metabolism			
PAAG_06329	3-hydroxybutyryl-CoA dehydrogenase	2.40	107.88
PAAG_02664	3-ketoacyl-CoA thiolase	2.20	245.70
PAAG_07746	3-ketoacyl-CoA thiolase	2.00	93.78
PAAG_03447	Acetyl-CoA acetyltransferase	2.17	145.13
PAAG_05454	Acyl-CoA dehydrogenase	2.00	211.80
PAAG_03116	Acyl-coenzyme A oxidase	2.46	89.66
PAAG_06309	Enoyl-CoA hydratase	1.57	227.79
PAAG_06392	Enoyl-CoA hydrataseily protein	1.57	29.07
PAAG_05690	Esterase D	2.26	145.43
PAAG_05984	Glutaryl-CoA dehydrogenase	1.56	210.74

PAAG_03960	Isopentenyl-diphosphate Delta-isomerase	1.65	53.10
PAAG_00976	LiPid Depleted family member	1.70	17.46
PAAG_11860	Nonspecific lipid-transfer protein _ Transport	1.58	95.15
PAAG_01928	Peroxisomal dehydratase	1.59	47.87
PAAG_05093	Succinyl-CoA:3-ketoacid-coenzyme A	1.68	205.21
PAAG_01557	Short-chain dehydrogenase	2.10	5.24
PAAG_01269	Diacylglycerol pyrophosphate Phosphatase	1.87	5.37
Metabolism of vitamins, cofactors, and prosthetic groups			
PAAG_01227	3-methyl-2-oxobutanoatehydroxymethyltransferase	2.11	25.62
PAAG_03709	5-formyltetrahydrofolate ciclo-ligase	2.59	21.64
PAAG_00851	6,7-dimethyl-8-ribityllumazine synthase	2.46	37.65
PAAG_07321	Pyridoxine biosynthesis protein PDX1	1.52	115.30
PAAG_03345	Phosphotyrosine protein phosphatase	9.31	34.90
PAAG_08427	Aldose reductase	1.65	27.09
PAAG_03106	ThiJ/PfpI family protein	5.31	75.64
PAAG_03631	1,2-oxophytodienoate reductase	1.58	264.85
PAAG_03741	Hydrolase-HD superfamily protein	5.01	11.17
PAAG_11532	Arylamine N-acetyltransferase 1	1.90	23.01
PAAG_06083	Dienelactone hydrolase family protein	2.12	82.35
PAAG_07875	Lactoylglutathione lyase	2.07	27.49
PAAG_00293	Quinone oxidoreductase	3.31	83.85
PAAG_00566	Aflatoxin B1 aldehyde reductase member 2	3.25	177.32
PAAG_04966	Hydrolase	1.52	117.50
2. ENERGY			
Glycolysis and gluconeogenesis			
PAAG_02682	Fructose-1,6-bisphosphatase	1.57	116.33
PAAG_01995	Fructose-bisphosphate aldolase	1.56	319.12
PAAG_06172	Glucokinase	2.18	178.62
PAAG_08468	Glyceraldehyde-3-phosphate dehydrogenase	1.53	373.46
PAAG_11035	Pyruvate dehydrogenase protein X component	1.66	226.61
Ethanol production			
PAAG_00403	Alcohol dehydrogenase	5.88	287.75
PAAG_04541	Alcohol dehydrogenase	6.33	247.18
PAAG_08911	Alcohol dehydrogenase	1.62	73.52
PAAG_03910	Aldehyde dehydrogenase	1.70	123.61
PAAG_02050	Pyruvate decarboxylase	1.66	216.82
Pentose-phosphate pathway			
PAAG_00633	Glucose-6-phosphate 1-dehydrogenase	1.77	153.57
PAAG_05940	Deoxyribose-phosphate aldolase	1.67	69.76
PAAG_05146	Ribose 5-phosphate isomerase A	1.92	41.82

Tricarboxylic-acid pathway			
PAAG_02732	2-oxoglutarate dehydrogenase E1	1.60	473.32
PAAG_08075	Citrate synthase	1.95	259.33
PAAG_08915	Dihydrolipoamide succinyltransferase	2.13	185.60
PAAG_00588	Fumarate hydratase	2.04	226.02
PAAG_00856	Isocitrate dehydrogenase subunit 1	1.56	209.92
PAAG_00053	Malate dehydrogenase	1.59	426.26
PAAG_01725	Succinate dehydrogenase flavoprotein subunit	3.46	197.78
PAAG_06103	Succinate dehydrogenase iron-sulfur subunit	3.29	61.54
PAAG_00417	Succinyl-CoA ligase subunit alpha	1.71	226.10
PAAG_05048	3-isopropylmalate dehydratase large subunit	2.57	521.25
Glyoxylate cycle			
PAAG_06951	Isocitrate lyase	2.99	303.75
PAAG_04542	Malate synthase	1.73	267.72
Methylcytrate cycle			
PAAG_04550	2-methylcitrate synthase	2.67	426.54
PAAG_04559	2-methylcitrate dehydratase	2.00	435.38
Electron transport and membrane-associated energy conservation			
PAAG_05605	ATP synthase delta chain	4.23	71.72
PAAG_05576	ATP synthase gamma chain	2.17	145.13
PAAG_08037	ATP synthase subunit beta	4.06	364.59
PAAG_08551	ATP synthase subunit g	2.44	82.59
PAAG_04820	ATPase alpha subunit	3.59	391.46
PAAG_12575	Cytochrome b5	1.59	17.14
PAAG_08088	Cytochrome b-c1 complex subunit 2	3.13	124.12
PAAG_06268	Cytochrome c	1.52	130.71
PAAG_07246	Cytochrome c oxidase subunit VIa	1.54	107.19
PAAG_07672	Ubiquinol-cytochrome c reductase subunit 7	3.76	43.06
PAAG_12013	NADH dehydrogenase subunit 5	1.93	4.76
3. CELL CYCLE and DNA PROCESSING			
PAAG_00883	ATP-dependent DNA helicase	1.52	134.49
PAAG_00170	Chromosome transmission fidelity protein	1.96	71.92
PAAG_06491	DNA repair and recombination protein RAD26	2.31	60.70
PAAG_07273	DNA replication licensing factor mcm5	1.51	154.90
PAAG_01520	DNA-binding protein HGH1	2.20	34.09
PAAG_05824	MACRO domain-containing protein	2.08	74.54
PAAG_00294	Replication factor-A protein	1.85	83.06
PAAG_06486	DNA polymerase alpha catalytic subunit	9.40	48.89
PAAG_06260	Calcineurin binding protein	1.73	22.48

PAAG_07192	Microtubule-associated protein RP/EB family member 3	3.21	70.37
PAAG_05476	ADP-ribosylation factor family protein	2.49	20.77
PAAG_06202	CENP-Q a CENPA-CAD centromere complex subunit	2.24	22.35
4. TRANSCRIPTION			
PAAG_08917	Histone H2a	1.91	62.19
PAAG_08918	Late histone H2B.L4	2.01	80.59
PAAG_07099	Histone H3.3	2.27	58.96
PAAG_07098	Histone H4.1	1.85	125.77
PAAG_00126	Histone H4.2	2.25	147.14
PAAG_01558	CBF/NF-Y family transcription factor	2.91	31.93
PAAG_04814	Nucleic acid-binding protein	2.42	171.63
PAAG_04726	Pirin	1.65	118.47
PAAG_01710	Polymerase II polypeptide D	1.96	140.07
PAAG_00469	Transcription elongation factor spt4	2.38	16.67
PAAG_02276	ATP-dependent RNA helicase suv3	1.52	98.19
PAAG_02801	tRNA ligase	1.88	62.55
PAAG_02255	mRNA decapping hydrolase	2.29	113.71
PAAG_03277	Pre-mRNA-processing factor 39	3.86	94.59
PAAG_06168	Peptidyl-prolyl cis-trans isomerase cypE	1.74	78.28
PAAG_11921	Pre-mRNA-splicing factor	1.62	253.01
PAAG_00714	Nuclear transport factor 2 domain-containing	1.79	19.16
PAAG_04767	U4/U6 small nuclear ribonucleoprotein PRP4	6.23	10.98
PAAG_01394	Poly(A) RNA polymerase cid14	1.98	85.58
PAAG_02434	C6 zinc finger domain containing protein	1.79	64.12
PAAG_04647	RNA binding protein	2.57	34.86
PAAG_00992	Heterogeneous nuclear ribonucleoprotein HRP1	2.33	6.29
5. PROTEIN SYNTHESIS			
PAAG_06367	40S ribosomal protein S11	1.56	139.88
PAAG_04965	60S ribosomal protein L31	1.78	115.41
PAAG_07550	60S ribosomal protein L42	1.57	79.91
PAAG_01412	40S ribosomal protein S17	2.05	74.55
PAAG_08153	50S ribosomal protein L6	3.07	25.83
PAAG_08285	50S ribosomal protein L12	1.78	131.23
PAAG_01731	54S ribosomal protein L37	1.60	31.99
PAAG_00302	Exportin-1	2.22	82.74
PAAG_00747	Eukaryotic translation initiation factor 2 subunit gamma	1.60	173.40
PAAG_02582	Elongation factor 2	2.78	57.31
PAAG_07381	Eukaryotic peptide chain release factor subunit 1	2.03	93.13
PAAG_02071	Glutamyl-tRNA synthetase	2.46	334.35
PAAG_08702	Seryl-tRNA synthetase	1.82	207.91
PAAG_05103	Threonyl-tRNA synthetase	1.73	101.26
PAAG_04742	Valyl-tRNA synthetase	1.72	318.84

PAAG_05969	Translation initiation factor 2[a]	2.77	18.49
PAAG_00772	Translation initiation factor 3 subunit J	2.52	100.81
6. PROTEIN FATE			
PAAG_01726	26S protease regulatory subunit 8	2.36	93.03
PAAG_03191	26S proteasome non-ATPase regulatory subunit 1	1.72	125.14
PAAG_05962	26S proteasome non-ATPase regulatory subunit 3	2.10	143.38
PAAG_05029	26S proteasome regulatory subunit RPN9	1.63	84.03
PAAG_02026	Ankyrin repeat protein	2.23	19.75
PAAG_02772	Endosomal peripheral membrane protein	19.29	53.87
PAAG_09122	FK506-binding protein	1.86	31.95
PAAG_02974	Glutaredoxin domain-containing protein	3.27	41.85
PAAG_01854	Golgi apparatus membrane protein TVP18	1.70	46.95
PAAG_03161	GTP-binding protein ypt5	2.40	79.88
PAAG_06255	Mitochondrial co-chaperone GrpE	2.26	194.69
PAAG_03772	Mitochondrial import inner translocase subunit tim9	1.64	27.00
PAAG_00109	Mitochondrial intermembrane subunit Tim	5.69	6.03
PAAG_05417	Mitochondrial-processing peptidase subunit beta	1.90	175.07
PAAG_07490	Monothiol glutaredoxin-5	1.83	84.84
PAAG_05788	Peptidyl-prolyl cis-trans isomerase A2	1.68	152.72
PAAG_00739	Peptidyl-prolyl cis-trans isomerase B	3.25	112.77
PAAG_07509	Peptidyl-prolyl cis-trans isomerase ssp1	1.53	79.96
PAAG_06250	Peptidylprolyl isomerase	1.82	35.93
PAAG_03101	Prefoldin subunit 1	1.73	69.84
PAAG_00852	Proteasome component C1	1.60	134.41
PAAG_03536	Proteasome component PRE5	1.58	142.38
PAAG_00071	Proteasome component Y7	1.58	136.20
PAAG_08141	Proteasome subunit alpha type-4	1.58	135.25
PAAG_11221	Pyroglutamyl peptidase type	1.59	33.40
PAAG_12392	T-complex protein 1 subunit zeta	4.80	100.78
PAAG_00295	Ubiquitin carboxyl-terminal hydrolase	2.23	132.99
PAAG_02254	Ubiquitin carboxyl-terminal hydrolase	1.86	65.44
PAAG_04282	UBX domain-containing protein	1.64	51.91
PAAG_07890	Vacuolar-sorting protein snf7_Endocytosis	1.83	23.51
PAAG_07500	Xaa-Pro aminopeptidase	4.52	130.01
PAAG_00664	Aspartyl aminopeptidase	1.54	193.14
7. PROTEIN WITH BINDING FUNCTION or COFACTOR REQUIREMENT			
PAAG_11982	YbgI/family dinuclear metal center protein	2.49	17.59
PAAG_04391	Progesterone binding protein	3.95	92.85
PAAG_08648	GTP-binding protein RBG1	2.63	41.64
PAAG_11679	Chaperone protein clpB	1.97	172.93
8. CELLULAR TRANSPORT, TRANSPORT FACILITIES and TRANSPORT ROUTES			

PAAG_00555	Coatomer subunit epsilon	3.47	23.96
PAAG_08359	Coatomer subunit alpha	1.72	170.24
PAAG_08103	EF hand domain-containing protein	7.40	66.14
PAAG_01500	GTP-binding protein SAS1	2.05	55.97
PAAG_08093	GTP-binding protein ypt3	1.99	159.56
PAAG_00326	Heavy metal ion transporter, putative	1.57	28.57
PAAG_12133	Lactose permease	8.25	10.93
PAAG_06752	Mitochondrial ATPase inhibitor, IATP family protein	2.76	69.19
PAAG_04243	Na+/K+-exchanging ATPase alpha chain	2.04	47.88
PAAG_04276	Phosphatidylinositol transporter	1.89	94.54
PAAG_07341	Transport protein particle subunit bet5	9.74	15.65
PAAG_12424	Voltage-dependent anion channel protein 1	1.51	12.17

9. CELLULAR COMMUNICATION/SIGNAL TRANSDUCTION MECHANISM

PAAG_00332	cAMP-regulated phosphoprotein family protein Igo1	1.61	45.71
PAAG_02599	Phosphorelay intermediate protein YPD1	1.50	28.29
PAAG_01602	Ras-like GTP-binding protein	4.20	19.24
PAAG_04274	Protein phosphatase inhibitor 2 (IPP-2)	4.58	46.79

10. CELL RESCUE, DEFENSE and VIRULENCE

Stress response

PAAG_00871	30 kDa heat shock protein	3.43	223.90
PAAG_08059	Heat shock protein	2.25	900.66
PAAG_01262	Hsp70-like protein	1.53	456.40
PAAG_11262	Hsp7-like protein	1.69	549.72
PAAG_05142	10 kDa heat shock protein	2.26	164.83

Detoxification

PAAG_01454	Catalase	2.72	334.92
PAAG_05860	Glutamate-cysteine ligase	5.56	28.19
PAAG_04164	Superoxide dismutase Cu/Zn SOD1	3.38	58.63
PAAG_02725	Superoxide dismutase Fe/Mn SOD2	3.71	153.18
PAAG_02926	Superoxide dismutase Fe/Mn SOD5	2.55	98.31
PAAG_05292	Glutathione reductase	1.61	153.12
PAAG_03931	Glutathione S-transferase Gst3	4.71	90.39

11. BIOGENESIS OF CELLULAR COMPONENTS

Cell wall

PAAG_00651	Alpha-1,3-glucan synthase	3.04	11.53
PAAG_01874	Dolichol-phosphate mannosyltransferase	1.58	23.58
PAAG_01136	Beta-hexosaminidase	4.81	46.84
PAAG_08038	1,4-alpha-glucan-branching enzyme	1.94	144.62

Cytoskeleton/strucutural proteins

PAAG_00564	Actin	1.96	106.74
PAAG_07185	Actin like protein 2/3 complex, subunit 5	5.14	69.65
PAAG_08252	Clathrin light chain	1.64	101.04
PAAG_00529	Cytoskeletal adaptor protein SagA	1.52	121.01
PAAG_07958	Fimbrin	1.62	219.14

12. MISCELLANEOUS

PAAG_05905	Programmed cell death protein 5	2.34	21.95
PAAG_00493	Autophagy-related protein 3	2.36	64.46
PAAG_00008	Alpha/beta hydrolase fold family protein	1.84	21.77
PAAG_02650	C2 domain-containing protein	2.66	47.03
PAAG_06512	CHCH domain-containing protein	1.68	24.79
PAAG_03152	CobW domain-containing protein	1.53	170.14
PAAG_00367	CUE domain-containing protein	2.69	35.59
PAAG_04610	DUF28 domain-containing protein	1.51	23.30
PAAG_04422	EKC/KEOPS complex, subunit Pcc1	1.98	10.55
PAAG_02068	Elicitor protein	1.82	59.29
PAAG_03427	Endonuclease/exonuclease/phosphatase	3.23	4.70
PAAG_00503	HAD-superfamily hydrolase	3.02	181.77
PAAG_05037	HHE domain-containing protein	2.68	24.15
PAAG_01976	LEA domain protein	2.64	57.47
PAAG_01717	MGS207 protein	1.89	46.16
PAAG_07872	MS8	2.16	45.34
PAAG_07821	NAD dependent epimerase	2.12	97.47
PAAG_04851	Osmotic growth protein	1.81	242.10
PAAG_05720	SAP domain-containing protein	2.03	43.01
PAAG_03330	Dihydrolipoyl dehydrogenase	1.68	332.08
PAAG_01556	FAD dependent oxidoreductase superfamily	1.52	73.84
PAAG_03774	S-(hydroxymethyl)glutathione dehydrogenase	2.08	44.92

13. UNCLASSIFIED

PAAG_00297	Hypothetical protein	1.67	97.23
PAAG_00335	Hypothetical protein	1.56	115.90
PAAG_00340	Hypothetical protein	2.42	199.39
PAAG_00835	Hypothetical protein	2.14	26.12
PAAG_01284	Hypothetical protein	2.48	6.39
PAAG_01952	Hypothetical protein	1.76	24.79
PAAG_02001	Hypothetical protein	2.55	36.96
PAAG_02121	Hypothetical protein	2.80	16.92
PAAG_02336	Hypothetical protein	3.47	97.80
PAAG_02375	Hypothetical protein	4.39	12.29
PAAG_03072	Hypothetical protein	1.68	10.84
PAAG_03648	Hypothetical protein	1.77	11.51

PAAG_03740	Hypothetical protein	2.57	83.52
PAAG_03925	Hypothetical protein	6.85	26.26
PAAG_04303	Hypothetical protein	5.68	31.87
PAAG_04335	Hypothetical protein	2.65	31.38
PAAG_05351	Hypothetical protein	1.74	16.28
PAAG_05403	Hypothetical protein	1.51	10.37
PAAG_05565	Hypothetical protein	2.77	6.84
PAAG_05624	Hypothetical protein	6.39	22.79
PAAG_05856	Hypothetical protein	16.67	14.91
PAAG_05957	Hypothetical protein	1.69	34.28
PAAG_06248	Hypothetical protein	4.29	18.33
PAAG_06376	Hypothetical protein	1.51	5.44
PAAG_06851	Hypothetical protein	2.86	27.69
PAAG_08671	Hypothetical protein	2.29	84.51
PAAG_11138	Hypothetical protein	12.27	9.89
PAAG_11142	Hypothetical protein	2.34	22.05
PAAG_11323	Hypothetical protein	2.11	16.44
PAAG_11405	Hypothetical protein	2.63	5.91
PAAG_11937	Hypothetical protein	1.85	5.82
PAAG_11980	Hypothetical protein	1.67	6.46
PAAG_12043	Hypothetical protein	1.59	22.08
PAAG_12169	Hypothetical protein	2.35	24.31
PAAG_12334	Hypothetical protein	4.83	17.69
PAAG_12439	Hypothetical protein	1.82	21.67
PAAG_12504	Hypothetical protein	2.38	16.99
PAAG_12514	Hypothetical protein	1.72	11.91
PAAG_12554	Hypothetical protein	1.63	10.92
PAAG_12676	Hypothetical protein	4.51	23.59

[a] Identification of differentially regulated proteins from *Paracoccidioides* genome database (http://www.broadinstitute.org/annotation/genome/paracoccidioides_brasiliensis/MultiHome.html) using the ProteinLynx Global Server vs. 2.4 (PLGS) (Waters Corporation, Manchester, UK).

[b] Proteins annotation from *Paracoccidioides* genome database or by homology from NCBI database (http://www.ncbi.nlm.nih.gov/)

[c] Acetate/Glucose means: The level of expression in yeast cells derived from cultured in sodium acetate divided by the level in the control yeast cells cultured in glucose.

[d] Biological process of differentially expressed proteins from MIPS (http://mips.helmholtz-muenchen.de/funcatDB/) and Uniprot databases (http://www.uniprot.org/).

Supplemental Table 3: Proteins down-regulated in *Paracoccidioides brasiliensis* isolate Pb03 after growth for 48 hours in sodium acetate as carbon source.

Accession number[a]	Protein Description[b]	Acetate/Glucose Ratio[c]	Score
Functional categories[d]			
1. METABOLISM			
Amino acid metabolism			
PABG_06909	1,2-dihydroxy-3-keto-5-methylthiopentenedioxygenase	0.23	11.72
PABG_01773	2-oxoisovalerate dehydrogenase subunit beta	0.56	120.02
PABG_00108	3-hydroxyanthranilate 3,4-dioxygenase	0.19	45.89
PABG_11179	3-isopropylmalate dehydratase, large subunit	0.41	146.54
PABG_02157	Acetolactate synthase	0.37	122.57
PABG_07568	Acetolactate synthase small subunit	0.22	175.79
PABG_03090	Aromatic-amino-acid aminotransferase	0.66	299.19
PABG_02890	Aspartate aminotransferase	0.45	284.18
PABG_12180	Aspartate kinase	0.59	63.83
PABG_07381	Bisphosphate-3'-nucleotidase	0.52	147.20
PABG_04202	Branched-chain-amino-acid aminotransferase	0.55	190.07
PABG_04676	Cysteine synthase	0.59	296.70
PABG_02415	Histidinol-phosphate aminotransferase	0.53	34.25
PABG_03086	Homocitrate synthase	0.28	145.45
PABG_07083	Ketol-acid reductoisomerase	0.40	419.20
PABG_03730	L-ornithine 5-monooxygenase	0.02	241.80
PABG_00309	Methionine adenosyltransferase 2 subunit beta	0.64	69.10
PABG_01063	Peptide methionine sulfoxide reductase	0.53	100.68
PABG_11793	N-acetyltransferase ats1	0.57	17.95
PABG_01248	NAD-specific glutamate dehydrogenase	0.55	552.67
PABG_01996	Phospho-2-dehydro-3-deoxyheptonate aldolase	0.64	71.04
PABG_06940	Phosphoserine aminotransferase	0.57	168.29
PABG_04656	Serine hydroxymethyltransferase	0.50	213.34
PABG_07147	Serine hydroxymethyltransferase	0.54	219.71
Nitrogen, sulfur and selenium metabolism			
PABG_05255	Urease accessory protein ureG	0.48	59.38
PABG_01063	Peptide methionine sulfoxide reductase	0.53	100.68
Nucleotide/nucleoside/nucleobase metabolism			
PABG_01175	Adenine phosphoribosyltransferase	0.25	67.51
PABG_05356	Adenylate kinase isoenzyme 2, mitochondrial	0.43	66.20
PABG_07789	Bifunctional dihydrofolate reductase-thymidylate synthase	0.31	33.70
PABG_06118	GMP synthase	0.46	52.44
PABG_05573	Non-canonical purine NTP pyrophosphatase	0.59	14.83
PABG_00254	Nucleoside-diphosphate-sugar epimerase	0.34	62.39

PABG_03400	Nucleolysin TIA-1	0.49	55.81
PABG_07260	Orotidine 5'-phosphate decarboxylase	0.47	98.75
PABG_05432	Phosphoribosylformylglycinamidine synthase	0.54	217.10
PABG_01097	UTP-glucose-1-phosphate uridylyltransferase	0.46	256.19
C-compound and carbohydrate metabolism			
PABG_01560	4-nitrophenylphosphatase	0.36	63.15
PABG_02592	Epoxide hydrolase	0.46	28.74
PABG_03197	Mannose-1-phosphate guanyltransferase	0.50	143.35
PABG_03225	Glyoxylate reductase	0.11	22.07
PABG_04017	2-nitropropane dioxygenase	0.55	71.46
PABG_04506	Alpha,alpha-trehalose-phosphate synthase	0.19	37.58
PABG_05374	2,5-diketo-D-gluconic acid reductase A	0.59	33.73
PABG_07675	Sterigmatocystin 8-O-methyltransferase	0.12	166.61
PABG_07861	Glycogen synthase kinase-3 beta	0.25	142.36
Lipid, fatty acid and isoprenoid metabolism			
PABG_03423	Acetoacetyl-CoA synthase	0.48	119.14
PABG_07087	Delta(3,5)-Delta(2,4)-Enoyl-CoA isomerase	0.51	68.68
PABG_07557	Diphosphomevalonate decarboxylase	0.47	69.71
PABG_03585	Fatty acid synthase subunit beta dehydratase	0.58	617.58
PABG_06772	Geranylgeranyl pyrophosphate synthetase	0.48	61.18
PABG_07800	Peroxisomal multifunctional enzyme	0.19	555.41
PABG_01991	3-ketoacyl-CoA thiolase	0.62	42.84
Metabolism of vitamins, cofactors, and prosthetic groups			
PABG_04074	Methylenetetrahydrofolate reductase	0.19	116.91
PABG_07767	Ethanolamine utilization protein eutG	0.47	141.06
2. ENERGY			
Glycolysis and gluconeogenesis			
PABG_03640	6-phosphofructokinase subunit beta	0.66	230.81
PABG_12188	Aldose 1-epimerase	0.61	52.05
PABG_03332	Phosphoglycerate kinase	0.41	347.11
PABG_02300	Pyruvate decarboxylase	0.66	267.86
Pentose-phosphate pathway			
PABG_01586	Glucose-6-phosphate 1-dehydrogenase	0.41	172.63
PABG_05454	Ribokinase	0.60	28.91
Tricarboxylic-acid pathway			
PABG_04595	ATP citrate lyase subunit	0.56	109.54
PABG_03242	Dihydrolipoamide branched chain transacylase	0.35	110.16
PABG_04020	Succinate dehydrogenase flavoprotein subunit	0.60	109.47

Electron transport and membrane-associated energy conservation			
PABG_02983	Mitochondrial ribosomal protein subunit S24	0.53	40.17
PABG_07006	Regulatory protein suaprga1	0.61	266.45
PABG_06504	Vacuolar ATP synthase subunit E	0.55	109.50
PABG_05301	Vacuolar ATP synthase subunit B	0.43	213.75
PABG_07507	Cytochrome c oxidase assembly factor 6	0.54	78.25
3. CELL CYCLE AND PROCESSING			
PABG_04022	Ankyrin repeat protein	0.61	46.20
PABG_04744	Cell division control protein	0.21	9.90
PABG_04850	GMF family protein	0.29	18.13
PABG_07186	Mitochondrial genome maintenance protein Mgr2	0.60	26.18
PABG_02962	Mitogen-activated protein kinase	0.63	105.14
PABG_06608	Neuronal-specific septin-3	0.27	153.40
PABG_05575	Nucleosome 6 protein	0.46	114.72
PABG_05403	Septin-4	0.48	93.84
PABG_03696	Tubulin alpha-2 chain	0.63	123.44
PABG_00486	Tubulin beta chain	0.20	70.65
PABG_00273	UV excision repair protein Rad23	0.53	53.41
PABG_12413	DUF89 domain-containing protein	0.66	164.34
4. TRANSCRIPTION			
PABG_11363	ATP-dependent RNA helicase Eif4a	0.28	117.95
PABG_11364	ATP-dependent RNA helicase eIF4A	0.11	16.79
PABG_04293	ATP-dependent RNA helicase sub2	0.43	108.63
PABG_05371	Cellular nucleic acid-binding protein	0.49	122.42
PABG_03581	DNA-binding protein HGH1	0.59	43.10
PABG_11509	Elongation factor 1-alpha	0.35	359.10
PABG_02107	Mediator-RNA polymerase II transcription subunit 10	0.27	5.65
PABG_01229	Mitochondrial transcription factor 1	0.51	189.29
PABG_01162	mRNA binding post-transcriptional regulator (Csx1)	0.36	84.51
PABG_04343	Nascent polypeptide-associated complex subunit alpha	0.56	67.83
PABG_04281	Nascent polypeptide-associated complex subunit beta	0.53	60.11
PABG_04720	Peroxiredoxin Q/BCP	0.49	112.27
PABG_01645	Small nuclear ribonucleoprotein Sm D1	0.43	19.49
PABG_00932	Transcription initiation factor IIA gamma chain	0.55	11.79
PABG_04830	U2 small nuclear ribonucleoprotein A	0.27	11.84
5. PROTEIN SYNTHESIS			
PABG_00387	54S ribosomal protein L3	0.67	78.63
PABG_06347	40S ribosomal protein S19	0.66	147.03
PABG_02155	Ribosomal protein L28/L40	0.63	22.59
PABG_02911	40S ribosomal protein S12	0.63	72.80

PABG_07658	40S ribosomal protein S2	0.56	189.04
PABG_01950	50S ribosomal protein L13	0.53	29.45
PABG_01430	60S acidic ribosomal protein P0	0.35	160.38
PABG_05118	60S ribosomal protein L3	0.46	5.55
PABG_11216	60S ribosomal protein L37	0.60	90.44
PABG_06660	Eukaryotic translation initiation factor 3 subunit F	0.50	66.54
PABG_03044	Mitochondrial 54S ribosomal protein YmL36	0.56	11.00
PABG_03981	Cysteinyl-tRNA synthetase	0.38	51.51
PABG_06894	Elongation factor 1-gamma 1	0.63	287.29
PABG_05335	Elongation factor 2	0.43	586.23
PABG_00251	Elongation factor G	0.54	64.06
PABG_05563	Eukaryotic peptide chain release factor subunit 1	0.57	84.41
PABG_01480	Eukaryotic translation initiation factor 2 subunit 3	0.48	89.03
PABG_07154	Eukaryotic translation initiation factor 3 subunit K	0.42	16.34
PABG_02322	Glutamyl-tRNA synthetase	0.48	223.86
PABG_04136	Ubiquitin-conjugating enzyme	0.42	5.95
PABG_06435	Initiation factor 5A-4	0.59	47.56
PABG_04471	Leucyl-tRNA synthetase	0.64	220.71
PABG_06626	Methionyl-tRNA synthetase	0.61	132.63
PABG_01455	Translation initiation factor 3 subunit J	0.36	69.21
6. PROTEIN FATE			
PABG_07221	Monothiol glutaredoxin-5	0.60	104.02
PABG_07175	Chaperone protein dnaK	0.65	125.30
PABG_06307	Calcium/calmodulin-dependent protein kinase	0.45	68.52
PABG_00950	Ubiquitin-activating enzyme E1 Y	0.57	310.78
PABG_11351	26S protease regulatory subunit 10B	0.39	111.68
PABG_02198	26S protease regulatory subunit 6A	0.32	88.15
PABG_03773	26S protease regulatory subunit 7	0.63	70.22
PABG_03369	26S proteasome non-ATPase regulatory subunit 10	0.58	105.85
PABG_05889	26S proteasome non-ATPase regulatory subunit 11	0.57	47.81
PABG_05717	26S proteasome non-ATPase regulatory subunit 12	0.41	51.83
PABG_05698	26S proteasome non-ATPase regulatory subunit 3	0.53	127.20
PABG_01672	Prolyl peptidase	0.64	107.27
PABG_01465	Proteasome subunit beta type-3	0.63	44.40
PABG_06432	Polyadenylate-binding protein, cytoplasmic and nuclear	0.66	384.29
7. PROTEIN WITH BINDING FUNCTION OR COFACTOR REQUIREMENT			
PABG_06250	NTF2 and RRM domain-containing protein	0.48	50.86
PABG_01158	Zinc finger protein GIS2	0.59	51.25
PABG_05824	Glycolipid transfer protein HET-C2	0.65	107.15
PABG_02905	GTP-binding protein 128up	0.64	52.98
PABG_03284	GTP-dependent nucleic acid-binding protein engD	0.36	154.36
PABG_07851	GTP-binding protein ypt1	0.46	74.35

8. CELLULAR TRANSPORT, TRANSPORT FACILITIES and TRANSPORT ROUTES			
PABG_04417	GTP-binding nuclear protein GSP1/Ran	0.22	175.04
PABG_04401	Transmembrane 9 superfamily protein	0.08	12.75
PABG_04567	Coatomer subunit gamma-2	0.52	49.85
PABG_07340	EF hand domain-containing protein	0.61	109.59
PABG_03328	Aliphatic sulfonates import ATP-binding protein ssuB 1	0.63	114.21
PABG_02315	Peroxisomal membrane protein receptor Pex19	0.45	11.98
PABG_01589	Cation transporter ChaC	0.51	16.67
PABG_07473	Vacuolar-sorting protein snf7	0.21	35.99
9. CELLULAR COMMUNICATION/SIGNAL TRANSDUCTION MECHANISM			
PABG_06708	Adenosine kinase	0.64	109.86
PABG_02751	Rab GDP-dissociation inhibitor	0.58	278.20
PABG_11289	Tyrosine-protein kinase	0.57	21.16
10. CELL RESCUE, DEFENSE AND VIRULENCE			
Stress response			
PABG_00736	DNA damage-inducible protein	0.48	104.96
PABG_06249	Heat shock protein	0.14	879.10
Detoxification			
PABG_00718	Thioredoxin	0.58	47.81
PABG_03023	Thioredoxin reductase	0.52	101.38
11. BIOGENESIS OF CELLULAR COMPONENTS			
Cell wall			
PABG_11875	Alpha 1,3-glucosidase	0.47	48.58
PABG_05175	N-acetylglucosamine-induced protein 1	0.51	15.98
Cytoskeleton/structural proteins			
PABG_05049	Coronin-6	0.63	213.15
PABG_06210	F-actin-capping protein subunit beta	0.52	29.41
PABG_06519	Chitin biosynthesis protein	0.61	94.35
PABG_06867	Actin-66	0.13	236.57
PABG_04150	GPI-anchored cell wall protein	0.10	39.24
12. MISCELLANEOUS			
PABG_01116	Molybdopterin synthase small subunit CnxG	0.54	11.63
PABG_02713	PCI domain-containing protein	0.38	96.05
PABG_05425	NAP family protein	0.55	58.11
PABG_11354	Zinc metalloprotease	0.62	45.32
PABG_04682	Type 2A phosphatase activator tip41	0.35	44.69
PABG_07380	VHS domain-containing protein	0.24	33.10

13. UNCLASSIFIED

PABG_05526	Hypothetical protein	0.55	27.23
PABG_00682	Hypothetical protein	0.64	161.75
PABG_01378	Hypothetical protein	0.27	10.73
PABG_07518	Hypothetical protein	0.41	19.97
PABG_07299	Hypothetical protein	0.35	117.35
PABG_03948	Hypothetical protein	0.29	129.65
PABG_00435	Hypothetical protein	0.24	19.02
PABG_07406	Hypothetical protein	0.10	18.11
PABG_03302	Hypothetical protein	0.63	54.55
PABG_01272	Hypothetical protein	0.14	11.18
PABG_01577	Hypothetical protein	0.42	4.70
PABG_02043	Hypothetical protein	0.64	17.76
PABG_02066	Hypothetical protein	0.45	16.11
PABG_02498	Hypothetical protein	0.30	12.58
PABG_03079	Hypothetical protein	0.45	46.30
PABG_03144	Hypothetical protein	0.30	10.89
PABG_03291	Hypothetical protein	0.52	10.80
PABG_03565	Hypothetical protein	0.36	49.64
PABG_03721	Hypothetical protein	0.19	15.13
PABG_03735	Hypothetical protein	0.60	5.35
PABG_03992	Hypothetical protein	0.47	11.18
PABG_04002	Hypothetical protein	0.44	12.31
PABG_04756	Hypothetical protein	0.63	17.54
PABG_05090	Hypothetical protein	0.66	32.77
PABG_05343	Hypothetical protein	0.02	6.91
PABG_06426	Hypothetical protein	0.23	5.99
PABG_06921	Hypothetical protein	0.23	17.93
PABG_11229	Hypothetical protein	0.64	6.33
PABG_11333	Hypothetical protein	0.11	5.95
PABG_11463	Hypothetical protein	0.60	40.98
PABG_11948	Hypothetical protein	0.33	24.46
PABG_12207	Hypothetical protein	0.60	21.50
PABG_12415	Hypothetical protein	0.65	9.57
PABG_12441	Hypothetical protein	0.35	16.88
PABG_12446	Hypothetical protein	0.26	6.08
PABG_12574	Hypothetical protein	0.60	16.37
PABG_11804	Hypothetical protein	0.07	32.99
PABG_12023	Hypothetical protein	0.27	16.18
PABG_12033	Hypothetical protein	0.61	11.84
PABG_07597	Hypothetical protein	0.60	26.57
PABG_05701	Hypothetical protein	0.50	11.83
PABG_03826	Hypothetical protein	0.61	16.57

PABG_06575	Hypothetical protein	0.55	21.23
PABG_03151	Hypothetical protein	0.56	28.09
PABG_05579	Hypothetical protein	0.66	48.37
PABG_11583	Hypothetical protein	0.66	23.08

[a] Identification of differentially regulated proteins from *Paracoccidioides* genome database (http://www.broadinstitute.org/annotation/genome/paracoccidioides_brasiliensis/MultiHome.html) using the ProteinLynx Global Server vs. 2.4 (PLGS) (Waters Corporation, Manchester, UK).

[b] Proteins annotation from *Paracoccidioides* genome database or by homology from NCBI database (http://www.ncbi.nlm.nih.gov/).

[c] Acetate/Glucose means: The level of expression in yeast cells derived from cultured in sodium acetate divided by the level in the control yeast cells cultured in glucose.

[d] Biological process of differentially expressed proteins from MIPS (http://mips.helmholtz-muenchen.de/funcatDB/) and Uniprot databases (http://www.uniprot.org/).

Supplemental Table 4: Proteins up-regulated in *Paracoccidioides brasiliensis* isolate Pb03 after growth for 48 hours in sodium acetate as carbon source.

Accession number[a]	Protein Description[b]	Acetate/Glucose Ratio[c]	Score
Functional categories[d]			
1. METABOLISM			
Amino acid metabolism			
PABG_07394	4-hydroxyphenylpyruvate dioxygenase	4.05	253.46
PABG_00589	Alanine-glyoxylate aminotransferase	2.46	92.50
PABG_11192	Amino-acid acetyltransferase, mitochondrial	1.55	5.50
PABG_07531	Asparagine synthetase	1.88	122.47
PABG_02806	Aspartate aminotransferase	1.96	91.85
PABG_02012	Choline dehydrogenase	1.54	145.33
PABG_04712	Glutamate-5-semialdehyde dehydrogenase	2.04	183.29
PABG_03010	Glutamine synthetase	1.84	93.06
PABG_04990	Glycine cleavage T-protein	1.92	23.45
PABG_05965	Histidine biosynthesis trifunctional protein	1.63	17.44
PABG_07392	Homogentisate 1,2-dioxygenase	3.97	198.61
PABG_04732	Isochorismatase domain containing 2b	2.01	54.50
PABG_01965	Kynureninase	2.00	94.33
PABG_03129	Kynurenine-oxoglutarate transaminase	2.12	146.59
PABG_07533	Methionine aminopeptidase	1.51	64.41
PABG_07390	Maleylacetoacetate isomerase	2.66	111.96
PABG_02827	Ornithine aminotransferase	2.62	242.23
PABG_02447	Pentafunctional AROM polypeptide	3.05	206.59
PABG_03361	S-adenosylmethionine synthetase	1.91	203.87
PABG_01280	L-threonine 3-dehydrogenase	4.03	90.39
PABG_00544	TPA: putative Conserved lysine-rich protein	1.89	296.22
Nitrogen, sulfur and selenium metabolism			
PABG_00102	Ureidoglycolate hydrolase	5.42	17.84
PABG_07028	Formamidase	4.45	240.33
PABG_03480	Nitroreductase	1.65	87.22
PABG_02398	Urea carboxylase	1.60	416.19
Nucleotide/nucleoside/nucleobase metabolism			
PABG_04433	Adenylosuccinate lyase	1.58	95.31
PABG_06340	Inosine-5'-monophosphate dehydrogenase IMD2	1.69	316.83
PABG_06368	Quinone oxidoreductase	2.66	184.61
PABG_01949	Uricase	1.52	59.50
Phosphate metabolism			
PABG_04460	Serine/threonine protein kinase	4.94	16.22

C-compound and carbohydrate metabolism			
PABG_00225	4-coumarate-CoA ligase	1.57	193.77
PABG_01732	Tautomerase/MIF	4.05	90.54
PABG_05538	Lactonohydrolase	1.91	94.83
PABG_02864	Mannitol-1-phosphate 5-dehydrogenase	1.53	241.02
PABG_00813	NADPH-dependent D-xylose reductase	1.82	155.84
PABG_04877	Quinone oxidoreductase	2.06	174.79
PABG_01695	Retrograde regulation protein	2.89	65.11
PABG_01914	Ribulokinase	1.73	53.46
PABG_12460	Salicylate hydroxylase	1.57	47.49
PABG_06330	4-carboxymuconolactone decarboxylase family protein	1.58	53.38
PABG_06193	6-phosphogluconolactonase	2.08	86.31
Lipid, fatty acid and isoprenoid metabolism			
PABG_02112	2-succinylbenzoate-CoA ligase	1.53	183.90
PABG_00747	3-ketoacyl-CoA thiolase A	1.52	209.23
PABG_05999	3-ketoacyl-acyl carrier protein reductase	3.90	29.01
PABG_05972	3-oxoacyl-(acyl-carrier protein) reductase	1.89	331.40
PABG_01791	Acyl-CoA dehydrogenase	1.71	78.53
PABG_03016	Enoyl-CoA hydratase	1.77	19.23
PABG_02855	Acyl-CoA-binding protein	1.77	89.55
PABG_00955	Acyl-CoA N-acyltransferase	3.78	51.19
Metabolism of vitamins, cofactors, and prosthetic groups			
PABG_01387	6,7-dimethyl-8-ribityllumazine synthase	1.84	37.06
PABG_06591	Delta-aminolevulinic acid dehydratase	3.15	86.93
PABG_01549	NUDIX domain-containing protein	27.49	17.47
PABG_04836	Nudix hydrolase	1.82	36.29
PABG_00890	Phosphopantothenate-cysteine ligase	2.24	46.28
Secondary metabolism			
PABG_06389	Imidazole glycerol phosphate synthase hisHF	3.16	55.33
PABG_06397	Imidazole glycerol phosphate synthase hisHF	3.21	177.12
2. ENERGY			
Glycolysis and gluconeogenesis			
PABG_06480	Glucokinase GLK1	1.68	42.70
PABG_02052	Glucose-6-phosphate isomerase	2.16	217.75
PABG_00022	Glyceraldehyde-3-phosphate dehydrogenase	1.56	363.42
PABG_01237	Hexokinase	1.73	107.40
Ethanol production			
PABG_04316	Alcohol dehydrogenase GroES domain-containing protein	2.88	279.02

PABG_12402	Alcohol dehydrogenase 1	2.66	212.74
Pentose-phosphate pathway			
PABG_02360	Ribose-phosphate pyrophosphokinase	1.64	173.62
Tricarboxylic-acid pathway			
PABG_03210	2-oxoglutarate dehydrogenase E1	1.53	486.63
PABG_11957	Aconitate hydratase, mitochondrial	1.89	405.25
PABG_04594	ATP-citrate synthase	4.00	343.90
PABG_01382	Isocitrate dehydrogenase subunit 1	1.69	216.34
PABG_03494	Pyruvate dehydrogenase E1 component subunit alpha	1.87	278.19
PABG_03772	Succinate dehydrogenase flavoprotein subunit	2.66	276.05
Methylcytrate cycle			
PABG_04323	Methylisocitrate lyase	2.54	265.71
Electron transport and membrane-associated energy conservation			
PABG_06161	ATP synthase delta chain	3.25	28.85
PABG_12007	ATP synthase F0 subunit 8	1.84	107.56
PABG_11057	ATP synthase subunit alpha, mitochondrial	1.63	458.48
PABG_07285	ATP synthase subunit beta	1.87	349.38
PABG_06178	ATP synthase subunit delta,	1.97	59.54
PABG_05268	Cytochrome c oxidase polypeptide Vib	1.79	19.26
PABG_06935	Formate dehydrogenase	6.10	137.07
PABG_07303	F-type H+-transporting ATPase subunit epsilon	1.54	14.76
PABG_12311	NADH-ubiquinone oxidoreductase 49 kDa, mitochondrial	1.56	11.77
PABG_11661	Succinate dehydrogenase assembly factor 2, mitochondrial	1.63	91.85
PABG_05474	Vacuolar ATP synthase catalytic subunit A	1.88	247.75
PABG_03708	NADH-ubiquinone oxidoreductase 12 kDa subunit	2.98	22.65
PABG_03177	Ubiquinol-cytochrome c reductase subunit 6	6.17	32.84
PABG_06958	12-oxophytodienoate reductase	3.19	284.78
PABG_04666	Cytochrome b5	1.64	22.16
PABG_11490	Electron transfer flavoprotein-ubiquinone oxidoreductase	9.02	10.87
3. CELL CYCLE and DNA PROCESSING			
PABG_05569	Cell cycle control protein cwf14	2.09	15.92
PABG_02067	Mitochondrial genome maintenance protein MGM101	1.76	73.79
PABG_04448	Meiosis specific protein Hop1	2.20	45.43
PABG_03596	SNF7 family protein Fti1/Did2	3.67	15.15
PABG_05201	Septin-7	2.12	150.23
PABG_11327	Proliferating cell nuclear antigen	2.03	284.78
4. TRANSCRIPTION			
PABG_00085	Pirin	2.55	95.05

PABG_06262	PHD finger protein	2.03	18.92
PABG_06274	NuA3 HAT complex component NTO1	4.01	60.61
PABG_06004	Poly(A) polymerase PAPa	2.77	56.98
PABG_01856	Splicing factor spf30	1.77	28.68
PABG_03761	tRNA (guanine(37)-N1)-methyltransferase	2.71	79.13
PABG_03438	Transcription factor RfeF	1.56	76.06
PABG_05850	U1 small nuclear ribonucleoprotein	1.54	33.37
PABG_12042	U2 small nuclear ribonucleoprotein B	1.51	26.05
PABG_00485	U2 snRNP-associated protein Uap2	2.05	43.68
PABG_01474	U4/U6.U5 tri-snRNP-associated protein	2.59	50.62
PABG_00260	DNA-directed RNA polymerase III subunit Rpc31	2.17	46.98
PABG_05962	Basic helix-loop-helix transcription factor Yas1p	5.32	90.70
PABG_01008	Zinc finger protein	1.78	59.80
5. PROTEIN SYNTHESIS			
PABG_06421	30S ribosomal protein S7	1.66	163.76
PABG_04888	37S ribosomal protein S5	4.68	18.45
PABG_03113	50S ribosomal protein L24	1.52	19.86
PABG_01500	60S ribosomal protein L11	2.75	70.92
PABG_12185	60S ribosomal protein L28	1.84	310.74
PABG_06407	Cytochrome P450 monooxygenase	4.99	17.08
PABG_06666	Mitochondrial ribosomal protein YmL8	1.65	33.50
PABG_12047	Ran-specific GTPase-activating protein 1	1.58	265.86
PABG_01633	Ribosomal protein L30	1.80	59.78
PABG_06017	TCTP family protein	1.90	53.61
PABG_01959	67 kDa polymerase-associated factor PAF67	1.84	93.92
PABG_02129	Elongation factor 1-alpha	2.10	59.90
PABG_05845	Elongation factor 2	2.79	142.18
PABG_01416	Eukaryotic translation initiation factor 3 110 kDa subunit	1.84	109.69
PABG_06490	Eukaryotic translation initiation factor 3 subunit B	2.41	192.82
PABG_01208	Eukaryotic translation initiation factor 3 subunit I	1.74	106.67
PABG_02641	Translation initiation factor 4B	2.31	206.77
PABG_01301	Lysine-tRNA ligase	1.84	135.04
PABG_05580	Seryl-tRNA synthetase	2.86	265.30
PABG_07397	Lysyl-tRNA synthetase	2.42	145.34
6. PROTEIN FATE			
PABG_00967	T-complex protein 1 subunit alpha	2.68	164.60
PABG_01488	Peptidyl-prolyl cis-trans isomerase B	1.59	111.53
PABG_06135	TCTP family protein	1.59	106.15
PABG_06572	T-complex protein 1 subunit beta	1.53	91.90
PABG_07652	FK506-binding protein	2.33	77.53
PABG_07742	T-complex protein 1 subunit eta	2.12	117.58
PABG_01434	Chaperone protein dnaJ	1.58	78.19

PABG_05205	Intermembrane space import and assembly protein	2.25	25.77
PABG_00818	Mitochondrial import inner membrane translocase subunit tim9	1.54	11.98
PABG_01181	NADH dehydrogenase (ubiquinone) 1 beta subcomplex 8	5.77	78.45
PABG_00491	Ubiquitin-like modifier SUMO	1.53	25.45
PABG_03958	Subtilase-type proteinase psp3	1.66	123.42
PABG_05357	26S proteasome regulatory subunit rpn-8	2.10	84.59
PABG_05859	Ubiquitin thiolesterase	1.62	20.56
PABG_06586	T-complex protein 1 subunit beta	5.36	186.67
PABG_07230	Xaa-Pro aminopeptidase I	2.40	182.17
PABG_07373	Proteasome subunit alpha type-4	1.81	137.44
PABG_01386	Proteasome subunit alpha type-3	1.56	141.66
PABG_05365	V Chain V	1.67	78.82
PABG_06849	Carboxypeptidase Y	2.63	94.09
7. PROTEIN WITH BINDING FUNCTION or COFACTOR REQUIREMENT			
PABG_03848	YjeF-related protein	1.68	53.33
PABG_03778	Nuclear localization sequence-binding protein	3.16	48.38
PABG_03796	Translation machinery-associated protein 22	3.18	13.29
PABG_03042	APAF1-interacting protein	1.52	50.27
PABG_04194	Progesterone binding protein	2.69	82.62
PABG_02026	RNA-binding protein Vip1	1.62	152.84
8. CELLULAR TRANSPORT, TRANSPORT FACILITIES and TRANSPORT ROUTES			
PABG_06877	ATPase_c domain-containing protein	1.57	215.25
PABG_06615	Heavy metal ion transporter, putative	1.75	31.52
PABG_00598	Galactose-proton symport	1.54	22.94
PABG_01896	GTP-binding protein SAS1	3.52	40.46
PABG_03783	Exocyst complex component Sec10	2.59	102.59
PABG_12318	DUF726 domain-containing protein	1.67	41.63
9. CELLULAR COMMUNICATION/SIGNAL TRANSDUCTION MECHANISM			
PABG_06817	Neuronal calcium sensor 1	1.72	16.47
PABG_03846	WD repeat-containing protein	7.39	38.28
PABG_00188	Phosphatase 2A regulatory B subunit	1.87	50.26
PABG_01056	Kinase binding protein	1.75	33.99
PABG_05936	CAMK/CAMKL/KIN4 protein kinase	5.77	78.45
PABG_04460	Serine/threonine protein kinase	4.94	16.22
10. CELL RESCUE, DEFENSE AND VIRULENCE			
Stress response			
PABG_01369	Heat shock protein	2.86	235.05
PABG_02373	Heat shock protein	1.77	243.44
PABG_00374	Heat shock protein Hsp88	1.71	643.84
PABG_00350	Heat shock protein SSB	1.75	325.75

PABG_05342	Hsp70-like protein	1.56	747.87
Detoxification			
PABG_03954	Superoxide dismutase Cu/Zn SOD1	2.16	72.78
PABG_03204	Superoxide dismutase Fe/Mn SOD2	2.52	147.87
PABG_00431	Superoxide dismutase Cu/Zn SOD3	1.58	43.93
PABG_03387	Superoxide dismutase Fe/Mn SOD5	1.76	168.45
PABG_01943	Peroxisomal catalase	7.86	400.41
PABG_04219	Glutathione peroxidase	3.61	32.22
PABG_00949	Glutathione S-transferase Gst3	1.63	209.16
PABG_06156	Protein disulfide-isomerase	2.27	174.38
PABG_05451	Serine/threonine protein phosphatase 2A	2.81	18.58
PABG_00720	Cytochrome c peroxidase	3.20	257.66
11. BIOGENESIS OF CELLULAR COMPONENTS			
Cell wall			
PABG_07783	Antigenic cell wall protein	2.55	44.49
PABG_06590	Glucan 1,3-beta-glucosidase	3.38	31.35
PABG_04069	Neutral alpha-glucosidase AB	1.56	224.70
Cytoskeleton/strucutural proteins			
PABG_01263	Actin	2.02	97.21
PABG_07733	Actin lateral binding protein	1.66	183.02
PABG_03455	Clathrin light chain	2.17	101.18
12. MISCELLANEOUS			
PABG_01011	Urg3	1.58	90.54
PABG_01127	Short chain dehydrogenase/reductase	1.86	37.43
PABG_06951	Polysaccharide deacetylase family protein	3.96	185.15
PABG_01628	Adenosine deaminase	1.58	24.48
PABG_06653	CUE domain-containing protein	2.40	11.68
PABG_02064	DUF833 domain-containing protein	1.60	98.02
PABG_11267	Alkaline phosphatase	3.09	79.08
PABG_05421	Glyoxylate reductase	1.50	31.50
PABG_04660	Propionate-CoA ligase	1.56	35.02
PABG_03731	Peroxisomal dehydratase	1.52	39.28
PABG_06197	S-formylglutathione hydrolase	3.11	19.17
PABG_02094	Globin	3.36	51.68
13. UNCLASSIFIED			
PABG_01748	Hypothetical protein	2.89	38.06
PABG_00361	Hypothetical protein	46.44	34.74
PABG_00446	Hypothetical protein	1.64	26.97
PABG_05798	Hypothetical protein	1.89	48.03

PABG_00679	Hypothetical protein	1.52	17.78
PABG_01780	Hypothetical protein	1.94	18.43
PABG_01814	Hypothetical protein	2.18	30.82
PABG_01892	Hypothetical protein	2.51	4.89
PABG_02578	Hypothetical protein	4.23	298.74
PABG_03540	Hypothetical protein	4.58	11.31
PABG_03999	Hypothetical protein	2.17	16.92
PABG_04137	Hypothetical protein	2.06	43.70
PABG_05041	Hypothetical protein	1.83	50.89
PABG_05293	Hypothetical protein	5.54	5.76
PABG_05692	Hypothetical protein	2.81	6.16
PABG_07502	Hypothetical protein	3.16	10.93
PABG_11028	Hypothetical protein	2.16	28.49
PABG_11204	Hypothetical protein	2.18	44.75
PABG_11386	Hypothetical protein	5.86	10.38
PABG_11594	Hypothetical protein	9.51	10.87
PABG_11755	Hypothetical protein	2.89	22.06
PABG_12078	Hypothetical protein	1.53	5.39
PABG_12239	Hypothetical protein	105.53	10.55
PABG_12338	Hypothetical protein	4.75	6.03
PABG_12351	Hypothetical protein	11.89	12.24
PABG_12386	Hypothetical protein	1.81	18.19
PABG_12408	Hypothetical protein	1.58	5.77
PABG_12656	Hypothetical protein	2.53	6.17
PABG_03766	Hypothetical protein	1.53	59.76
PABG_06624	Hypothetical protein	1.57	40.31
PABG_01741	Hypothetical protein	2.05	108.18
PABG_01683	Hypothetical protein	7.30	34.10
PABG_02970	Hypothetical protein	2.65	104.93
PABG_06275	Hypothetical protein	1.55	76.58

[a] Identification of differentially regulated proteins from *Paracoccidioides* genome database (http://www.broadinstitute.org/annotation/genome/paracoccidioides_brasiliensis/MultiHome.html) using the ProteinLynx Global Server vs. 2.4 (PLGS) (Waters Corporation, Manchester, UK).

[b] Proteins annotation from *Paracoccidioides* genome database or by homology from NCBI database (http://www.ncbi.nlm.nih.gov/).

[c] Acetate/Glucose means: The level of expression in yeast cells derived from cultured in sodium acetate divided by the level in the control yeast cells cultured in glucose.

[d] Biological process of differentially expressed proteins from MIPS (http://mips.helmholtz-muenchen.de/funcatDB/) and Uniprot databases (http://www.uniprot.org/).

Supplemental Table 5: Proteins down-regulated in *Paracoccidioides brasiliensis* isolate Pb339 after growth for 48 hours in sodium acetate as carbon source.

Accession number[a]	Protein Description[b]	Acetate/Glucose Ratio[c]	Score
Functional categories[d]			
1- METABOLISM			
Amino acid metabolism			
PADG_01536	Glutamine synthetase	0.006	189.43
PADG_01305	Argininosuccinate lyase	0.56	138.41
PADG_04356	Cystathionine gamma-synthase	0.56	47.23
PADG_05888	Aspartokinase	0.36	52.77
PADG_06955	Tryptophan synthase	0.49	45.67
PADG_00210	Glycine dehydrogenase	0.37	364.02
PADG_00402	5-carboxymethyl-2-hydroxymuconate semialdehyde	0.31	41.71
PADG_07845	Imidazole glycerol phosphate synthase hisHF	0.64	65.71
PADG_07269	Phenylacetate 2-hydroxylase	0.54	37.80
PADG_05058	Chorismate mutase	0.34	18.79
PADG_01789	Anthranilate phosphoribosyltransferase	0.56	33.26
PADG_00386	Phospho-2-dehydro-3-deoxyheptonate aldolase	0.63	102.63
PADG_03167	3-isopropylmalate dehydratase	0.26	242.64
PADG_06671	3-isopropylmalate dehydrogenase A	0.57	142.25
PADG_08225	Acetolactate synthase small subunit	0.47	37.94
PADG_01993	Acetoacetyl-coenzyme A synthetase	0.18	140.90
PADG_03032	Ornithine decarboxylase	0.25	26.09
PADG_01404	Aspartate aminotransferase	0.33	177.33
PADG_02726	Cysteine synthase	0.57	160.19
PADG_04570	Branched-chain-amino-acid aminotransferase	0.45	247.14
PADG_08662	Cystathionine beta-lyase	0.36	43.57
PADG_04522	Homoserine kinase	0.64	62.14
PADG_07241	Dihydroxy-acid dehydratase	0.38	32.19
Nitrogen, sulfur and selenium metabolism			
PADG_07471	2-nitropropane dioxygenase	0.24	49.64
PADG_08696	GPR/FUN34 family protein	0.65	24.05
Nucleotide/nucleoside/nucleobase metabolism			
PADG_07918	Pyrimidine and pyridine-specific 5'-nucleotidase	0.33	18.78
PADG_02246	Adenosine kinase	0.47	76.39
PADG_04721	Amidophosphoribosyltransferase	0.51	65.16
PADG_06585	GMP synthase	0.62	149.68
PADG_12229	Phosphoribosylaminoimidazole carboxylase, ATPase subunit	0.44	15.42
PADG_07585	Inosine-5'-monophosphate dehydrogenase IMD2	0.30	199.70
PADG_06747	DNA-directed RNA polymerase II subunit RPB1	0.23	134.66

PADG_05472	GMP synthase	0.58	88.64
PADG_01424	Inosine-uridine preferring nucleoside hydrolase	0.39	37.33
PADG_08530	Thymidylate synthase	0.17	24.38
PADG_08434	Nicotinamide mononucleotide adenylyltransferase	0.66	44.15
PADG_00209	Guanine deaminase	0.36	47.55
PADG_04293	Adenine phosphoribosyltransferase	0.36	28.72
PADG_05812	CTP synthase	0.62	26.72
PADG_11922	Uridine kinase	0.45	27.11
PADG_05643	Ribonucleotide reductase R2 subunit variant	0.33	32.31
PADG_00988	Ribonuclease T2	0.13	18.40
PADG_07888	Eukaryotic translation initiation factor 5A	0.60	61.25
Compound and carbohydrate metabolism			
PADG_00315	Carbonic anhydrase	0.35	22.16
PADG_01636	4-hydroxyphenylpyruvate dioxygenase	0.38	43.44
PADG_02625	4-coumarate-CoA ligase	0.30	157.12
PADG_03943	Phosphomannomutase	0.47	77.85
PADG_08474	Mannose-1-phosphate guanyltransferase	0.27	137.39
PADG_04761	Glucosidase I	0.66	119.08
PADG_04900	Alpha,alpha-trehalose-phosphate synthase	0.42	68.93
PADG_02145	Glycogen phosphorylase	0.37	210.39
PADG_08244	Neutral trehalase	0.34	58.59
PADG_05778	Glycogen synthase	0.23	30.08
PADG_12009	Trehalose 6-phosphate synthase	0.65	21.34
PADG_05419	UDP-glucose 4-epimerase	0.67	27.75
PADG_00561	Galactokinase	0.56	97.74
PADG_06878	Nuclear protein SNF4	0.01	6.06
PADG_07319	Sporulation-regulated protein	0.52	176.16
PADG_04754	General amidase	0.13	22.46
PADG_03984	Glucosamine-fructose-6-phosphateaminotransferase	0.19	187.73
Lipid, fatty acid and isoprenoid metabolism			
PADG_02244	(R)-benzylsuccinyl-CoA dehydrogenase	0.34	113.46
PADG_04827	Acyl-coenzyme A synthetase O-MACS	0.64	28.94
PADG_08214	Diphosphomevalonate decarboxylase	0.62	11.51
PADG_01291	Enoyl-CoA hydratase	0.50	67.28
PADG_05184	Ethanolamine-phosphate cytidylyltransferase	0.42	60.36
PADG_00255	Fatty acid synthase subunit beta dehydratase	0.29	779.10
PADG_02174	Geranylgeranyl pyrophosphate synthetase	0.30	80.02
PADG_00685	Hydroxymethylglutaryl-CoA synthase	0.61	91.51
PADG_01786	NMDA receptor-regulated protein	0.45	65.05
PADG_00221	Short-chain dehydrogenase	0.01	18.54
PADG_00204	Sterol 24-C-methyltransferase	0.54	16.68
PADG_00244	Trans-2-enoyl-CoA reductase	0.51	148.67

PADG_05733	60 kDa lysophospholipase	0.53	32.35
PADG_01677	Acetyl-coenzyme A synthetase	0.55	444.46
Metabolism of vitamins, cofactors, and prosthetic groups			
PADG_04250	C-1-tetrahydrofolate synthase	0.41	204.60
PADG_07528	Cysteine desulfurase	0.52	84.11
PADG_12043	Folylpolyglutamate synthase	0.66	216.61
PADG_01126	Molybdopterin synthase large subunit CnxH	0.60	33.05
PADG_05564	Porphobilinogen deaminase	0.07	17.82
PADG_00607	Riboflavin synthase alpha chain	0.60	105.09
PADG_11535	Folylpolyglutamate synthase	0.50	76.60
2- ENERGY			
Glycolysis and gluconeogenesis			
PADG_00192	6-phosphofructokinase	0.65	228.35
PADG_01896	Phosphoglycerate kinase	0.29	440.10
Pentose-phosphate pathway			
PADG_07771	6-phosphogluconolactonase	0.31	84.60
PADG_04989	Ribose 5-phosphate isomerase A	0.50	66.11
PADG_11295	Ribose-phosphate pyrophosphokinase 3	0.13	14.25
PADG_11296	Ribose-phosphate pyrophosphokinase 3	0.35	107.68
Tricarboxylic-acid pathway			
PADG_00317	Succinyl-CoA ligase subunit beta	0.30	241.32
PADG_02260	Succinyl-CoA ligase subunit alpha	0.41	172.36
Electron transport and membrane-associated energy conservation			
PADG_00688	F-type H+-transporting ATPase subunit h	0.55	12.42
PADG_04729	ATP synthase D chain, mitochondrial	0.57	97.65
PADG_06978	Cytochrome c	0.22	46.71
PADG_01841	Cytochrome c oxidase assembly protein COX19	0.35	11.31
PADG_06995	Cytochrome c oxidase subunit 6b	0.59	22.32
PADG_08460	NADPH dehydrogenase	0.16	27.45
PADG_11605	NADPH-cytochrome P450 reductase	0.51	18.52
PADG_06956	Vacuolar ATP synthase subunit B	0.66	192.96
PADG_12152	ATP synthase subunit g	0.48	42.19
3- CELL CYCLE AND DNA PROCESSING			
PADG_00656	Non-histone chromosomal protein 6	0.32	72.14
PADG_00466	Mitochondrial genome maintenance protein	0.59	43.94
PADG_07835	Replication factor-A protein	0.58	73.25
PADG_05798	Single-strand binding protein family	0.34	108.62
PADG_05900	Transcription elongation factor 1	0.05	6.16

PADG_02359	Cell division control protein	0.14	175.26
PADG_05714	Cell division control protein	0.42	127.64
PADG_05683	Cell division control protein	0.59	533.91
PADG_07477	Ankyrin repeat protein	0.51	22.46
PADG_11711	ATP-dependent RNA helicase eIF4A	0.09	148.50
PADG_08634	Bud emergence protein	0.22	45.52
PADG_08425	CBS domain-containing protein	0.45	5.61
PADG_07070	Cell division control protein	0.23	111.87
PADG_11337	Chromodomain helicase hrp3	0.43	42.40
PADG_03005	Dynein light chain	0.06	27.84
PADG_05837	Glycoprotein FP21	0.42	71.95
PADG_11743	Meiotic recombination protein DMC1	0.04	18.98
PADG_00951	Microtubule-associated protein RP/EB family	0.08	17.08
PADG_05875	Centromere/microtubule-binding protein CBF5	0.61	28.47
PADG_11857	Mitotic checkpoint protein BUB3	0.31	97.97
PADG_05893	Nucleosome assembly protein	0.44	222.87
PADG_08676	RNA binding effector protein Scp160	0.46	80.06
PADG_00128	Tubulin alpha chain	0.15	139.30
PADG_08316	Tubulin alpha-1 chain	0.36	45.78

4-TRANSCRIPTION

PADG_08081	DNA-binding protein HEXBP	0.50	97.05
PADG_00718	histone chaperone asf1	0.33	19.61
PADG_01455	KH domain RNA-binding protein	0.49	39.05
PADG_04307	mRNA binding post-transcriptional regulator	0.44	107.67
PADG_04730	Nascent polypeptide-associated complex subunit alpha	0.48	82.97
PADG_04657	Nascent polypeptide-associated complex subunit beta	0.34	89.53
PADG_06931	Nitrogen regulatory protein DAL80	0.09	16.37
PADG_00067	Polymerase (RNA) II (DNA directed) polypeptide D	0.55	55.09
PADG_06666	RNA splicing factor Pad-1	0.46	107.95
PADG_01232	TFIIH basal transcription factor complex p52 subunit	0.60	11.53
PADG_00034	Transcription elongation factor S-II	0.52	27.66
PADG_03406	Transcription initiation factor IIA small subunit	0.49	10.47
PADG_06752	Transcription initiation factor TFIID subunit 9	0.29	6.02
PADG_02825	Splicing factor	0.03	7.00
PADG_03988	LSM domain-containing protein	0.04	5.79
PADG_00205	Pre-mRNA-splicing factor slt11	0.43	23.81
PADG_04107	Pre-mRNA-splicing factor srp1	0.23	39.87
PADG_01999	Small nuclear ribonucleoprotein Sm D3	0.48	23.87
PADG_02752	116 kDa U5 small nuclear ribonucleoprotein component	0.64	175.86
PADG_11945	Dicer-like protein 1	0.55	17.75
PADG_05468	U2 small nuclear ribonucleoprotein A	0.35	41.01
PADG_05210	tRNA pseudouridine synthase	0.13	6.27

5- PROTEIN SYNTHESIS

PADG_00785	Ribosomal protein S15	0.48	40.22
PADG_01026	60S ribosomal protein L43	0.63	51.64
PADG_04118	60S ribosomal protein L38	0.67	71.05
PADG_04588	60S ribosomal protein L22	0.60	108.74
PADG_04862	50S ribosomal protein Mrp49	0.14	41.45
PADG_00333	40S ribosomal protein S16	0.40	118.42
PADG_00354	40S ribosomal protein S17	0.60	106.93
PADG_01083	60S ribosomal protein L32	0.53	87.21
PADG_06048	40S ribosomal protein S27	0.63	43.46
PADG_01914	Ribosomal protein L35	0.58	40.50
PADG_02056	50S ribosomal protein L12	0.12	77.69
PADG_02797	54S ribosomal protein L3	0.39	23.68
PADG_04030	60S acidic ribosomal protein P0	0.42	87.86
PADG_04475	Small subunit ribosomal protein YMR-31	0.08	25.98
PADG_05244	60S ribosomal protein L44	0.42	91.24
PADG_05573	54S ribosomal protein L19	0.02	12.21
PADG_06266	40S ribosomal protein S9	0.51	60.26
PADG_06502	40S ribosomal protein S20	0.66	60.72
PADG_06599	40S ribosomal protein S25	0.35	128.23
PADG_00044	28 kDa ribonucleoprotein	0.54	72.82
PADG_07583	Ribosomal protein S21E	0.41	94.11
PADG_07685	40S ribosomal protein S13-1	0.49	138.04
PADG_08152	40S ribosomal protein S26E	0.53	74.30
PADG_08453	Large subunit ribosomal protein L6	0.47	37.26
PADG_02691	Eukaryotic translation initiation factor 6	0.64	68.59
PADG_04948	H/ACA ribonucleoprotein complex subunit 1	0.31	28.80
PADG_05561	Serine/threonine-protein kinase RIO2	0.58	24.50
PADG_06315	Ribosome maturation protein SDO1	0.30	32.79
PADG_04810	GTP-binding nuclear protein GSP1/Ran	0.27	195.81
PADG_11083	Ribosomal protein L13	0.23	25.38
PADG_12373	40S ribosomal protein S30	0.25	14.06
PADG_02206	DnaJ homolog subfamily B member 4	0.19	72.99
PADG_05118	Translation initiation factor 3 subunit K	0.52	46.32
PADG_04672	ATP-dependent RNA helicase SUB2	0.05	167.39
PADG_00692	Elongation factor 1-alpha	0.36	358.93
PADG_02896	Elongation factor 1-beta	0.56	52.70
PADG_08125	Elongation factor 2	0.50	693.37
PADG_01949	Elongation factor Tu	0.56	288.95
PADG_01891	translation initiation factor RLI1	0.46	137.06
PADG_05879	Eukaryotic peptide chain release factor subunit 1	0.39	89.77
PADG_07977	Eukaryotic translation initiation factor 1A	0.62	74.56
PADG_04210	Eukaryotic translation initiation factor 2 beta subunit	0.31	51.86
PADG_06160	Eukaryotic translation initiation factor 2 subunit alpha	0.13	25.23

PADG_04083	Eukaryotic translation initiation factor 2 subunit gamma	0.55	172.47
PADG_01389	Eukaryotic translation initiation factor 3 subunit 8	0.37	151.50
PADG_02296	Eukaryotic translation initiation factor 3 subunit F	0.56	77.19
PADG_00438	Eukaryotic translation initiation factor 3 subunit G	0.36	24.30
PADG_11111	Nuclear transport factor 2	0.27	36.71
PADG_02588	Protein phosphatase PP2A regulatory subunit B	0.43	55.01
PADG_00041	Ran GTPase-activating protein	0.42	149.41
PADG_06110	Translation factor SUI1	0.20	49.36
PADG_01079	Translation initiation factor 4B	0.59	106.95
PADG_00457	Translation initiation factor 4G	0.47	194.73
PADG_00080	Translation initiation factor eIF3	0.58	98.81
PADG_11904	Translational activator GCN1	0.46	250.07
PADG_05164	Transport protein SEC13	0.36	11.01
PADG_11157	tRNA (cytosine-5-)-methyltransferase NCL1	0.61	71.74
PADG_07962	MADS box transcription factor Mcm1	0.12	25.06
PADG_04962	Aspartyl-tRNA synthetase	0.42	58.09
PADG_02340	Methionyl-tRNA synthetase	0.27	102.74
PADG_04116	Methionyl-tRNA synthetase	0.39	39.58
PADG_04949	Threonyl-tRNA synthetase	0.62	134.68
PADG_03642	Tryptophanyl-tRNA synthetase	0.40	23.39
PADG_03689	Tyrosyl-tRNA synthetase	0.51	111.10

6- PROTEIN FATE

PADG_01432	Peptidyl-prolyl cis-trans isomerase NIMA-interacting 4	0.66	13.47
PADG_05011	Peptidyl-prolyl cis-trans isomerase	0.60	16.83
PADG_08049	Peptidyl-prolyl cis-trans isomerase cyp15	0.53	18.35
PADG_05124	Prefoldin subunit 3	0.10	5.68
PADG_04034	Mitochondrial protein import protein MAS5	0.29	156.98
PADG_08340	Ubiquitin fusion degradation protein	0.59	43.97
PADG_07804	Transport protein sec23	0.35	157.52
PADG_04883	Transport protein SEC24	0.26	73.58
PADG_07515	UBX domain-containing protein	0.48	54.37
PADG_08048	T-complex protein 1 subunit beta	0.45	164.83
PADG_01114	Importin subunit alpha-1a	0.20	57.31
PADG_05884	Mitochondrial import inner membrane translocase TIM8	0.51	29.77
PADG_05740	SNARE domain-containing protein	0.18	11.15
PADG_06439	NEDD8-conjugating enzyme Ubc12	0.60	24.02
PADG_07156	Histone acetyltransferase type B catalytic subunit	0.44	97.29
PADG_04880	Mitogen-activated protein kinase	0.41	18.33
PADG_02197	DNA damage tolerance protein rad31	0.36	10.74
PADG_07925	Ubiquitin-conjugating enzyme	0.30	22.05
PADG_01992	Mitochondrial-processing peptidase subunit alpha	0.37	29.13
PADG_11423	A-factor-processing enzyme	0.57	50.03
PADG_06359	Bleomycin hydrolase	0.46	68.67

PADG_05335	Iron sulfur cluster assembly protein	0.57	49.04
PADG_06655	Coatomer subunit delta	0.17	58.08
PADG_00300	26S protease regulatory subunit 8	0.26	130.16
PADG_12469	26S proteasome non-ATPase regulatory subunit 6	0.55	115.87
PADG_04234	26S proteasome non-ATPase regulatory subunit 8	0.51	39.33
PADG_00071	26S proteasome regulatory subunit RPN10	0.62	23.37
PADG_08095	26S proteasome regulatory subunit rpn-8	0.21	61.66
PADG_03944;	26S proteasome non-ATPase regulatory subunit 10	0.40	104.76
PADG_06276	O-sialoglycoprotein endopeptidase	0.22	11.99
PADG_07929	Ubiquitin carboxyl-terminal hydrolase	0.53	119.33
PADG_11319	Ubiquitin-conjugating enzyme variant MMS2	0.49	97.58
PADG_00634	Vacuolar protease A	0.56	64.16
PADG_06815	Xaa-Pro dipeptidase	0.47	50.79

7- PROTEIN WITH BINDING FUNCTION OR COFACTOR REQUIREMENT

PADG_03895	Dynein light chain LC8-type	0.33	18.65
PADG_00011	Actin binding protein	0.53	76.87
PADG_03390	Molybdenum cofactor synthesis protein cinnamon	0.57	15.55
PADG_01032	Curved DNA-binding protein	0.46	178.28
PADG_05381	RNA-binding protein	0.23	10.31
PADG_02022	Clathrin light chain	0.66	57.40
PADG_01849	GTP-dependent nucleic acid-binding protein engD	0.60	225.76
PADG_02207	GTP-binding protein	0.17	37.00
PADG_08304	GTP-binding protein YPTM2	0.18	126.10
PADG_04420	Peptide methionine sulfoxide reductase msrA	0.41	59.54
PADG_05308	Type 2A phosphatase activator tip41	0.17	75.35
PADG_11347	TIA1 cytotoxic granule-associated RNA binding protein	0.37	59.17

8- CELLULAR TRANSPORT, TRANSPORT FACILITIES AND TRANSPORT ROUTES

PADG_07957	Ferric reductase transmembrane component 7	0.64	34.72
PADG_00622	Arsenical pump-driving ATPase	0.35	60.57
PADG_04852	EH domain binding protein epsin 2	0.63	23.32
PADG_00282	GTP-binding protein SAS1	0.14	40.32
PADG_02686	Reduced viability upon starvation protein	0.56	28.49
PADG_00442	Arf gtpase-activating protein	0.38	48.44
PADG_03551	F-actin-capping protein subunit alpha	0.31	107.29
PADG_00937	Ras-related protein Rab-5C	0.12	119.27
PADG_02833	ADP-ribosylation factor	0.41	113.72
PADG_07930	ARP2/3 complex 20 kDa subunit	0.46	75.83
PADG_02401	ARP2/3 complex 21 kDa subunit	0.53	39.72
PADG_07014	Vesicular-fusion protein sec17	0.60	39.59

9- CELLULAR COMMUNICATION/SIGNAL TRANSDUCTION MECHANISM

PADG_02300	Protein phosphatase 2C	0.66	95.94

PADG_02153	Mitogen-activated protein kinase HOG1	0.33	20.37
PADG_11275	CMGC/MAPK protein kinase	0.23	115.16
PADG_11742	MAP Kinase Interacting Kinase	0.43	26.77
PADG_02800	Adenylyl cyclase-associated protein	0.40	22.60
PADG_02017	Calmodulin	0.53	78.01
10- CELL RESCUE, DEFENSE AND VIRULENCE			
Stress response			
PADG_04379	Heat shock protein STI1	0.39	430.59
PADG_02030	Hsp90 co-chaperone Cdc37	0.49	215.55
PADG_07715	Heat shock protein	0.13	913.35
Detoxification			
PADG_03163	Cytochrome c peroxidase	0.42	190.52
PADG_05628	Disulfide-isomerase tigA	0.66	136.92
PADG_03500	Glutamate-cysteine ligase	0.44	24.59
PADG_02218	Glutathione synthetase	0.35	6.79
PADG_00529	Glutaredoxin	0.22	43.50
PADG_03161	Thioredoxin	0.44	47.29
PADG_05504	Thioredoxin	0.29	64.81
PADG_05344	Peroxiredoxin Q/BCP	0.41	72.62
PADG_01263	Superoxide dismutase Fe/Mn SOD6	0.06	6.04
11-BIOGENESIS OF CELLULAR COMPONENTS			
Cell wall			
PADG_08120	glucosamine 6-phosphate N-acetyltransferase	0.52	50.16
Cytoskeleton/structural proteins			
PADG_07249	Actin binding protein	0.50	213.57
PADG_12076	Actin	0.12	130.34
PADG_12077	Actin	0.05	277.77
PADG_12426	1,4-alpha-glucan-branching enzyme	0.57	149.20
PADG_02125	Actin	0.34	61.89
PADG_00945	Actin related protein 2/3 complex, subunit 5	0.47	26.96
PADG_05538	Actin	0.18	196.88
12- MISCELLANEOUS			
PADG_04260	HET-C protein	0.66	59.08
PADG_05341	Fimbrin	0.12	136.68
PADG_00967	Golgi complex component Cog3	0.20	66.05
PADG_03226	P450 monooxygenase	0.18	41.23
PADG_03397;	DNA-directed RNA polymerase	0.54	34.40
PADG_03288	ATP NAD kinase	0.32	15.25
PADG_08290	KOW motif domain-containing protein	0.50	43.87

PADG_12310	Histidinol dehydrogenase	0.34	24.25
PADG_12196	Nucleolar protein 58	0.10	50.34
PADG_11353	Signal recognition particle subunit SRP72	0.51	133.11
PADG_11302	VosA	0.54	43.80
PADG_02846	Glutaredoxin domain-containing protein	0.50	32.28
PADG_02664	SAP domain-containing protein	0.66	14.73
PADG_03121	DUF757 domain-containing protein	0.39	5.75
PADG_00694	Ankyrin repeat protein	0.63	29.01
PADG_01160	PCI domain-containing protein	0.13	75.47
PADG_03244	HD domain-containing protein	0.45	46.86
PADG_03382	DUF866 domain-containing protein	0.66	18.76
PADG_08034	Dienelactone hydrolase family protein	0.50	44.15
PADG_12437	EF hand domain-containing protein	0.42	167.04
PADG_00999	CAP20 protein	0.17	12.03
PADG_03830	WD repeat-containing protein 1-B	0.64	274.62

13-UNCLASSIFIED

PADG_08451	Hypothetical protein	0.20	34.33
PADG_04879	Hypothetical protein	0.06	17.15
PADG_00237	Hypothetical protein	0.28	56.24
PADG_05340	Hypothetical protein	0.60	146.99
PADG_08212	Hypothetical protein	0.52	24.19
PADG_12237	Hypothetical protein	0.27	4.84
PADG_01021	Hypothetical protein	0.10	45.59
PADG_04869	Hypothetical protein	0.44	69.49
PADG_03654	Hypothetical protein	0.48	32.32
PADG_07452	Hypothetical protein	0.27	22.59
PADG_00046	Hypothetical protein	0.11	18.66
PADG_00222	Hypothetical protein	0.18	87.21
PADG_00388	Hypothetical protein	0.35	24.52
PADG_00440	Hypothetical protein	0.30	28.00
PADG_07979	Hypothetical protein	0.58	70.27
PADG_00541	Hypothetical protein	0.52	33.49
PADG_00555	Hypothetical protein	0.50	16.23
PADG_00769	Hypothetical protein	0.07	14.58
PADG_00921	Hypothetical protein	0.08	27.52
PADG_00944	Hypothetical protein	0.45	66.92
PADG_01148	Hypothetical protein	0.28	6.29
PADG_01285	Hypothetical protein	0.50	36.81
PADG_01287	Hypothetical protein	0.63	48.47
PADG_05491	Hypothetical protein	0.28	37.75
PADG_01409	Hypothetical protein	0.44	6.58
PADG_02092	Hypothetical protein	0.22	49.52
PADG_02307	Hypothetical protein	0.31	44.23

PADG_02346	Hypothetical protein	0.62	6.37
PADG_02671	Hypothetical protein	0.11	5.02
PADG_02759	Hypothetical protein	0.14	91.01
PADG_03110	Hypothetical protein	0.34	9.25
PADG_03135	Hypothetical protein	0.04	6.28
PADG_03159	Hypothetical protein	0.24	5.67
PADG_03428	Hypothetical protein	0.43	26.01
PADG_03612	Hypothetical protein	0.48	16.32
PADG_03631	Hypothetical protein	0.06	44.77
PADG_03645	Hypothetical protein	0.13	11.83
PADG_03660	Hypothetical protein	0.58	131.28
PADG_03827	Hypothetical protein	0.38	23.83
PADG_04057	Hypothetical protein	0.21	116.34
PADG_05921	Hypothetical protein	0.11	17.62
PADG_04357	Hypothetical protein	0.36	72.76
PADG_04423	Hypothetical protein	0.66	21.64
PADG_04494	Hypothetical protein	0.55	58.26
PADG_04512	Hypothetical protein	0.66	17.30
PADG_05274	Hypothetical protein	0.02	15.43
PADG_05408	Hypothetical protein	0.31	21.89
PADG_05462	Hypothetical protein	0.30	83.91
PADG_05935	Hypothetical protein	0.39	44.40
PADG_06220	Hypothetical protein	0.14	17.50
PADG_06435	Hypothetical protein	0.11	22.82
PADG_06473	Hypothetical protein	0.27	18.61
PADG_06690	Hypothetical protein	0.55	81.80
PADG_06798	Hypothetical protein	0.11	10.65
PADG_07205	Hypothetical protein	0.44	6.83
PADG_07264	Hypothetical protein	0.63	15.30
PADG_02475	Hypothetical protein	0.16	36.57
PADG_07414	Hypothetical protein	0.61	29.26
PADG_07520	Hypothetical protein	0.62	40.32
PADG_07935	Hypothetical protein	0.01	6.06
PADG_08037	Hypothetical protein	0.27	24.34
PADG_08116	Hypothetical protein	0.39	44.75
PADG_08238	Hypothetical protein	0.15	26.79
PADG_08305	Hypothetical protein	0.50	19.26
PADG_08342	Hypothetical protein	0.47	73.54
PADG_08368	Hypothetical protein	0.18	156.18
PADG_08413	Hypothetical protein	0.29	42.13
PADG_08480	Hypothetical protein	0.64	72.47
PADG_08483	Hypothetical protein	0.63	39.18
PADG_08693	Hypothetical protein	0.28	41.79
PADG_11091	Hypothetical protein	0.04	6.89

PADG_11366	Hypothetical protein	0.17	27.08
PADG_11406	Hypothetical protein	0.13	5.15
PADG_11572	Hypothetical protein	0.62	5.85
PADG_11593	Hypothetical protein	0.01	5.68
PADG_11622	Hypothetical protein	0.02	5.13
PADG_11992	Hypothetical protein	0.37	4.73
PADG_12058	Hypothetical protein	0.11	5.46
PADG_12194	Hypothetical protein	0.46	16.62
PADG_05205	Hypothetical protein	0.46	6.04
PADG_00735	Hypothetical protein	0.19	107.46
PADG_12364	Hypothetical protein	0.32	6.42

[a] Identification of differentially regulated proteins from *Paracoccidioides* genome database (http://www.broadinstitute.org/annotation/genome/paracoccidioides_brasiliensis/MultiHome.html) using the ProteinLynx Global Server vs. 2.4 (PLGS) (Waters Corporation, Manchester, UK).

[b] Proteins annotation from *Paracoccidioides* genome database or by homology from NCBI database (http://www.ncbi.nlm.nih.gov/).

[c] Acetate/Glucose means: The level of expression in yeast cells derived from cultured in sodium acetate divided by the level in the control yeast cells cultured in glucose.

[d] Biological process of differentially expressed proteins from MIPS (http://mips.helmholtz-muenchen.de/funcatDB/) and Uniprot databases (http://www.uniprot.org/).

Supplemental Table 6: Proteins up-regulated in *Paracoccidioides brasiliensis* isolate Pb339 after growth for 48 hours in sodium acetate as carbon source.

Accession number[a]	Protein Description[b]	Acetate/Glucose Ratio[c]	Score
Functional categories[d]			
1- METABOLISM			
Amino acid metabolism			
PADG_04686	Glutamine synthetase	8.93	59.90
PADG_05085	Delta-1-pyrroline-5-carboxylate dehydrogenase	1.86	297.72
PADG_04419	Carbapenem antibiotics biosynthesis protein carD	1.77	47.21
PADG_05337	Gamma-glutamyl phosphate reductase	6.95	207.31
PADG_03825	NAD-specific glutamate dehydrogenase	2.47	760.59
PADG_00663	Homoserine dehydrogenase	3.83	164.03
PADG_02456	Cystathionine gamma-lyase	2.18	67.15
PADG_11705	L-serine dehydratase	3.02	70.21
PADG_06213	Phosphoserine aminotransferase	1.59	188.76
PADG_05896	D-3-phosphoglycerate dehydrogenase	1.51	69.27
PADG_06301	Imidazoleglycerol-phosphate dehydratase	1.60	45.04
PADG_01286	Homoisocitrate dehydrogenase	1.87	80.02
PADG_08092	L-aminoadipate-semialdehyde dehydrogenase large subunit	1.98	211.00
PADG_08452	3',5'-bisphosphate nucleotidase	2.63	47.97
PADG_07369	Isovaleryl-CoA dehydrogenase	1.63	258.19
PADG_00637	Arginase	2.88	59.92
PADG_07029	Acetylornithine aminotransferase	1.80	95.62
PADG_04516	NADP-specific glutamate dehydrogenase	2.65	163.29
PADG_08176	Cobalamin-independent synthase	2.79	78.70
PADG_01886	Adenosylhomocysteinase	1.91	236.81
PADG_03058	Succinate-semialdehyde dehydrogenase	2.33	240.51
PADG_01228	3-hydroxybutyryl-CoA dehydrogenase	1.87	141.99
PADG_07274	Anthranilate synthase component 2	2.13	283.23
PADG_07366	Methylcrotonoyl-CoA carboxylase subunit alpha	1.92	139.22
PADG_02214	4-aminobutyrate aminotransferase	1.62	231.77
PADG_00066	tRNA methyltransferase Trm5	2.05	93.01
PADG_01314	YggS family pyridoxal phosphate enzyme	5.78	98.63
PADG_03671	Phenylpyruvate tautomerase	2.03	141.35
PADG_03964	Fumarylacetoacetate hydrolase domain-containing protein	2.27	119.23
PADG_04142	Fumarylacetoacetate hydrolase domain-containing protein	2.81	50.39
Nitrogen, sulfur and selenium metabolism			
PADG_01697	Carbonic anhydrase	2.23	44.05
PADG_07674	Carbonic anhydrase	2.40	182.02
PADG_06490	Formamidase	1.68	237.65
PADG_08009	Monoxygenase	1.53	45.63

PADG_00734	Urea carboxylase	5.50	185.29
PADG_02728	Sulfite oxidase	1.67	153.46
PADG_02048	Nitroreductase family protein	1.55	84.01
Nucleotide/nucleoside/nucleobase metabolism			
PADG_08098	Adenylate kinase cytosolic	4.65	93.05
PADG_02183	ADP-ribose pyrophosphatase	6.15	77.89
PADG_04340	DNA-directed RNA polymerase II subunit RPB2	2.78	188.52
PADG_06897	mRNA turnover protein	5.23	12.90
PADG_08066	Purine nucleoside phosphorylase	1.71	28.86
PADG_12503	RNA-directed DNA polymerase	2.84	83.25
PADG_01100	Uracil phosphoribosyltransferase	2.72	38.01
PADG_06197	Xanthine dehydrogenase	3.77	207.86
Phosphate metabolism			
PADG_01617	Phosphotransmitter protein Ypd1	1.89	15.33
PADG_06273	Calcineurin subunit B	1.69	18.99
C-compound and carbohydrate metabolism			
PADG_01372	Mannitol-1-phosphate 5-dehydrogenase	1.52	267.33
PADG_03278	Myo-inositol-1-phosphate synthase	1.74	134.21
PADG_04687	3-beta-hydroxysteroid dehydrogenase	1.61	64.42
PADG_04939	Succinyl-CoA:3-ketoacid-coenzyme A transferase subunit B	1.52	175.46
PADG_06765	NADP-dependent leukotriene B4 12-hydroxydehydrogenase	4.51	81.09
PADG_03268	NADPH-dependent D-xylose reductase	1.89	169.53
PADG_07618	Vanillin dehydrogenase	2.27	111.12
PADG_08722	Glycogen synthase kinase 3 beta	1.68	123.02
PADG_02847	HpcH/HpaI aldolase	2.49	101.30
Lipid, fatty acid and isoprenoid metabolism			
PADG_00513	2-succinylbenzoate-CoA ligase	2.07	164.96
PADG_06876	3-hydroxyisobutyryl-CoA hydrolase	3.15	187.30
PADG_01687	3-ketoacyl-CoA thiolase	1.71	307.68
PADG_04495	4-coumarate-CoA ligase	2.18	94.45
PADG_08468	4-hydroxyphenylpyruvate dioxygenase	1.69	234.68
PADG_02751	Acetyl-CoA acetyltransferase/ tiolase	1.51	195.73
PADG_02597	Acetyl-CoA hydrolase	1.59	17.87
PADG_02991	Acyl-coenzyme A oxidase/ desidrogenase	1.56	194.48
PADG_07023	Carnitine O-acetyltransferase	9.11	220.24
PADG_05783	Farnesyl pyrophosphate synthetase	1.56	128.79
PADG_00254	Fatty acid synthase subunit alpha reductase	4.09	511.16
PADG_00608	Formyl-coenzyme A transferase	1.66	148.41
PADG_07031	Hydroxymethylglutaryl-CoA lyase	1.92	134.59
PADG_05281	Propionate-CoA ligase	2.05	21.27

PADG_07699	S-formylglutathione hydrolase	1.57	69.52
PADG_01486	Short chain dehydrogenase/reductase family	2.17	122.05
Metabolism of vitamins, cofactors, and prosthetic groups			
PADG_08108	Coproporphyrinogen III oxidase	3.52	78.55
PADG_05490	Molybdopterin binding domain-containing protein	1.76	89.22
PADG_05947	Nicotinate-nucleotide pyrophosphorylase	1.53	211.13
PADG_06088	Ubiquinone biosynthesis protein coq-4	1.77	47.39
PADG_04032	Uroporphyrinogen decarboxylase	1.79	127.64
Secondary metabolism			
PADG_02981	ThiJ/PfpI family protein	5.21	207.87
ENERGY			
Glycolysis and gluconeogenesis			
PADG_05109	2,3-bisphosphoglycerate-independent phosphoglycerate mutase	1.75	179.69
PADG_05951	Aldose 1-epimerase	1.52	35.78
PADG_01706	Fructose-1,6-bisphosphatase	1.93	123.19
PADG_02411	Glyceraldehyde-3-phosphate dehydrogenase	2.25	404.23
PADG_11132	Phosphoglucomutase	1.85	521.06
Ethanol production			
PADG_04701	Alcohol dehydrogenase	4.63	246.56
PADG_11405	Alcohol dehydrogenase 1	1.89	209.72
Pentose-phosphate pathway			
PADG_04604	Transketolase	1.88	362.84
PADG_07420	Transaldolase	1.52	339.23
PADG_00780	Ribose-phosphate pyrophosphokinase	2.86	169.19
PADG_07217	Ribose-phosphate pyrophosphokinase	2.01	39.11
PADG_11977	Ribokinase	2.05	57.87
Tricarboxylic-acid pathway			
PADG_01762	2-oxoglutarate dehydrogenase E1	1.65	419.90
PADG_04993	ATP-citrate synthase subunit 1	2.02	287.66
PADG_01546	Citrate lyase subunit beta	2.77	92.07
PADG_08119	Fumarate hydratase	3.25	180.84
PADG_12250	Pyruvate dehydrogenase kinase	3.65	59.22
PADG_07213	Pyruvate dehydrogenase protein X component	1.83	254.39
Methylcytrate cycle			
PADG_04710	2-methylcitrate synthase	2.32	421.12
PADG_04709	Mitochondrial 2-methylisocitrate lyase	2.98	225.72

Electron transport and membrane-associated energy conservation

PADG_05750	Cytochrome c oxidase subunit Via	1.88	35.10
PADG_07813	ATP synthase gamma chain	1.91	130.08
PADG_02561	ATPase alpha subunit	1.93	446.71
PADG_00171	Cytochrome b2	2.91	217.80
PADG_06221	Formate dehydrogenase	3.88	167.37
PADG_04175	Inorganic pyrophosphatase	1.69	221.03
PADG_05343	NADH-ubiquinone oxidoreductase 21.3 kDa subunit	1.60	16.70
PADG_06201	Oxidoreductase ucpA	1.64	69.11
PADG_05436	Ubiquinol-cytochrome c reductase iron-sulfur subunit	1.73	45.49
PADG_04501	Ubiquinol-cytochrome c reductase subunit 7	5.84	31.65
PADG_04319	V-type ATPase, G subunit	4.30	162.12
PADG_01519	NADPH dehydrogenase	3.94	134.21
PADG_06196	12-oxophytodienoate reductase	3.03	393.26

3- CELL CYCLE AND DNA PROCESSING

PADG_01391	DNA repair and recombination protein RAD26	1.57	114.81
PADG_06911	DNA repair and recombination protein pif1	1.87	18.51
PADG_08606	DNA mismatch repair protein Msh3	2.44	71.26
PADG_04056	14-3-3 protein epsilon	1.71	265.12
PADG_02724	Asparagine-rich protein	1.72	56.47
PADG_05369	Cell division control protein	1.54	26.77
PADG_02157	Cytoskeletal adaptor protein SagA	2.00	119.38
PADG_05906	Histone H2a	6.64	85.50
PADG_05907	Histone H2B type 1-A	1.84	100.20
PADG_11679	Proliferating cell nuclear antigen	1.65	254.32
PADG_04004	Serine/threonine-protein kinase Chk2	76.71	27.88
PADG_06182	Transcriptional repressor TUP1	1.98	204.90
PADG_02900	Tubulin beta chain	1.73	44.21

4- TRANSCRIPTION

PADG_07629	C2H2 finger domain-containing protein	4.27	54.51
PADG_00873	Histone H3	2.55	76.34
PADG_00872	Histone H4	3.48	127.89
PADG_07134	Histone H4.2	3.33	152.75
PADG_04910	NGG1-interacting factor 3	1.80	22.23
PADG_04966	Phosducin family protein	1.73	36.21
PADG_02473	Pirin	3.49	21.15
PADG_07509	Transcription initiation factor TFIID subunit 6	1.92	20.86
PADG_08345	Transcriptional regulator	2.27	32.84
PADG_05885	Cell cycle control protein cwf14	1.98	35.57
PADG_03696	Nuclear polyadenylated RNA-binding protein Nab2	2.87	26.71
PADG_02996	PAB1 binding protein	2.71	70.85

PADG_05545	Pre-mRNA-splicing factor ATP-dependent RNA helicase	3.33	105.36
PADG_04796	Pre-mRNA-splicing factor rse1	3.62	196.23
PADG_01783	Splicing factor 3a subunit 2	4.76	30.86
PADG_05587	U2 small nuclear ribonucleoprotein B	1.53	70.06
PADG_11352	Transcription factor RfeF	1.98	30.54
PADG_03431	G4 quadruplex nucleic acid binding protein	2.34	120.50
5- PROTEIN SYNTHESIS			
PADG_12324	40S ribosomal protein S19	2.05	170.31
PADG_06680	40S ribosomal protein S22	2.20	130.72
PADG_03315	40S ribosomal protein S4	1.58	253.27
PADG_07803	60S ribosomal protein L12	1.56	151.54
PADG_05939	60S ribosomal protein L27a	1.54	121.40
PADG_03781	60S ribosomal protein L30	2.66	63.90
PADG_11585	60S ribosomal protein L37	2.58	50.69
PADG_11379	60S ribosomal protein L5	1.85	256.30
PADG_02888	60S ribosomal protein L6	1.67	238.98
PADG_01568	Mitochondrial 54S ribosomal protein YmL36	90.96	11.32
PADG_02064	NAM9+ protein	2.74	48.36
PADG_06768	rRNA 2'-O-methyltransferase fibrillarin	1.96	69.01
PADG_05787	ATP-dependent RNA helicase FAL1	2.76	87.65
PADG_06265	Elongation factor 1-gamma 1	1.93	284.67
PADG_04016	Eukaryotic translation initiation factor 3 subunit A	3.35	164.70
PADG_08033	Eukaryotic translation initiation factor 3 subunit B	1.98	176.04
PADG_00626	Eukaryotic translation initiation factor 3 subunit E	5.04	97.58
PADG_01865	Eukaryotic translation initiation factor 3 subunit H	3.60	82.97
PADG_06681	Importin subunit beta-1	1.55	44.67
PADG_06997	Nuclear cap-binding protein	1.52	23.87
PADG_05199	Nuclear cap-binding protein subunit 2	2.90	4.89
PADG_02339	Nucleoporin-17	2.75	58.96
PADG_02908	Ubiquitin-like modifier SUMO	2.43	20.75
PADG_04863	Leucyl-tRNA synthetase	2.54	190.09
PADG_07732	Aspartyl-tRNA synthetase	4.75	31.38
PADG_08472	Lysyl-tRNA synthetase	3.98	221.46
6- PROTEIN FATE			
PADG_00501	DnaJ domain-containing protein	2.06	109.44
PADG_00928	T-complex protein 1 subunit gamma	1.67	141.38
PADG_01565	Calreticulin	3.92	91.58
PADG_05129	UDP-glucose:glycoprotein glucosyltransferase	3.13	105.89
PADG_06998	Transport protein SEC31	2.57	188.97
PADG_04795	Deubiquitination-protection protein dph1	2.27	119.91
PADG_05032	Hsp90 binding co-chaperone (Sba1)	1.81	55.05
PADG_05094	T-complex protein 1 subunit zeta	1.58	142.62

PADG_08484	T-complex protein 1 subunit epsilon	4.35	126.45
PADG_08587	FK506-binding protein	1.60	33.10
PADG_00590	Cyclin-K	4.28	23.20
PADG_03040	GTP-binding protein ypt5	4.92	93.94
PADG_07064	Intermembrane space import and assembly protein	1.87	41.46
PADG_00741	Peroxisomal targeting signal 2 receptor	2.46	15.21
PADG_00910	Serine/threonine-protein kinase ksg1	1.59	21.74
PADG_02997	Kinase family protein	1.61	73.19
PADG_07558	Ubiquitin carboxyl-terminal hydrolase	3.43	148.30
PADG_12186	Ankyrin repeat protein	4.66	54.84
PADG_06766	Mitochondrial-processing peptidase subunit beta	2.75	189.90
PADG_08328	ATP-dependent Clp protease ATP-binding subunit clpX	1.72	479.84
PADG_03221	Saccharolysin	1.80	232.98
PADG_03290	Tripeptidyl-peptidase	3.13	124.82
PADG_04167	Aspartyl aminopeptidase	2.24	236.72
PADG_05193	Xaa-Pro aminopeptidase	1.87	175.50
PADG_06051	26S proteasome regulatory subunit rpn5	4.69	96.71
PADG_02636	26S protease regulatory subunit 4	1.72	55.81
PADG_03735	Prolyl peptidase	1.56	60.12
PADG_04877	26S proteasome non-ATPase regulatory subunit 13	1.69	115.17
PADG_04076	Proteasome component C11	1.60	98.31
PADG_05160	Dipeptidyl-peptidase	1.70	278.49
PADG_12323	peptidyl-prolyl cis-trans isomerase	3.51	133.30
PADG_08442	Proteasome component Y13	2.44	151.73
PADG_00051	26S protease regulatory subunit 8	8.27	134.43
PADG_02735	Proteasome component PRE6	4.59	136.67
PADG_03982	Proteasome component C1	1.51	120.68
PADG_05560	26S proteasome regulatory subunit rpn-1	2.05	122.81
PADG_04451	COP9 signalosome complex subunit 5	2.53	46.07
PADG_11128	26S protease regulatory subunit 6B	1.86	119.51
PADG_01652	E3 ubiquitin-protein ligase HUWE1	1.88	183.85
PADG_06314	Carboxypeptidase Y	2.44	102.34
PADG_07460	Vacuolar aminopeptidase	2.26	163.45

7-PROTEIN WITH BINDING FUNCTION OR COFACTOR REQUIREMENT

PADG_00352	SH3 domain-containing protein	1.56	45.03
PADG_02134	coatomer subunit epsilon	1.62	57.89
PADG_03098	DUF858 domain-containing protein	2.36	16.46
PADG_07317	RNA binding domain-containing protein	2.34	38.76
PADG_03459	Replication factor-A protein	1.96	42.03
PADG_11421	Histone H2A.Z	3.96	107.71
PADG_01566	APAF1-interacting protein	1.97	73.96
PADG_04559	Progesterone binding protein	3.70	86.55
PADG_06294	Hsp70 nucleotide exchange factor fes1	1.97	34.23

PADG_00554	Rho GTPase	4.37	21.28
8-CELLULAR TRANSPORT, TRANSPORT FACILITIES AND TRANSPORT ROUTES			
PADG_07508	CRAL/TRIO domain-containing protein	4.35	78.39
PADG_08401	Phosphatidylinositol-phosphatidylcholine transfer protein	4.40	28.31
PADG_02640	ATP-binding cassette sub-family F member 2	2.80	88.18
PADG_04302	Trafficking protein particle complex subunit 3	1.92	33.27
PADG_06033	NIPSNAP family protein	2.63	229.81
PADG_08423	Vacuolar protein sorting-associated protein	1.80	75.40
9-CELLULAR COMMUNICATION/SIGNAL TRANSDUCTION MECHANISM			
PADG_01243	Rab GDP-dissociation inhibitor	1.78	309.06
PADG_01787	1-phosphatidylinositol phosphodiesterase	2.06	59.81
PADG_02845	Integrin beta-1-binding protein	1.70	92.25
PADG_06778	TGF-beta signaling pathway	4.25	57.42
PADG_06103	GTPase activating protein	4.38	72.15
PADG_11474	HAL protein kinase	1.91	42.79
PADG_05608	GTP-binding protein ypt7	2.73	17.23
10-CELL RESCUE, DEFENSE AND VIRULENCE			
Stress response			
PADG_00778	Hsp70	1.77	149.35
PADG_02895	Heat shock protein	2.26	155.71
PADG_03562	Hsp70-like protein	1.62	482.62
PADG_05139	Heat shock 70 kd protein cognate 1	2.15	99.91
PADG_02785	Heat shock protein Hsp88	2.24	683.66
Disease, virulence and defense			
PADG_01479	Gamma-glutamyltranspeptidase	1.51	184.59
Detoxification			
PADG_01954	Superoxide dismutase Fe/Mn SOD5	1.73	125.51
PADG_01755	Superoxide dismutase Fe/Mn SOD2	2.24	99.33
PADG_07418	Superoxide dismutase Cu/Zn SOD1	2.27	114.85
PADG_01400	Superoxide dismutase Cu/Zn SOD4	1.80	61.42
PADG_01551	Thioredoxin reductase	1.69	81.39
PADG_00324	Peroxisomal catalase	3.57	356.41
PADG_04587	Peroxiredoxin HYR1	1.89	73.03
11. BIOGENESIS OF CELLULAR COMPONENTS			
Cell wall			
PADG_07913	Chitin synthase	4.81	40.27
PADG_03872	Chitin synthase	1.76	58.96

12- MISCELLANEOUS

PADG_06763	Septum formation protein Maf	2.09	27.03
PADG_01499	ISWI chromatin-remodeling complex ATPase ISW1	1.94	73.30
PADG_02565	FAS1 domain-containing protein	2.49	27.57
PADG_00111	PKHD-type hydroxylase TPA1	3.47	73.21
PADG_00422	Actin cytoskeleton protein (VIP1)	2.56	140.32
PADG_03031	CobW domain-containing protein	78.49	121.17
PADG_03436	3' exoribonuclease family protein	5.74	12.63
PADG_03526	M protein repeat protein	2.90	183.53
PADG_03534	lipase/esterase family protein	8.49	49.12
PADG_04223	2-dehydropantoate 2-reductase	2.65	38.96
PADG_04477	mediator of RNA polymerase II transcription subunit 18	2.12	34.05
PADG_06202	Arp2/3 complex subunit Arc16	4.42	133.09
PADG_07469	RNase III domain-containing protein	1.64	81.95
PADG_07627	4-carboxymuconolactone decarboxylase family protein	2.09	49.25
PADG_11060	viral A-type inclusion protein repeat protein	1.60	112.06
PADG_11652	Poly(rC)-binding protein	1.92	229.44
PADG_11131	oligoribonuclease	1.91	15.84
PADG_05356	isochorismatase domain-containing protein	5.65	119.19
PADG_11752	ATP-binding cassette sub-family G member 4	1.65	24.04
PADG_12274	YjeF family domain-containing protein	2.18	58.70
PADG_03959	ARP2/3 actin-organizing complex subunit Sop2	2.99	177.81
PADG_12252	Phosphotransferase enzyme family protein	1.84	27.91
PADG_03276	S-(hydroxymethyl)glutathione dehydrogenase	2.57	132.79
PADG_06906	Triosephosphate isomerase	2.20	203.21

13-UNCLASSIFIED

PADG_00085	Hypothetical protein	2.81	144.28
PADG_00452	Hypothetical protein	3.74	22.84
PADG_00472	Hypothetical protein	5.43	39.06
PADG_00496	Hypothetical protein	10.27	64.83
PADG_01009	Hypothetical protein	1.67	17.58
PADG_01010	Hypothetical protein	1.59	223.24
PADG_01130	Hypothetical protein	10.05	13.74
PADG_01204	Hypothetical protein	1.84	24.73
PADG_01488	Hypothetical protein	1.53	121.99
PADG_01639	Hypothetical protein	1.58	18.75
PADG_01818	Hypothetical protein	4.15	13.10
PADG_01867	Hypothetical protein	1.54	93.10
PADG_02114	Hypothetical protein	1.68	46.34
PADG_02336	Hypothetical protein	10.07	11.27
PADG_02343	Hypothetical protein	3.09	121.43
PADG_02658	Hypothetical protein	7.78	42.62
PADG_02678	Hypothetical protein	2.50	27.16

PADG_02948	Hypothetical protein	2.51	31.04
PADG_02967	Hypothetical protein	1.61	324.58
PADG_03210	Hypothetical protein	1.75	36.54
PADG_03410	Hypothetical protein	11.70	6.83
PADG_03429	Hypothetical protein	2.05	22.15
PADG_03570	Hypothetical protein	1.86	26.11
PADG_03745	Hypothetical protein	2.13	5.13
PADG_03785	Hypothetical protein	11.66	48.20
PADG_03835	Hypothetical protein	2.78	15.35
PADG_03886	Hypothetical protein	3.78	105.12
PADG_04002	Hypothetical protein	2.60	33.65
PADG_04243	Hypothetical protein	1.55	24.34
PADG_04343	Hypothetical protein	1.76	22.53
PADG_04389	Hypothetical protein	2.13	16.92
PADG_04430	Hypothetical protein	3.08	22.69
PADG_04457	Hypothetical protein	3.08	29.71
PADG_04907	Hypothetical protein	3.07	62.07
PADG_05152	Hypothetical protein	1.60	17.34
PADG_05157	Hypothetical protein	6.80	25.47
PADG_05445	Hypothetical protein	4.94	5.68
PADG_05600	Hypothetical protein	77.87	17.39
PADG_05703	Hypothetical protein	1.79	38.74
PADG_06037	Hypothetical protein	1.56	16.30
PADG_06080	Hypothetical protein	3.66	48.50
PADG_06136	Hypothetical protein	1.54	7.14
PADG_06179	Hypothetical protein	2.19	21.43
PADG_06514	Hypothetical protein	1.61	12.22
PADG_06893	Hypothetical protein	2.17	11.70
PADG_07103	Hypothetical protein	1.69	16.18
PADG_07355	Hypothetical protein	2.67	67.39
PADG_07402	Hypothetical protein	6.20	21.50
PADG_07670	Hypothetical protein	1.64	70.44
PADG_08218	Hypothetical protein	2.72	21.19
PADG_08724	Hypothetical protein	1.94	65.47
PADG_11063	Hypothetical protein	1.81	5.88
PADG_11100	Hypothetical protein	4.89	10.55
PADG_11101	Hypothetical protein	3.57	69.11
PADG_11247	Hypothetical protein	1.71	10.44
PADG_11360	Hypothetical protein	4.95	12.00
PADG_11437	Hypothetical protein	23.50	5.36
PADG_11941	Hypothetical protein	80.02	6.19
PADG_12124	Hypothetical protein	3.30	22.94
PADG_12272	Hypothetical protein	2.17	12.38
PADG_12309	Hypothetical protein	1.81	18.83

PADG_12353	Hypothetical protein	36.57	17.78
PADG_12502	Hypothetical protein	11.61	16.41
PADG_06898	Hypothetical protein	1.75	63.05
PADG_01935	Hypothetical protein	2.28	113.43
PADG_00627	Hypothetical protein	9.28	55.50
PADG_01632	Hypothetical protein	2.11	29.79
PADG_02887	Hypothetical protein	1.99	90.86
PADG_04612	Hypothetical protein	7.43	21.66
PADG_08603	Hypothetical protein	3.52	10.80
PADG_01626	Hypothetical protein	3.48	52.96
PADG_07214	Hypothetical protein	1.63	37.18
PADG_01630	Hypothetical protein	1.90	62.33
PADG_04817	Hypothetical protein	2.02	37.78
PADG_01047	Hypothetical protein	4.23	43.43

[a] Identification of differentially regulated proteins from *Paracoccidioides* genome database (http://www.broadinstitute.org/annotation/genome/paracoccidioides_brasiliensis/MultiHome.html) using the ProteinLynx Global Server vs. 2.4 (PLGS) (Waters Corporation, Manchester, UK).

[b] Proteins annotation from *Paracoccidioides* genome database or by homology from NCBI database (http://www.ncbi.nlm.nih.gov/).

[c] Acetate/Glucose means: The level of expression in yeast cells derived from cultured in sodium acetate divided by the level in the control yeast cells cultured in glucose.

[d] Biological process of differentially expressed proteins from MIPS (http://mips.helmholtz-muenchen.de/funcatDB/) and Uniprot databases (http://www.uniprot.org/).

Supplemental Table 7: Proteins down-regulated in *Paracoccidioides brasiliensis* isolate PbEPM83 after growth for 48 hours in sodium acetate as carbon source.

Accession number[a]	Protein Description[b]	Acetate/Glucose Ratio[c]	Score
Functional categories[d]			
1- METABOLISM			
Amino acid metabolism			
PADG_03984	Glucosamine-fructose-6-phosphateaminotransferase	0.11	374.05
PADG_05888	Aspartokinase	0.57	65.69
PADG_06955	Tryptophan synthase	0.33	90.45
PADG_02914	Aminomethyltransferase	0.54	348.25
PADG_08648	D-3-phosphoglycerate dehydrogenase	0.47	37.89
PADG_01621	Aspartate aminotransferase	0.38	273.91
PADG_07010	Urease accessory protein ureG	0.59	93.75
PADG_01536	Glutamine synthetase	0.46	55.97
PADG_07146	Pyrroline-5-carboxylate reductase	0.19	16.90
PADG_04689	Acetylglutamate kinase	0.60	205.14
PADG_00888	Argininosuccinate synthase	0.55	297.70
PADG_01404	Aspartate aminotransferase	0.52	253.15
PADG_04356	Cystathionine gamma-synthase	0.62	74.93
PADG_03500	Glutamate-cysteine ligase	0.52	34.07
PADG_01615	Homocitrate synthase	0.32	243.77
PADG_04487	Chorismate synthase	0.57	23.59
PADG_00386	Phospho-2-dehydro-3-deoxyheptonate aldolase	0.60	95.20
PADG_00215	Aromatic-L-amino-acid decarboxylase	0.52	83.41
PADG_02263	5-proFAR isomerase	0.51	22.11
PADG_08304	Acetolactate synthase small subunit	0.46	123.00
PADG_06671	3-isopropylmalate dehydrogenase A	0.51	93.20
Nucleotide/nucleoside/nucleobase metabolism			
PADG_04293	Adenine phosphoribosyltransferase	0.38	116.43
PADG_06112	Phosphoribosylaminoimidazole-succinocarboxamidesynthase	0.47	26.67
PADG_06585	GMP synthase	0.57	159.49
PADG_00331	Uricase	0.58	119.92
PADG_08530	Thymidylate synthase	0.54	53.15
PADG_06897	mRNA turnover protein	0.32	6.51
C-compound and carbohydrate metabolism			
PADG_01697	Carbonic anhydrase	0.61	10.44
PADG_01745	Mannose-1-phosphate guanyltransferase	0.62	155.31
PADG_03943	Phosphomannomutase	0.48	189.31
PADG_08474	Mannose-1-phosphate guanyltransferase	0.47	174.14
PADG_04374	UTP-glucose-1-phosphate uridylyltransferase	0.19	237.33

PADG_08100	NADP:D-xylose dehydrogenase	0.44	5.38
PADG_04900	Alpha,alpha-trehalose-phosphate synthase	0.62	64.63
PADG_12009	Trehalose 6-phosphate synthase/phosphatase	0.55	5.74
Lipid, fatty acid and isoprenoid metabolism			
PADG_02751	Acetyl-CoA acetyltransferase	0.49	250.18
PADG_00254	Fatty acid synthase subunit alpha reductase	0.55	713.59
PADG_00255	Fatty acid synthase subunit beta dehydratase	0.59	846.61
PADG_00434	Long-chain-fatty-acid-CoA ligase	0.59	38.09
PADG_02789	3-ketoacyl-CoA thiolase	0.42	63.41
PADG_03194	3-ketoacyl-CoA thiolase B	0.60	184.05
PADG_05130	Long-chain specific acyl-CoA dehydrogenase	0.62	85.67
PADG_05431	Phosphomevalonate kinase	0.40	39.02
Metabolism of vitamins, cofactors, and prosthetic groups			
PADG_02384	Delta-aminolevulinic acid dehydratase	0.33	16.71
PADG_05357	Thiamine-phosphate pyrophosphorylase	0.49	28.11
PADG_07528	Methylenetetrahydrofolate reductase	0.38	165.22
PADG_00464	Biotin-protein ligase	0.54	133.36
Secondary metabolism			
PADG_00262	Inositol monophosphatase	0.51	66.08
2- ENERGY			
Glycolysis and gluconeogenesis			
PADG_03813	Hexokinase	0.64	195.24
PADG_07202	Fructose-2,6-bisphosphatase	0.29	25.21
Tricarboxylic-acid pathway			
PADG_07213	Pyruvate dehydrogenase protein X component	0.40	343.13
PADG_04827	Acyl-coenzyme A synthetase O-MACS	0.62	17.07
PADG_04993	ATP-citrate synthase subunit 1	0.54	395.54
Electron transport and membrane-associated energy conservation			
PADG_02912	Vacuolar ATP synthase subunit C 1	0.64	146.07
PADG_03175	Vacuolar ATP synthase subunit F	0.63	82.02
PADG_04596	Vacuolar ATP synthase 16 kDa proteolipid subunit	0.51	6.33
PADG_08391	Plasma membrane ATPase	0.24	52.75
PADG_12152	F-type H+-transporting ATPase subunit g	0.25	46.39
3- CELL CYCLE AND DNA PROCESSING			
PADG_08684	WD repeat protein Cac2	0.40	61.63
PADG_02683	UV excision repair protein RAD23	0.64	60.74
PADG_01646	AAA family ATPase Pontin	0.64	65.77

PADG_04047	Serine/threonine-protein phosphatase PP1	0.63	6.63
PADG_01405	Protein phosphatase PP2A regulatory subunit A	0.30	85.86
PADG_06697	Poly(A) polymerase pla1	0.31	17.81
PADG_03531	Elongation factor 1-alpha	0.38	108.28
PADG_02359	Cell division control protein	0.40	62.16
PADG_02900	Tubulin beta chain	0.35	96.42
PADG_00128	Tubulin alpha chain	0.21	191.55
PADG_12076	Actin beta/gamma 1	0.66	133.20
PADG_12077	Actin beta/gamma 1	0.43	230.47
PADG_07477	Ankyrin repeat protein	0.06	5.83
PADG_02069	C-type cyclin	0.28	4.81
PADG_02763	Cyclin-dependent kinases regulatory subunit	0.55	35.60
PADG_03637	Cell division control protein	0.31	34.92
PADG_06182	Transcriptional repressor TUP1	0.56	218.31
PADG_11857	Cell cycle arrest protein BUB3	0.49	107.61
PADG_05885	Cell cycle control protein cwf14	0.60	28.49
PADG_00932	Eukaryotic translation initiation factor 3	0.57	88.07
PADG_05893	Nucleosome assembly protein	0.39	202.55

4- TRANSCRIPTION

PADG_07962	MADS box transcription factor Mcm1	0.25	28.80
PADG_04307	mRNA binding post-transcriptional regulator (Csx1)	0.49	133.52
PADG_05545	Pre-mRNA-splicing factor ATP-dependent RNA helicase	0.41	105.77
PADG_01783	Splicing factor 3a subunit 2	0.46	72.45
PADG_08423	Transcriptional regulator	0.36	84.89
PADG_03074	Transcription elongation factor spt5	0.56	64.74
PADG_00568	General negative regulator of transcription subunit 1	0.54	111.85
PADG_05975	Exosome complex exonuclease RRP4	0.03	5.20
PADG_00718	Histone chaperone asf1	0.58	19.36
PADG_01455	KH domain RNA-binding protein	0.59	119.48

5- PROTEIN SYNTHESIS

PADG_02445	40S ribosomal protein S15	0.63	76.46
PADG_03315	40S ribosomal protein S4	0.63	224.26
PADG_04493	SUMO-conjugating enzyme ubc9	0.45	29.86
PADG_00080	Translation initiation factor eIF3	0.45	158.08
PADG_04672	ATP-dependent RNA helicase SUB2	0.21	179.09
PADG_07073	Nonsense-mediated mRNA decay protein	0.29	71.83
PADG_00342	Eukaryotic translation initiation factor 3	0.33	74.44
PADG_00626	Eukaryotic translation initiation factor 3 subunit E	0.18	141.47
PADG_08033	Eukaryotic translation initiation factor 3 subunit B	0.52	135.30
PADG_08592	Eukaryotic translation initiation factor 4E-1	0.15	56.33
PADG_07285	RNA binding domain-containing protein	0.53	103.27
PADG_11711		0.25	188.21

PADG_00002	Alanyl-tRNA synthetase	0.47	446.82
PADG_04962	Aspartyl-tRNA synthetase	0.65	108.86
PADG_04116	Methionyl-tRNA synthetase	0.39	32.26
6- PROTEIN FATE			
PADG_00050	T-complex protein 1 subunit alpha	0.52	215.94
PADG_00928	T-complex protein 1 subunit gamma	0.22	223.15
PADG_03441	T-complex protein 1 subunit alpha	0.63	313.99
PADG_05108	Prefoldin beta subunit	0.42	58.76
PADG_05124	Prefoldin subunit 3	0.44	11.47
PADG_04034	Mitochondrial protein import protein MAS5	0.31	166.98
PADG_04048	Small COPII coat GTPase sar1	0.47	61.99
PADG_08048	T-complex protein 1 subunit beta	0.52	352.83
PADG_01114	Importin subunit alpha-1a	0.22	52.42
PADG_02637	Ubiquitin-conjugating enzyme	0.65	121.06
PADG_06439	NEDD8-conjugating enzyme Ubc12	0.66	39.57
PADG_07925	Ubiquitin-conjugating enzyme	0.43	33.75
PADG_03793	Oligosaccharyltransferase alpha subunit ostA	0.53	32.06
PADG_05837	Glycoprotein FP21	0.65	121.93
PADG_02625	4-coumarate-CoA ligase	0.49	271.98
PADG_01021	Actin monomer binding protein	0.54	68.19
PADG_05099	Calcium/calmodulin-dependent protein kinase type I	0.17	11.53
PADG_06655	Coatomer subunit delta	0.60	71.28
PADG_00300	26S protease regulatory subunit 8	0.33	138.38
PADG_02636	26S protease regulatory subunit 4	0.59	53.96
PADG_06851	26S proteasome non-ATPase regulatory subunit 11	0.60	65.33
PADG_08095	26S proteasome regulatory subunit rpn-8	0.51	95.00
PADG_00051	26S protease regulatory subunit 8	0.41	87.43
PADG_00599	26S protease regulatory subunit 6A	0.29	96.20
PADG_11701	26S protease subunit RPT4 [	0.51	25.28
PADG_05428	Proteasome maturation factor	0.60	52.17
PADG_06051	26S proteasome regulatory subunit rpn5	0.57	74.27
7- PROTEIN WITH BINDING FUNCTION OR COFACTOR REQUIREMENT			
PADG_00011	Actin binding protein	0.47	85.48
PADG_03098	DUF858 domain-containing protein	0.44	38.14
PADG_07714	NTF2 and RRM domain-containing protein	0.48	50.15
PADG_02924	G2/M phase checkpoint control protein Sum2	0.42	171.06
PADG_06294	Hsp70 nucleotide exchange factor fes1	0.36	7.56
PADG_02207	GTP-binding protein	0.49	47.49
8- CELLULAR TRANSPORT, TRANSPORT FACILITIES AND TRANSPORT ROUTES			
PADG_08263	Outer mitochondrial membrane protein porin 1	0.60	96.07
PADG_08725	Translin-associated protein X	0.50	26.51

PADG_00282	GTP-binding protein SAS1	0.41	70.36
PADG_02203	Membrane biogenesis protein Yop1	0.39	12.67
PADG_02686	Reduced viability upon starvation protein	0.66	37.98
PADG_04100	Clathrin heavy chain 1	0.65	372.85
PADG_03551	F-actin-capping protein subunit alpha	0.30	79.37
PADG_07756	F-actin-capping protein subunit beta	0.49	47.59
PADG_04965	Coatomer subunit gamma-1	0.57	143.97
PADG_07014	Vesicular-fusion protein sec17	0.45	107.29
PADG_05839	Transport protein particle subunit bet5	0.34	21.89
9- CELLULAR COMMUNICATION/SIGNAL TRANSDUCTION MECHANISM			
PADG_01787	1-phosphatidylinositol phosphodiesterase	0.48	46.91
PADG_02300	Protein phosphatase 2C	0.59	112.83
PADG_08337	GTP-binding protein rho1	0.56	160.54
PADG_02153	Mitogen-activated protein kinase HOG1	0.59	38.32
PADG_06243	cAMP-independent regulatory protein pac2	0.42	17.03
10- CELL RESCUE, DEFENSE AND VIRULENCE			
Stress response			
PADG_03180	DNA damage-inducible protein	0.59	93.63
PADG_03095	Mitochondrial peroxiredoxin PRX1	0.22	198.88
PADG_02761	Heat shock protein SSB1	0.64	332.21
PADG_00778	Hsp70	0.55	240.21
PADG_07715	Heat shock protein	0.19	881.46
Detoxification			
PADG_00529	Glutaredoxin	0.39	45.72
PADG_02846	Glutaredoxin domain-containing protein	0.37	47.47
PADG_01551	Thioredoxin reductase	0.58	84.67
PADG_03161	Thioredoxin	0.55	41.19
11-BIOGENESIS OF CELLULAR COMPONENTS			
Cell wall			
PADG_05937	chitin synthase activator	0.33	39.53
12- MISCELLANEOUS			
PADG_02587	COP9 signalosome complex subunit 4	0.54	60.09
PADG_03343	developmental protein fluG	0.43	42.01
PADG_00922	bud site selection protein	0.48	142.57
PADG_05341	fimbrin	0.32	237.90
PADG_00219	actin-like protein arp9	0.64	56.54
PADG_00260	DNA-binding protein HGH1	0.49	47.76
PADG_01052	3-demethylubiquinone-9 3-methyltransferase	0.43	33.32
PADG_01160	PCI domain-containing protein	0.30	88.65

PADG_01487	OTU domain-containing protein 6B	0.45	26.71
PADG_01688	DlpA domain-containing protein	0.51	59.74
PADG_03012	FluG domain-containing protein	0.59	41.19
PADG_04223	2-dehydropantoate 2-reductase	0.47	35.81
PADG_05580	PP-loop family protein	0.59	28.42
PADG_11395	K(+)/H(+) antiporter 1	0.43	78.21
PADG_11982	vacuolar protein sorting-associated protein	0.31	101.46
PADG_12125	phytanoyl-CoA dioxygenase family protein	0.56	58.50
PADG_12381	rab geranylgeranyl transferase escort protein	0.42	16.77
PADG_01032	DNA-binding protein, 42 kDa	0.66	173.77
PADG_04030	60S acidic ribosomal protein P0	0.67	159.12
PADG_04420	Peptide methionine sulfoxide reductase msrA	0.56	91.23
PADG_05308	Type 2A phosphatase activator tip41	0.65	64.33

13-- UNCLASSIFIED

PADG_04012	Hypothetical protein	0.63	22.15
PADG_03005	Hypothetical protein	0.32	39.52
PADG_11649	Hypothetical protein	0.66	17.20
PADG_03698	Hypothetical protein	0.66	26.03
PADG_00602	Hypothetical protein	0.66	32.42
PADG_02526	Hypothetical protein	0.49	11.04
PADG_02349	Hypothetical protein	0.26	11.64
PADG_02919	Hypothetical protein	0.64	39.48
PADG_03431	Hypothetical protein	0.57	181.38
PADG_05627	Hypothetical protein	0.58	61.62
PADG_00206	Hypothetical protein	0.63	36.67
PADG_00211	Hypothetical protein	0.64	75.91
PADG_00316	Hypothetical protein	0.24	17.13
PADG_00421	Hypothetical protein	0.50	26.80
PADG_02887	Hypothetical protein	0.21	80.60
PADG_00541	Hypothetical protein	0.27	12.51
PADG_00939	Hypothetical protein	0.52	10.45
PADG_01287	Hypothetical protein	0.52	19.35
PADG_01516	Hypothetical protein	0.56	27.11
PADG_01857	Hypothetical protein	0.45	35.81
PADG_02044	Hypothetical protein	0.19	38.01
PADG_02086	Hypothetical protein	0.39	66.57
PADG_02439	Hypothetical protein	0.41	12.34
PADG_02478	Hypothetical protein	0.30	14.23
PADG_04924	Hypothetical protein	0.50	80.63
PADG_02666	Hypothetical protein	0.23	27.74
PADG_03185	Hypothetical protein	0.64	31.76
PADG_04430	Hypothetical protein	0.39	37.36
PADG_04438	Hypothetical protein	0.07	5.78

PADG_04457	Hypothetical protein	0.44	12.33
PADG_04509	Hypothetical protein	0.35	10.73
PADG_05294	Hypothetical protein	0.60	10.47
PADG_05408	Hypothetical protein	0.61	17.33
PADG_06620	Hypothetical protein	0.07	5.36
PADG_07103	Hypothetical protein	0.57	40.93
PADG_07495	Hypothetical protein	0.28	29.75
PADG_07520	Hypothetical protein	0.54	70.84
PADG_07633	Hypothetical protein	0.43	27.89
PADG_08037	Hypothetical protein	0.64	34.90
PADG_08065	Hypothetical protein	0.52	22.79
PADG_04586	Hypothetical protein	0.33	17.06
PADG_04311	Hypothetical protein	0.64	66.10
PADG_08345	Hypothetical protein	0.17	16.41
PADG_08715	Hypothetical protein	0.65	155.19
PADG_01583	Hypothetical protein	0.39	16.15
PADG_08368	Hypothetical protein	0.61	196.20
PADG_11090	Hypothetical protein	0.53	23.18
PADG_11191	Hypothetical protein	0.57	20.26
PADG_00187	Hypothetical protein	0.62	75.89
PADG_11593	Hypothetical protein	0.00	10.93
PADG_11719	Hypothetical protein	0.02	5.47
PADG_11913	Hypothetical protein	0.49	22.81
PADG_11921	Hypothetical protein	0.55	9.39
PADG_12050	Hypothetical protein	0.57	23.38
PADG_12244	Hypothetical protein	0.39	13.13

[a] Identification of differentially regulated proteins from *Paracoccidioides* genome database (http://www.broadinstitute.org/annotation/genome/paracoccidioides_brasiliensis/MultiHome.html) using the ProteinLynx Global Server vs. 2.4 (PLGS) (Waters Corporation, Manchester, UK).

[b] Proteins annotation from *Paracoccidioides* genome database or by homology from NCBI database (http://www.ncbi.nlm.nih.gov/).

[c] Acetate/Glucose means: The level of expression in yeast cells derived from cultured in sodium acetate divided by the level in the control yeast cells cultured in glucose.

[d] Biological process of differentially expressed proteins from MIPS (http://mips.helmholtz-muenchen.de/funcatDB/) and Uniprot databases (http://www.uniprot.org/).

Supplemental Table 8: Proteins up-regulated in *Paracoccidioides brasiliensis* isolate PbEPM83 after growth for 48 hours in sodium acetate as carbon source.

Accession number[a]	Protein Description[b]	Acetate/Glucose Ratio[c]	Score
Functional categories[d]			
1- METABOLISM			
Amino acid metabolism			
PADG_00210	Glycine dehydrogenase	2.70	371.67
PADG_05085	Delta-1-pyrroline-5-carboxylate dehydrogenase	3.20	366.33
PADG_04062	Peptidase family protein	2.05	117.81
PADG_08662	Cystathionine beta-lyase	2.35	61.59
PADG_02726	Cysteine synthase	2.59	219.17
PADG_01886	Adenosylhomocysteinase	1.98	341.59
PADG_04522	Homoserine kinase	2.01	60.82
PADG_08376	Aspartate-semialdehyde dehydrogenase	1.94	178.88
PADG_00405	Choline dehydrogenase	1.78	133.41
PADG_00402	5-carboxymethyl-2-hydroxymuconate semialdehyde dehydrogenase	1.55	124.04
PADG_01228	3-hydroxybutyryl-CoA dehydrogenase	1.76	173.26
PADG_00336	Prephenate dehydrogenase	2.02	86.09
PADG_07214	Precorrin-2 dehydrogenase	5.61	63.03
PADG_02728	Sulfite oxidase	1.58	174.66
PADG_08465	Fumarylacetoacetase	1.61	284.68
PADG_07609	Dihydroxy-acid dehydratase	1.82	169.14
PADG_04570	Branched-chain-amino-acid aminotransferase	1.86	192.92
PADG_07370	Methylcrotonoyl-CoA carboxylase beta chain	1.70	192.95
PADG_00643	Mitochondrial methylglutaconyl-CoA hydratase	2.31	137.03
PADG_01328	Ornithine aminotransferase	1.64	218.66
PADG_00637	Arginase	1.57	83.84
PADG_00663	Homoserine dehydrogenase	1.85	165.59
PADG_05277	Serine hydroxymethyltransferase	1.71	250.23
PADG_01963	Glycine cleavage system H protein	1.52	117.87
PADG_08604	ATP phosphoribosyltransferase	1.75	36.85
PADG_00349	Kynureninase	2.15	34.44
PADG_08466	Homogentisate 1,2-dioxygenase	2.93	196.05
PADG_00875	Pentafunctional AROM polypeptide	1.75	475.88
PADG_03466	3-hydroxyisobutyrate dehydrogenase	1.52	250.46
Nitrogen, sulfur and selenium metabolism			
PADG_01150	2-nitropropane dioxygenase	1.64	121.25
PADG_01061	Cyanate hydratase	3.94	68.89
PADG_03852	HIRA interacting protein	1.76	29.45
PADG_00446	Oxidoreductase 2-nitropropane dioxygenase family	2.47	266.23

Nucleotide/nucleoside/nucleobase metabolism			
PADG_02246	Adenosine kinase	1.58	109.66
PADG_04340	DNA-directed RNA polymerase II subunit RPB2	2.06	193.11
PADG_06424	DNA-directed RNA polymerase III subunit RPC1	1.57	315.75
PADG_08066	Purine nucleoside phosphorylase	1.61	44.65
PADG_07918	Pyrimidine 5'-nucleotidase	2.04	15.15
PADG_02493	Ureidoglycolate lyase	6.09	17.60
C-compound and carbohydrate metabolism			
PADG_02123	Aflatoxin B1 aldehyde reductase member 2	2.23	144.99
PADG_00401	Glucosamine-6-phosphate isomerase	1.53	21.02
PADG_06765	NADP-dependent leukotriene B4 12-hydroxydehydrogenase	2.40	92.25
PADG_03859	NADP-dependent mannitol dehydrogenase	1.81	171.99
PADG_00604	Phosphoacetylglucosamine mutase	1.70	300.70
PADG_03710	Retrograde regulation protein	1.82	168.78
PADG_04312	UDP-N-acetylglucosamine pyrophosphorylase	1.52	253.34
Lipid, fatty acid and isoprenoid metabolism			
PADG_01687	3-ketoacyl-CoA thiolase	1.96	309.73
PADG_06721	3-oxoacyl-[acyl-carrier-protein] reductase	2.39	44.20
PADG_06805	Acyl-CoA dehydrogenase	2.47	272.08
PADG_07023	Carnitine O-acetyltransferase	2.15	254.86
PADG_06425	Delta(3,5)-Delta(2,4)-dienoyl-CoA isomerase	1.86	131.58
PADG_01209	Enoyl-CoA hydratase	2.08	267.66
PADG_12025	Glutaryl-CoA dehydrogenase	1.55	224.08
PADG_07031	Hydroxymethylglutaryl-CoA lyase	2.29	117.10
PADG_07411	NAD-dependent 15-hydroxyprostaglandin dehydrogenase	2.21	47.96
PADG_00601	Peroxisomal dehydratase	3.01	145.59
PADG_05281	Propionate-CoA ligase	3.50	103.15
PADG_07699	S-formylglutathione hydrolase	1.65	70.58
PADG_02527	Short chain dehydrogenase family protein	2.46	25.33
PADG_04939	Succinyl-CoA:3-ketoacid-coenzyme A transferase subunit B	2.23	227.51
PADG_00244	Trans-2-enoyl-CoA reductase	2.39	228.05
Metabolism of vitamins, cofactors, and prosthetic groups			
PADG_03598	3-methyl-2-oxobutanoatehydroxymethyltransferase	1.65	56.16
PADG_03213	5-formyltetrahydrofolate cyclo-ligase	1.58	46.61
PADG_03983	6,7-dimethyl-8-ribityllumazine synthase	1.72	81.54
PADG_04879	Uroporphyrinogen-III synthase	2.40	11.99
PADG_00821	Glutamyl-tRNA synthetase	2.69	436.08
PADG_05490	Molybdopterin binding domain-containing protein	1.68	105.44
PADG_01126	Molybdopterin synthase large subunit CnxH	1.63	10.02
PADG_03697	Protoporphyrinogen oxidase	1.54	65.69
PADG_12043	Cysteine desulfurase, mitochondrial	2.06	286.83

Secondary metabolism			
PADG_04899	Metallo-beta-lactamase domain-containing protein	2.48	48.87
PADG_02981	ThiJ/PfpI family protein	1.99	176.19
2-ENERGY			
Glycolysis and gluconeogenesis			
PADG_06187	6-phosphofructo-2-kinase	1.88	118.86
PADG_00852	Aldolase	4.07	27.60
PADG_01706	Fructose-1,6-bisphosphatase	1.56	173.53
Ethanol production			
PADG_04701	Alcohol dehydrogenase	4.64	212.97
PADG_11405	Alcohol dehydrogenase 1	3.52	195.36
PADG_03099	Aldehyde dehydrogenase	1.50	145.31
PADG_03403	Aldehyde dehydrogenase A	2.18	161.09
PADG_00714	Pyruvate decarboxylase	1.52	326.01
Tricarboxylic-acid pathway			
PADG_01762	2-oxoglutarate dehydrogenase E1	1.56	503.51
PADG_04994	ATP-citrate-lyase	1.55	215.40
PADG_08387	Citrate synthase	2.18	304.62
PADG_06494	Dihydrolipoyl dehydrogenase	1.61	417.52
PADG_08119	Fumarate hydratase	1.79	220.38
PADG_02592	Fumarate reductase	1.74	388.88
PADG_03977	Isocitrate dehydrogenase subunit 1	1.65	231.54
PADG_07210	Malate dehydrogenase	1.62	408.49
PADG_03268	NADPH-dependent D-xylose reductase	1.52	43.52
PADG_00052	Succinate dehydrogenase flavoprotein subunit	2.25	188.33
PADG_08013	Succinate dehydrogenase iron-sulfur subunit	4.24	62.30
PADG_02260	Succinyl-CoA ligase subunit alpha	1.55	212.60
Glyoxylate cycle			
PADG_01483	Isocitrate lyase	1.99	295.45
PADG_04702	Malate synthase	2.11	260.12
Methylcytrate cycle			
PADG_04710	2-methylcitrate synthase	2.62	439.39
PADG_04718	2-methylcitrate dehydratase	1.89	507.90
PADG_04709	Mitochondrial 2-methylisocitrate lyase	1.67	272.44
Electron transport and membrane-associated energy conservation			
PADG_02561	ATPase alpha subunit	3.46	551.56

PADG_02745	NADH-ubiquinone oxidoreductase	2.67	22.20
PADG_04397	cytochrome c oxidase subunit 4, mitochondrial	1.61	44.68
PADG_04501	ubiquinol-cytochrome c reductase subunit 7	2.47	18.67
PADG_05343	NADH-ubiquinone oxidoreductase 21.3 kDa subunit	2.09	4.29
PADG_06978	Cytochrome c	3.25	124.44
PADG_06995	Cytochrome c oxidase polypeptide VIb	1.97	43.20
PADG_07042	ATP synthase subunit 5	1.55	139.19
PADG_08373	F-type H+-transporting ATPase subunit epsilon	1.93	21.50
PADG_08292	Cytochrome-c oxidase chain VIIc	1.62	6.83
PADG_02578	ATP synthase subunit 4	1.96	127.09
PADG_03747	Alternative oxidase	3.55	31.20
PADG_04729	ATP synthase D chain, mitochondrial	2.28	60.01
PADG_05750	Cytochrome c oxidase subunit 5a	2.34	120.55
PADG_02468	F-type H+-transporting ATP synthase subunit	1.89	32.29
PADG_07813	ATP synthase gamma chain	1.85	92.56
PADG_08349	ATP synthase subunit beta	4.44	414.51
PADG_07789	ATP synthase delta chain	4.96	84.73
PADG_08394	Cytochrome b-c1 complex subunit 2	3.77	224.93
PADG_01841	Cytochrome c oxidase assembly protein COX19	1.90	54.09
PADG_00688	F-type H+-transporting ATPase subunit h	5.20	19.80
PADG_11981	V-type H+-transporting ATPase subunit A	1.93	284.14
PADG_05290	Cytochrome b5	1.80	30.70
PADG_12148	NADH-ubiquinone oxidoreductase 78 kDa subunit	2.63	11.93
3-CELL CYCLE AND DNA PROCESSING			
PADG_08606	DNA mismatch repair protein Msh3	2.30	44.93
PADG_01391	DNA repair and recombination protein RAD26	2.09	164.70
PADG_00237	Histone-lysine N-methyltransferase	2.94	40.25
PADG_04614	Prohibitin-1	1.66	99.13
PADG_07835	Replication factor-A protein	1.84	99.63
PADG_05798	Single-strand binding protein family	1.54	155.48
PADG_00759	Prefoldin subunit 4	1.94	49.66
PADG_01668	Centrin-3	1.90	28.73
PADG_05906	Histone H2a	2.49	69.68
PADG_00422	Actin cytoskeleton protein (VIP1)	1.53	206.56
4- TRANSCRIPTION			
PADG_02752	116 kDa U5 small nuclear ribonucleoprotein component	1.87	242.69
PADG_07629	C2H2 finger domain-containing protein	3.29	91.62
PADG_00873	Histone H3	1.87	86.33
PADG_00872	Histone H4	2.09	123.77
PADG_07134	Histone H4.2	2.06	153.08
PADG_04521	Mediator of RNA polymerase II transcription subunit 5	2.73	53.58
PADG_02555	RNA binding domain-containing protein	1.92	289.49

PADG_06666	RNA splicing factor Pad-1	1.75	125.55
PADG_05900	Transcription elongation factor 1	1.70	16.43
PADG_05924	ATP-dependent RNA helicase DHH1	2.27	118.07
PADG_05415	ATP-dependent RNA helicase suv3	1.75	42.86
PADG_02783	RNA-binding La domain-containing protein	1.57	131.64
PADG_02825	Splicing factor	1.73	14.02
PADG_05587	U2 small nuclear ribonucleoprotein B	2.56	81.31
PADG_04301	WD repeat-containing protein	1.74	17.61
PADG_06487	D-tyrosyl-tRNA(Tyr) deacylase	1.59	27.94
5- PROTEIN SYNTHESIS			
PADG_05562	Large subunit ribosomal protein L23	1.76	22.58
PADG_00627	Large subunit ribosomal protein L49	2.26	48.06
PADG_08453	Large subunit ribosomal protein L6	2.89	25.90
PADG_11743	Ribosomal RNA-processing protein 7	1.81	47.80
PADG_01854	Small subunit ribosomal protein S11	1.98	12.57
PADG_04475	Small subunit ribosomal protein YMR-31	2.07	48.83
PADG_07519	50S ribosomal protein L1	2.42	4.69
PADG_02056	50S ribosomal protein L12	2.20	127.81
PADG_01647	50S ribosomal protein L24	1.61	25.15
PADG_05177	54S ribosomal protein L9	1.66	10.54
PADG_05847	Brix domain-containing protein	2.61	45.74
PADG_05206	Mitochondrial 54S ribosomal protein L38	1.55	17.56
PADG_11083	Ribosomal protein L13	1.94	24.15
PADG_04449	Ribosomal protein L23e	1.80	91.17
PADG_03829	Ribosomal protein S18	1.62	54.89
PADG_05118	Translation initiation factor 3 subunit K	1.74	46.73
PADG_03046	Elongation factor G 1	1.90	269.60
PADG_04083	Eukaryotic translation initiation factor 2 subunit gamma	2.41	160.88
PADG_05388	Asparaginyl-tRNA synthetase	1.80	147.91
PADG_08472	Lysyl-tRNA synthetase	2.07	243.09
PADG_05897	Seryl-tRNA synthetase	1.72	275.50
PADG_00821	Glutamyl-tRNA synthetase	2.69	436.08
6-PROTEIN FATE			
PADG_02895	ATP-dependent Clp protease ATP-binding subunit ClpB	1.50	191.00
PADG_00501	DnaJ domain-containing protein	2.66	49.04
PADG_08587	FK506-binding protein	1.79	39.06
PADG_06992	Mitochondrial co-chaperone GrpE	1.93	212.32
PADG_05129	UDP-glucose:glycoprotein glucosyltransferase	1.76	256.94
PADG_02431	Translocation protein SEC66	1.53	24.26
PADG_04241	Coatomer subunit alpha	1.77	227.55
PADG_00839	Diphthine synthase	1.61	23.41
PADG_02197	DNA damage tolerance protein rad31	1.51	4.87

PADG_04063	Histidine kinase M7	1.83	59.52
PADG_07156	Histone acetyltransferase type B catalytic subunit	1.56	168.09
PADG_06766	Mitochondrial-processing peptidase subunit beta	2.05	230.10
PADG_05980	Protein kinase byr1	1.53	33.13
PADG_07834	Ubiquitin carboxyl-terminal hydrolase	2.22	163.85
PADG_05335	Iron sulfur cluster assembly protein	1.50	74.19
PADG_04167	Aspartyl aminopeptidase	1.73	270.11
PADG_08109	Gamma-aminobutyric acid receptor associated protein	1.64	15.26
PADG_04125	Mitochondrial presequence protease	2.10	384.78
PADG_03982	Proteasome component C1	1.50	132.00
PADG_03965	Proteasome component Pre4	1.65	114.48
PADG_08442	Proteasome component Y13	1.70	152.27
PADG_07422	Subtilase-type proteinase psp3	1.57	97.95
PADG_05193	Xaa-Pro aminopeptidase	2.10	149.15
PADG_12323	Peptidyl-prolyl cis-trans isomerase	1.69	172.73
7- PROTEIN WITH BINDING FUNCTION OR COFACTOR REQUIREMENT			
PADG_00352	SH3 domain-containing protein	2.05	47.10
PADG_03091	WD repeat-containing protein	12.84	16.91
PADG_06997	Nuclear cap-binding protein	3.98	30.03
8- CELLULAR TRANSPORT, TRANSPORT FACILITIES AND TRANSPORT ROUTES			
PADG_05084	Ctr copper transporter family protein	2.40	5.70
PADG_07415	Phosphatidylinositol transporter	4.55	37.70
PADG_01440	ADP,ATP carrier protein	1.65	136.43
PADG_01847	Stomatin family protein	2.36	33.02
PADG_02640	ATP-binding cassette sub-family F member 2	1.70	137.14
PADG_04883	Transport protein SEC24	2.15	60.43
PADG_07288	Polyubiquitin binding protein	1.72	27.32
PADG_06998	Transport protein SEC31	1.51	197.35
9- CELL RESCUE, DEFENSE AND VIRULENCE			
Stress response			
PADG_03963	30 kDa heat shock protein	2.37	226.88
PADG_08369	Heat shock protein	2.23	833.68
PADG_03562	Hsp70-like protein	1.54	536.57
PADG_00430	Heat shock protein SSC1	1.81	606.34
Detoxification			
PADG_01954	Superoxide dismutase Fe/Mn SOD5	2.28	90.74
PADG_07418	Superoxide dismutase Cu/Zn SOD1	2.49	76.85
PADG_01755	Superoxide dismutase Fe/Mn SOD2	3.13	141.53
PADG_03423	Glutathione S-transferase Gst3	2.74	143.10
PADG_04587	Peroxiredoxin HYR1	1.57	17.20

PADG_00324	Peroxisomal catalase	2.00	318.42
PADG_07815	Disulfide-isomerase	1.73	224.03
11-BIOGENESIS OF CELLULAR COMPONENTS			
Cell wall			
PADG_02865	Cell wall biogenesis protein phosphatase Ssd1	1.75	88.42
12- MISCELLANEOUS			
PADG_12145	Uracil-regulated protein 1	1.96	94.70
PADG_11421	Histone H2A.Z	1.77	93.26
PADG_07836	Quinone oxidoreductase	3.32	197.36
PADG_08034	Dienelactone hydrolase family protein	1.62	94.41
PADG_05010	Arrestin domain-containing protein	1.65	68.59
PADG_03638	Oxidoreductase	2.11	17.77
PADG_03436	3' exoribonuclease family protein	2.63	30.70
PADG_03526	M protein repeat protein	1.92	345.35
PADG_03544	Ser/Thr protein phosphatase family protein	1.62	198.85
PADG_00345	HHE domain-containing protein	1.55	21.23
PADG_01862	Stress responsive A/B barrel domain-containing protein	3.18	16.31
PADG_03031	CobW domain-containing protein	2.61	216.78
PADG_03316	MYB DNA-binding domain-containing protein	2.14	37.99
PADG_02596	Transcriptional regulatory protein SIN3	1.72	79.43
PADG_12204	Hydroxyacylglutathione hydrolase	1.54	39.73
13-UNCLASSIFIED			
PADG_05474	Hypothetical protein	1.79	143.49
PADG_11446	Hypothetical protein	1.64	38.40
PADG_00046	Hypothetical protein	2.64	26.87
PADG_00060	Hypothetical protein	1.55	59.84
PADG_00388	Hypothetical protein	3.00	45.95
PADG_00459	Hypothetical protein	2.89	44.14
PADG_00465	Hypothetical protein	1.57	14.24
PADG_00496	Hypothetical protein	3.66	63.52
PADG_00646	Hypothetical protein	1.67	72.31
PADG_00674	Hypothetical protein	1.55	41.06
PADG_01488	Hypothetical protein	2.17	199.11
PADG_01618	Hypothetical protein	3.02	16.62
PADG_01727	Hypothetical protein	4.66	36.73
PADG_01855	Hypothetical protein	8.31	62.66
PADG_01867	Hypothetical protein	1.56	110.12
PADG_01991	Hypothetical protein	2.19	5.66
PADG_01885	Hypothetical protein	5.48	16.89
PADG_01560	Hypothetical protein	2.63	11.15
PADG_02272	Hypothetical protein	2.56	12.28

PADG_02301	Hypothetical protein	5.83	5.69
PADG_02307	Hypothetical protein	2.18	65.50
PADG_02336	Hypothetical protein	2.85	6.14
PADG_02557	Hypothetical protein	2.05	51.81
PADG_02633	Hypothetical protein	1.79	22.17
PADG_02658	Hypothetical protein	1.55	51.55
PADG_02758	Hypothetical protein	1.67	47.43
PADG_02759	Hypothetical protein	1.80	76.93
PADG_02858	Hypothetical protein	1.75	45.83
PADG_02878	Hypothetical protein	1.80	27.97
PADG_03340	Hypothetical protein	2.52	57.47
PADG_03570	Hypothetical protein	2.33	23.64
PADG_07896	Hypothetical protein	3.09	33.95
PADG_07064	Hypothetical protein	6.48	44.18
PADG_03579	Hypothetical protein	2.14	20.54
PADG_03612	Hypothetical protein	1.63	11.84
PADG_03660	Hypothetical protein	1.57	134.38
PADG_03761	Hypothetical protein	1.61	27.17
PADG_03785	Hypothetical protein	1.67	50.65
PADG_03995	Hypothetical protein	1.73	9.73
PADG_04057	Hypothetical protein	2.06	135.28
PADG_04229	Hypothetical protein	1.57	192.60
PADG_04256	Hypothetical protein	1.67	15.97
PADG_04423	Hypothetical protein	2.89	43.34
PADG_04439	Hypothetical protein	1.82	53.57
PADG_04494	Hypothetical protein	2.11	16.49
PADG_04627	Hypothetical protein	4.86	11.06
PADG_04685	Hypothetical protein	1.59	26.74
PADG_04806	Hypothetical protein	2.25	22.68
PADG_04907	Hypothetical protein	4.26	54.11
PADG_04953	Hypothetical protein	1.92	32.62
PADG_05104	Hypothetical protein	1.75	17.69
PADG_05157	Hypothetical protein	6.53	30.67
PADG_05701	Hypothetical protein	1.51	105.71
PADG_05703	Hypothetical protein	1.68	58.47
PADG_01796	Hypothetical protein	2.63	35.34
PADG_06021	Hypothetical protein	1.98	17.33
PADG_06136	Hypothetical protein	3.17	56.11
PADG_06239	Hypothetical protein	2.69	11.40
PADG_06846	Hypothetical protein	2.96	5.36
PADG_06986	Hypothetical protein	1.51	10.53
PADG_06974	Hypothetical protein	3.21	5.12
PADG_07075	Hypothetical protein	1.66	23.18
PADG_07298	Hypothetical protein	2.04	17.30

PADG_07565	Hypothetical protein	5.36	39.97
PADG_07696	Hypothetical protein	2.22	21.16
PADG_07768	Hypothetical protein	2.63	50.70
PADG_07793	Hypothetical protein	1.64	16.47
PADG_08152	Hypothetical protein	1.69	75.18
PADG_08214	Hypothetical protein	1.58	52.38
PADG_08420	Hypothetical protein	1.67	32.45
PADG_08478	Hypothetical protein	6.24	16.95
PADG_08689	Hypothetical protein	1.50	17.72
PADG_11044	Hypothetical protein	1.90	11.47
PADG_11111	Hypothetical protein	1.74	34.44
PADG_07689	Hypothetical protein	2.11	107.03
PADG_11157	Hypothetical protein	1.62	65.96
PADG_11170	Hypothetical protein	1.55	10.91
PADG_11357	Hypothetical protein	4.71	9.10
PADG_11487	Hypothetical protein	7.10	29.09
PADG_11558	Hypothetical protein	1.52	12.09
PADG_11833	Hypothetical protein	1.82	169.57
PADG_11904	Hypothetical protein	3.51	729.03
PADG_12072	Hypothetical protein	1.68	22.65
PADG_12182	Hypothetical protein	6.69	38.51
PADG_12186	Hypothetical protein	1.54	71.59
PADG_12285	Hypothetical protein	1.87	6.72
PADG_12292	Hypothetical protein	4.43	5.03
PADG_12311	Hypothetical protein	1.73	11.36
PADG_12392	Hypothetical protein	1.59	34.40
PADG_00580	Hypothetical protein	1.55	47.40
PADG_07449	Hypothetical protein	2.43	54.99
PADG_03559	Hypothetical protein	5.98	11.45
PADG_12408	Hypothetical protein	1.68	28.98
PADG_12411	Hypothetical protein	1.63	5.73
PADG_12419	Hypothetical protein	3.62	18.83
PADG_12447	Hypothetical protein	2.01	56.85
PADG_12503	Hypothetical protein	2.41	302.59

[a] Identification of differentially regulated proteins from *Paracoccidioides* genome database (http://www.broadinstitute.org/annotation/genome/paracoccidioides_brasiliensis/MultiHome.html) using the ProteinLynx Global Server vs. 2.4 (PLGS) (Waters Corporation, Manchester, UK).

[b] Proteins annotation from *Paracoccidioides* genome database or by homology from NCBI database (http://www.ncbi.nlm.nih.gov/).

[c] Acetate/Glucose means: The level of expression in yeast cells derived from cultured in sodium acetate divided by the level in the control yeast cells cultured in glucose.

[d] Biological process of differentially expressed proteins from MIPS (http://mips.helmholtz-muenchen.de/funcatDB/) and Uniprot databases (http://www.uniprot.org/).

Supplemental Table 10: Synthesis of the proteins related to the main metabolic pathways in *Paracoccidioides lutzii* and *P. brasiliensis* isolates after growth for 48 hours in sodium acetate as carbon source.

Functional categories[a] / Protein description[b]	Acetate/Glucose Ratio[c]				Acession number[d]
Isolates	***Pb*01**	***Pb*03**	***Pb*339**	***Pb*EPM83**	
1. ENERGY					
Glycolysis / Gluconeogenesis					
UTP-glucose-1-phosphate uridylyltransferase	0.1060	*	*	0.1921	PAAG_06817; PADG_04374
Glycogen synthase	2.3158	*	0.2000	*	PAAG_07276; PADG_05778
1,4-alpha-glucan-branching enzyme	1.9364	*	*	*	PAAG_08038
Glycogen phosphorylase	*	*	0.3650	*	PADG_02145
Phosphoglucomutase	*	*	1.8547	*	PADG_11132
Glucokinase	2.1820	1.6758	*	*	PAAG_06172; PABG_06480
Hexokinase	0.5411	1.7294	*	0.6444	PAAG_01015; PABG_01237; PADG_03813
Glucose-6-phosphate isomerase	*	2.1592	*	*	PABG_02052
Phosphofructokinase 1	0.0286	0.6565	0.6475	*	PAAG_01583; PABG_03640; PADG_00192
Fructose-1,6-bisphosphatase	1.5726	*	1.9291	1.5608	PAAG_02682; PADG_01706
Fructose-biphosphate aldolase	1.5640	*	*	4.0431	PAAG_01995; PADG_00852
Triosephosphate isomerase	*	*	2.1992	*	PADG_06906
Glyceraldehyde-3-phosphate dehydrogenase	1.5272	1.5622	2.2502	*	PAAG_08468; PABG_00022; PADG_02411
Phosphoglycerate kinase	*	0.4094	0.2854	*	PABG_03332; PADG_01896
Phosphoglycerate mutase	*	*	1.7510	*	PADG_05109
6-phosphofructo-2-kinase	0.6565	*	*	*	PAAG_03643
Fructose-2,6-bisphosphatase	*	*	*	0.2902	PADG_07202
Ethanol production					
Aldehyde dehydrogenase A	*	*	*	2.18	PADG_03403
Aldehyde dehydrogenase	1.7035	*	*	*	PAAG_03910
Pyruvate decarboxylase	1.6585	*	*	1.5160	PAAG_02050; PADG_00714
Alcohol dehydrogenase 1	5.8833	2.6590	1.8945	3.5222	PAAG_00403; PABG_04316; PADG_11405
Alcohol dehydrogenase	*	2.8854	4.6278	4.6365	PABG_04316; PADG_04701
Alcohol dehydrogenase	2.3540	0.4684	*	*	PAAG_08911; PABG_07767
Citrate cycle (TCA cycle)					
Acetyl-CoA hydrolase	*	*	0.5468	*	PADG_02597
Acetyl-coenzyme A synthetase	*	*	1.5934	*	PADG_01677
Aconitate hydratase	2.5739	1.8855	*	2.0604	PAAG_05048; PABG_11957; PADG_11845

ATP-citrate synthase subunit 1	*	3.9958	2.0159	0.5420	PABG_04594; PADG_04993
ATP-citrate-lyase	*	0.5640	*	1.5492	PABG_04595; PADG_04994
Citrate lyase subunit beta	*	*	2.7667	*	PADG_01546
Citrate synthase	1.9503	*	*	2.1828	PAAG_08075; PADG_08387
Dihydrolipoamide succinyltransferase	2.1272	*	*	*	PAAG_08915
Dihydrolipoyl dehydrogenase	0.0395	*	*	1.6093	PAAG_03330; PADG_06494
Fumarate hydratase	2.0430	*	3.2527	1.7921	PAAG_00588; PADG_08119
Fumarate reductase	*	*	*	1.7370	PADG_02592
Isocitrate dehydrogenase [NAD] subunit 1	1.5573	1.6896	*	1.6513	PAAG_00856; PABG_01382; PADG_03977
Malate dehydrogenase	1.5893	*	*	1.6212	PAAG_00053; PADG_07210
Oxoglutarate dehydrogenase	1.6015	1.5253	1.6444	1.5575	PAAG_02732; PABG_03210; PADG_01762
Pyruvate dehydrogenase complex dihydrolipoamide acetyltransferase	1.6615	*	1.8264	0.4023	PAAG_11035; PADG_07213
Pyruvate dehydrogenase kinase	*	*	3.6490	*	PADG_12250
Succinate dehydrogenase [ubiquinone] flavoprotein subunit	3.4568	2.6561	*	2.2497	PAAG_01725; PABG_03772; PADG_00052
Succinate dehydrogenase [ubiquinone] iron-sulfur subunit	3.2987	*	*	4.2371	PAAG_06103; PADG_06553; PADG_08013
Succinyl-CoA sintetase subunit alpha	1.7090	*	0.4054	1.5504	PAAG_00417; PADG_02260
Glyoxylate cycle					
Isocitrate lyase	2.9921	*	*	1.9860	PAAG_06951; PABG_01483
Malate synthase	1.7279	*	*	2.1061	PAAG_04542; PADG_04702
Oxidation of fatty acids					
3-hydroxybutyryl-CoA dehydrogenase	2.4003	*	1.8680	1.7645	PAAG_06329; PADG_01228
3-ketoacyl-CoA thiolase	2.1333	1.5187	1.7094	1.7562	PAAG_02664; PABG_00747; PADG_01687
3-ketoacyl-CoA thiolase B, peroxisomal	*	*	*	0.5984	PADG_03194
60 kDa lysophospholipase	*	*	0.5333	*	PADG_05733
Acyl-CoA dehydrogenase	2.0032	1.7105	*	2.4653	PAAG_05454; PABG_01791; PADG_06805
Acyl-coenzyme A desidrogenase	2.4629	*	1.5613	*	PAAG_03116; PADG_02991
Carnitine O-acetyltransferase	*	*	*	2.1491	PADG_07023
Delta(3,5)-Delta(2,4)-dienoyl-CoA isomerase	*	0.5139	*	1.8556	PABG_07087; PADG_06721
Enoyl-CoA hydratase	1.5675	1.7676	*	2.0790	PAAG_06309; PABG_03016; PADG_01209

Enoyl-CoA hydratase/isomerase family protein	1.5699	*	*	0.5033	PAAG_06392; PADG_01291
Short chain dehydrogenase family protein	*	*	*	2.4576	PADG_02527
Short-chain dehydrogenase	4.7118	*	0.1428	*	PAAG_01557; PADG_00221
Synthesis and degradation of ketone bodies					
Acetyl-CoA acetyltransferase	2.1667	*	1.5126	*	PAAG_03447; PADG_02751
Hydroxymethylglutaryl-CoA synthase	*	*	0.6010	*	PADG_00685
Hydroxymethylglutaryl-CoA lyase	*	*	1.9153	2.2882	PADG_07031
Succinyl-CoA:3-ketoacid-coenzyme A transferase	1.6768	*	1.5178	2.2355	PAAG_05093; PADG_04939
Acetoacetate-CoA ligase	*	0.4800	0.1778	*	PABG_03423; PADG_01993
Fatty acid biosynthesis					
3-oxoacyl-[acyl-carrier-protein] reductase	0.2060	*	*	2.3929	PAAG_03123; PADG_06721
Acyl-coenzyme A synthetase	*	*	0.5963	0.6245	PADG_04827
Fatty acid synthase subunit alpha	*	*	4.0867	0.5526	PADG_00254
Fatty acid synthase subunit beta dehydratase	0.3496	0.5839	0.2939	0.5910	PAAG_01524; PABG_03585; PADG_00255
Long-chain-fatty-acid-CoA ligase	*	*	*	0.5856	PADG_00434
Trans-2-enoyl-CoA reductase	*	*	0.5134	2.3908	PADG_00244
Methylcitrate cycle					
2-methylcitrate synthase	2.6721	*	2.3207	2.6157	PAAG_04550; PADG_04710
2-methylcitrate dehydratase	2.0037	*	*	1.8910	PAAG_04559; PADG_04718
Methylisocitrate lyase	*	2.5429	2.9785	1.6659	PABG_04323; PADG_04709
Propionate-CoA ligase	*	1.5638	2.0471	3.5024	PABG_04660; PADG_05281
Electron transport and membrane-associated energy conservation					
NADH-ubiquinone oxidoreductase 21.3 kDa subunit	*	*	1.5948	2.0924	PADG_05343
Alternative oxidase, mitochondrial	*	*	*	3.5486	PADG_03747
ATP synthase delta chain	*	3.2513	*	1.5543	PABG_06161; PADG_07042
ATP synthase F1, gamma subunit	2.1728	*	1.9140	1.8508	PAAG_05576; PADG_07813
ATP synthase subunit 4	*	*	*	1.9560	PADG_02578
ATP synthase subunit alpha	0.0678	1.6317	1.9289	3.4632	PAAG_04820; PABG_11057; PADG_02561
ATP synthase subunit beta	4.0577	1.8668	*	4.4407	PAAG_08037; PABG_07285; PADG_08349
ATP synthase subunit D	*	*	0.5723	2.2771	PADG_04729

ATP synthase subunit delta	4.2276	1.9723	*	4.9575	PAAG_05605; PABG_06178;PADG_07789
ATP synthase subunit G	2.4386	*	*	*	PAAG_08551
Cytochrome b5	*	1.6289	*	*	PABG_04666
Cytochrome b-c1 complex subunit 2	3.1252	*	*	3.7722	PAAG_08088; PADG_08394
Cytochrome c	1.5212	*	0.2200	3.2504	PAAG_06268; PADG_06978
Cytochrome c oxidase assembly protein COX19	*	*	0.3454	1.9027	PADG_01841
Cytochrome c oxidase polypeptide VIb	*	1.7915	*	1.5998	PABG_05268; PADG_08292
NADH-ubiquinone oxidoreductase 49 kDa subunit, mitochondrial	*	1.5429	*	2.6265	PABG_12311; PADG_12148
NADPH dehydrogenase	*	*	2.7925	*	PADG_01519
Putative cytochrome c oxidase subunit VIa	*	*	1.8851	*	PADG_05750
Ubiquinol-cytochrome c reductase subunit 7	*	*	5.8276	*	PADG_04501
2. CELL WALL					
Chitin synthase class V	*	*	4.8078	*	PADG_07913
Chitin biosynthesis protein	*	0.6085	*	*	PABG_06519
Glucan 1,3-beta-glucosidase	*	1.5845	*	*	PABG_06330
Glucosamine-fructose-6-phosphate aminotransferase	0.0947	*	0.1893	0.1098	PAAG_00850; PADG_03984
Sterol 24-C-methyltransferase	*	*	0.5381	*	PADG_00204
Glucosamine-6-phosphate deaminase	*	*	*	1.5413	PADG_00401
Phosphoacetylglucosamine mutase	*	*	*	1.6978	PADG_00604
UDP-N-acetylglucosamine pyrophosphorylase	*	*	*	1.5221	PADG_04312
3. AMINO ACID DEGRADATION					
Methionine, threonine, valine leucine and isoleucine					
2-oxoisovalerate dehydrogenase subunit beta	1.6422	0.5631	*	*	PAAG_01194; PABG_01773
3-hydroxyisobutyrate dehydrogenase	*	*	*	1.5232	PADG_03466
Adenosylhomocysteinase	1.9887	*	1.9063	1.9792	PAAG_02859; PADG_01886
Branched-chain amino acid aminotransferase	0.2930	0.5525	0.4502	1.8625	PAAG_04401
Cystathionine beta-synthase	*	0.5917	*	*	PABG_04676
Cystathionine gamma-lyase	*	*	2.1645	*	PADG_02456
Dihydrolipoamide branched chain transacylase	*	0.3502	*	*	PABG_03242
Isovaleryl-CoA dehydrogenase	*	*	1.6305	*	PADG_07369
Methylcrotonoyl-CoA carboxylase beta chain	1.5500	*	*	1.7011	PAAG_04103; PADG_07370

Methylcrotonoyl-CoA carboxylase subunit alpha	*	*	1.9142	*	PADG_07366
Methylmalonate-semialdehyde dehydrogenase	1.6596	*	*	*	PAAG_07036
Mitochondrial methylglutaconyl-CoA hydratase	*	*	*	2.3069	PADG_00643
Threonine dehydratase	2.3523	*	*	*	PAAG_03168
Threonine, alanine, glycine and serine					
Alanine aminotransferase	1.7302	*	*	*	PAAG_08207
Alanine-glyoxylate aminotransferase	*	2.4552	*	*	PABG_00589
Glycine cleavage system H protein	*	*	*	1.5237	PADG_01963
Glycine cleavage system T protein	*	*	*	0.5432	PADG_02914
Glycine dehydrogenase	1.5611	1.9209	0.3708	2.7044	PAAG_1568; PABG_04990; PADG_00210
L-serine dehydratase	*	*	3.0201	*	PADG_11705
Serine hydroxymethyltransferase	*	0.5413	*	*	PABG_07147
Threonine dehydratase	*	4.0242	*	*	PABG_01280
Aspartate					
Aspartate aminotransferase	0.9755	1.9558	0.3257	0.4548	PABG_02806; PADG_01404
Arginine, histidine, glutamate and proline					
Arginase	*	*	2.8753	1.5659	PADG_00637
1-pyrroline-5-carboxylate dehydrogenase	3.7092	*	1.8568	3.1996	PAAG_05253, PADG_05085
4-aminobutyrate aminotransferase	*	*	1.6145	*	PADG_02214
Amino-acid acetyltransferase	*	1.5500	*	*	PABG_11192
Glutamate decarboxylase	0.3816	*	*	*	PAAG_03506
Glutamate dehydrogenase	*	*	2.6447	*	PADG_04516
Glutamate-5-semialdehyde dehydrogenase	1.7370	2.0399	6.9476	*	PAAG_07954; PABG_04712; PADG_05337
Glutamine synthetase	*	1.8440	0.0060	0.4642	PABG_03010; PADG_01536
Ornithine aminotransferase	*	2.6378	*	1.6393	PABG_02827; PADG_01328
Succinate-semialdehyde dehydrogenase	*	*	2.3322	*	PADG_03058
Phenylalanine, tyrosine, lysine and tryptophan					
4-hydroxyphenylpyruvate dioxygenase	*	4.0525	1.6926	*	PABG_07394; PADG_08468
Fumarylacetoacetase	1.8464	*	*	1.6096	PAAG_08163; PADG_08465
Glutaryl-CoA dehydrogenase	1.5648	*	*	1.5538	PAAG_05984; PADG_12025
Homogentisate 1,2-dioxygenase	2.8449	3.9693	*	2.9274	PAAG_08164; PABG_07392; PADG_08466
Kynureninase	*	1.9978	*	2.1469	PABG_01965; PADG_00349

Kynurenine-oxoglutarate transaminase	3.3878	2.1199	*	*	PAAG_02644; PABG_03129
Maleylacetoacetate isomerase	1.8658	2.6612	*	*	PAAG_08162; PABG_07390
Phenylpyruvate tautomerase	*	*	2.0329	*	PADG_03671
4. STRESS RESPONSE / DETOXIFICATION					
Cytochrome c peroxidase	*	3.2024	0.4209	*	PABG_00720; PADG_03163
Glutamate-cysteine ligase	5.5711	*	0.4408	0.5170	PAAG_05860; PADG_03500
Glutathione peroxidase	*	3.6064	*	*	PABG_04219;
Glutathione synthetase	*	*	0.3462	*	PADG_02218
Heat shock 70 kd protein cognate 1	*	*	2.1446	*	PADG_05139
Heat shock protein 30 kDa	3.4272	*	*	2.3727	PAAG_00871; PADG_03963
Heat shock protein Hsp88	*	1.7109	2.2386	*	PABG_00374; PADG_02785;
Heat shock protein STI1	*	*	0.3898	*	PADG_04379
Hsp70	*	*	1.7698	0.5490	PADG_00778
Hsp75-like protein	0.6087	*	*	0.6386	PAAG_07775; PADG_02761
Hsp90-like protein	0.0729	*	0.1264	0.1902	PAAG_05679; PADG_07715
Peroxisomal catalase P	2.7216	7.8608	3.5746	1.9969	PAAG_01454; PADG_00324; PABG_01943
Subtilase-type proteinase psp3	*	1.6536	*	*	PABG_03958
Superoxide dismutase SOD1 Cu/Zn	3.3803	2.1639	2.2682	2.4857	PAAG_04164; PABG_03954; PADG_07418
Superoxide dismutase SOD2 Fe/Mn	3.7060	2.5223	2.2353	3.1283	PAAG_02725; PABG_03204; PADG_01755
Superoxide dismutase SOD3 Cu/Zn	*	1.5782	*	*	PABG_00431
Superoxide dismutase SOD4 Cu/Zn	*	*	1.7988	*	PADG_01400
Superoxide dismutase SOD5 Fe/Mn	2.5451	1.5782	1.7258	2.2816	PAAG_02926 PABG_03387 PADG_01954
Thioredoxin	*	*	*	0.5506	PADG_03161
Thioredoxin reductase	*	0.5212	1.6851	0.5843	PABG_03023; PADG_01551

[a]Biological process of differentially expressed proteins from MIPS (http://mips.helmholtz-muenchen.de/funcatDB/) and Uniprot databases (http://www.uniprot.org/).

[b]Proteins annotation from *Paracoccidioides* genome database or by homology from NCBI database (http://www.ncbi.nlm.nih.gov/).

[c]Acetate/Glucose means: The level of expression in yeast cells derived from cultured in sodium acetate divided by the level in the control yeast cells cultured in glucose, in the differents isolates: *P. lutzii* (*Pb*01) and *P. brasiliensis* (*Pb*03, *Pb*339, and *Pb*EPM83).

[d]Identification of differentially regulated proteins from *Paracoccidioides* genome database (http://www.broadinstitute.org/annotation/genome/paracoccidioides_brasiliensis/MultiHome.html) using the ProteinLynx Global Server vs. 2.4 (PLGS) (Waters Corporation, Manchester, UK).
*Constitutive protein or not regulated.

Supplemental Table 4: Proteins up-regulated in *Paracoccidioides brasiliensis* isolate 03 after growth for 48 hours in sodium acetate as carbon source.

Accession number[a]	Protein Description[b]	Acetate/Glucose Ratio[c]	Score
Functional categories[d]			
1. METABOLISM			
Amino acid metabolism			
PABG_07394	4-hydroxyphenylpyruvate dioxygenase	4.05	253.46
PABG_00589	Alanine-glyoxylate aminotransferase	2.46	92.50
PABG_11192	Amino-acid acetyltransferase, mitochondrial	1.55	5.50
PABG_07531	Asparagine synthetase	1.88	122.47
PABG_02806	Aspartate aminotransferase	1.96	91.85
PABG_02012	Choline dehydrogenase	1.54	145.33
PABG_04712	Glutamate-5-semialdehyde dehydrogenase	2.04	183.29
PABG_03010	Glutamine synthetase	1.84	93.06
PABG_04990	Glycine cleavage T-protein	1.92	23.45
PABG_05965	Histidine biosynthesis trifunctional protein	1.63	17.44
PABG_07392	Homogentisate 1,2-dioxygenase	3.97	198.61
PABG_04732	Isochorismatase domain containing 2b	2.01	54.50
PABG_01965	Kynureninase	2.00	94.33
PABG_03129	Kynurenine-oxoglutarate transaminase	2.12	146.59
PABG_07533	Methionine aminopeptidase	1.51	64.41
PABG_07390	Maleylacetoacetate isomerase	2.66	111.96
PABG_02827	Ornithine aminotransferase	2.62	242.23
PABG_02447	Pentafunctional AROM polypeptide	3.05	206.59
PABG_03361	S-adenosylmethionine synthetase	1.91	203.87
PABG_01280	L-threonine 3-dehydrogenase	4.03	90.39
PABG_00544	TPA: putative Conserved lysine-rich protein	1.89	296.22
Nitrogen, sulfur and selenium metabolism			
PABG_00102	Ureidoglycolate hydrolase	5.42	17.84
PABG_07028	Formamidase	4.45	240.33
PABG_03480	Nitroreductase	1.65	87.22
PABG_02398	Urea carboxylase	1.60	416.19
Nucleotide/nucleoside/nucleobase metabolism			
PABG_04433	Adenylosuccinate lyase	1.58	95.31
PABG_06340	Inosine-5'-monophosphate dehydrogenase IMD2	1.69	316.83
PABG_06368	Quinone oxidoreductase	2.66	184.61
PABG_01949	Uricase	1.52	59.50
Phosphate metabolism			
PABG_04460	Serine/threonine protein kinase	4.94	16.22

C-compound and carbohydrate metabolism			
PABG_00225	4-coumarate-CoA ligase	1.57	193.77
PABG_01732	Tautomerase/MIF	4.05	90.54
PABG_05538	Lactonohydrolase	1.91	94.83
PABG_02864	Mannitol-1-phosphate 5-dehydrogenase	1.53	241.02
PABG_00813	NADPH-dependent D-xylose reductase	1.82	155.84
PABG_04877	Quinone oxidoreductase	2.06	174.79
PABG_01695	Retrograde regulation protein	2.89	65.11
PABG_01914	Ribulokinase	1.73	53.46
PABG_12460	Salicylate hydroxylase	1.57	47.49
PABG_06330	4-carboxymuconolactone decarboxylase family protein	1.58	53.38
PABG_06193	6-phosphogluconolactonase	2.08	86.31
Lipid, fatty acid and isoprenoid metabolism			
PABG_02112	2-succinylbenzoate-CoA ligase	1.53	183.90
PABG_00747	3-ketoacyl-CoA thiolase A	1.52	209.23
PABG_05999	3-ketoacyl-acyl carrier protein reductase	3.90	29.01
PABG_05972	3-oxoacyl-(acyl-carrier protein) reductase	1.89	331.40
PABG_01791	Acyl-CoA dehydrogenase	1.71	78.53
PABG_03016	Enoyl-CoA hydratase	1.77	19.23
PABG_02855	Acyl-CoA-binding protein	1.77	89.55
PABG_00955	Acyl-CoA N-acyltransferase	3.78	51.19
Metabolism of vitamins, cofactors, and prosthetic groups			
PABG_01387	6,7-dimethyl-8-ribityllumazine synthase	1.84	37.06
PABG_06591	Delta-aminolevulinic acid dehydratase	3.15	86.93
PABG_01549	NUDIX domain-containing protein	27.49	17.47
PABG_04836	Nudix hydrolase	1.82	36.29
PABG_00890	Phosphopantothenate-cysteine ligase	2.24	46.28
Secondary metabolism			
PABG_06389	Imidazole glycerol phosphate synthase hisHF	3.16	55.33
PABG_06397	Imidazole glycerol phosphate synthase hisHF	3.21	177.12
2. ENERGY			
Glycolysis and gluconeogenesis			
PABG_06480	Glucokinase GLK1	1.68	42.70
PABG_02052	Glucose-6-phosphate isomerase	2.16	217.75
PABG_00022	Glyceraldehyde-3-phosphate dehydrogenase	1.56	363.42
PABG_01237	Hexokinase	1.73	107.40
Ethanol production			
PABG_04316	Alcohol dehydrogenase GroES domain-containing protein	2.88	279.02

PABG_12402	Alcohol dehydrogenase 1	2.66	212.74
Pentose-phosphate pathway			
PABG_02360	Ribose-phosphate pyrophosphokinase	1.64	173.62
Tricarboxylic-acid pathway			
PABG_03210	2-oxoglutarate dehydrogenase E1	1.53	486.63
PABG_11957	Aconitate hydratase, mitochondrial	1.89	405.25
PABG_04594	ATP-citrate synthase	4.00	343.90
PABG_01382	Isocitrate dehydrogenase subunit 1	1.69	216.34
PABG_03494	Pyruvate dehydrogenase E1 component subunit alpha	1.87	278.19
PABG_03772	Succinate dehydrogenase flavoprotein subunit	2.66	276.05
Methylcytrate cycle			
PABG_04323	Methylisocitrate lyase	2.54	265.71
Electron transport and membrane-associated energy conservation			
PABG_06161	ATP synthase delta chain	3.25	28.85
PABG_12007	ATP synthase F0 subunit 8	1.84	107.56
PABG_11057	ATP synthase subunit alpha, mitochondrial	1.63	458.48
PABG_07285	ATP synthase subunit beta	1.87	349.38
PABG_06178	ATP synthase subunit delta,	1.97	59.54
PABG_05268	Cytochrome c oxidase polypeptide Vib	1.79	19.26
PABG_06935	Formate dehydrogenase	6.10	137.07
PABG_07303	F-type H+-transporting ATPase subunit epsilon	1.54	14.76
PABG_12311	NADH-ubiquinone oxidoreductase 49 kDa, mitochondrial	1.56	11.77
PABG_11661	Succinate dehydrogenase assembly factor 2, mitochondrial	1.63	91.85
PABG_05474	Vacuolar ATP synthase catalytic subunit A	1.88	247.75
PABG_03708	NADH-ubiquinone oxidoreductase 12 kDa subunit	2.98	22.65
PABG_03177	Ubiquinol-cytochrome c reductase subunit 6	6.17	32.84
PABG_06958	12-oxophytodienoate reductase	3.19	284.78
PABG_04666	Cytochrome b5	1.64	22.16
PABG_11490	Electron transfer flavoprotein-ubiquinone oxidoreductase	9.02	10.87
3. CELL CYCLE and DNA PROCESSING			
PABG_05569	Cell cycle control protein cwf14	2.09	15.92
PABG_02067	Mitochondrial genome maintenance protein MGM101	1.76	73.79
PABG_04448	Meiosis specific protein Hop1	2.20	45.43
PABG_03596	SNF7 family protein Fti1/Did2	3.67	15.15
PABG_05201	Septin-7	2.12	150.23
PABG_11327	Proliferating cell nuclear antigen	2.03	284.78
4. TRANSCRIPTION			
PABG_00085	Pirin	2.55	95.05

PABG_06262	PHD finger protein	2.03	18.92
PABG_06274	NuA3 HAT complex component NTO1	4.01	60.61
PABG_06004	Poly(A) polymerase PAPa	2.77	56.98
PABG_01856	Splicing factor spf30	1.77	28.68
PABG_03761	tRNA (guanine(37)-N1)-methyltransferase	2.71	79.13
PABG_03438	Transcription factor RfeF	1.56	76.06
PABG_05850	U1 small nuclear ribonucleoprotein	1.54	33.37
PABG_12042	U2 small nuclear ribonucleoprotein B	1.51	26.05
PABG_00485	U2 snRNP-associated protein Uap2	2.05	43.68
PABG_01474	U4/U6.U5 tri-snRNP-associated protein	2.59	50.62
PABG_00260	DNA-directed RNA polymerase III subunit Rpc31	2.17	46.98
PABG_05962	Basic helix-loop-helix transcription factor Yas1p	5.32	90.70
PABG_01008	Zinc finger protein	1.78	59.80
5. PROTEIN SYNTHESIS			
PABG_06421	30S ribosomal protein S7	1.66	163.76
PABG_04888	37S ribosomal protein S5	4.68	18.45
PABG_03113	50S ribosomal protein L24	1.52	19.86
PABG_01500	60S ribosomal protein L11	2.75	70.92
PABG_12185	60S ribosomal protein L28	1.84	310.74
PABG_06407	Cytochrome P450 monooxygenase	4.99	17.08
PABG_06666	Mitochondrial ribosomal protein YmL8	1.65	33.50
PABG_12047	Ran-specific GTPase-activating protein 1	1.58	265.86
PABG_01633	Ribosomal protein L30	1.80	59.78
PABG_06017	TCTP family protein	1.90	53.61
PABG_01959	67 kDa polymerase-associated factor PAF67	1.84	93.92
PABG_02129	Elongation factor 1-alpha	2.10	59.90
PABG_05845	Elongation factor 2	2.79	142.18
PABG_01416	Eukaryotic translation initiation factor 3 110 kDa subunit	1.84	109.69
PABG_06490	Eukaryotic translation initiation factor 3 subunit B	2.41	192.82
PABG_01208	Eukaryotic translation initiation factor 3 subunit I	1.74	106.67
PABG_02641	Translation initiation factor 4B	2.31	206.77
PABG_01301	Lysine-tRNA ligase	1.84	135.04
PABG_05580	Seryl-tRNA synthetase	2.86	265.30
PABG_07397	Lysyl-tRNA synthetase	2.42	145.34
6. PROTEIN FATE			
PABG_00967	T-complex protein 1 subunit alpha	2.68	164.60
PABG_01488	Peptidyl-prolyl cis-trans isomerase B	1.59	111.53
PABG_06135	TCTP family protein	1.59	106.15
PABG_06572	T-complex protein 1 subunit beta	1.53	91.90
PABG_07652	FK506-binding protein	2.33	77.53
PABG_07742	T-complex protein 1 subunit eta	2.12	117.58
PABG_01434	Chaperone protein dnaJ	1.58	78.19

PABG_05205	Intermembrane space import and assembly protein	2.25	25.77
PABG_00818	Mitochondrial import inner membrane translocase subunit tim9	1.54	11.98
PABG_01181	NADH dehydrogenase (ubiquinone) 1 beta subcomplex 8	5.77	78.45
PABG_00491	Ubiquitin-like modifier SUMO	1.53	25.45
PABG_03958	Subtilase-type proteinase psp3	1.66	123.42
PABG_05357	26S proteasome regulatory subunit rpn-8	2.10	84.59
PABG_05859	Ubiquitin thiolesterase	1.62	20.56
PABG_06586	T-complex protein 1 subunit beta	5.36	186.67
PABG_07230	Xaa-Pro aminopeptidase I	2.40	182.17
PABG_07373	Proteasome subunit alpha type-4	1.81	137.44
PABG_01386	Proteasome subunit alpha type-3	1.56	141.66
PABG_05365	V Chain V	1.67	78.82
PABG_06849	Carboxypeptidase Y	2.63	94.09

7. PROTEIN WITH BINDING FUNCTION or COFACTOR REQUIREMENT

PABG_03848	YjeF-related protein	1.68	53.33
PABG_03778	Nuclear localization sequence-binding protein	3.16	48.38
PABG_03796	Translation machinery-associated protein 22	3.18	13.29
PABG_03042	APAF1-interacting protein	1.52	50.27
PABG_04194	Progesterone binding protein	2.69	82.62
PABG_02026	RNA-binding protein Vip1	1.62	152.84

8. CELLULAR TRANSPORT, TRANSPORT FACILITIES and TRANSPORT ROUTES

PABG_06877	ATPase_c domain-containing protein	1.57	215.25
PABG_06615	Heavy metal ion transporter, putative	1.75	31.52
PABG_00598	Galactose-proton symport	1.54	22.94
PABG_01896	GTP-binding protein SAS1	3.52	40.46
PABG_03783	Exocyst complex component Sec10	2.59	102.59
PABG_12318	DUF726 domain-containing protein	1.67	41.63

9. CELLULAR COMMUNICATION/SIGNAL TRANSDUCTION MECHANISM

PABG_06817	Neuronal calcium sensor 1	1.72	16.47
PABG_03846	WD repeat-containing protein	7.39	38.28
PABG_00188	Phosphatase 2A regulatory B subunit	1.87	50.26
PABG_01056	Kinase binding protein	1.75	33.99
PABG_05936	CAMK/CAMKL/KIN4 protein kinase	5.77	78.45
PABG_04460	Serine/threonine protein kinase	4.94	16.22

10. CELL RESCUE, DEFENSE AND VIRULENCE

Stress response

PABG_01369	Heat shock protein	2.86	235.05
PABG_02373	Heat shock protein	1.77	243.44
PABG_00374	Heat shock protein Hsp88	1.71	643.84
PABG_00350	Heat shock protein SSB	1.75	325.75

PABG_05342	Hsp70-like protein	1.56	747.87
Detoxification			
PABG_03954	Superoxide dismutase Cu/Zn SOD1	2.16	72.78
PABG_03204	Superoxide dismutase Fe/Mn SOD2	2.52	147.87
PABG_00431	Superoxide dismutase Cu/Zn SOD3	1.58	43.93
PABG_03387	Superoxide dismutase Fe/Mn SOD5	1.76	168.45
PABG_01943	Peroxisomal catalase	7.86	400.41
PABG_04219	Glutathione peroxidase	3.61	32.22
PABG_00949	Glutathione S-transferase Gst3	1.63	209.16
PABG_06156	Protein disulfide-isomerase	2.27	174.38
PABG_05451	Serine/threonine protein phosphatase 2A	2.81	18.58
PABG_00720	Cytochrome c peroxidase	3.20	257.66
11. BIOGENESIS OF CELLULAR COMPONENTS			
Cell wall			
PABG_07783	Antigenic cell wall protein	2.55	44.49
PABG_06590	Glucan 1,3-beta-glucosidase	3.38	31.35
PABG_04069	Neutral alpha-glucosidase AB	1.56	224.70
Cytoskeleton/strucutural proteins			
PABG_01263	Actin	2.02	97.21
PABG_07733	Actin lateral binding protein	1.66	183.02
PABG_03455	Clathrin light chain	2.17	101.18
12. MISCELLANEOUS			
PABG_01011	Urg3	1.58	90.54
PABG_01127	Short chain dehydrogenase/reductase	1.86	37.43
PABG_06951	Polysaccharide deacetylase family protein	3.96	185.15
PABG_01628	Adenosine deaminase	1.58	24.48
PABG_06653	CUE domain-containing protein	2.40	11.68
PABG_02064	DUF833 domain-containing protein	1.60	98.02
PABG_11267	Alkaline phosphatase	3.09	79.08
PABG_05421	Glyoxylate reductase	1.50	31.50
PABG_04660	Propionate-CoA ligase	1.56	35.02
PABG_03731	Peroxisomal dehydratase	1.52	39.28
PABG_06197	S-formylglutathione hydrolase	3.11	19.17
PABG_02094	Globin	3.36	51.68
13. UNCLASSIFIED			
PABG_01748	Hypothetical protein	2.89	38.06
PABG_00361	Hypothetical protein	46.44	34.74
PABG_00446	Hypothetical protein	1.64	26.97
PABG_05798	Hypothetical protein	1.89	48.03

PABG_00679	Hypothetical protein	1.52	17.78
PABG_01780	Hypothetical protein	1.94	18.43
PABG_01814	Hypothetical protein	2.18	30.82
PABG_01892	Hypothetical protein	2.51	4.89
PABG_02578	Hypothetical protein	4.23	298.74
PABG_03540	Hypothetical protein	4.58	11.31
PABG_03999	Hypothetical protein	2.17	16.92
PABG_04137	Hypothetical protein	2.06	43.70
PABG_05041	Hypothetical protein	1.83	50.89
PABG_05293	Hypothetical protein	5.54	5.76
PABG_05692	Hypothetical protein	2.81	6.16
PABG_07502	Hypothetical protein	3.16	10.93
PABG_11028	Hypothetical protein	2.16	28.49
PABG_11204	Hypothetical protein	2.18	44.75
PABG_11386	Hypothetical protein	5.86	10.38
PABG_11594	Hypothetical protein	9.51	10.87
PABG_11755	Hypothetical protein	2.89	22.06
PABG_12078	Hypothetical protein	1.53	5.39
PABG_12239	Hypothetical protein	105.53	10.55
PABG_12338	Hypothetical protein	4.75	6.03
PABG_12351	Hypothetical protein	11.89	12.24
PABG_12386	Hypothetical protein	1.81	18.19
PABG_12408	Hypothetical protein	1.58	5.77
PABG_12656	Hypothetical protein	2.53	6.17
PABG_03766	Hypothetical protein	1.53	59.76
PABG_06624	Hypothetical protein	1.57	40.31
PABG_01741	Hypothetical protein	2.05	108.18
PABG_01683	Hypothetical protein	7.30	34.10
PABG_02970	Hypothetical protein	2.65	104.93
PABG_06275	Hypothetical protein	1.55	76.58

[a] Identification of differentially regulated proteins from *Paracoccidioides* genome database (http://www.broadinstitute.org/annotation/genome/paracoccidioides_brasiliensis/MultiHome.html) using the ProteinLynx Global Server vs. 2.4 (PLGS) (Waters Corporation, Manchester, UK).

[b] Proteins annotation from *Paracoccidioides* genome database or by homology from NCBI database (http://www.ncbi.nlm.nih.gov/).

[c] Acetate/Glucose means: The level of expression in yeast cells derived from cultured in sodium acetate divided by the level in the control yeast cells cultured in glucose.

[d] Biological process of differentially expressed proteins from MIPS (http://mips.helmholtz-muenchen.de/funcatDB/) and Uniprot databases (http://www.uniprot.org/).

Conclusões

4. CONCLUSÕES

Após analisar o proteoma de isolados membros de diferentes espécies filogenéticas do gênero *Paracoccidioides:* *Pb*339, *Pb*03, *Pb*EPM83e *Pb*01 na fase leveduriforme na presença de acetato de sódio como fonte de carbono podemos concluir:

- Os membros das quatro espécies filogenéticas avaliadas conseguiram sobreviver na presença de acetato de sódio como fonte de carbono, no entanto houve uma redução na biomassa em todos isolados em relação a glicose como observado pelo peso seco celular;

- A análise do perfil proteômico revelou a reorganização do metabolismo durante o crescimento em acetato de sódio como fonte de carbono com aumento nos níveis de expressão de proteínas relacionadas à gliconeogênese, estresse e degradação dos aminoácidos nos quatro isolados avaliados.

- Diferenças entre os isolados foram observadas como aumento nos níveis de expressão de proteínas pertencentes ao ciclo glioxalato,TCA e cadeia respiratória no *Pb*EPM83 e *Pb01*; a produção de etanol e a β-oxidação foi observada no *Pb01* e *Pb*EPM83;o ciclo de metilcitrato apresentaram elevada expressão de enzimas no *Pb339*. Os perfis proteômico indicam que os quatro isolados reorganizam o metabolismo para o uso do acetato uma fonte não preferencial de carbono.

Referências Bibliográficas

REFERÊNCIAS BIBLIOGRÁFICAS

ARAÚJO SA. PRADO LG. VELOSO JM. PEDROSO ER. Case of recurrent Paracoccidioidomycosis: 25 years after initial treatment. Braz J Infect Dis. 13:394. 2009.

ASAKURA M. OKUNO T. TAKANO Y. Multiple contributions of peroxisomal metabolic function to fungal pathogenicity in *Colletotrichum lagenarium*. Appl Environ Microbiol. 72:6345-6354. 2006.

ASKEW C. SELLAM A. EPP E. HOGUES H. MULLICK A. NANTEL A. WHITEWAY M. Transcriptional regulation of carbohydrate metabolism in the human pathogen *Candida albicans*. PLoS Pathog. 5:e1000612. 2009

BAGAGLI. E. FRANCO. M. BOSCO. SM. HEBELER-BARBOSA F. TRINCA LA. MONTENEGRO MR. High frequency of *Paracoccidioides brasiliensis* infection in armadillos (*Dasypus novemcinctus*): an ecological study. Med. Mycol. 41:217–223. 2003.

BAGAGLI. E. THEODORO RC. BOSCO SMG. McEWEN JG. *Paracoccidioides brasiliensis*: phylogenetic and ecological aspects. Mycopathologia. 165:197–207. 2008.

BARELLE CJ. PRIEST CL. MacCALLUM DM. GOW NA. ODDS FC. BROWN AJ. Niche-specific regulation of central metabolic pathways in a fungal pathogen. Cell. Microbiol. 8:961–971. 2006.

BASTOS KP. BAILÃO AM. BORGES CL. FARIA FP. FELIPE MS. SILVA MG. MARTINS WS. FIÚZA RB. PEREIRA M. SOARES CM. The transcriptome analysis of early morphogenesis in *Paracoccidioides brasiliensis* mycelium reveals novel and induced genes potentially associated to the dimorphic process. BMC Microbiol. 10:7-29. 2007.

BLOTTA MH. MAMONI RL. OLIVEIRA SJ. NOUÉR SA. PAPAIORDANOU PM. GOVEIA A. CAMARGO ZP. Endemic regions of paracoccidioidomycosis in Brazil: a clinical and epidemiologic study of 584 cases in the southeast region. Am J Trop Med Hyg. 61:390–394. 1999.

BOCCA AL. AMARAL AC. TEIXEIRA MM. Paracoccidioidomycosis: eco-epidemiology. taxonomy and clinical and therapeutic issues. Future Microbiol. 8:1177–1191. 2013.

BOWYER P. DE LUCAS JR & TURNER G. Regulation of the expression of the isocitrate lyase gene (acuD) of *Aspergillus nidulans*. Mol Gen Genet .242:484–489. 1994.

BROCK M. Fungal metabolism in host niches. Curr Opin Microbiol 12:371–376. 2009.

BROWN GD. DENNING DW. GOW NA. LEVITZ SM. NETEA MG. WHITE TC. Hidden killers: human fungal infections. Sci Transl Med 4:165rv113. 2012.

BRUMMER E. CASTANEDA E. RESTREPO A. Paracoccidioidomycosis: an update. Clin Microbiol Rev. 6:89-117. 1993.

BRUMMER E. HANSON LH. RESTREPO A. STEVENS DA. *In vivo* and *in vitro* activation of pulmonary macrophages by IFN-gamma for enhanced killing of *Paracoccidioides brasiliensis* or *Blastomyces dermatitidis*. J Immunol. 140: 786–2789. 1988a.

BRUMMER E. HANSON LH. RESTREPO A. STEVENS DA. Intracellular multiplication of *Paracoccidioides brasiliensis* in macrophages: killing and restriction of multiplication by activated macrophages. Infect Immun. 57:2289–2294. 1989.

BRUMMER E. HANSON LH. STEVENSDA. Gamma-interferon activation of macrophages for killing of *Paracoccidioides brasiliensis* and evidence for nonoxidative mechanisms. Int J Immunopharmacol .10:945–952. 1988b.

BUITRAGO MJ. CUENCA-ESTRELLA M. Current epidemiology and laboratory diagnosis of endemic mycoses in Spain. Enferm Infecc Microbiol Clin. 30: 407-413. 2012.

CANO MI. CISALPINO PS. GALINDO I. RAMIREZ JL. MORTARA RA. DA SILVEIRA JF. Electrophoretic karyotypes and genome sizing of the pathogenic fungus *Paracoccidioides brasiliensis*. J. Clin. Microbiol. 36:742–747. 1998.

CARRERO LL. NIÑO-VEGA G. TEIXEIRA MM. CARVALHO MJ. SOARES CM. PEREIRA M. JESUINO RS. McEWEN JG. MENDOZA L. TAYLOR JW. FELIPE MS. SAN-BLAS G. New *Paracoccidioides brasiliensis* isolate reveals unexpected genomic variability in this human pathogen. Fungal Genet Biol. 45:605-612. 2008.

CASAL M. PAIVA S. QUEIROS O. SOARES-SILVA I. Transport of carboxylic acids in yeasts. FEMS Microbiol Rev. 32:974–994. 2008.

CHAKIR M. PERIDY O. CAPY P. PLA E. DAVID JR. Adaptation to alcoholic fermentation in *Drosophila*: a parallel selection imposed by environmental ethanol and acetic acid. Proc Natl Acad Sci. 90:3621–3625. 1993.

CONRAD R. KLOSE M. Anaerobic conversion of carbon dioxide to methane. acetate and propionate on washed rice roots. FEMS Microbiol Ecol. 30:147-155. 1999.

COONEY NM. KLEIN BS. Fungal adaptation to the mammalian host: it is a new world. after all. Curr Opin Microbiol. 11: 11–516. 2008.

CORREDOR GG. CASTAÑO JH. PERALTA LA. DÍEZ S. ARANGO M. MCEWEN J. RESTREPO A. Isolation of *Paracoccidioides brasiliensis* from the nine-banded armadillo *Dasypus novemcinctus*. in an endemic area for paracoccidioidomycosis in Colombia. Rev Iberoam Micol. 16:216-220. 1999.

COSTA M. BORGES CL. BAILÃO AM. MEIRELLES GV. MENDONÇA YA. DANTAS SF. DE FARIA FP. FELIPE MS. MOLINARI-MADLUM EE. MENDES-GIANNINI MJ. FIUZA RB. MARTINS WS. PEREIRA M. SOARES CM. Transcriptome profiling of *Paracoccidioides brasiliensis* yeast-phase cells recovered from infected mice brings new insights into fungal response upon host interaction. Microbiology. 153:4194–4207 2007.

COZZONE AJ. Regulation of acetate metabolism by protein phosphorylation in enteric bacteria. Annu Rev Microbiol. 52:127–164. 1998.

CRUZ AHS. BROCK M. ZAMBUZZI-CARVALHO PF. SANTOS-SILVA LK. TROIAN RF. GÓES AM. SOARES CMA. PEREIRA M. Phosphorylation is the major mechanism regulating isocitrate lyase activity in *Paracoccidioides brasiliensis* yeast cells. The FEBS J. 278:2318–2332. 2011.

DE FARIAS MR. CONDAS LA. RIBEIRO MG. BOSCO SDE M. MURO MD. WERNER J. THEODORO RC. BAGAGLI E. MARQUES SA. FRANCO M. Paracoccidioidomycosis in a dog: case report of generalized lymphadenomegaly. Mycopathologia. 172:147–152. 2011.

DE MATOS WB. DOS SANTOS GMC. DA SILVA UEB. GONÇALVES E DA G DO R. DA SILVA. AR. Paracoccidioidomycosis in the state of Maranhão. Brazil: geographical and clinical aspects. Rev Soc Bras Med Trop. 45:385-389. 2012.

DE VIRGILIO C. BURCKERT N. BARTH G. NEUHAUS JM. BOLLER T. WIEMKEN A. Cloning and disruption of a gene required for growth on acetate but not on ethanol: the acetyl-coenzyme A synthetase gene of *Saccharomyces cerevisiae*. Yeast. 8:1043–1051. 1992.

DELNEGRO G. LACAZ CS. FIORILLO AM. *Paracoccidioides brasiliensis*. Morphology. Evolutionary Cycle. Maintenance of Saprophytic Life. Biology. Virulence. Systematic Position. In: Paracoccidioidomycosis. South American Blastomycosis. Sarvier São Paulo: 11–21. 1992.

DERENGOWSKI LS. TAVARES AH. SILVA S. PROCÓPIO LS. FELIPE MS. SILVA-PEREIRA I. Macrophages and in vitro nutritional stress condition: Upregulation of glyoxylate cycle genes upon *Paracoccidioides brasiliensis* internalization by murine. Med Mycol. 46:125–134. 2008.

DERISI JL. IYER VR. BROWN PO. Exploring the metabolic and genetic control of gene expression on a genomic scale. Science. 278:680–686. 1997.

DESJARDINS CA. CHAMPION MD. HOLDER JW. MUSZEWSKA A. GOLDBERG J. BAILÃO AM. BRIGIDO MM. FERREIRA ME. GARCIA AM. GRYNBERG M. GUJJA S. HEIMAN DI. HENN MR. KODIRA CD. LEÓN-NARVÁEZ H. LONGO LV. MA LJ. MALAVAZI I. MATSUO AL. MORAIS FV. PEREIRA M. RODRÍGUEZ-BRITO S. SAKTHIKUMAR S. SALEM-IZACC SM. SYKES SM. TEIXEIRA MM. VALLEJO MC. WALTER ME. YANDAVA C. YOUNG S. ZENG Q. ZUCKER J. FELIPE MS. GOLDMAN GH. HAAS BJ. McEWEN JG. NINO-VEGA G. PUCCIA R. SAN-BLAS G. SOARES CM. BIRREN BW. CUOMO CA. Comparative genomic analysis of human fungal pathogens causing paracoccidioidomycosis. PLoS Genetics.7:e1002345. 2011.

DIXON GH. KORNBERG HL. LUND P. Biochim Biophys. Acta. 41:217-233. 1960.

EBEL F. SCHWIENBACHER M. BEYER J. HEESEMANN J. BRAKHAGE AA. BROCK M. Analysis of the regulation. expression. and localization of the isocitrate lyase from *Aspergillus fumigatus*. a potential target for antifungal drug development. Fungal Genet Biol. 43:476-489. 2006.

EGI M. BELLOMO R. STACHOWSKI E. FRENCH CJ. HART GK. HEGARTY C. BAILEY M. Blood glucose concentration and outcome of critical illness: the impact of diabetes. Crit Care Med. 36:2249-55. 2008.

FAN W. KRAUS PR. BOILY MJ. HEITMAN J. *Cryptococcus neoformans* gene expression during murine macrophage infection. Eukaryot Cell. 4:1420–1433. 2005.

FELDMESSER M. KRESS Y. NOVIKOFF P. CASADEVALL A. *Cryptococcus neoformans* is a facultative intracellular pathogen in murine pulmonary infection. Infect Immun. 68:4225–4237. 2000.

FELIPE MS. ANDRADE RV. ARRAES FB. NICOLA AM. MARANHÃO AQ. TORRES FA. SILVA-PEREIRA I. POÇAS-FONSECA MJ. CAMPOS EG. MORAES LM. ANDRADE PA. TAVARES AH. SILVA SS. KYAW CM. SOUZA DP. PEREIRA M. JESUÍNO RS. ANDRADE EV. PARENTE JA. OLIVEIRA GS. BARBOSA MS. MARTINS NF. FACHIN AL. CARDOSO RS. PASSOS GA. ALMEIDA NF. WALTER ME. SOARES CM. CARVALHO MJ. BRÍGIDO MM; PbGENOME NETWORK. Transcriptional profiles of the human pathogenic fungus *Paracoccidioides brasiliensis* in mycelium and yeast cells. J Biol Chem. 280:24706–24714. 2005.

FELIPE MS. ANDRADE RV. PETROFEZA SS. MARANHÃO AQ. TORRES FA. ALBUQUERQUE P. ARRAES FB. ARRUDA M. AZEVEDO MO. BAPTISTA AJ. BATAUS LA. BORGES CL. CAMPOS EG. CRUZ MR. DAHER BS. DANTAS A. FERREIRA MA. GHIL GV. JESUINO RS. KYAW CM. LEITÃO L. MARTINS CR. MORAES LM. NEVES EO. NICOLA AM. ALVES ES. PARENTE JA. PEREIRA M. POÇAS-FONSECA MJ. RESENDE R. RIBEIRO BM. SALDANHA RR. SANTOS SC. SILVA-PEREIRA I. SILVA MA. SILVEIRA E. SIMÕES IC. SOARES RB. SOUZA DP. DE-SOUZA MT. ANDRADE EV. XAVIER MA. VEIGA HP. VENANCIO EJ. CARVALHO MJ. OLIVEIRA AG. INOUE MK. ALMEIDA NF. WALTER ME. SOARES CM. BRÍGIDO MM. Transcriptome characterization of the dimorphic and pathogenic fungus *Paracoccidioides brasiliensis* by EST analysis. Yeast. 20:263–271. 2003.

FERNANDEZ E. FERNANDEZ M. MORENO F. RODICIO R. Transcriptional regulation of the isocitrate lyase encoding gene in *Saccharomyces cerevisiae*. FEBS Lett. 333:238–242. 1993.

FERNÁNDEZ-ARENAS E. CABEZÓN V. BERMEJO C. ARROYO J. NOMBELA C. DIEZ-OREJAS R. GIL C. Integrated proteomics and genomics strategies bring new insight into *Cândida albicans* response upon macrophage interaction. Mol Cell Proteomics. 6:460-778. 2007.

FILLER SG. SHEPPARD DC. Fungal invasion of normally non-phagocytic host cells. PLoS Pathog. 2:e129. 2006.

FLECK CB. SCHOBEL F. BROCK M. Nutrient acquisition by pathogenic fungi: nutrient availability. pathway regulation. and differences in substrate utilization. Int J Med Microbiol. 301:400–407. 2011.

FRADIN C. DE GROOT P. MacCALLUM D. SCHALLER M. KLIS F. ODDS FC. HUBE B. Granulocytes govern the transcriptional response. morphology and proliferation of *Candida albicans* in human blood. Mol Microbiol. 56:397–415. 2005.

FRANCO M. BAGAGLI E. SCAPOLIO S. LACAZ C DA S. A critical analysis of isolation of *Paracoccidioides brasiliensis* from soil. Med Mycol. 38:185-191. 2000.

FRANCO M. MONTENEGRO MR. MENDES RP. MARQUES SA. DILLON ML. MOTA NGS. Paracoccidioidomycosis: a recently proposed classification of its clinical forms. Rev Soc Bras Med Trop. 20:129–132. 1987.

FRANCO M. Host parasite relationships in paracoccidioidomycosis. J Med Vet Mycol. 25:5–18. 1987.

FROHNER IE. BOURGEOIS C. YATSYK K. MAJER O. KUCHLER K. *Cândida albicans* cell surface superoxide dismutases degrade host-derives reativem oxigeno species to escape innate immune surveillance. Mol Microbiol. 71:240-252. 2009.

GERSTMEIR R. WENDISCH VF. SCHNICKE S. RUAN H. FARWICK M. REINSCHEID D. EIKMANNS BJ. Acetate metabolism and its regulation in *Corynebacterium glutamicum*. Biotechnol. 4:99-122. 2003.

GEZUELE E. Aislamiento de *Paracoccidioides* sp. de heces de un pingüino de lia Antártida. In: Proceedings IV International Symposium on Paracoccidioidomycosis. 10–14. 1989.

GOLDMAN GH. DOS REIS MARQUES E. DUARTE RIBEIRO DC. DE SOUZA BERNARDES LA. QUIAPIN AC. VITORELLI PM. SAVOLDI M. SEMIGHINI CP.

DE OLIVEIRA RC. NUNES LR. TRAVASSOS LR. PUCCIA R. BATISTA WL. FERREIRA LE. MOREIRA JC. BOGOSSIAN AP. TEKAIA F. NOBREGA MP. NOBREGA FG. GOLDMAN MH. Expressed sequence tag analysis of the human pathogen *Paracoccidioides brasiliensis* yeast phase: identification of putative homologues of *Candida albicans* virulence and pathogenicity genes. Eukariot Cell. 2:34–48. 2003.

GURVITZ A. ROTTENSTEINER H. The biochemistry of oleate induction: transcriptional upregulation and peroxisome proliferation. BBA-Mol Cell Res. 1763: 1392–1402. 2006.

HAHN RC. MACEDO AM. FONTES CJ. BATISTA RD. SANTOS NL. HAMDAN JS. Randomly amplified polymorphic DNA as a valuable tool for epidemiological studies of *Paracoccidioides brasiliensis*. J Clin Microbiol. 41:2849–2854. 2003.

HAHN RC. MACEDO AM. SANTOS NL. RESENDE JC. HAMDAN JS. Characterization of *Paracoccidioides brasiliensis* atypical isolates by random amplified polymorphic DNA analysis. Rev Iberoam Micol. 19:49–51. 2002.

HAMEL RD. APPANNA VD. Modulation of TCA cycle enzymes and aluminum stress in *Pseudomonas fluorescens*. J Inorg Biochem. 87:1-8. 2001.

HARTIG A. SIMON MM. SCHUSTER T. DAUGHERTY JR. YOO HS. COOPER TG. Differentially regulated malate synthase genes participate in carbon and nitrogen metabolism of *S. cerevisiae*. Nucleic Acids Res. 20:5677-5686. 1992.

HARVER RA. FERRIER DR. Ciclo do ácido cítrico. Bioquímica Ilustrada. Artmed. 5ª ed. 109-116. 2012. 528p.

HEBELER-BARBOSA F. MORAIS FV. MONTENEGRO MR. KURAMAE EE. MONTES B. MCEWEN JG. BAGAGLI E. PUCCIA R. Comparison of the sequences of the internal transcribed spacer regions and PbGP43 genes of *Paracoccidioides brasiliensis* from patients and armadillos (*Dasypus novemcinctus*). J Clin Microbiol. 41:5735– 5737. 2003.

HILTUNEN JK. MURSULA AM. ROTTENSTEINER H. WIERENGA RK. KASTANIOTIS AJ. GURVITZ A. The biochemistry of peroxisomal beta-oxidation in the yeast *Saccharomyces cerevisiae*. FEMS Microbiol Rev. 27:35–64. 2003.

HOHMANN S. Osmotic stress signaling and osmoadaptation in yeasts. Microbiol Mol Biol R. 66:300–372. 2002.

HÖNER ZU. BENTRUP K. MICZAK A. SWENSON DL. RUSSELL DG. Characterization of activity and expression of isocitrate lyase in *Mycobacterium avium* and *Mycobacterium tuberculosis*. J Bacteriol. 181:7161–7167. 1999.

HUNG GC. BROWN CR. WOLFE AB. LIU JJ. CHIANG HL. Degradation of the gluconeogenic enzymes fructose-1.6-bisphosphatase and malate dehydrogenase is mediated by distinct proteolytic pathways and signaling events. J Biol Chem. 279: 49138–49150. 2004.

IBRAHIM-GRANET O. DUBOURDEAU M. LATGE´ JP. AVE P. HUERRE M. BRAKHAGE AA. BROCK M. Methylcitrate synthase from *Aspergillus fumigatus* is essential for manifestation of invasive aspergillosis. Cell Microbiol. 10:134-148. 2008.

IDNURM A. HOWLETT BJ. Isocitrate lyase is essential for pathogenicity of the fungus *Leptosphaeria maculans* to canola (*Brassica napus*). Eukaryot Cell 1:719-724. 2002.

IKEDA Y. YAMAMOTO J. OKAMURA M. FUJINO T. TAKAHASHI S. TAKEUCHI K. OSBORNE TF. YAMAMOTO TT. ITO S. SAKAI J. Transcriptional regulation of the murine acetyl-CoA synthetase 1 gene through multiple clustered binding sites for sterol regulatory element-binding proteins and a single neighboring site for *Sp1*. J Biol Chem. 276: 419–3426. 2001.

KISPAL G. CSEKO J. ALKONYI I. SANDOR A. Isolation and characterization of carnitine acetyltransferase from *S. cerevisiae*. Biochim Biophys Acta. 1085:217–222. 1991.

KLEIN HP. JAHNKE L. Effects of aeration on formation and localization of the acetyl coenzyme A synthetases of *Saccharomyces cerevisiae*. J Bacteriol. 137:179–184. 1979.

KORNBERG H L. KREBS HA. Synthesis of cell constituents from C2-units by a modified tricarboxylic acid cycle. Nature. 179:988–991. 1957.

KORNBERG HL. MADSEN NB. Synthesis of C4-dicarboxylic acids from acetate by a glyoxylate bypass of the tricarboxylic acid cycle. Biochim Biophys Acta. 24:651–653. 1957.

KORNBERG. HL. The role and control of the glyoxylate cycle in *Escherichia coli*. Biochem J. 99:1-11. 1966.

KUNZE M. KRAGLER F. BINDER M. HARTIG A. GURVITZ A. Targeting of malate synthase 1 to the peroxisomes of *Saccharomyces cerevisiae* cells depends on growth on oleic acid medium. Eur J Biochem. 269:915-922. 2002.

LI W. METIN B. WHITE TC. HEITMAN J. Organization and evolutionary trajectory of the mating type (MAT) locus in dermatophyte and dimorphic fungal pathogens. Eukaryot Cell. 9:46–58. 2010.

LIN YY. LU JY. ZHANG J. WALTER W. DANG W. WAN J. TAO SC. QIAN J. ZHAO Y. BOEKE JD. BERGER SL. ZHU H. Protein acetylation microarray reveals that NuA4 controls key metabolic target regulating gluconeogenesis. Cell. 136:1073–1084 2009.

LODI T. FERRERO I. Isolation of the DLD gene of *Saccharomyces cerevisiae* encoding the mitochondrial enzyme D-lactate ferricytochrome c oxidoreductase. Mol Gen Genet. 238:315–324. 1999.

LOIKKANEN I. HAGHIGHI S. VAINIO S. PAJUNEN A. Expression of cytosolic acetyl-CoA synthetase gene is developmentally regulated. Mech Dev. 115:139–141. 2002.

LORENZ MC. BENDER JA. FINK GR. Transcriptional response of *Candida albicans* upon internalization by macrophages. Eukaryot Cell. 3: 1076–1087. 2004.

LORENZ MC. FINK GR. Life and death in a macrophage: role of the glyoxylate cycle in virulence. Eukaryot Cell. 1:657–662. 2002.

LORENZ MC. FINK GR. The glyoxylate cycle isrequired for fungal virulence. Nature. 412:83-86. 2001.

LORENZ MC. Carbon catabolite control in *Cândida albicans*: new wrinkles in metabolism. MBio. 4:e00034-13. 2013.

LUTZ A. A pseudococcidic mycosis localized in the mouth and observed in Brazil. A contribution to the knowledge of American hyphoblastomycoses. Brasil Med. 22:121–141. 1908.

MARTINEZ R. Epidemiology of Paracoccidioidomycoses. Rev Soc Bras Med Trop. 57 Suppl 19:11-20. 2015.

MARTINEZ. R. Paracoccidioidomycosis: the dimension of the problem of a neglected disease. Rev Soc Bras Med Trop. 43:480. 2010.

MATUTE DR. McEWEN JG. PUCCIA R. MONTES BA. SAN-BLAS G. BAGAGLI E. RAUSCHER JT. RESTREPO A. MORAIS F. NIÑO-VEGA G. TAYLOR JW. Cryptic speciation and recombination in the fungus *Paracoccidioides brasiliensis* as revealed by gene genealogies. Mol Biol Evol. 23:65–73. 2006a.

MATUTE DR. SEPULVEDA EV. QUESADA LM. GOLDMAN GH. TAYLOR JW. RESTREPO A. McEWEN JG. Microsatellite analysis of three phylogenetic species of *Paracoccidioides brasiliensis*. J Clin Microbiol. 44:2153–2157. 2006b.

MATUTE DR. TORRES IP. SALGADO-SALASAR C. RESTREPO A. McEWEN JG. Background selection at the chitin synthase II (*chs2*) locus in *Paracoccidioides brasiliensis* species complex. Fungal Genet Biol. 44:57–367. 2007.

McEWEN JG. RESTREPO BI. SALAZAR ME. RESTREPO A. Nuclear staining of *Paracoccidioides brasiliensis* conidia. J Med Vet Mycol. 25: 343–345. 1987.

McEWEN. JG. GARCIA AM. ORTIZ BL. BOTERO S. RESTREPO A. In search of the natural habitat of *Paracoccidioides brasiliensis*. Arch Med Res. 26:305–306. 1995.

MCKINNEY JD. HÖNER ZU BENTRUP K. MUÑOZ-ELÍAS EJ. MICZAK A. CHEN B. CHAN WT. SWENSON D. SACCHETTINI JC. JACOBS WR JR. RUSSELL DG. Persistence of *Mycobacterium tuberculosis* in macrophages and mice requires the glyoxylate shunt enzyme isocitrate lyase. Nature. 406:735-738. 2000.

MITSUNORI N. SELITRENNIKOFF CP. A Method to Assay Glyoxylate cycle inhibitors for antifungals. Fungal Genet Biol. 55:121-130. 2002.

MOLINARI-MADLUM EE. FELIPE MS. SOARES CM. Virulence of *Paracoccidioides brasiliensis* isolates can be correlated to groups defined by random amplified polymorphic DNA analysis. Med Mycol. 37:269–276. 1999.

MONTOYA AE. MORENO MN. RESTREPO A. McEWEN JG. Electrophoretic karyotype of clinical isolates of *Paracoccidioides brasiliensis*. Fungal Genet. Biol. 21: 223–227. 1997.

MUNÕZ-ELIAS EJ. MCKINNEY JD. *Mycobacterium tuberculosis* isocitrate lyases 1 and 2 are jointly required for in vivo growth and virulence. Nat Med 11:638–644. 2005.

NAKAZAWA M. MINAMI T. TERAMURA K. KUMAMOTO S. HANATO S. TAKENAKA S. UEDA M. INUI H. NAKANO Y. MIYATAKE K. Molecular characterization of a bifunctional glyoxylate cycle enzyme. malate synthase/isocitrate lyase. in *Euglena gracilis*. Comp Biochem Physiol B Biochem Mol Biol. 141:445-452. 2005.

NIIMI M. FIRTH NA. CANNON RD. Antifungal drug resistance of oral fungi. Odontology. 98:15–25. 2010.

NINÕ-VEGA G. CALCAGNO AM. SAN-BLAS G. SAN-BLAS F. GOODAY GW. GOW NAR. RFLP analysis reveals marked geographical isolation between strains of *Paracoccidioides brasiliensis*. Med Mycol. 38:437–441. 2000.

NUNES LR. COSTA DE OLIVEIRA R. LEITE DB. DA SILVA VS. DOS REIS MARQUES E. DA SILVA FERREIRA ME. RIBEIRO DC. DE SOUZA BERNARDES

LA. GOLDMAN MH. PUCCIA R. TRAVASSOS LR. BATISTA WL. NÓBREGA MP. NOBREGA FG. YANG DY. DE BRAGANÇA PEREIRA CA. GOLDMAN GH. Transcriptome analysis of *Paracoccidioides brasiliensis* cells undergoing mycelium-to-yeast-transition. Eukaryot Cell. 4: 115–2128. 2005.

OLIVAS I. ROYUELA M. ROMERO B. MONTEIRO MC. MÍNGUEZ JM. LABORDA F. DE LUCAS JR. Ability to grow on lipids accounts for the fully virulent phenotype in neutropenic mice of *Aspergillus fumigatus* null mutants in the key glyoxylate cycle enzymes. Fungal Genet Biol. 45:45-60. 2007.

ONO MA. BRACARENSE AP. MORAIS HS. TRAPP SM. BELITARDO DR. CAMARGO ZP. Canine paracoccidioidomycosis: a seroepidemiologic study. Med Mycol. 39:277–282. 2001.

PADILLA-GUERRERO IE. BARELLI L. GONZÁLEZ-HERNÁNDEZ GA. TORRES-GUZMÁN JC. BIDOCHKA MJ. Flexible metabolism in *Metarhizium anisopliae* and Beauveria bassiana: role of the glyoxylate cycle during insect pathogenesis. Microbiology. 155:3166–3175. 2011.

PANUNTO-CASTELO A1. FREITAS-DA-SILVA G. BRAGHETO IC. MARTINEZ R. ROQUE-BARREIRA MC. *Paracoccidioides brasiliensis* exoantigens: recognition by IgG from patients with different clinical forms of paracoccidioidomycosis. Microbes Infect. 5:1205-1211. 2003.

PIGOSSO LL. PARENTE AFA. COELHO ASG. SILVA LP. BORGES CL. BAILÃO AM. SOARES CMA. Comparative proteomics in the genus *Paracoccidioides*. Fungal Genet Biol. 60:87–100. 2013.

PINZAN CF. Immunological basis for the gender differences in murine *Paracoccidioides brasiliensis* infection. PLoS One. 5:e10757. 2010.

PLAVELL RB. WOODWARD DO. The Regulation of Synthesis of Krebs Cycle Enzymes in *Neurospora* by Catabolite and Product Repression. Eur J Biochem. 13:548-663. 1970.

PRADO M. SILVA MB. LAURENTI. R. TRAVASSOS LR. TABORDA CP. Mortality due to systemic mycoses as a primary cause of death or in association with AIDS in Brazil: a review from 1996 to 2006. Mem Inst Oswaldo Cruz. 104:513–521. 2009.

PRICE MS. BETANCOURT-QUIROZ M. PRICE JL. TOFFALETTI DL. VORA H. HU G. KRONSTAD JW. PERFECT JR. *Cryptococcus neoformans* requires a functional glycolytic pathway for disease but not persistence in the host. MBio. 2:e00103-11. 2011.

PRIGNEAU AO. PORTA JA. POUDRIER S. COLONNA-ROMANO T. NOEL. MARESCA B. Genes involved in beta-oxidation. energy metabolism and glyoxylate cycle are induced by *Candida albicans* during macrophage infection. Yeast. 20:723–730 2003.

RAMIREZ MA. LORENZ MC. Mutations in alternative carbon utilization pathways in *Candida albicans* attenuate virulence and confer pleiotropic phenotypes. Eukaryot Cell. 6:280–290. 2007.

RESTREPO A. TOBÓN A. *Paracoccidioides brasiliensis*. In: MANDELL GL. BENNETT JE. DOLLIN R. (Eds). Principles and Practice of Infectious Diseases. Philadelphia. 3062–3068. 2005.

RESTREPO A. The ecology of *Paracoccidioides brasiliensis*: a puzzle still unsolved. Sabouraudia 23:323–334. 1985.

RESTREPO-MORENO A. Paracoccidioidomycosis. In: Dismukes. WE. Pappas PG. Sobel J. (Eds.) Clinical Mycology. Oxford University Press. New York. p. 328–345. 2003.

ROONEY PJ. KLEIN BS. Linking fungal morphogenesis with virulence. Cell Microbiol. 4:127-137. 2002.

RUBIN-BEJERANO I. FRASER I. GRISAFI P. FINK GR. Phagocytosis by neutrophils induces an amino acid deprivation response in *Saccharomyces cerevisiae* and *Candida albicans*. Proc Natl Acad Sci. 100:11007–11012. 2003.

SALGADO-SALAZAR C. JONES LR. RESTREPO A. McEWEN JG. The human fungal pathogen *Paracoccidioides brasiliensis* (Onygenales: *Ajellomycetaceae*) is a complex of two species: phylogenetic evidence from five mitochondrial markers. Cladistics. 26:610-624. 2010.

SAN BLAS F. Ultrastructure of spore formation in *Paracoccidioides brasiliensis*. J Med Vet Mycol. 24:203–210. 1986.

SAN-BLAS G. NINO-VEGA G. ITURRIAGA T. *Paracoccidioides brasiliensis* and paracoccidioidomycosis: molecular approaches to morphogenesis. diagnosis. epidemiology. taxonomy and genetics. Med Mycol. 40:225–242. 2002.

SAN-BLAS G. NIÑO-VEGA G. *Paracoccidioides brasiliensis*: chemical and molecular tools for research on cell walls antifungals diagnosis taxonomy Mycopathologia. 165:183-195. 2008.

SAN-BLAS G. VERNET D. Induction of the synthesis of cell wall alpha-1.3-glucan in the yeast like form of *Paracoccidioides brasiliensis* strain IVIC Pb9 by fetal calf serum. Infect Immun.15:897–902. 1977.

SAN-BLAS G. Paracoccidioidomycosis and its etiologic agent *Paracoccidioides brasiliensis*. J Med Vet Mycol. 31:99-113. 1993.

SANO A. NISHIMURA K. MIYAJI M. Effects of sex hormones on sexual difference of experimental paracoccidioidomycosis. Review Japanese. 40:1-8. 1999.

SANTT O. PFIRRMANN T. BRAUN B. JURETSCHKE J. KIMMIG P. SCHEEL H. HOFMANN K. THUMM M. WOLF DH. The yeast GID complex. a novel ubiquitin ligase (E3) involved in the regulation of carbohydrate metabolism. Mol Biol Cell. 19:3323–3333. 2008.

SCORZONI L. DE PAULA E SILVA AC. SINGULANI JDE L. LEITE FS. DE OLIVEIRA HC. DA SILVA RA. FUSCO-ALMEIDA AM. MENDES-GIANNINI MJ. Comparison of virulence between Paracoccidioides brasiliensis and *Paracoccidioides lutzii* using *Galleria mellonella* as a host model. Virulence. 6:766-776. 2015.

SELITRENNIKOFF CP. NAKATA M. New cell wall targets for antifungal drugs. Curr Opin Investig Drugs. 4:200-205. 2003.

SHANKAR J. WU TD. CLEMONS KV. MONTEIRO JP. MIRELS LF. STEVENS DA. Influence of 17β-estradiol on gene expression of *Paracoccidioides* during mycelia-to-yeast transition. PLoS One. 6: e28402. 2011.

SHIKANAI-YASUDA MA. BENARD G. HIGAKI Y. DEL NEGRO GM. HOO S. VACCARI EH. GRYSCHEK RC. SEGURADO AA. BARONE AA. ANDRADE DR. Randomized trial with itraconazole. ketoconazole and sulfadiazine in paracoccidioidomycosis. Med Mycol. 40:411–417. 2002.

SHIKANAI-YASUDA MA. QUEIROZ-TELLES F. MENDES RP. COLOMBO AL. MORETTI ML. GRUPO DE CONSULTORES DO CONSENSO EM PARACOCCIDIOIDOMICOSE. Consenso em Paracoccidioidomicose. Rev Soc Bras Med Trop. 39:297–310. 2006.

SHIKANAI-YASUDA MA. Pharmacological management of para- coccidioidomycosis. Expert Opin. Pharmacother. 6:385–397. 2005.

SHIMAZU T. HIRSCHEY MD. HUANG JY. HO LT. VERDIN E. Acetate metabolism and aging: An emerging connection. Mech Ageing Dev. 7-8:511-516. 2010.

SILVA-VERGARA ML. MARTINEZ R. CHADU A. MADEIRA M. FREITAS-SILVA G. LEITE MAFFEI CM. Isolation of a *Paracoccidioides brasiliensis* strain from the soil of a coffee plantation in Ibiá. State of Minas Gerais. Brazil. Med Mycol. 36:37-42. 1998.

SMITH H. Questions about the behaviour of bacterial pathogens in vivo. Philos Trans R Soc Lond B Biol Sci. 355: 551–564. 2000.

SOARES CMA. MADLUN EE. DA SILVA SP. PEREIRA M. FELIPE MS. Characterization of *Paracoccidioides brasiliensis* isolates by random amplified polymorphic DNA analysis. J Clin Microbiol. 33:505–507. 1995.

SPLENDORE A. Zymonematoses with localization in the mouth cavity observed in Brazil. Bull Soc Path Exot. 5:13–319. 1912.

STARAI VJ. CELIC I. COLE RN. BOEKE JD. ESCALANTE-SEMERENA JC. Sir2-dependent activation of acetyl-CoA synthetase by deacetylation of active lysine. Science. 298:2390–2392. 2002.

STARAI VJ. ESCALANTE-SEMERENA JC. Identification of the protein acetyltransferase (Pat) enzyme that acetylates acetyl-CoA synthetase in *Salmonella enterica*. Science. 298:2250–2262. 2004.

TALHARI C. DE SOUZA JV. PARREIRA VJ. REINEL D. TALHARI S. Oral exfoliative cytology as a rapid diagnostic tool for paracoccidioidomycosis. Mycoses. 51:177–178. 2008.

TAVARES AH. SILVA SS. DANTAS A. CAMPOS EG. ANDRADE RV. MARANHÃO AQ. BRÍGIDO MM. PASSOS-SILVA DG. FACHIN AL. TEIXEIRA SM. PASSOS GA. SOARES CM. BOCCA AL. CARVALHO MJ. SILVA-PEREIRA I. FELIPE MS. Early transcriptional response of *Paracoccidioides brasiliensis* upon internalization by murine macrophages. Microbes Infect. 9:583–590. 2007.

TEIXEIRA M DE M. THEODORO RC. DERENGOWSKI LDA S. NICOLA AM. BAGAGLI E. FELIPE MS. Molecular and morphological data supports the existence of a sexual cycle in species of the genus *Paracoccidioides*. Eukaryot Cell. 12:380–389. 2013.

TEIXEIRA MM. THEODORO RC. DE CARVALHO MJ. FERNANDES L. PAES HC. HAHN RC. MENDONZA L. BAGAGLI E. SAN-BLAS G. FELIPE MS. Phylogenetic analysis reveals a high level of speciation in the *Paracoccidioides* genus. Mol Phylogenet Evol. 52:273–283. 2009.

TERÇARIOLI GR. BAGAGLI E. REIS GM. THEODORO RC. BOSCO SDE M. MACORIS SA. RICHINI-PEREIRA VB. Ecological study of *Paracoccidioides brasiliensis* in soil: growth ability. conidia production and molecular detection. BMC Microbiol. 7:92. 2007.

THEODORO RC. CANDEIAS JM. ARAÚJO JP JR. BOSCO SDE M. MACORIS SA. PADULA LO. FRANCO M. BAGAGLI E. Molecular detection of *Paracoccidioides brasiliensis* in soil. Med. Mycol. 43:725–729. 2005.

THEODORO RC. TEIXEIRA M DE M. FELIPE MS. PADUAN K DOS S. RIBOLLA PM. SAN-BLAS G. BAGAGLI E. Genus *Paracoccidioides*: species recognition and biogeographic aspects. PLoS ONE. 7:e37694. 2012.

TOVY A. HERTZ R. SIMAN-TOV R. SYAN S. FAUST D. GUILLEN N. ANKRI S. Glucose starvation boosts *Entamoeba histolytica* virulence. PLoS Negl Trop Dis. 5:e1247. 2011.

TRAVASSOS LR. TABORDA CP. New advances in the development of a vaccine against paracoccidioidomycosis. Front Microbiol. 3:212. 2012.

TRAVASSOS LR. TABORDA CP. Paracoccidioidomycosis: advances in treatment incorporating modulators of the immune response. J. Invasive Fungal Infect. 5:1–6. 2011.

TRAVIS SM. CONWAY BA. ZABNER J. SMITH JJ. ANDERSON NN. SINGH PK. GREENBERG EP. WELSH MJ. Activity of abundant antimicrobials of the human airway. Am J Respir Cell Mol Biol. 20:872–879. 1999.

TREJO-CHAVEZ A. RAMÍREZ-ROMERO R. ANCER-RODRIGUEZ J. NEVAREZ-GARZA AM. RODRIGUEZ-TOVAR LE. Disseminated paracoccidioidomycosis in a Southern two toed sloth (*Choloepusdidactylus*). J Comp Pathol. 144:231–234. 2011.

TRELEASE RN. BECKER WM. BURKER JJ. Cytochemical localization of malate synthase in glyoxysomes. J Cell Biol. 60:483-495. 1974.

TURCOTTE B. LIANG XB. ROBERT F. SOONTORNGUN N. Transcriptional regulation of nonfermentable carbon utilization in budding yeast. FEMS Yeast Res. 10:2-13. 2010.

VIEIRA G DE D. ALVES T DE C. LIMA SM. CAMARGO LM. SOUZA CM. Paracoccidioidomycosis in a western Brazilian Amazon State: clinical-epidemiologic profile and spatial distribution of the disease. Rev Soc Bras Med Trop. 47:63-68. 2014.

VYLKOVA S. CARMAN AJ. DANHOF HA. COLLETTE JR. ZHOU H. LORENZ MC. The fungal pathogen *Candida albicans* autoinduces hyphal morphogenesis by raising extracellular pH. MBio. 2:e00055–e00011. 2011.

WANG ZY. THORNTON CR. KERSHAW MJ. DEBAO L. TALBOT NJ. The glyoxylate cycle is required for temporal regulation of virulence by the plant pathogenic fungus *Magnaporthe grisea*. Mol Microbiol. 47:1601-1612. 2003.

WAYNE LG. LIN KY. Glyoxylate metabolism and adaptation of *Mycobacterium tuberculosis* to survival under anaerobic conditions. Infect Immun. 37:32-39. 1982.

WOLFE AJ. The acetate switch. Microbiol Mol Biol Rev. 69:12–50. 2005.

WOODNUTT G. PARKER DS. Acetate metabolism by tissues of the rabbit. Comp Biochem Physiol B. 85:487–490. 1986.

YAMASHITA H. FUKUURA A. NAKAMURA T. KANEYUKI T. KIMOTO M. HIEMORI M. TSUJI H. Purification and partial characterization of acetyl-coA synthetase in rat liver mitochondria. J Nutr Sci Vitaminol. 48:359–364. 2002.

ZAMBUZZI-CARVALHO PF. CRUZ AHS. SANTOS-SILVA LK. GOES AM. SOARES CM. PEREIRA M. The malate synthase of *Paracoccidioides brasiliensis* Pb01

is required in the glyoxylate cycle and in the allantoin degradation pathway. Med Mycol. 7:734-744. 2009.